INTERVENTION WITH THE HSP90 MODULATOR KU-32 IMPROVES CHRONIC EXPERIMENTAL DIABETIC NEUROPATHY

By

Michael J. Urban

Submitted to the graduate degree program in Neuroscience and the Graduate Faculty of The University of Kansas in partial fulfillment of the requirements for the degree of Doctor of Philosophy.

Rick T. Dobrowsky, Ph.D., Chairperson

Brian S.J. Blagg, Ph.D.

Thomas E. Prisinzano, Ph.D.

Douglas E. Wright, Ph.D.

Brian D. Ackley, Ph.D.

Date Defended: 8 December 2014

The Dissertation Committee for Michael J. Urban certifies that this is the approved version of the following dissertation:

INTERVENTION WITH THE HSP90 MODULATOR KU-32 IMPROVES CHRONIC EXPERIMENTAL DIABETIC NEUROPATHY

Rick T. Dobrowsky, Ph.D., Chairperson

Date Approved: 8 December 2014

ABSTRACT

Inducing the heat shock response (HSR) through Hsp90 inhibition augments heat shock protein (Hsp) support and may improve several aspects of neurodegenerative phenotypes. Several Hsps serve as molecular chaperones that assist in the folding of nascent polypeptides (client proteins) into their mature conformations. They also act as intracellular triage units that refold damaged proteins, stabilize protein complexes, solubilize protein aggregates, and help clear irreparable proteins. A confounding issue surrounding Hsp90 inhibitors is their inability to generate therapeutic windows that dissociate cytotoxic client protein degradation from HSR induction. Our novel C-terminal Hsp90 inhibitor, **KU-32**, induces the HSR while divesting client protein degradation, thus expanding the dose range for neuroprotection.

After 16 weeks of streptozotocin (STZ)-induced Type 1 diabetes in Swiss-Webster mice, KU-32 was intraperitoneally injected weekly at a dose of 20 mg/kg KU-32 (~ 43 mM Captisol/saline vehicle) for 10 weeks. Untreated diabetic mice developed significant reductions in motor and sensory nerve conduction velocities and worsening thermal and mechanical hypoalgesia. KU-32 intervention time-dependently restored these deficits back to untreated non-diabetic levels, without adversely affecting non-diabetic mice. Further, untreated diabetic mice exhibited a 31% reduction in hindpaw intraepidermal nerve fiber (iENF) density by 16 weeks, which remained consistent until study completion. KU-32 improved diabetic iENF density to within 11% of non-diabetic levels by 26 weeks.

To assess mitochondrial function, a 96-well Extracellular Flux (XF96) Analyzer was used to measure oxygen consumption rates (OCRs) for lumbar (L4-L6) dorsal root ganglia (DRG) isolated and cultured upon study completion at 26 weeks. Treatment with the ATP synthase inhibitor oligomycin reduced diabetic OCRs by ~ 80%, indicating that diabetic

DRG devote most of their basal oxygen consumption to ATP synthesis. This is over twice that of untreated non-diabetic DRG at ~ 35%. KU-32 treatment in STZ-diabetes improved OCR reductions to ~ 40%, signifying vast improvements to ATP synthesis efficiency. Upon protonophore injection, DRG from KU-32-treated diabetic mice exhibited a much higher rebound in OCRs compared to diabetes alone, suggesting possible improvements in resiliency to prolonged metabolic stress. Overall, these data suggest that the neuroprotective effects of KU-32 at more chronic stages of diabetic peripheral neuropathy (DPN) may stem from the drug's ability to improve mitochondrial function and nerve fiber innervation.

KU-32 pharmacokinetic (PK) analyses were also performed on DPN-relevant tissues to verify successful drug distribution and elimination from these tissues after intraperitoneal (IP) or oral gavage (OG) treatments. The results showed that KU-32 was rapidly absorbed and distributed to DPN-relevant tissues within 30 minutes of IP treatment and one hour of gavage. Temporal PK analyses suggested that 99.9% of KU-32 distributed to these tissues was eliminated within ~ 30 hours of treatment. This was consistent with findings from an 8-week intervention study, which showed virtually no detectable levels of KU-32 present in diabetic and non-diabetic tissues one week after final treatment. In support of the ongoing hypothesis that inducible Hsp70 is essential for KU-32's neuroprotective effects in DPN, we showed that drug distribution to DPN-relevant tissues were indistinguishable between wild-type C57BL/6 and Hsp70 KO mice. OG also increased drug elimination half-lives for all examined tissues compared to IP treatments, suggesting that OG drug delivery may beneficially increase drug exposure duration.

ACKNOWLEDGEMENTS

I must first thank God for protecting, guiding, and developing me through the numerous trials and tribulations of my life.

To my wife Katherine ("Katie") and our boys Joseph, Erik, Khoen, and Jace: I would not be where I am today without your love, patience, and support. To my parents Joseph and Carol and my siblings Audra, Jeremy, and Joshua, thanks for your unwavering support, love, and encouragement during graduate school and in life.

To Dr. Rick Dobrowsky, thank you for your mentorship, faith in my ability, and willingness to take me under your wing as a Neuroscience graduate student. Early on, you challenged me to think outside-the box . . . something I feel you might have since regretted. Nevertheless, your push ignited a spark that has inspired a career in molecular neuroscience.

Dr. Dobrowsky and Dr. Blagg, thank you for allowing me the freedom to explore the field of molecular neuroscience in pursuit of solving the KU-32 enigma.

To Dr. Brian Blagg, thank you for your mentorship and entrusting me with such a demanding and rewarding project. Without you, there would not have been a collaboration with Dr. Dobrowsky and I would not be where I am today. I truly appreciate everything you have done for me and my research career.

To past and present Dobrowsky and Blagg lab members who have helped me along the way, especially Drs. James McGuire, Cuijuan (Melanie) Yu, Kevin Farmer, Liang Zhang, Pan Pan, and Jiacheng Ma, thank you for your contributions to this work and your friendship. I am especially grateful to Drs. Brian Blagg, Joe Burlison, and Huiping Zhao for the development and synthesis of KU-32, which made this work possible.

To Joana Krise and Dr. Roger Rajewski at The University of Kansas's Biotechnology Innovation and Optimization Center, thank you for providing the technical consult and equipment needed to conduct the pharmacokinetic analyses for KU-32.

To Drs. Rick Dobrowsky, Brian Blagg, Thomas Prisinzano, Douglas Wright, and Brian Ackley, thank you for serving on my committees and your patience and understanding for the extenuating circumstances surrounding this dissertation defense.

This work would not have been possible without funding from the Juvenile Diabetes Research Foundation and the National Institutes of Health.

Finally, to my mentors and friends in the United States Army and Kansas Army National Guard, thank you for allowing me to pursue my educational goals and to better serve my country through scientific achievement. I will use my scientific and military knowledgebase to further basic understanding of the neuropathology associated with blast-induced traumatic brain injury, with the hope of one day developing effective pharmacotherapeutic options to treat our blast casualties. I dedicate this dissertation to my fallen brethren and sistren who have made the ultimate sacrifice to defend the values that make this nation great.

You are not forgotten.

TABLE OF CONTENTS

CHAPTER III: KU-32 PHARMACOKINETIC ANALYSES **Page**

LIST OF FIGURES

LIST OF TABLES

LIST OF ABBREVIATIONS

17-AAG	17-(allylamino)-17-demethoxy geldanamycin
3-DG	3-deoxyglucosone
ABC	avidin-biotin complex
ACE	angiotensin-converting enzyme
AD	Alzheimer's disease
ADA	American Diabetes Association
ADP	adenosine diphosphate
AGE	advanced glycation end-product
AHA1	ATPase homologue 1
ALS	amyotrophic lateral sclerosis
ALS	anterolateral system
AMPK	adenosine monophosphate-dependent protein kinase
ANOVA	analysis of variance
ANS	autonomic nervous system
AP-1	activating-protein-1
AR	aldose reductase
ARI	aldose reductase inhibitor
ATP	adenosine triphosphate
AUC	area under the curve
autoreactive T_h cell	autoreactive helper T lymphocyte
BAG-1	Bcl-2-associated athanogene
BBB	blood-brain barrier
BCS	body condition score
BDNF	brain-derived neurotrophic factor
BER	base excision repair
BMI	body mass index
cAMP	cyclic adenosine monophosphate
CC	central compartment
CD3	cluster of differentiation-3
Cdc37	cell division cycle 37 homolog, *S. cerevisiae*
CHIP	C-terminus of Hsc70/Hsp70-interacting protein
CMAP	compound muscle action potential
$C_{i\text{-}30}$	drug concentration at 30-minute time point
$C_{i\text{-}60}$	drug concentration at 60-minute time point
C_{max}	maximum drug concentration
CMF	cow's milk formula
CML	N-ε-(carboxymethyl)lysine
CN III	cranial nerve III (oculomotor)

CN IV	cranial nerve IV (trochlear)
CN VI	cranial nerve VI (abducens)
CN VII	cranial nerve VII (facial)
CN X	cranial nerve X (vagus)
CNS	central nervous system
C_o	drug concentration at time zero
COX-1	cyclooxygenase-1
COX-2	cyclooxygenase-2
CPE	carboxypeptidase E
CREB	cAMP-response element binding
CSK	C-terminal Src kinase
CSPα	cysteine string protein α
CTLA4	cytotoxic T-lymphocyte antigen 4 gene
CTL	cytotoxic T lymphocyte
CTS	carpal tunnel syndrome
CVB4	HEV-B coxsackievirus B4
d3KU-32	trideutero KU-32
DAF-16	abnormal dauer formation-16
DAG	1,2-diacylglycerol
DAISY	Diabetes Autoimmunity Study in the Young
DAN	diabetic autonomic neuropathy
DCCT	Diabetes Control and Complications Trial
DIPP	Finnish Type 1 Diabetes Prediction and Prevention Project
DKA	diabetic ketoacidosis
DMEM	dulbecco's modified eagle's medium
DPN	diabetic peripheral neuropathy
DPP	Diabetes Prevention Program
DPP-4	diaminopeptidase-4
DRG	dorsal root ganglia
DSPN	diabetic sensorimotor polyneuropathy
EDTA	ethylenediaminetetraacetic acid
eIF4E	eukaryotic translation initiation factor-4E
EMG	electromyogram
ENDIT	European Nicotinamide Diabetes Intervention Trial
Endo	endoneurium
Epi	epineurium
ER	endoplasmic reticulum
ERK	extracellular-signal-regulated kinase
EV	extrinsic vessel
FAD	flavin adenine dinucleotide, oxidized

$FADH_2$	flavin adenine dinucleotide, reduced
FCCP	carbonylcyanide-4-(trifluoromethoxy)-phenylhydrazone
FCRL3	Fc receptor-like 3 gene
FDA	Food and Drug Administration
FFA	free fatty acid
FINDIA	Finnish Dietary Intervention Trial for the Prevention of Type 1 Diabetes
FKHR	forkhead in rhabdomyosarcoma
FoxO	forkhead box "other"
FPG	fasting plasma glucose
FTO	fat mass and obesity-associated gene
GABA	γ-aminobutyric acid
$GABA_B$	γ-aminobutyric acid, class B
GAD	glutamic acid decarboxylase
GAD-65	glutamic acid decarboxylase-65-kDa
GAD-67	glutamic acid decarboxylase-67-kDa
GADA	glutamic acid decarboxylase autoantibody
GAP-43	growth-associated protein-43
GCK	glucokinase gene
GDA	geldanamycin
GDM	gestational diabetes mellitus
GEF	guanine nucleotide exchange factor
GLP-1	glucagon-like peptide-1
GLP-1R	glucagon-like peptide-1 receptor
GLUT-1	glucose transporter-1
GLUT-2	glucose transporter-2
GLUT-3	glucose transporter-3
GLUT-4	glucose transporter-4
Grb2	growth factor receptor-bound protein-2
GSH	glutathione, reduced
GSK-3β	glycogen synthase kinase-3β
GSSH	glutathione, oxidized
GWAS	genome-wide association studies
HbA_{1C}	glycated hemoglobin
HD	Huntington's disease
HEV-B	human enterovirus B
HLA	human leukocyte antigen
HOP	Hsp70/Hsp90-organizing protein
HRP	horseradish peroxidase
Hsc70	heat shock cognate - 70 kDa

HSF1	heat shock factor 1
Hsp	heat shock protein
Hsp40	heat shock protein - 40 kDa
Hsp70	heat shock protein - 70 kDa
Hsp70 KO	inducible Hsp70.1/Hsp70.3 double knockout
Hsp72	inducible heat shock protein - 72 kDa (Hsp70)
Hsp90	heat shock protein - 90 kDa
HSR	heat shock response
IA-2A	insulinoma-associated protein-2 autoantibody
IAAs	insulin autoantibodies
IACUC	Institutional Animal Care and Use Committee
IADPSG	International Association of Diabetes and Pregnancy Study Groups
IAPP	islet amyloid polypeptide
IB	immunoblotting
IC_{50}	drug concentration needed to inhibit protein activity by half
ICA	islet-cell cytoplasmic autoantibody
IDDM	insulin-dependent diabetes mellitus
IDF	International Diabetes Federation
iENF	intraepidermal nerve fiber
IFG	impaired fasting glucose
IGFBP-3	insulin-like growth factor-binding protein-3
IGF-I	insulin-like growth factor-I
IGF-IR	insulin-like growth factor-I receptor
IGT	impaired glucose tolerance
IGTN	impaired glucose tolerance neuropathy
IHC	immunohistochemistry
IKK-β	inhibitor of nuclear factor-κB (NF-κB) kinase β
IL-1β	interleukin-1β
IL-6	interleukin-6
INS	insulin gene
IP	intraperitoneal
IP-10	interferon-γ-inducible protein-10
IP-PK	intraperitoneal pharmacokinetic
IR	insulin receptor
IR-A	insulin receptor - A
IR-B	insulin receptor - B
IRS-1	insulin receptor substrate-1
IRS-2	insulin receptor substrate-2
iTRAQ	isobaric tags for relative and absolute quantification
IV	intravenous

IV-PK	intravenous pharmacokinetic
J protein	J-domain-containing protein
JNK	c-Jun N-terminal kinase
K_{ATP} channel	potassium-ATP channel
k_e	drug elimination rate constant
KO	knockout
LADA	latent autoimmune diabetes in adults
LC/MS/MS	liquid chromatography-tandem (triple quadrupole) mass spectrometry
LCK	lymphocyte cell-specific protein-tyrosine kinase
LDL	low-density lipoprotein
LIT	linear ion trap
LOQ	limit of quantification
LYP	lymphoid tyrosine phosphatase
MAPK	mitogen-activated protein kinase
MBP	myelin basic protein
MCF7	human breast adenocarcinoma
MDM2	murine double minute-2
MEK-1	MAPK/ERK kinase 1
mGluR5	metabotropic glutamate receptor-5
MHC	major histocompatibility complex
mHtt	mutant huntingtin
MI	myo-inositol
MIP	macrophage inflammatory protein
MNCV	motor nerve conduction velocity
MRC	maximal respiratory capacity
mRIPA	modified radioimmunoprecipitation assay
MS	multiple sclerosis
MTBE	methyl *tert*-butyl ether
mtHsp70	mitochondrial Hsp70
mTOR	mammalian target of rapamycin
NAD^+	nicotinamide adenine dinucleotide, oxidized
NADH	nicotinamide adenine dinucleotide, reduced
NADPH	nicotinamide adenine dinucleotide phosphate, reduced
NCV	nerve conduction velocity
NDDG	National Diabetes Data Group
NFATC2	nuclear factor of activated T-cells-2
NF-κB	nuclear factor-κB
NGF	nerve growth factor
NGS	normal goat serum

NIDDM	non-insulin-dependent diabetes mellitus
NIH	National Institutes of Health
NMDA	*N*-methyl-D-aspartic acid, or glutamate
NMDAR	*N*-methyl-D-aspartic acid receptor
NSAID	non-steroidal antiinfammatory drug
NT-3	neurotrophin-3
OCR	oxygen consumption rate
OCT	optimal cutting temperature compound
OG	oral gavage
OG-PK	oral gavage pharmacokinetic
OGT	O-GlcNAc transferase
OGTT	oral glucose tolerance test
p	phosphorylated
P2-C	protein 2-C
PAG	periaqueductal gray
PAI-1	plasminogen activator inhibitor-1
PAR	poly(ADP-ribose)
PARP	poly(ADP-ribose) polymerase
PBS	phosphate buffered saline
PBS-T	phosphate buffered saline with tween-20
PC	peripheral compartment
PD	Parkinson's disease
PDK1	phosphoinositide-dependent kinase-1
PDZK3	PSD-95/Dlg-A/ZO-1 (PDZ) domain-containing-3
Peri	perineurium
PGP 9.5	ubiquitin C-terminal hydrolase
PI	phosphatidylinositol
PI3K	phosphatidylinositol 3-kinase
PIP2	phosphatidylinositol 4,5-bisphosphate
PIP3	phosphatidylinositol 3,4,5-triphosphate
PK	pharmacokinetic
PKA	protein kinase A
PKB/Akt	protein kinase-B
PKC	protein kinase C
PMP22	peripheral myelin protein 22
pooled nerves	sciatic, tibial, and sural nerves
PPARG	peroxisome proliferator-activated receptor-γ gene
PPAR-γ	peroxisome proliferator-activated receptor-γ
PTEN	phosphatase and tensin homolog
PTPN22	tyrosine-protein phosphatase non-receptor type 22 gene
Q	ubisemiquinone

QST	quantitative sensory threshold
RAGE	receptor for advanced glycation end-products
raptor	regulatory-associated protein of mTOR
Ras	rat sarcoma
RNS	reactive nitrosative species
ROS	reactive oxygen species
RTK	receptor tyrosine kinase
RV	radicular vessels
SAR	structure-activity relationship
SBMA	spinal & bulbar muscular atrophy
SC	Schwann cell
SDS	sodium dodecyl sulfate
SDS-PAGE	sodium dodecyl sulfate-polyacrylamide gel electrophoresis
SEM	standard error of the mean
Ser	serine
SGLT-1	sodium-dependent glucose transporter-1
Shc	Src (sarcoma) homology 2 domain-containing
SILAC	stable isotope labeling of amino acids in culture
SLC2A2	glucose transporter-2 gene
SLC830A8	zinc transporter-8 gene
SNAP	sensory nerve action potential
SNCV	sensory nerve conduction velocity
SNP	single nucleotide polymorphism
SNRI	serotonin-norepinephrine reuptake inhibitor
SOD	superoxide dismutase
Src	Rous sarcoma
SRC	spare respiratory capacity
SSRI	selective serotonin reuptake inhibitor
STZ	streptozotocin
SW	Swiss-Webster
$t_{1/2}$	drug elimination half-life
T1DM	type 1 diabetes mellitus
T2DM	type 2 diabetes mellitus
TCA	tricarboxylic acid
TCF7L2	transcription factor 7-like 2 gene
TCP1	tailless complex polypeptide 1
TCR	T cell receptor
TGF-β1	transforming growth factor-β1
Thr	threonine
TNF-α	tumor necrosis factor-α

TOM70	translocase of outer mitochondrial membrane 70-kDa
tPA	tissue plasminogen activator
TRAP-1	TNF receptor-associate protein-1
T_{reg} cell	regulatory T lymphocyte
TRiC	TCP1-ring complex
TRIGR	Trial to Reduce IDDM in the Genetically at Risk
TSC2	tuberous sclerosis complex 2
UDP-*O*-GlcNAc	uridine diphosphate-*N*-acetyl-D-glucosamine
UKPDS	United Kingdom Prospective Diabetes Study
Vav1 GEF	Vav 1 guanine nucleotide exchange factor
VDCC	voltage-dependent calcium channel
VEGF	vascular endothelial growth factor
VNTR	variable number of tandem repeat
WHF	whey-based hydrolyzed formula
WHO	World Health Organization
WT B6	wild-type C57BL/6
ZAP-70	ζ-chain (TCR) associated protein kinase-70-kDa
ZnT8A	zinc transporter-8 autoantibody
β cell	pancreatic β cell
$\Delta\Psi m$	mitochondrial inner membrane potential

CHAPTER I: INTRODUCTION

SECTION 1. DIABETES MELLITUS

1.1. Epidemiology of Diabetes Mellitus

By 2030, diabetes mellitus will affect over 550 million people worldwide, or one in every ten adults.[1-3] Diabetes mellitus is a heterogeneous group of metabolic disorders characterized by persistent hyperglycemia that results from dysfunctional insulin signaling.[4] This non-communicable disease accounts for 8% of global mortality in adults (ages 20-79), and will presumably become the seventh leading cause of death by 2030.[1-2, 5] Diabetes has reached epidemic levels, generating serious international health concerns and igniting public health awareness initiatives by the United Nations and its member states (most notably the United States, China, India, the Russian Federation, Brazil, and Mexico).[2, 6-8]

The International Diabetes Federation (IDF) affirms that *half* of the approximate 371 million adults currently living with diabetes are *undiagnosed* and *unaware* of their condition.[1] This is partially attributed to the reality that 80% of all diabetics live in low- and middle-income regions.[1-2, 9-10] Financial hardships, lack of insurance coverage, socioeconomic barriers, uncoordinated care, and shortages in healthcare professionals often hinder the timely acquisition of appropriate health care in these regions.[8-13] In countries undergoing rapid urbanization and development, increases in population, lifespan, and sedentary lifestyles often boost the number of Type 2 diabetic patients flooding the local medical treatment facilities.[3, 5, 7-11, 14-15] While Type 1 diabetes typically requires lifesaving medical interventions and diagnosis early in life, Type 2 diabetes generally develops much later and may take several years from disease onset to reach a clinical diagnosis (discussed in-depth in **Classification of Diabetes Mellitus**).[4, 9, 14, 16-20] Besides the occasional periodic

health assessment, the detection of Type 2 diabetes ultimately requires the patient to recognize health abnormalities and to willingly seek out medical attention.[4, 9, 14] For these reasons, diabetes prevalence estimates must consider the likely lag in clinical diagnoses.

As alluded to previously, the global burden of diabetes is not evenly distributed. While the top ten most populated countries account for ~ 63% of adult diabetes cases (ages 20-79), it is the smaller countries that are experiencing the worst of the epidemic.[1-3, 5, 7-11] In fact, the highest comparative prevalence[†] of diabetes lies in the Middle East (Kuwait, Bahrain, Saudi Arabia, and Qatar at 22-24%) and several Pacific island states [Federated States of Micronesia[††], Kiribati, Nauru, Tuvalu, Vanuatu, and the Marshall Islands at 22-37%].[1] Comparative prevalence in these regions is often two to three times greater than any other region (*e.g.* United States at 9.4%, Mexico at 15.6%, India at 9.0%, and China at 8.8%).[1]

In the United States, diabetes affects about 7% of the total population, with 2012 reports confirming at least 22.3 million cases.[12] In U.S. adults (ages 20-79), clinically diagnosed diabetics account for ~ 8% of the subpopulation, while another 3% remain presumably undiagnosed.[1-2] This prevalence will likely exceed 25% by 2050.[21] With this dreary forecast, the economic burden of diabetes in the United States has not gone unrealized.[12, 21]

Medical treatments for diabetes mellitus cost the United States nearly $176 billion in 2012, a 30% increase since 2007.[12] Over one-quarter of these expenditures were attributed to prescription medications.[12] In fact, while U.S. medication costs reached $286 billion in 2012, $50 billion worth of this medication went to treat diabetes.[12] The average U.S. diabetic spends ~ 2.3 times more each year on medical care than the typical non-diabetic.[12, 21] Unfortunately, the disease's burden does not end here. Diabetic complications can often

[†] In contrast to national prevalence, comparative prevalence alleviates region-specific variations in age by normalizing to world population age profiles, thereby ensuring more appropriate comparisons
[††] The Federated States of Micronesia is the global leader with 37.2% comparative prevalence

deteriorate a person's health to the point of lethality. Health deterioration not only impacts the patient's quality of life and mental state, but it also distresses surrounding family members and friends.[12-13, 20, 22] Premature mortality can also decimate household incomes and family savings. During these economically challenging times in the Untied States, the untimely deaths of 246,000 diabetics amounted to $18.5 billion in lost productivity in 2012.[12] These societal burdens will continue to grow as the diabetes foothold strengthens.

Despite its global prevalence and societal burdens, there is still a pressing need to develop new drugs that effectively treat diabetes and its associated complications. Although controlled insulin therapy significantly decelerates the rate of progression of diabetes, complications still develop and represent a significant risk to the overall deterioration of a person's health.[23-25] Unfortunately, medicinal treatment options for diabetic complications are limited in that they typically offer monosymptomatic relief or target single pathogenic mechanisms commonly associated with hyperglycemia.[26] This is especially true in the treatment of diabetic peripheral neuropathy (DPN).[26] DPN patients commonly exhibit multiple clinical symptoms that lead physicians to prescribe several medications to address individual symptoms.[27] This partially drives diabetes medication costs and increases the potential risks for drug-drug, drug-nutrient, and drug-disease interactions.[12, 27] For these reasons, DPN could benefit from a more multifaceted therapeutic approach.

Herein, an examination of diabetes mellitus and its substantial burden upon the nervous system will be conducted. Further discussion will emphasize the development of DPN (**SECTION 2**), modern pharmacotherapeutics (**SECTION 3**), and the therapeutic potential associated with targeting heat shock proteins (**SECTION 4**). Preliminary work (2010 Master's Thesis) will also be summarized in **SECTION 4**.[28]

1.2. Clinical Diagnosis and Classification of Diabetes Mellitus

To better understand the modern consensus concerning the classification and clinical diagnosis of diabetes mellitus, a short historical review regarding their derivation follows. This review introduces the condition of prediabetes alongside present-day clinical diagnostic measurements. Modern clinical diagnostic criteria and classifications will be discussed subsequently in their respective sections.

1.2.1. Historical Prelude

In 1979, the National Diabetes Data Group (NDDG) published the *first* widely accepted classification system and clinical diagnostic criteria for diabetes mellitus.[29-30] The publication elicited prompt support by the World Health Organization (WHO) and sparked a global push for standardization amongst the clinical diabetes community.[29, 31] The NDDG and WHO collectively established what became commonly known as insulin-dependent diabetes mellitus (IDDM), non-insulin-dependent diabetes mellitus (NIDDM), gestational diabetes mellitus (GDM), and malnutritional diabetes.[29-32] These categories were based largely upon clinical manifestations and pharmacologic requirements, such as insulin-dependency.[29-32] Over time, diabetes mellitus became a label used to describe several disorders that merely shared hyperglycemic phenotypes, but were otherwise etiologically distinct.[29-32] With advancements in diabetes etiology imminent, this classification system became obsolete by the turn of the century.[29]

In contrast, clinical diagnostic criteria utilized metabolic screening techniques that have been largely preserved in the clinic today [*i.e.* 2-hour oral glucose tolerance test (OGTT) and fasting plasma glucose (FPG) measurements].[29-32] These diagnostic parameters enabled

differentiation between diabetes, non-diabetes, and impaired glucose tolerance in children as well as pregnant and non-pregnant adults.[29-32]

1.2.2. Establishment of Prediabetes

After nearly two decades of etiological advancements in diabetes, committees were established by the American Diabetes Association[†] (ADA) and the WHO[††] to modernize diabetes diagnostic criteria and classifications.[29, 33-34] These committees expanded upon the impaired glucose tolerance condition previously outlined by the NDDG and WHO.[29-31, 33-34] They recognized the presence of an intermediate metabolic state that manifests between normal glucose homeostasis and the lower diagnostic limits for clinical diabetes.[29, 33-34] Although this intermediate state is not a clinical entity per se, it serves as an important biomarker for patients at serious risk of developing diabetes and associated cardiovascular[†††] complications.[4, 18-20, 29, 33, 35-36] Patients with this "prediabetes" condition exhibit particular metabolic anomalies: impaired glucose tolerance *and/or* impaired fasting glucose.[29-32, 34, 36]

1.2.3. Impaired Glucose Tolerance and Impaired Fasting Glucose

Impaired glucose tolerance (IGT) is determined using the 2-hour OGTT in accordance with WHO standards.[31, 37] Venous plasma glucose levels are measured two hours after the oral administration of 75 g anhydrous glucose (dissolved in water).[4, 29, 31, 33, 35, 37] Plasma glucose levels of 140-199 mg/dl (7.8-11.0 mM) are considered positive for IGT.[4, 29, 33, 35]

Impaired fasting glucose (IFG) was introduced by the ADA in 1997 and requires venous FPG measurements after eight hours of caloric restriction.[29, 33, 38] According to 2003 ADA standards, patients with FPG levels of 100-125 mg/dl (5.6-6.9 mM) are positive for IFG.[4, 29, 33, 35] However, the WHO and the IDF did not adopt the ADA's IFG changes in 2003.

[†] Expert Committee on Diagnosis and Classification of Diabetes Mellitus; 1997 and 2003
[††] WHO Consultation; 1998
[†††] Microvascular deterioration is often already underway

Instead, they retain use of the original IFG lower cutoff of 110 mg/dl (6.1 mM) established back in 1997.[29, 33, 35] Both of these metabolic anomalies, IGT and IFG, are elevated in patients with clinical diabetes (discussed below).

1.2.4. Glycated Hemoglobin

In addition to IFG and IGT, the detection of glycated hemoglobin (HbA_{1C}) enables physicians to assess long-term changes in blood-glucose levels over an 8-12 week period.[4, 38-42] HbA_{1C} represents a group of naturally occurring, non-enzymatic, post-translational modifications known as advanced glycation end-products (AGEs), whose levels become exacerbated during prolonged periods of hyperglycemia [discussed in-depth in **Advanced Glycation End-Products**].[39, 41-48] HbA_{1C} levels are generally expressed as a percentage of total hemoglobin within a collected whole blood sample using a standard A1C meter.[40-42] Prediabetes HbA_{1C} levels generally range between 5.7-6.4%.[4, 40-41] Based upon HbA_{1C} and FBG data from 2005-2008, prediabetes presumably affects ~ 35% of the current U.S. adult population over 20 years of age and 50% of the elderly over 65 years.[20] After much debate concerning test standardization, availability, and storage, an international consensus was finally achieved in 2009 regarding the clinical use of HbA_{1C} for diagnosis.[35, 40-41]

1.2.5. Clinical Diagnosis of Diabetes Mellitus

1.2.5.1. Diagnostic Criteria for Diabetes Mellitus

In addition to prediabetes screening, IFG, IGT, and HbA_{1C} metabolic tests provide the diagnostic parameters required for the clinical diagnosis of diabetes.[4, 29, 33-35, 38-41] Simply put, individuals with IFG, IGT, or HbA_{1C} results that exceed the prediabetes parameters described above meet the clinical diagnostic criteria for diabetes.[4, 29, 33-35, 38-41] Conversely, individuals with test results below prediabetes parameters are non-diabetic.[4, 29, 33-35, 38-41]

Test selection is ultimately time-, resource-, and physician-dependent. In dire situations, a patient displaying classic hyperglycemia symptoms can be clinically diagnosed by a random plasma glucose measurement of 200 mg/dl (11.1 mM) or greater.[4, 38] While these diagnostic criteria address most types of diabetes, gestational diabetes mellitus remains an exception.

1.2.5.2. Diagnostic Criteria for Gestational Diabetes Mellitus

In determining gestational diabetes mellitus (GDM), women are administered the 75 g OGTT at 24-28 weeks of pregnancy.[4, 49] After an 8-hour overnight fast, venous plasma glucose levels are measured immediately before glucose ingestion (FPG) and again 1-hour and 2-hours later (OGTT).[4, 49] GDM is diagnosable if any of the following criteria are met: FPG > 5.1 mM; 1-hour OGTT > 10.0 mM; or 2-hour OGTT > 8.5 mM.[4, 49] These criteria were established by the 2008-2009 International Association of Diabetes and Pregnancy Study Groups (IADPSG) with input from several international obstetrical and diabetes organizations, including the ADA.[4] In 2013, the WHO adopted this criteria as well.[49]

1.2.6. Classification of Diabetes Mellitus

ADA and WHO modernization efforts near the turn of the century produced the more appropriate, etiology-based diabetes classification system in use today.[29, 33-35, 49] Dysfunctional insulin signaling underlies all types of diabetes mellitus. The main types of diabetes mellitus include: Type 1, Type 2, and gestational diabetes mellitus.

1.2.6.1. Type 1 Diabetes Mellitus (T1DM)

1.2.6.1.1. Epidemiology of T1DM

Type 1 diabetes mellitus (T1DM), formerly known as insulin-dependent diabetes mellitus (IDDM) or, comprises 5-10% of all diabetic cases.[20] T1DM is the third most

common chronic childhood disease[†], affecting an estimated 490,000 children (ages 0-14) worldwide in 2011.[1, 50] This global prevalence is increasing by an average of 3% each year.[20] Significant differences in geographic distribution also exist. Northern European nations, such as Sweden, Norway, Finland, and the United Kingdom, are amongst the world leaders in T1DM prevalence in children (ages 0-14 years).[1, 50] As one travels south to Italy, Spain, and France, these incidents taper down to nearly half.[1, 50] In contrast, the United States does not share Europe's geographic distribution and is much more evenly dispersed.[50] This is likely attributed to the inherent, widespread ethnic diversity of the United States.[50]

Type 1 diabetes affects an estimated 970,000 Americans, or 0.34% of the total U.S. population.[51] Approximately 20%[†] of these Type 1 diabetics are children and young adults (0.24% of Americans under 20 years).[51-52] Furthermore, T1DM accounts for over 80% of all new diabetes cases in children and young adults (under 20 years).[20, 50] Age, race, and sex have no noticeable impact upon T1DM prevalence.[1, 51]

1.2.6.1.2. Pathogenesis and Natural History of T1DM

T1DM is a relapsing-remitting autoimmune disease in which pancreatic β cells in the islets of Langerhans and/or circulating insulin are selectively targeted through immune-mediated elimination.[53-56] This results in a severe compromise of the body's systemic insulin supply and a lifelong dependence upon exogenous insulin.[55] The pathogenesis and natural history of T1DM are reviewed herein.

A revolutionary T1DM pathogenic model was proposed by Eisenbarth in 1986.[57-58] Eisenbarth's model proposed that the extended periods of prediabetes, which are commonly observed in patients prior to clinical disease onset, are linked to the additional polyendocrine

[†] Asthma and obesity are the most common

[†] Extrapolation from 2010 (1) T1DM prevalence (0.24%) and (2) population census (82,267,556) reporting for Americans under 20 years of age.

deficiencies and the chronic autoimmunity [islet-cell cytoplasmic autoantibodies (ICAs)] also observed in these patients.[57-58] This was reinforced by clinical immunosuppressive therapies (*i.e.* antithymocyte globulin and cyclosporine A) of the time, which favorably hindered Type 1 diabetes progression.[57-60] Unfortunately, the specific mechanisms and putative stimuli responsible for triggering this autoimmunity and the reasons why β cells and insulin are progressively and selectively targeted remain unclear to this day.[53, 61-65]

Clinical T1DM generally manifests as the functional integrity and/or viability of a patient's pancreatic β cell population approaches 10-20%.[53, 66] Hence, there is a distinct delay between the initial onset of autoimmunity and the development of overt diabetes.[53] This prediabetic period can vary in duration from weeks to several years before ultimately developing into clinical T1DM.[62, 65-66] What's more, the mere presence of circulating autoantibodies does not necessarily guarantee that a patient will always develop clinical Type 1 diabetes.[62, 66-67] For a long time it was thought that this autoimmune assault occurs uninterrupted and at a constant rate until all β cells were destroyed.[53, 57] Although complete β cell loss does frequently occur in most patients within 2-3 years of clinical onset, it is now known that some individuals never actually lose all of their β cell function.[53, 67-70] Also, the pathological development of T1DM progresses more realistically in waves of autoimmune bombardment as opposed to previous notions of a more constant, full frontal assault.[53-54, 56]

Autoimmunity in T1DM is a cyclic process.[53-54, 56, 65] Under normal conditions, peripheral tolerance is afforded by regulatory T lymphocytes (T_{reg} cells) that suppress autoreactive helper T lymphocytes (autoreactive T_h cells) that manage to escape negative selection in the thymus (*i.e.* central tolerance).[53, 65, 71] In most T1DM cases, a gradual disequilibrium between these two groups develops over time.[53, 65] This leads to the

accumulation of autoreactive T_h cells that can infiltrate the pancreatic islets most likely via the pancreatic lymph nodes.[53, 64-65] During early pathogenic stages, a trailing upsurge of T_{reg} cell production usually restores homeostatic restraint over the autoreactive T_h cells until the next influx occurs.[53, 65] Unfortunately, the effectiveness of each successive T_{reg} cell ramp up lessens over time until eventually the T_{reg} cells are unable to contain the amplifying number of autoreactive T_h cells.[65, 67, 71] These autoreactive T_h cells bind to autoantigen-presenting pancreatic β cells to initiate an adaptive immune response.[65, 71] Consequently, cytotoxic T lymphocytes (CTLs or "killer" T cells) and B lymphocyte-generated autoantibodies are recruited to the islets, where inflammation (insulitis) ensues.[65, 71]

Interestingly, pancreatic β cells also begin to proliferate during this inflammatory process.[69-70] This is presumed to be a compensatory mechanism (negative feedback) triggered in response to diminished insulin support. [52, 64, 65] Alas, these attempts only intensify subsequent autoimmune cycles by increasing β cell target availability.[53, 56, 69-70, 72]

As insulitis develops, malnutrition and hyperglycemia set in.[56] This forces a patient to either undergo exogenous insulin-replacement therapy or risk death.[56] Within weeks of initiating subcutaneous insulin therapy, patients frequently experience a phenomenon known as the "honeymoon period," wherein a partial-to-complete correction of hyperglycemia can occur.[56, 70, 72] During this short-lived period, the amount of required insulin usually drops to less than 0.5 units of insulin/kg/day.[73] It has been proposed that this supplementation temporarily reduces glucotoxicity to the point that some recovery of endogenous insulin secretion is able to take place.[72] This is also likely aided by β cell proliferation attempts.[70] Although only half of T1DM children experience a significant honeymoon phase, this phase

can last up to two years.[56, 74-75] Regardless, hyperglycemia inevitably returns, bringing with it an increased requirement for exogenous insulin and the risk for chronic complications.[56]

1.2.6.1.3. Risk Factors for T1DM

Although the underlying factors associated with T1DM autoimmunity remain elusive, several exogenous factors are known to encourage autoimmune progression.[53, 63, 65, 76] These entail both hereditary and environmental risk factors.[53, 63, 65, 76]

1.2.6.1.3.1. Hereditary Risk Factors for T1DM

There is a strong genetic basis for the development of T1DM. The risk of developing T1DM increases nearly 15-fold (~ 5%) in Americans with Type 1 diabetic siblings or parents.[51, 77] Concordance rates in dizygotic (fraternal) twins are slightly higher at 6-10%.[77] Interestingly, while children of Type 1 diabetic mothers have about a 2% chance of developing Type 1 diabetes, children of diseased fathers are higher at around 7%.[77] This suggests some sex-linked genetic tendencies. Since monozygotic twins share nearly identical genotypes and associated phenotypes (*e.g.* disease susceptibility and development), identical twin studies are generally used to distinguish exclusive genetic predisposition from environmental contributing factors in disease etiology. Although T1DM concordance rates historically range between 30-50%, a more recent U.S. study has shown that more long-term observations increase disease concordance rates to ~ 65% by 60 years of age.[78-82] In this same study, T1DM concordance rates were only 15-20% by 20 years of age.[82] Hence, while clinical disease onset in identical twins may be more discordant early on, concordance rates increase over time.[82] Collectively, these data refute an exclusive genetic basis for T1DM.

Linkage analyses between two T1DM first-degree relatives (especially between siblings) have identified several broad, genomic regions that contribute to overall T1DM risk.[58] The

identification of these inherited risk factors has been significantly accelerated with the recent advent of genome-wide association studies (GWAS).[83-84] Collectively, over 50 genomic loci have been identified to affect T1DM development.[84-86] Nearly all of these regions encode genes involved in immunity, insulin production, and metabolism.[53, 84] However, most of these identified risk factors have only marginal impacts upon T1DM development.[85] Therefore, only the four most well-established, high risk loci will be addressed.

1.2.6.1.3.1.1. Human Leukocyte Antigen

The strongest region of the genome associated with T1DM development is found on the short arm of chromosome 6 (locus 6p21.3), a large region encoding components of the human leukocyte antigen (HLA) system.[53, 76, 83-84] The HLA system is the major histocompatibility complex (MHC) in humans.[87] These HLA genes encode a wide variety of cell surface proteins that enable the immune system to distinguish "self" from "non-self," or impending pathogenic threats.[62, 67, 76, 87-88] The HLA region of chromosome 6 contains over 200 genes that are susceptible to massive amounts of genetic polymorphisms; some of these genes have over a hundred alleles. [62, 67, 76, 87-88]

Several HLA alleles have been shown to either accelerate or protect against pancreatic autoimmunity.[4, 62, 67, 76, 87, 89] For instance, HLA class II-derived proteins are found only on the surfaces of cells rooted in bodily defense mechanisms (*e.g.* macrophages, dendritic cells, B lymphocytes, and islet epithelial cells).[76] These membrane proteins present proteolytic fragments of endocytosed pathogens/short viral peptides as antigens for targeted elimination. The HLA class II gene variants HLR-DR and HLA-DQ confer 40-50% of known inherited T1DM risk.[62, 90] In contrast, some class II HLA-DR and HLA-DQ alleles (*e.g.* DRB1*0403, DRB1*1401, and DQB1*0602) may actually protect against disease progression.[91-93]

Several HLA class I alleles can also accelerate (*e.g.* HLA-A*24, A*30 and B*18) or protect (*e.g.* HLA-A*01, A*03, A*28, B*14, and B*56) against T1DM progression.[62, 94] HLA class I-derived proteins, which are found on nearly all cells, present proteolytic fragments from infiltrating pathogens and viruses for immune-mediated elimination.[62, 76, 87] Although HLA class I gene variants have historically been regarded as secondary to class II variant disease associations, evidence of their role in T1DM progression is increasing.[62] Nevertheless, how HLA class I and class II variants specifically thwart or facilitate central or peripheral tolerance is not fully understood.[4, 62, 76, 83, 87]

1.2.6.1.3.1.2. Lymphoid Tyrosine Phosphatase

Another gene implicated in T1DM risk is *PTPN22* (*tyrosine-protein phosphatase non-receptor type 22*) on chromosome 1p13.[62, 84, 95] This encodes lymphoid tyrosine phosphatase (LYP), which negatively regulates T cell receptor (TCR) signaling.[62, 84, 95] TCR signaling is what causes naïve $CD4^+$ T cells to differentiate into T_{reg} and autoreactive T_h cells in the thymus if they are autoantigen-reactive.[95] This results in the termination of autoreactive T_h cells and the dispatch of policing T_{reg} cells to the periphery.[95] Naïve $CD4^+$ T cells that survive the thymic screening process then enter circulation in search of antigen-presenting, HLA-derived proteins.[71, 95] In the periphery, TCR signaling triggers naïve $CD4^+$ T cell differentiation as well as an adaptive immune response.[71, 95]

TCR signaling initiates once antigen-presenting HLA-derived proteins bind to TCRs.[95] This activates a complex network of kinases, adaptor proteins, and phosphatases.[95] TCR signaling also prompts LYP to dissociate from its inhibitory complex with C-terminal Src kinase (CSK) to begin dephosphorylating regulatory tyrosine residues on TCR signaling molecules: ζ-Chain (TCR) associated protein kinase-70-kDa (ZAP-70); lymphocyte cell-

specific protein-tyrosine kinase (LCK); cluster of differentiation-3 (CD3); and Vav 1 guanine nucleotide exchange factor (Vav1 GEF).[83-84, 95] Hence, LYP antagonizes TCR signaling. Many Type 1 diabetics possess a single nucleotide polymorphism (SNP) within the encoding region of the *PTPN22* gene (C1858T).[84, 96] This corresponds to an arginine substitution for tryptophan at residue 620 (R620W), which disrupts normal LYP:CSK interactions, thus increasing LYP activity.[84, 96-97] If autoantigen-reactive naïve $CD4^+$ T cells fail to differentiate in the thymus due to TCR signal inhibition, then they can escape to the periphery.[96-97] Why these cells later activate in the periphery remains unknown.[96-97]

Additionally, this particular SNP is often accompanied by a significant increase in proinsulin:C-peptide ratios, suggesting impairment in insulin processing or a surge in systemic insulin demand (discussed further in **Zinc Transporter-8 Autoantibodies and Zinc in Insulin Processing**).[84, 98-99] Thus, this SNP may not only aids naïve $CD4^+$ T cell escape, but may also somehow compromise the functional integrity of the β cells.

1.2.6.1.3.1.3. Cytotoxic T-Lymphocyte Antigen-4

The *CTLA4* (cytotoxic T-lymphocyte antigen 4) gene on chromosome 2q33 is also implicated in T1DM risk.[62, 83] This same region is also implicated in several autoimmune disorders, including: Rheumatoid Arthritis; Celiac Disease; Multiple Sclerosis; and autoimmune endocrinopathies (*e.g.* Autoimmune Addison's Disease, Primary Biliary Cirrhosis, and Graves' Disease).[100-105] *CTLA4* encodes a glycoprotein co-receptor that translocates to the cell membrane in response to TCR signaling in activated $CD4^+$ T cells.[106] CTLA4 reduces TCR signaling through its interactions with homodimeric CD80 and/or CD86 on antigen-presenting cells.[106] It is thought that this docking inhibits TCR signaling by enhancing phosphatase activity, competing with co-stimulatory CD28 for ligands, and

disrupting lipid raft and ZAP-70 microcluster formation in $CD4^+$ T cells.[106] Hence, these mechanisms serve as intracellular "brakes" for accidental responses to autoantigens.

The CTLA4 SNP +49A/G, which results in an alanine substitution for threonine at residue 17 (A17T) of the leader sequence, is strongly associated with T1DM risk.[107-109] It is thought that this site mutation alters this protein's post-translational processing in the endoplasmic reticulum (ER), thus hindering its glycosylation and vesicular integration.[108] As a result, CTLA4's inhibitory actions are compromised, reducing T cell stimulatory thresholds and increasing the likelihood of autoimmunity.[109]

1.2.6.1.3.1.4. Insulin

Finally, genetic variations in the insulin gene itself (*INS* on chromosome 11p15.5) have naturally been suspected in T1DM development.[83] However, genetic polymorphisms and variable number of tandem repeats (VNTRs) upstream of *INS* gene have no affect on β cell autoimmunity.[62, 76, 84, 96, 110] With that said, insulin autoantibodies (IAAs) are usually the first detectible autoantibodies to appear in children.[111] Since *INS* risk genotypes generally weaken insulin expression in the thymus, it is possible that screening for insulin-reactive $CD4^+$ T cells is compromised.[62, 112] Hence, *INS* genetic variants are more likely to affect tolerance to circulating insulin versus the β cell autoimmunity.[62, 85, 112-113]

1.2.6.1.3.2. Environmental Risk Factors for T1DM

Environmental factors, including infectious agents, dietary and nutritional influences, and even psychological stressors, have been proposed to trigger pancreatic autoimmunity in T1DM.[58] These environmental risks and associated hypotheses are discussed below.

Infectious agents, such as viruses, bacteria, and parasites, may contribute to T1DM autoimmunity either by: (1) directly infecting the β cells; (2) triggering host-mediated

proinflammatory/cytotoxic cytokine release, wherein β cells become collateral damage; or (3) presenting antigens that mimic normal β cell peptides to induce immune cross-reactivity.[53, 58] Of these infectious agents, viruses are the most strongly implicated.

1.2.6.1.3.2.1. Viruses

Human enterovirus B species (HEV-Bs) have long been implicated as possible conduits for inducing autoimmunity in T1DM. The HEV-B coxsackievirus B4 (CVB4) produces protein 2-C (P2-C), which closely resembles glutamic acid decarboxylase (GAD), a common enzyme in many neurons and pancreatic β cells (discussed in-depth in **Glutamic Acid Decarboxylase Autoantibodies**).[76, 114] It is thought that this mimicry could either mask the virus from immune-mediated elimination or cause the immune system to target GAD instead.[76] Furthermore, in response to nearby HEV-B (CVB and Echovirus) infections and replication, pancreatic islets secrete proinflammatory cytokines [*e.g.* tumor necrosis factor-α (TNF-α) and interleukin-6 (IL-6)] and chemotactic proteins [*e.g.* IL-8, interferon-γ-inducible protein-10 (IP-10), macrophage inflammatory protein (MIP)-1a, and MIP-1b].[115-117] As a result, close proximity HEV-B infections cause the pancreatic islet cells to draw non-specific inflammation back towards the islets themselves, resulting in insulitis.[117] This is the "fertile field hypothesis" of T1DM development.[114, 118]

1.2.6.1.3.2.2. Parasites

Alternatively, the "hygiene hypothesis" proposes that the removal/prevention of certain pathogens, such as parasitic worms, through public health measures may actually counteract protective immunomodulation normally afforded by the parasite for survival.[114, 119] In other words, a decline in parasitic infestation may actually increase one's susceptibility to Type 1 diabetes.[114, 119] This is supported by trend analysis studies with the human helminth

Enterobius vermicularis.[120] Infestations involving this pinworm, which used to infect nearly half of the U.S. and European childhood population in the 1950s, has declined steadily over the past few decades with improvements in personal hygiene.[120] This pinworm can modulate the development of the mucosal immune system and promote a more humoral immune responsive-type (versus cell-mediated) to better ensure its own survival.[120] Consequently, this reduces overall T cell expression.[120] With T1DM prevalence on the rise and pinworm infections in decline, this supports the hygiene hypothesis.[120] Of course, good hygiene has also been argued to prevent T1DM.[121] Regardless, this hypothesis raises questions as to whether tiny parasites can trigger T1DM autoimmunity.

1.2.6.1.3.2.3. Gut Microbiota

Inflammatory bowel diseases (*e.g.* Crohn's Disease) have demonstrated the ability of gut microbiota to severely impact the immune system and to modulate autoimmunity.[114, 122-123] Although the disruption of gut microbiota affects T1DM development in mice, examining these effects in humans is still in its infancy.[58, 114, 122, 124] However, preliminary evidence suggests that such a disruption might exist in early childhood T1DM cases.[114, 124] In these T1DM cases, bacterial biodiversity in the gut diminishes over time and becomes less stable, suggesting a possible disease link.[124] Further, autoreactive T_h cells, which also originate in the gut's highly active immune system (*i.e.* mucosal lymphoid tissue) during early development, can disrupt peripheral tolerance and increase β cell targeting.[125-126] Even so, more studies are needed to explore these pathological implications in human T1DM.

1.2.6.1.3.2.4. Dietary Factors

Dietary factors can also significantly impact T1DM progression. According to the largely accepted "accelerator hypothesis," systemic increases in insulin demand in obese and

overweight patients (especially children) can actually lead to "drop-dead exhaustion" in pancreatic β cells.[114, 127] Further, exposures to certain dietary factors at early stages in life (neonate, infant, and toddler) can affect T1DM risk.[114] For example, breastfeeding reduces the risk of islet autoimmune development by supplying essential Zn^{2+} ions, nicotinamide, and vitamins C, D, and E.[114] Given the high permeability and immunological profile of the neonate/infant/toddler gut, it has been proposed that the early introduction of high caloric foods, such as potatoes, carrots, and even cow's milk, can prematurely accelerate insulin demands and disrupt peripheral tolerance.[76, 114, 125, 128-130] As the immune system matures and the gut thickens, intestinal permeability and immune reactions to these dietary factors decrease.[125] Hence, it is likely that these early developmental stages are more susceptible to the pathogenic effects of dietary factors than adults.[114]

Evidence of dietary factor influences upon autoantibody expression in T1DM patients is mounting. In the Finnish Dietary Intervention Trial for the Prevention of Type 1 Diabetes (FINDIA), newborn infants were either fed either cow's milk formula (CMF), whey-based hydrolyzed formula (WHF), or WHF without bovine insulin for the first six months of life (whenever breast milk was not available).[131] By three years of age, the prevalence of seropositivity for at least one autoantibody in these children was: 6.3% (CMF-fed); 4.9% (WHF-fed), and 2.6% (WHF without bovine insulin-fed).[131] While human and bovine insulin only differ by three amino acids (two in the A-chain and one in the B-chain), it is not surprising that antibodies developed against bovine insulin might cross-react with human insulin.[131-132] This suggests that if bovine insulin induces an adaptive immune response, the developed antibodies may double as IAAs to increase T1DM risk.[61, 131]

Perhaps more interesting is the Finnish Type 1 Diabetes Prediction and Prevention Project (DIPP), wherein infants possessing genetic polymorphisms for *INS*, *PTPN22*, or *CTLA-4* were screened for autoantibody expression.[133] In this study, infants were introduced and given CMF either before or after six months of age.[133] While both *PTPN22* (C1858T) and INS (-A23T) genotypes demonstrated autoantibody development [IAA, ICA, and insulinoma-associated protein-2 autoantibody (IA-2A)] in children receiving CMF before six months of age, only the *INS* (-A23T) genotype exhibited autoantibody expression with CMF introduction after six months.[133] These *INS* (-A23T) genotypes, but not *PTPN22* (C1858T), also developed autoantibodies against GAD (GADAs) independent of CMF introduction timelines.[133] An additional study combining dietary and hereditary risk factor assessments was the Trial to Reduce IDDM in the Genetically at Risk (TRIGR) study.[134] In this study, infants possessing high risk HLA alleles were either administered CMF or a casein hydrosylate formula alternative.[134] CMF-fed infants developed a significantly higher level of autoantibodies than infants fed casein hydrosylate formula.[134]

In summary, there appears to be significant interplay between genetic and environmental factors affecting autoimmune development in T1DM. These data suggest that autoimmune development is fed by multiple mechanisms that converge to increase T1DM risk. These risk factors ultimately encourage an adaptive immune response with autoantibodies that selectively target pancreatic β cells for elimination. Since the cell-mediated immunity has been addressed, autoantibody influences on T1DM development are reviewed below.

1.2.6.1.4. Autoantibodies in T1DM

Autoantibodies are present in 70-80% of newly diagnosed Type 1 diabetic patients.[135] As such, the serological detection of autoantibodies (*i.e.* autoantibody titers and definitive

autoantibody counts) has become a powerful indicator of autoimmune development in preclinical stages.[4, 62, 136] This is especially true for patients that possess high-risk HLA alleles, children, and young adults.[53, 136] In the previously mentioned identical twin study, the 65% T1DM concordance rate also corresponded to an autoantibody detection concordance rate of 78% by the same age (60 years).[82] This suggests a partial genetic basis for autoantibody development and supports the validity of this biomarker later in life. In this regard, the diagnosis of Latent Autoimmune Diabetes in Adults (LADA), a subtype of T1DM that develops later in life, is largely based on autoantibody seropositivity.[89]

There are currently over two dozen autoantibodies associated with T1DM.[53, 137] Among these autoantibodies, the most prevalent are the islet-cell cytoplasmic autoantibodies (ICAs) and insulin autoantibodies (IAAs), as well as autoantibodies against glutamic acid decarboxylase-65-kDa (GADAs), insulinoma-associated protein-2 (IA-2As), and zinc transporter-8 (ZnT8As).[137-143] The risk of developing T1DM increases significantly with each additional type of autoantibody developed. In the European Nicotinamide Diabetes Intervention Trial (ENDIT), 10-34-year old patients expressing only ICAs had a 2.2% risk of developing T1DM within the next five years.[135, 144] This risk increased to 17%, 39%, and 70% with the appearance of one, two, or three *additional* autoantibody(ies), respectively.[135, 144] Furthermore, the Diabetes Autoimmunity Study in the Young (DAISY) revealed that 89% of the children that express two or more islet-related autoantibodies developed T1DM.[145] This suggests that age significantly affects one's susceptibility to autoantibodies. While each of the above types of autoantibodies will be discussed shortly, the processing and secretion of insulin itself will first be reviewed in the context of ZnT8As to better enable subsequent discussions.

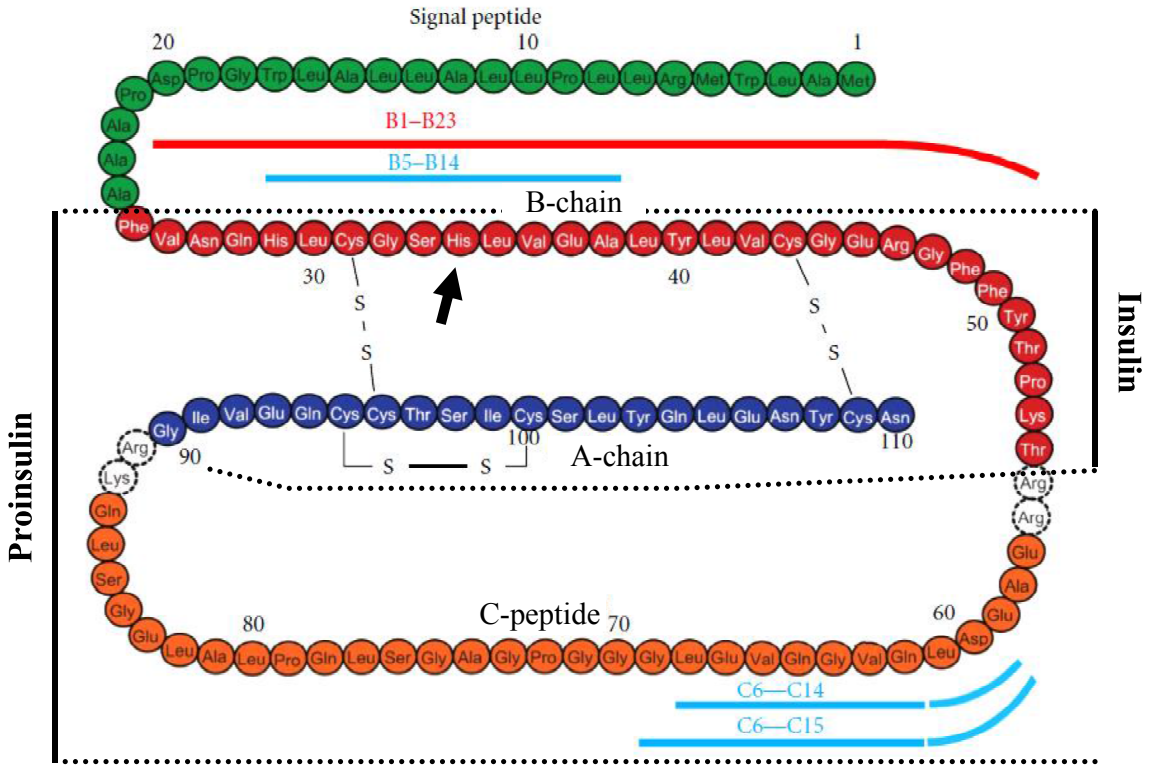

Figure 1. Structures of preproinsulin (all), proinsulin, and insulin. Arrow indicates the histidine residue at position B10 that coordinates with either one of two Zn^{2+} ions to form hexameric proinsulin. The signal peptide (green) and the C-peptide (orange) are cleaved during insulin processing. (Adapted from Kanatsuna *et al.*)[146]

1.2.6.1.4.1. Zinc Transporter-8 Autoantibodies and Zinc in Insulin Processing

ZnT8 is a pancreatic β cell-specific zinc transporter that localizes to the membrane of intracellular insulin secretory granules.[147] By regulating Zn^{2+} ions, ZnT8 serves a critical role in processing, storage, and secretion of insulin.[147] Insulin originates as the 110-amino acid precursor known as preproinsulin (**Figure 1**).[146, 148-149] Upon cleaving preproinsulin's signal sequence in the ER, monomeric proinsulin is transported into the Golgi apparatus where it is folded. Histidine at position B10 coordinates with either one of the two central Zn^{2+} ions to form hexameric proinsulin.[148-149] The prohormone convertases PC1/3 and PC2 and exoprotease carboxypeptidase E (CPE) then excise the C-peptides to produce hexameric insulin while en route to insulin secretory granules.[148-149] The two Zn^{2+} ions are co-secreted

with hexameric insulin via exocytosis and dissociate upon reaching the higher pH of the blood (~ 7.4).[148] These Zn^{2+} ions then inhibit K_{ATP} channels located on pancreatic α cell membranes to prevent glucagon secretion and glucagon-associated glycogenolysis in the liver.[150] Given that T1DM patients are hypoinsulinemic, it is not surprising that Type 1 diabetics also exhibit unusually high basal systemic glucagon levels.[150] This feeds systemic hyperglycemia even further and complicates insulin therapy. Hence, Zn^{2+} ions not only provide structural stability for insulin during its processing and secretion, but these cations also help regulate glucagon secretion.

Nearly 30% of Type 1 diabetic patients that test negative for all other known disease-associated autoantibodies test positive for ZnT8As.[138] Since the discovery of ZnT8As in 2007, these autoantibodies have been found in 55-65% of all new-onset T1DM cases.[143, 151] However, ZnT8A concentrations usually decrease after diagnosis to the point that they are only detectible in ~ 25% of patients 50 years later.[151-153] With this in mind, the functional importance of ZnT8 in T1DM etiology has not gone unexplored.[138] Most ZnT8As recognize the intracellular C-terminus of ZnT8.[137-138] Accordingly, the effects of *SLC830A8* (ZnT8 gene on chromosome 8q24.11) genetic variations upon ZnT8's C-terminal structure and associated disease susceptibility have been assessed.[86, 137-138] Interestingly, while *SLC830A8* SNPs increase Type 2 diabetes risk, Type 1 diabetes is unaffected.[137-138, 154-155] Although two additional loci [*FCRL3* (Fc receptor-like 3) gene on chromosome 1q23.1 and HLA class I regions] have been linked with ZnT8A seropositivity, SNP assessments at these loci have no impact upon T1DM risk as well.[153] Hence, while ZnT8As may serve as effective biomarkers, they are not under the same genetic control as the disease.[153, 155]

1.2.6.1.4.2. Insulin Autoantibodies

IAAs are found primarily in children below five years of age.[145-146] In this age group, children that persistently express IAAs nearly always develop T1DM within the next six years.[145] What's more, ~ 63% of the children that exhibit fluctuating IAA levels develop T1DM within ten years.[145] Hence, the level of IAA persistency in children can predict the age at which T1DM will most likely occur.[145]

As previously mentioned, genetic variations in *INS* reduce thymic insulin levels, thus crippling the autoreactive screening process for insulin and allowing naïve $CD4^+$ T cells to enter circulation. With that said, *anything* that causes pancreatic β cell death can trigger the presentation of β cellular debris (*e.g.* insulin, proinsulin, and C-peptide) by HLA-derived proteins.[146] Evasive autoreactive naïve $CD4^+$ T cells descend upon these presented antigens to induce cell-mediated and humoral immune responses.[146] The humoral immune response generates a multitude of autoantibodies, including IAAs.[146] Furthermore, autoreactive B lymphocytes that also manage to escape the negative selection process can also trigger immunopathogenesis.[146] Upon finding an antigenic match, B lymphocytes recruit T_h cells to help induce its differentiation into autoantibody-producing plasma cells.[146] In either case, plasma cells still generate IAAs, which bind to (pro)insulin A and B chains.[146, 156] HLA class I and class II-derived proteins can also bind (pro)insulin A and B chains as well as C-peptide.[146, 157-158] This could also elicit a humoral and/or cell-mediated immune response.

1.2.6.1.4.3. Glutamic Acid Decarboxylase Autoantibodies

Glutamic acid decarboxylase autoantibodies (GADAs) are detectible in 70-80% of new-onset T1DM patients and tends to persist throughout most of their lives.[137] About half of the patients that survive fifty years of T1DM still test positive for GADAs.[137, 151] These GADAs

primarily target the 65-kDa isoform (GAD-65) over the 67-kDA isoform (GAD-67).[137] GAD normally catalyzes the conversion of glutamate to the inhibitory neurotransmitter γ-aminobutyric acid (GABA). GABA is also found in pancreatic β cells, where it is thought to act in an autocrine/paracrine manner to modulate islet hormone secretion and aid β cell regeneration.[159-163] Hence, GADAs could compromise β cell (and neuronal) function and viability. GADAs are also the predominate autoantibody found in LADA patients, where its extended presence arguably helps distinguish it from Type 2 diabetes mellitus.[89]

1.2.6.1.4.4. Insulinoma-Associated Protein-2 Autoantibodies

IA-2As are found in 60-70% of new-onset T1DM cases.[137, 151, 164-165] However, these IA-2As are detectible in only ~ 6% of the diabetic population after 50 years of T1DM.[151] IA-2 is an inactive tyrosine phosphatase found in the membranes of neuroendocrine secretory granules.[164] Despite IA-2's implications in insulin secretion and β cell proliferation, the physiological functions of this enzyme are still unknown.[53, 164, 166]

1.2.6.1.4.5. Islet-Cell Cytoplasmic Autoantibodies

The "biochemical autoantibodies" (IA-2As, GADAs, IAAs, and ZnT8As) described above have islet autoantigens that have been specifically identified and cloned.[53, 137] In contrast, ICAs have no identified autoantigens other than the islet cells themselves.[137] Seropositivity for these polyclonal ICAs is determined using epifluorescent microscopy, wherein the patient's collected serum is incubated with human (blood-group O) pancreatic tissue samples.[137] Although ICAs are present in 70-80% of new-onset Type 1 diabetes, they are only detectible in ~ 5% in of Type 1 diabetics after ten years.[137] Nevertheless, ICAs were the first autoantibodies discovered in T1DM, and despite their seemingly ambiguous targeting of pancreatic β cells, remain a major part of T1DM developmental risk.[137]

1.2.6.1.5. Idiopathic T1DM

Idiopathic Type 1 diabetes mellitus is ambiguous by definition. Although idiopathic diabetics clearly develop stages of hypoinsulinemia, they are devoid of any evidence of autoimmunity.[4, 167] The natural history for this sect differs from other T1DM patients in that initial insulin therapy normally renders these diabetics normoglycemic for several years without any additional need for exogenous insulin treatment, so long as they watch their diet and maintain use of other glucose-regulating agents (discussed in-depth in **Targeting Hyperglycemia**).[167] This is reminiscent of an extremely long "honeymoon period."[167] Subsequent exogenous insulin requirements are generally only needed on a periodic basis.[4] Besides intermittent hyperglycemia, idiopathic diabetes is best characterized by sporadic bouts of "unprovoked" diabetic ketoacidosis (DKA).[167] DKA is a life-threatening event that usually only arises during the first manifestation of the disease or during periods of extreme insulin deficiency (discussed in-depth in **Targeting Hyperglycemia**).[4, 167] In idiopathic diabetics, DKA arises without warning when insulin levels plummet.[4, 167] Despite strong signs of genetic inheritance, no genes have been linked to idiopathic diabetes.[4, 167]

1.2.6.2. Type 2 Diabetes Mellitus (T2DM)

1.2.6.2.1. Epidemiology of T2DM

Type 2 diabetes mellitus (T2DM), formerly known as non-insulin-dependent diabetes mellitus (NIDDM) or adult-onset diabetes, comprises 90-95% of all diabetic cases.[4, 20, 168-169] Hence, the epidemiological statistics presented in the introductory section mostly pertain to T2DM. However, there are specific T2DM demographic trends that should be noted.

While T2DM has historically been considered a disease that affects the middle-aged and more senior population, the disease's prevalence in children is escalating.[169-176] In 2003, the

prevalence of T2DM in U.S. children (under 20 years) surpassed that of T1DM in several ethnic/racial groups, including: African Americans at 19.0:15.7 (T2DM:T1DM incidents per 100,000 children) and Asian/Pacific Islanders at 12.1:7.4 (T2DM:T1DM incidents per 100,000 children).[169, 172-177] In American adolescents (ages 15-19), the frequency of T2DM (per 100,000) is: 49.4 (Native Americans); 22.7 (Asian/Pacific Islanders); 19.4 (African Americans); 17.0 (Hispanics); and 5.6 (Non-Hispanic Whites).[176] This is thought to be partially linked to rising trends of childhood obesity, which increases T2DM risk.[171, 178-179]

There are also significant ethnic/racial differences in T2DM prevalence in adults. For instance, the highest documented prevalence of T2DM in the world is found in the Pima Indians of modern-day Arizona.[180-182] As of 2003, the prevalence of T2DM in these Native Americans culminated at 58% (ages 55-64), with an average body mass index (BMI) of 27.7 kg/m^2 (men) and 30.1 kg/m^2 (women).[182] Although overweight (BMI: 25-29.9 kg/m^2) and obese (BMI > 30 kg/m^2) phenotypes[†] are generally associated with increased T2DM risk, these BMI:T2DM risk correlations are only applicable within a particular race/ethnicity and do not necessarily hold true when comparing other groups.[180, 183]

Over 35% of the global Type 2 diabetic population resides in the Western Pacific, with a significant portion in East Asia.[3, 184-185] Although the population BMI for East Asians is far less than those of European descent, T2DM prevalence is still comparable to that of the United States.[3, 184-185] This is thought to be the result of higher visceral adiposity in Asian populations, which is thought to be more metabolically adverse (*i.e.* contributes more to lipotoxicity and insulin resistance).[184] These BMIs are consistent with Asian Americans as well.[186] However, despite lower BMIs, Asian Americans (*i.e.* Asian Indians, Filipinos, Vietnamese, Japanese, Koreans, and Chinese) are 30-50% more likely to develop T2DM

[†] 1998 standards established by the National Institutes of Health's National Heart, Lung, and Blood Institute

versus non-Hispanic White Americans.[186] Furthermore, regardless of BMI, the prevalence of T2DM in African Americans, Mexican Americans, and Puerto Ricans in the United States is 3-4% higher than non-Hispanic White Americans.[187-188] Hence, BMI affects T2DM risk differently within each race/ethnicity, and this risk is subject to environmental influence.

1.2.6.2.2. Pathogenesis and Natural History of T2DM

T2DM is characterized by a progressive loss of pancreatic β cell function within insulin-resistant individuals.[4, 35, 170, 178, 189-191] While both of these features develop well before the clinical onset of T2DM, the relative contributions of these factors have been the source of much controversy.[170] However, a study in the Pima Indians at the turn of the century helped put this debate to rest.[170, 180-181] The study showed that declining glucose tolerance in developing Type 2 diabetics results from the progressive loss of pancreatic β cell function, since overall insulin responsiveness did not change.[170, 180] This was later supported by the United Kingdom Prospective Diabetes Study (UKPDS), which showed that tightly maintaining normoglycemia pharmacologically does not prevent the deterioration of glucose regulation in developing Type 2 diabetics.[192-193] Hence, β cell dysfunction is the root cause of T2DM pathogenesis. However, insulin production and secretion are partially driven by plasma glucose levels.[149, 170] This means that anything that disrupts glucose clearance, including insulin resistance, decreases glucose "sensing" and intensifies insulin secretion.[149, 170, 191] This hyperactivity can amplify previously discrete anomalies, eventually causing dysfunction and death in pancreatic β cells.[149, 170, 191] As such, the relative contributions of both β cell dysfunction and insulin resistance in T2DM development are reviewed below. As a prelude, an imperative review of the glucose-mediated feedback system governing insulin production and secretion has been conducted.

1.2.6.2.2.1. Glucose Transport, Insulin Secretion, and Onset of Hyperglycemia

Pancreatic β cells respond to a variety of nutrients circulating in the blood, including glucose and other monosaccharides, free fatty acids, and amino acids.[149] However, glucose is the primary stimulus for insulin secretion.[149] Since DPN results from dysfunctional insulin signaling and associated glucotoxicity, the pathological implications of insulin's affect on glucose transport and its feedback mechanisms are discussed below.[44, 194-195]

Glucose is absorbed from the intestinal lumen by sodium-dependent glucose transporter-1 (SGLT-1), a cotransporter expressed on the apical membrane of enterocytes.[196] Glucose transporter-2 (GLUT-2), which is expressed on the enterocyte's basolateral membrane, then exports glucose into the blood for circulation.[44, 196-197] Upon reaching the pancreatic β cells, constitutively expressed GLUT-1 (humans) and GLUT-2 (rodents) permit glucose to flow freely into pancreatic β cells, where it is metabolized.[44, 149, 197-202] The initiation of glucose metabolism by glucokinase (hexokinase 4) is the "sensing" mechanism (rate-limiting step) for insulin secretion.[149, 198-201] Increases in intracellular ATP levels then inhibit ATP-sensitive potassium channels.[149, 198-201] This depolarizes the cell membrane and induces Ca^{2+} ion influx via voltage-dependent calcium channels (VDCCs).[149, 198-201] This causes insulin secretory granules to the cell membrane and secrete hexameric insulin.[148-149, 198-201]

Upon dissociation in the blood, monomeric insulin docks to insulin receptors on the cell membranes of muscle, adipose, and liver cells.[148, 203-207] This induces phosphatidylinositol 3-kinase/protein kinase-B (PI3K/Akt-)-mediated GLUT-4 vesicle translocation to the cell membrane, where it docks, fuses with the cell membrane, and facilitates glucose uptake.[207-209] Hence, dysfunctional insulin signaling causes these insulin-sensitive tissues to become malnourished, which jeopardizes their function and viability.[44]

On the other hand, the nervous system and pancreas can not afford to endure sustained periods of glucose deprivation. As such, neurons and endothelial cells of the blood-brain barrier (BBB) employ constitutively expressed, insulin-insensitive GLUT-3 and GLUT-1, respectively, for nutritional support.[44, 197, 210-212] Human β cells use GLUT-1 for nutritional support since they are the primary source of insulin supply.[44, 197, 202] Hence, GLUT-1 and GLUT-3 are open corridors for glucose influx. If insulin signaling is compromised and muscle, adipose, and hepatic tissues fail to assist in glucose clearance, there are no flood gates that can close to prevent glucose from entering the neurons and β cells. This results in glucotoxicity in neurons and the pancreas, which is often followed by lipotoxicity.[149] Glucotoxicity is further complicated by glucagon-induced hepatic glycogenolysis.[44, 150] What's more, hepatic gluconeogensis also promptly ensues in an attempt to mitigate "starving conditions" as detected by the liver.[44] These hepatic actions collectively increase glucose entry into the blood. Hence, hyperglycemia feeds upon itself.

Overall, dysfunctional insulin signaling disrupts normal glucose transport, thus resulting in muscle, adipose, and hepatic malnourishment, systemic hyperglycemia, and detrimental metabolic flux in neurons and pancreatic β cells. In T1DM, dysfunctional insulin signaling arises through the loss of β cells and systemic insulin supply through autoimmune bombardment.[4] In contrast, T2DM has historically been considered a metabolic disease.[4] However, islet-reactive T_h cells and autoantibodies have been found in various subgroups of T2DM patients.[213-218] This has given rise to new questions and concerns, primarily: (1) how pathogenically distinct are T1DM and T2DM and (2) how accurate is the current etiological classification system?[213] Nevertheless, the development of dysfunctional insulin signaling in Type 2 diabetes mellitus (as currently understood) is reviewed below.

1.2.6.2.2.2. Pancreatic β Cell Dysfunction and Associated Risk Factors

Pancreatic β cell dysfunction in T2DM is mainly characterized by diminished insulin production and secretion.[191] One explanation for these shortcomings is the loss of β cells. At autopsy, the pancreatic islets of T2DM patients often contain lesions with clear signs of inflammation and apoptosis (**Figure 2**).[219-222] These reductions can be as high as 60%.[222]

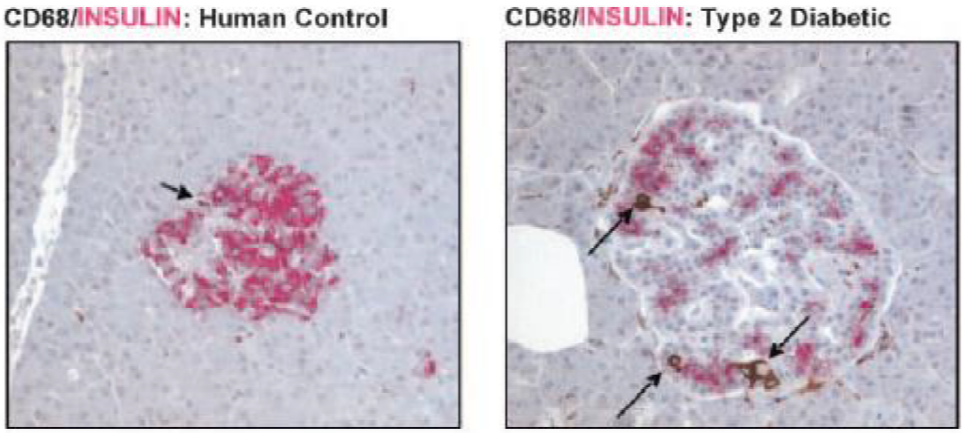

Figure 2. Inflammation in human islets. Double immunohistochemical staining for the macrophage marker CD68 (brown; arrows) and insulin (red) in non-diabetic (left) and Type 2 diabetic (right) islet sections indicate insulin depletion and immunologic infiltration.[220]

Decreases in β cell viability may be attributed to islet amyloid deposition (**Figure 3**).[223] This results from the aggregation of islet amyloid polypeptide (IAPP), or human amylin, a 37-amino acid polypeptide that is co-packaged and co-secreted with insulin.[224-226] IAPP normally fine-tunes the actions of insulin and glycemic control by suppressing glucagon secretion and slowing gastric emptying.[224-226] Why these IAPP aggregates form in T2DM patients is not well understood.[226] It is possible that an increase in insulin demand, while in the midst of worsening hyperglycemia and insulin resistance, boosts IAPP levels beyond the β cell's handling capacity.[226] It is also unknown whether this aggregation occurs inside the secretory granule or in the interstitial space after secretion.[226] Regardless, these aggregates disrupt normal β cell function, induce apoptosis, and incite islet inflammation.[226-227]

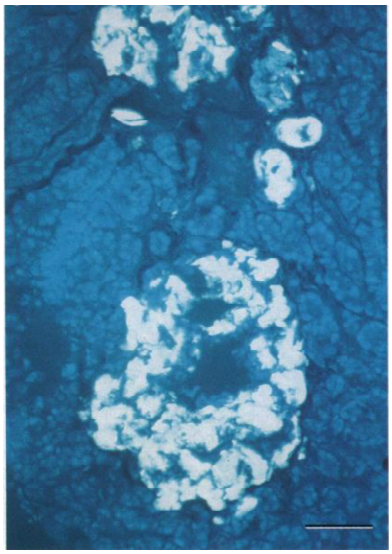

Figure 3. Islet amyloid deposition in human islets. Thioflavin S staining of islets from a Type 2 diabetic patient; islet amyloid deposition appears white (Bar = 50 μm).[223]

Pancreatic β cell loss also results from an acquired autoimmunity. In adults with classic phenotypic T2DM[†], β cell dysfunction strongly correlates to the presence of autoreactive T_h cells.[215] Age also significantly impacts the manner by which this autoimmunity develops.[215, 228-229] For instance, the prevalence of autoreactive T_h cells is ~ 64% in adults with T2DM versus ~ 42% in newly diagnosed children (ages < 18 years).[215, 229] On the other hand, autoantibody prevalence is much higher in Type 2 diabetic children (70-75%) than in it is in adults (~ 48%).[215, 228-229] Why these age-related differences occur is not well understood. Despite etiologic similarities between T1DM and this T2DM sect, there is reason to believe that some of the molecular targets, as well as the prevalence of shared autoantibodies, differ between these diseases.[214-215, 217, 230] It is also conceivable that autoimmunity in T2DM could be linked to phenotypic risk factors, such as obesity, which is uncharacteristic in T1DM. This notion partly stems from the propensity of obese individuals to develop various inflammatory disorders, including psoriasis and Crohn's Disease.[123, 217, 231-233]

[†] Diagnosis at ages 35-70 years and no history of DKA, ketonuria, or insulin therapy

1.2.6.2.2.2.1. Hereditary Risk Factors for Pancreatic β Cell Dysfunction

T2DM is affected by multiple genetic loci that collectively contribute to over 70% of T2DM risk.[234-236] In monozygotic twin studies, disease concordance rates of 17% and 76% were reached by 1 year and 15 years, respectively, following initial diagnosis of the first twin.[236] IGT concordance reached 96% by 15 years.[236] These data suggest a strong genetic influence upon T2DM development.

In terms of β cell function, genetic variants often affect glucose metabolism and insulin biosynthesis, processing, and secretion. For example, mutations in PC1/3 can hinder proinsulin processing in insulin secretory granules.[191, 237] In the gut, genetic polymorphisms in *TCF7L2* (*transcription factor 7-like 2*) reduce the expression of the incretin GLP-1 (glucagon-like peptide-1).[238] This hormone normally binds to GLP-1 receptors (GLP-1Rs) on β cells to enhance insulin secretion through the activation of cyclic AMP/protein kinase A (cAMP/PKA) signaling.[239] Of the 40^{+} susceptibility loci known to affect β-cell function in T2DM, *TCF7L2* SNPs have the strongest T2DM-associated risk to date.[169, 237, 240] Other examples of susceptible loci include *SLC2A2* (GLUT-2), *SLC830A8* (ZnT8), and *GCK* (glucokinase).[169, 237, 240] It is estimated that only 10% of the total genetic influences thought to affect β cell function in T2DM development have actually been identified.[169]

1.2.6.2.2.2.2. Environmental Risk Factors for Pancreatic β Cell Dysfunction

Environmental factors can influence genetic expression during fetal and neonatal programming and can affect one's future susceptibility to disease.[169, 234] Epigenetics is the study of how the environment interacts with the genome to chemically alter DNA and DNA-associated proteins and modify gene expression.[169, 234, 241-243] Many of these "epigenetic marks" are meiotically (genomic imprinting) and mitotically heritable.[169, 234, 241-243]

Examples of epigenetic marks include: DNA modifications (*e.g.* methylation); histone post-translational modifications (*e.g.* acetylation and phosphorylation); alternative nucleosome positioning; microRNAs; and oxidative/nitrosative damage.[234, 241] All of these epigenetic marks serve to translate environmental cues into lifelong epigenetic states.[234]

Epigenetic programming can adversely impact β cell development, neurohormonal weight control, and promote oncogenesis.[169, 244] Examples of contributing prenatal and early postpartum environmental factors include: xenobiotic chemicals, behavioral cues, low-dose radiation, and nutritional supplements.[243] Although the specific epigenetic factors and mechanisms governing intrauterine pancreatic programming are unclear, children of mothers with GDM exhibit a higher risk of developing obesity, glucose intolerance, and T2DM than children of obese mothers.[245-246] Conversely, it has also been proposed that if a newborn is equipped for a life of low-energy intake, he/she may face problems later in life with the adoption of high-energy diets and a more sedentary lifestyle.[169] Hence, the embryonic and neonatal environment can predispose a child to future disease development.

Epigenetic alterations are implicated in both β cell dysfunction and the development of autoimmunity.[242, 247] DNA methylation profiling of pancreatic islets from T2DM donors has shown differential DNA methylation within the promoter regions of over 250 genes relative to non-diabetic donor tissues or high-glucose-treated islet explants.[247] These disruptions in gene expression are linked to β cell dysfunction, apoptosis, adaptation of metabolic stress, and inflammation.[247] Whether or not these epigenetic alterations are the cause or an effect of T2DM remains to be determined. Epigenetic alterations in autoimmunity in T1DM are gaining momentum and may doubly apply to T2DM as well. Epigenetic marks in T1DM notably include: hypermethylation and hypomethylation of several genes in macrophages

and B lymphocytes as well as unfavorable alterations in microRNA levels of T_{reg} cells and the pancreas (affecting insulin exocytosis, development, and apoptosis).[242] Hence, epigenetics may have a critical role in T1DM and T2DM development.

1.2.6.2.2.3. Insulin Resistance and Associated Risk Factors

Insulin resistance is a major hallmark of T2DM.[248-250] Insulin resistance mainly results from hyperlipidemia and associated lipotoxicity.[248-250] Although mutations or defects in the insulin signaling machinery can exist and do affect insulin resistance, these cases are usually more rare.[249] Nonetheless, key mutations affecting insulin signaling and hyperlipidemic pathogenic contributions are reviewed below. Although the molecular components of the insulin signaling cascade are superficially introduced below, they will be covered more in-depth in the **Altered Insulin-Associated Neurotrophism in Diabetes Mellitus** section.

Adipocytes normally regulate systemic free fatty acid (FFA) circulation in the blood. However, high caloric intake and diminished physical activity can alter systemic FFA distribution and utilization. At the cellular level, protection against lipotoxicity is generally afforded by the storage of FFAs as triacylglycerides in small lipid droplets.[248-250] Under hyperlipidemic conditions in non-adipose cells (especially muscle cells), the intracellular storage capacities quickly depletes.[250] This results in the intracellular accumulation of FFAs and the production of adverse lipid products, such as diacylglycerol (DAG) and ceramide.[248, 250-253] DAG and ceramide activate select protein kinase C (PKC) isoforms that disrupt insulin signaling by phosphorylating and inhibiting insulin receptor substrate-1 (IRS-1), IRS-2, and Akt.[248-254] Inhibitory phosphorylations of IRS-1 and IRS-2 are also executed by the stress kinases JNK (c-Jun N-terminal kinase) and IKK-β [inhibitor of nuclear factor-κB (NF-κB) kinase β].[248-249, 254] JNK and IKK-β are activated in response to proinflammatory

cytokines (*e.g.* TNF-α), FFAs, reactive oxygen species, and ER stress, and they are implicated in the development of insulin resistance.[248-249, 254] These phosphorylations also inhibit PI3K/Akt-mediated GLUT-4 vesicle translocation. In addition, JNK and IKK-β phosphorylate and activate AP-1 (activating-protein-1) and NF-κB, respectively.[248-249, 254] This induces the expression of additional cytokines and perpetuates inflammation.[248-249, 254]

Only a few genetic variations have been linked to insulin resistance in T2DM. One of these gene products, *PPARG* (encoding PPAR-γ, peroxisome proliferator-activated receptor-γ), is the target for thiazolidinediones (discussed further in **Targeting Hyperglycemia**).[255] FFAs and eicosanoids (prostaglandins and leukotrienes) bind to PPAR-γ to permit the expression of genes associated with adipocyte differentiation and glucose homeostasis.[256] Thus, inducing PPAR-γ reduces insulin resistance by improving adipocyte proliferation, viability, and preventing the release of detrimental FFAs and cytokines, such as TNF-α.[169]

Other risk factors for insulin resistance include genetic variants for IRS-1, IRS-2, and IGF-I (insulin-like growth factor-I).[240, 257-259] The impact of these alterations will become evident in the future discussion on **Altered Insulin-Associated Neurotrophism in Diabetes Mellitus**. Finally, while over 40 gene variants have been linked to obesity, only variants in *FTO* (*fat mass and obesity-associated*) have been able to link BMI with T2DM risk.[191, 258, 260] Hence, the development of insulin resistance is more closely associated with obesity and sedentary lifestyle versus a genetic predisposition as seen with β cell dysfunction.

1.2.6.3. Gestational Diabetes Mellitus

GDM entails the development of glucose intolerance during pregnancy that is "not clearly overt diabetes."[178, 261] With the rise in obesity in women of childbearing age, this

distinction differentiates GDM from pre-GDM (women that are already/almost diabetic), which accounts for ~ 15% of diabetic pregnancy complications.[4, 261-262]

In the United States, GDM affects ~ 7% of all pregnancies (~ 200,000 cases each year), with the lowest rates occurring in African Americans (4%) and the highest rates occurring in Asian Americans (8.6%).[4, 262] GDM prevalence increases almost linearly as a woman ages from ~ 1% (ages 15-19) to ~ 16% (ages 45-beyond).[262] If GDM persists without intervention, the patient may likely develop clinical T2DM during the pregnancy or postpartum, posing serious health risks to both mother and child.[4, 20, 34, 49] The maternal risk of developing T2DM increases from 5-10% immediately after childbirth to 35-60% in the next 10-20 years.[20] This further supports age and BMI as risk factors for T2DM.

As previously mentioned, *in utero* epigenetic modifications can increase the risk of obesity, glucose intolerance, T1DM, and T2DM in the child if successful intervention is not achieved.[242, 245-246] In most cases, GDM is not diagnosed until 24-28 weeks of pregnancy unless it is caught at the initial visit with the physician.[261] This is partly attributed to the fact that most women with GDM have no apparent symptoms.[22] Exceptions to this screening frequency include women at high risk of GDM, such as patients with marked obesity, glycosuria, a personal history of GDM, or a strong family history of diabetes.[263]

Overall, despite their different etiologies, each type of diabetes induces hyperglycemia, which systemically alters an individual's metabolic state. This leads to a multitude of clinical symptoms and complications.

1.3. Symptoms and Complications of Hyperglycemia

Although the Ebers Papyrus arguably describes the first reported symptoms of diabetes mellitus about 3,500 years ago, the first indisputable symptomatic and treatment accounts

were recorded by the ancient Greek physician Aretaeus (81-138 AD).[264-267] It was Aretaeus that coined the term "diabetes" from the Greek word *diabaínein*, meaning "siphon" or "pipe-like," after making the following observations:

> Diabetes is . . . a melting down of the flesh and limbs into urine . . . life is disgusting and painful; thirst, unquenchable; excessive drinking, which, however, is disproportionate to the large quantity of urine, for more urine is passed; and one cannot stop them either from drinking or making water.[264]
>
> - Aretaeus, the Cappadocian

Hyperglycemic symptoms of diabetes mellitus include: frequent urination (polyuria); excessive thirst (polydipsia); increased appetite (polyphagia); blurred vision; unusual weight fluctuations; extreme fatigue; nausea; and slowly healing cuts or bruises.[4, 268] In addition, results from the Diabetes Control and Complications Trial (DCCT, 1983-1993) support the hypothesis that hyperglycemia contributes to the pathological progression of more chronic diabetic complications, such as diabetic neuropathy, cardiovascular disease, retinopathy, and nephropathy.[23, 44, 197] While our research mainly focuses on DPN, these other complications can foster neuropathic development. Thus, they will be addressed briefly in the context of DPN. The physiologic effects of acute diabetic complications will be addressed in the context of mismanaged insulin therapy in **Targeting Hyperglycemia**.

SECTION 2. DIABETIC PERIPHERAL NEUROPATHY

Diabetic peripheral neuropathy (DPN) is the overall attrition of peripheral nerve fibers that results from diabetes.[23, 46, 269-276] Affecting over half of the diabetic population, DPN is the most prevalent of the chronic complications.[271-272] These neuropathies mainly manifest as distal, symmetric, sensorimotor polyneuropathies, which entail both small and large nerve fiber deterioration in the extremities, partly resulting in progressive sensorimotor deficits.[271, 277] These sensorimotor deficits, combined with diminished microvascular support, promote

the development of non-healing foot ulcerations and gangrenous infections that ultimately require traumatic, lifesaving surgeries.[278] Incidentally, DPN is the leading cause of non-traumatic lower limb amputation in the United States, averaging ~ 82,000 each year.[20, 278] Sadly, over 85% of these amputations are thought to be preventable with early detection and proper therapeutic intervention.[20, 278] A patient's quality of life is further burdened by the increased likelihood of accidental injury (*e.g.* fractures, burns, contusions, lacerations, and frostbite) that often accompanies insensate neuropathies.[43]

Despite recent advances in DPN etiology, its prevalence, and its overall impact upon a patient's physical and mental well-being, there are few therapeutic options available to effectively treat DPN. In order to properly introduce modern pharmacotherapeutics and the need for new and effective drug treatment strategies, an examination of DPN pathogenesis follows. Herein, the morphological alterations and clinical manifestations that accompany DPN are reviewed and will be followed by an extensive look at the molecular mechanisms implicated in diabetic sensorimotor polyneuropathy (DSPN), the focus of this research.

2.1. Morphological and Clinical Manifestations in Diabetic Neuropathy

There are several forms of diabetic peripheral neuropathy. These neuropathies differ according to their symptoms, patterns of neurological involvement, course, risk factors, progression, and etiology.[274-276, 279] Although several DPN classification systems have been developed based upon various clinical manifestations or developmental patterns, the system proposed by Thomas and later adapted by Boulton and the Toronto Expert Panel on Diabetic Neuropathy (2009) is widely accepted today.[274-276, 279] This system divides DPN into focal and multifocal neuropathies and generalized, symmetric polyneuropathies.[274-276, 279]

2.1.1. Focal and Multifocal Neuropathies

Focal and multifocal neuropathies are generally asymmetric neuropathies that develop mostly in older T2DM patients.[270] Diabetic focal neuropathies consist of nerve entrapment and mononeuropathies.[270] The most common form of nerve entrapment is carpal tunnel syndrome (CTS), wherein compression of the median nerve in the wrist causes numbness, tingling or burning sensations, weakness, muscular atrophy, and potentially paralysis in the hands and fingers.[270, 280] Over one-third of the diabetic population is affected by CTS.[280-281] Other forms of entrapment involve the ulnar and radial nerves, the lateral cutaneous nerve of the thigh, and the peroneal and tibial nerves.[280] Tibial nerve entrapment can cause what is known as tarpal tunnel syndrome, wherein CTS-like symptoms develop in the feet.[280]

In contrast to the gradual progression of nerve entrapment, mononeuropathies develop abruptly as a result of localized vasculitis (inflammation of the blood vessels) and associated ischemia.[280] These mononeuropathies typically affect the peripheral nerves (median, ulnar, femoral, sciatic, sural, and peroneal), thoracic nerves, and, on more rare occasions, the cranial nerves (CN III, CN IV, CN VI, and CN VII).[270, 280] Mononeuropathic symptoms closely resemble those associated with nerve entrapment.

Multifocal neuropathies, as implied, affect multiple nerves at one time.[270, 274-275] These include the development of *multiple* mononeuropathies as well as cervical, thoracic, or lumbosacral radiculoplexopathies.[273-275] Lumbosacral radiculoplexopathy (also known as diabetic amyotrophy, proximal motor neuropathy, or Bruns-Garland Syndrome) entails neurodegeneration in the thighs, hips, legs, and/or buttocks presumably due to regionalized microvasculitis and ischemia.[273] This ultimately leads to muscular fatigue, atrophy, and diminished motor skills.[273]

2.1.2. Generalized Symmetric Polyneuropathies

The majority of DPN cases involve generalized, symmetric polyneuropathies. These include diabetic autonomic neuropathy, impaired glucose tolerance neuropathy, acute sensory neuropathy, and diabetic sensorimotor polyneuropathy.[276, 279]

2.1.2.1. Diabetic Autonomic Neuropathy

Diabetic autonomic neuropathy (DAN) is the most dangerous and least understood of the diabetic neuropathies.[282-283] Although usually diffuse, DAN can localize to particular visceral organ(s) and compromise their functional integrity.[283] DAN is further complicated by the fact that many visceral organs are dually innervated by both the parasympathetic and sympathetic nervous systems. .[282-283] This increases relative susceptibility of these organs to neurodegeneration and associated autonomic dysfunction.[282-283] As such, DAN can directly endanger a patient's life.[283]

Although the pathogenesis of DAN is not fully understood, evidence strongly suggests that autonomic neural imbalance results from chronic hyperglycemia and is multifactorial in nature.[282-283] DAN also appears to be length-dependent in that it initially targets the longest nerve fibers first.[282-283] This is extremely problematic given that the longest nerve of the autonomic nervous system (ANS), the vagus nerve (CN X), accounts for over 75% of all parasympathetic activity.[283-284]

DAN occurs in ~ 53% of T1DM and ~ 74% of T2DM patients.[285] Roughly 15% of these cases are considered moderate-to-severe.[285] DAN clinical symptoms can go unnoticed for a long time and can take years to develop.[282-283] Its symptoms ultimately depend upon which organ(s) have been affected.[283] DAN can cause myocardial ischemia, hypotension, cardiac arrhythmia, and cardiac infarction, which complicates hyperlipidemic and cardiovascular

complications already associated with diabetes.[282-283] DAN can cause: gastrointestinal irregularities (*e.g.* diarrhea, constipation, loss of bowel control, gastroparesis, heartburn, difficulty swallowing, nausea, and vomiting); genitourinary problems (*e.g.* erectile dysfunction, female sexual dysfunction, and loss of bladder sensation/control); improper sudomotor function (*e.g.* gustatory sweating, dry skin, heat intolerance); sleep apnea; irregular pupil constriction/dilation; and an overall unawareness of hypoglycemia.[282-283] Consequently, DAN can adversely impact a patient's quality of life and even endanger it.

2.1.2.2. Impaired Glucose Tolerance Neuropathy

Approximately 40% of patients described as having "idiopathic neuropathy" test positive for IGT.[276, 286-289] It is thought that these occurrences are the early stages of DPN.[276, 287] To test this hypothesis, the Impaired Glucose Tolerance Neuropathy (IGTN) study assessed whether lifestyle intervention (diet and exercise) could improve these neurodegenerative phenotypes.[287] The study was modeled after the Diabetes Prevention Program (DPP), which showed that intense diet and exercise can reduce IGT progression to T2DM by ~ 58%.[287, 290] In the IGTN study, diet and exercise partly restored cutaneous innervation (described shortly), which improved neuropathic pain.[287] This suggests that neuropathy can initiate before the clinical onset of diabetes and that lifestyle intervention is beneficial early on.

2.1.2.3. Acute Sensory Neuropathy

Acute sensory neuropathy is best described as an abrupt, intense, neuropathic pain.[270] Most patients describe an "electric shock"-like sensation (sharp, stabbing pains) in the lower extremities.[270] Frequent complaints include deep aching pains, constant burning sensations in the feet, and severe paresthesias (abnormal skin sensations).[270] Weight loss, depression, and sexual dysfunction are also common.[270, 279] These neuropathies are thought to result

from diverted microvascular support, which results due to poor glycemic control.[270, 279] Pharmacologic treatments for acute sensory neuropathy usually entail various analgesics.[270] Although this type of neuropathic pain usually resolves within a year, this is not usually the case in diabetic sensorimotor polyneuropathy (DSPN).[270, 274-275]

2.1.2.4. Diabetic Sensorimotor Polyneuropathy (DSPN)

DSPN is the most common type of diabetic neuropathy in the somatic nervous system and the focus of this research.[270, 273-275] DSPN is a symmetric neurodegenerative process that initiates in the more distal regions of small-caliber nerve fibers and progresses up the extremities (towards the midline).[270, 274-275] This compromises the functional integrity and viability of longer somatic nerves, thus leading to multiple clinical manifestations.[270]

2.1.2.4.1. Clinical Manifestations of DSPN

Generalized symmetric polyneuropathies are divided into atypical and typical subgroups to rule out non-diabetic sources of neuropathy in epidemiological and clinical research studies.[274-275] Atypical DPNs includes the acute sensory neuropathies and DANs, which develop intermittently throughout diabetes and have generally monophasic or relapsing courses.[275] In contrast, typical DPNs (DSPN) entail the development of chronic pain and sensorimotor deficits.[274-275] Given that atypical DPN diagnostic parameters are still underway and that our research is concerned with DSPN, only the diagnostic criteria for DSPN will be addressed.[274-275]

2.1.2.4.1.1. Electrophysiological and Sensory Assessments for DSPN

DSPN diagnostic criteria are based on electrophysiological and quantitative sensory threshold (QST) assessments.[274-275] Electrophysiological assessments generally entail both motor (MNCV) and sensory nerve conduction velocity (SNCV) measurements, which are

based on compound muscle action potentials (CMAPs) and sensory nerve action potentials (SNAPs), respectively. In human peroneal and sural nerves, DSPN gradually slows MNCV by approximately 0.5 m/s each year.[270, 291] DSPN reduces SNCV in the peroneal and sural nerves by 0.2 and 0.4 m/s each year, respectively.[270, 292] Although these deficits may appear minor at first, this becomes increasingly troublesome.

QST testing is a psychophysical type of analysis that measures somatosensory thresholds in response to incremental changes in stimulus intensity.[270] QST ultimately enables non-invasive assessments of both small- and large-fiber sensory function (discussed in-depth in **Somatosensory Nerve Fibers**).[293] QST diagnostic tools include: Biothesiometers to determine vibration perception thresholds; Semmes-Weinstein monofilaments (human version of von Frey monofilaments) for assessing mechanical hypoalgesia; and computer-driven thermal analyzers to measure temperature hypoalgesia.[293-294] QST ultimately enables progressive monitoring disease-induced changes in sensations.

2.1.2.4.1.2. Symptoms of DSPN

DSPN is characterized by both positive and negative symptoms that manifest primarily in the toes, feet, and legs.[274] Positive symptoms typically include paresthesias, which are best described as: burning, itching, throbbing, aching, prickling, "pins and needles," and constricting-like sensations.[43, 274] Tactile allodynias may also develop, causing typically non-noxious stimuli to be perceived as painful (*e.g.* brush of bed sheets or clothing draped over the skin).[43] These painful symptoms can lead to insomnia and physical injury as a patient attempts to avoid further aggravation of these "hot spots."

Physical injury can also result with the development of sensorimotor deficits, which comprise the negative symptoms of DSPN. [270] Although easily dismissible at first, these

deficits become increasingly problematic.[270, 295] Sensory deficits are commonly described as a "stocking and glove"-like perception of sensory loss and can lead to imbalance and physical injury.[270, 278] This increases the likelihood of developing non-healing foot ulcerations and gangrenous infections.[278] Although muscle weakness is much less common early on, atrophy can eventually occur in the small muscles of the feet and hands.[270, 272] Clinical signs of motor impairment often include diminished or absent ankle reflexes and occasionally (rare) loss of patellar reflexes.[270]

2.1.2.4.1.3. Clinical Diagnostic Criteria for DSPN

DSPN is divided into stages of progression based on QST and nerve conduction velocity (NCV) results.[274-275] Patients with **possible DSPN** either have positive symptoms, negative symptoms, *or* aberrant motor reflexes.[274-275] In **probable DSPN**, patients exhibit positive *or* negative symptoms *and* aberrant motor reflexes.[274-275] In **confirmed DSPN**, patients that meet the criteria for probable DSPN *also have* NCV deficits.[274-275] Finally, in **subclinical DSPN**, *only* NCV deficits are present.[274-275]

2.1.2.4.1.4. Alternative Small Fiber Neuropathy Assessments for DSPN

Small fiber neuropathy assessments can be used in the absence of NCV deficits in probable DSPN patients where DSPN is highly suspected.[275] In this regard, morphological assessments, such as skin punch biopsies and corneal confocal microscopy, are emerging as minimally invasive techniques to assess small sensory nerve fiber loss in patients.[275, 296] In skin biopsies, immunohistological analyses of intraepidermal nerve fiber (iENF) densities are used to assess changes in cutaneous innervation (*i.e.* C-fibers; discussed shortly).[275, 296] Recent studies show that iENF densities are significantly reduced in diabetic patients that still have normal NCVs.[297-298] These reductions are further exacerbated in patients

displaying clinical symptoms or signs of DSPN.[297] Intriguingly, assessments of small sensory corneal nerve fibers via corneal confocal microscopy strongly correlate with iENF loss and DSPN severity.[298] Hence, corneal confocal microscopy is gaining ground as a surrogate, non-invasive biomarker for DSPN.[298]

As a therapeutic side note, compounds that generally improve NCV and sensory deficits in rodents historically fail to exhibit clinical efficacy.[296, 299] Alternatively, morphological assessments, such as iENF density analysis or corneal confocal microscopy, may be more adept to predicting clinical efficacy since they can alleviate interspecies mechanistic differences.[296] Hence, iENF density analysis has been used as a morphological assessment to monitor both disease progression and drug efficacy in this research.

2.1.2.4.2. Somatosensory Nerve Fibers and Pain in DSPN

To better understand the development of somatosensory deficits in DSPN as well as the behavioral measurements used in this research, somatosensory nerve fibers are reviewed below. Since our research examines the effects of drug intervention upon thermal and mechanical hypoalgesia in STZ-diabetic mice, a special emphasis has been placed upon nociception (encoding/processing of potentially damaging, noxious stimuli) and pain.

2.1.2.4.2.1. Somatosensory Nerve Fibers

Somatosensory information is relayed to the central nervous system (CNS) by dorsal root ganglia (DRG).[300] DRG are pseudounipolar sensory neurons whose soma (cell bodies) lie clustered (in ganglia) in the intervertebral foramena of the spinal column.[300] These neurons have single axons (nerve fibers) that extend from peripheral tissues, such as the epidermis and dermis, to the dorsal horn lamina of the spinal cord.[300-301] At the distal termini, collateral branching increases sensitivity and broadens the neuron's receptive field.

Somatosensory nerve fibers consist of Aα-, Aβ-, Aδ-, and C-fibers.[302] Each type of fiber differs in its degree of myelination, conduction velocity, and type(s) of information it transmits.[300, 302-303] The thickness of the protective, dielectric myelin sheathe depends on neurotrophic signaling between myelinating Schwann cells (SCs) and the axons.[304-307] As myelin thickness increases, NCV also increases.[300, 302, 304-307] Aα-fibers are the most thickly myelinated fibers (12-20 μm in diameter) and the fastest conductors at 72-120 m/s.[300, 302] Aβ-fibers are more thinly myelinated (6-12 μm in diameter) and slower (6-72 m/s).[300, 302] Aα- and Aβ-fibers mainly transmit touch and proprioceptive information.[300, 302] The thinly myelinated Aδ-fibers (1-6 μm in diameter) transmit thermal and nociceptive information at 4-36 m/s.[300, 302] C-fibers are entirely unmyelinated, with diameters between 0.2-1.5 μm.[300, 302] C-fibers also transmit thermal and nociceptive information, but at a slower rate (0.4-2.0 m/s).[300, 302] C-fibers alternatively receive neurotrophic support from non-myelinating SCs, which surround multiple C-fibers to form Remak bundles.[305]

2.1.2.4.2.2. Nociception and Pain

Pain is a complex interpretation (percept) of *sensory outputs* combined with *emotional experiences*.[300-301, 303, 308] Although emotion does certainly influence pain, it is the relay of nociceptive information that is mainly compromised in DSPN. As such, it is important to distinguish between normal responses to non-noxious and noxious stimuli.

Thermal receptors and nociceptors are found at the free nerve endings of Aδ-fibers and C-fibers.[301, 303] At normal skin temperature (34ºC), warm receptors on C-fibers and cool receptors on Aδ-fibers fire continuously at 2-5 spikes/s.[300, 302] These thermal receptors fire most vigorously at 45ºC (warm receptors) and 25ºC (cool receptors).[300, 302] As temperatures fluctuate around these optimal temperatures, the firing rates decrease, altering the frequency

of transmissions to the CNS.[300, 302] As temperatures exceed 45ºC or fall below 5ºC, thermal receptor firing diminishes and heat (Aδ-fibers) and cold nociceptors (C-fibers) activate.[300, 302] Acute thermal pain tolerance can be measured in animals using the hot plate and cold plate tests, which assess hindpaw withdrawal latencies after abrupt exposures to extreme temperature changes.[308] Polymodal nociceptors on C-fibers also respond to noxious thermal stimuli.[300, 302] However, while heat and cold nociceptors typically evoke sharp painful sensations, polymodal nociceptors result in a slow, dull burning sensation.[300, 302] The latter can be measured using the Hargreaves behavioral test, which applies gradual, intensifying amounts of radiating heat to determine withdrawal latencies.[309]

Mechanical nociceptors respond to intense pressure.[300-302, 308] While polymodal nociceptors on C-fibers detect noxious blunt stimuli (*e.g.* pressing and pinching), mechanical nociceptors on Aδ-fibers sense pricking stimuli.[302, 310] Pricking pain thresholds can be assessed in animals by applying von Frey monofilaments to the plantar surface of the hindpaw and measuring withdrawal latencies.[303, 308] Hence, the von Frey and Hargreaves behavioral tests allow for Aδ-fiber and C-fiber nociceptive functions to be individually assessed. Both of these behavioral tests have been used in our research.

Thermal and nociceptive information is relayed to the primary somatosensory cortex by the anterolateral system (ALS).[300-302, 311] These sensory impressions are shunted through the secondary somatosensory cortex on to the somatosensory association cortex, where an overall perception of the stimuli is generated. In the case of pain, this oversimplification does not address the emotional contributions, the effects of ascending feeds to other regions of the brain, or the inhibitory effects of the descending periaqueductal gray (PAG) pathway. However, for the purposes of this research, it should be stressed that Aδ- and C-fiber

deterioration in DSPN compromises the initial sensing of noxious stimuli, which derails the perception of pain and results in hypoalgesia or hyperalgesia. The molecular mechanisms implicated in this deterioration are described below.

2.2. Neuropathogenesis in Diabetes Mellitus

DSPN is a multifactorial neurodegenerative disorder that arises from biochemical insults associated with glucotoxicity, altered neurotrophism, and ischemia.[44, 271, 275, 307] Although this discussion primarily focuses on the biochemical insults associated with DSPN, it should be noted that these mechanisms likely contribute to the development of all generalized symmetric polyneuropathies, especially DAN.

2.2.1. Glucotoxicity

As mentioned, dysfunctional insulin signaling disrupts normal glucose transport, thus resulting in adipose, muscle, and hepatic tissue malnourishment, systemic hyperglycemia, and excessive glucose influx into neurons. This abundance of glucose causes what is best described as "metabolic congestion" (**Figure 4**). In an attempt to metabolize and clear excess glucose, neurons employ alternative metabolic pathways that drain intracellular coenzyme and antioxidant resources. This forces neurons to reroute critical supplies in an attempt to support more crucial, life-sustaining functions. Unfortunately, chronic exposure to high glucose ultimately leads to a collapse in these critical functions and cell death. Glucotoxicity results from prolonged increases in metabolic flux through: glycolysis; Tricarboxylic Acid (TCA) Cycle; polyol pathway; hexosamine pathway; diacylglycerol-protein kinase C (DAG-PKC) pathway; non-enzymatic post-translational modifications (AGEs); and mitochondrial dysfunction. The neuropathological contributions for each of these mechanisms follow.

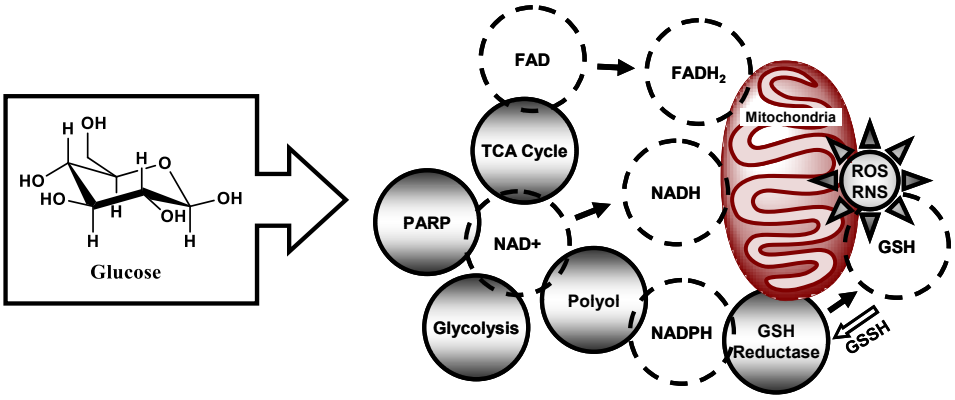

Figure 4. Conflicting metabolic demands in neurons during hyperglycemia. Overlapping regions indicate coenzyme (hashed) use by competing metabolic pathways, mitochondria, or glutathione reductase (solid) in glucose metabolism; reduced glutathione (GSH, hashed) replenishment is needed to effectively neutralize mitochondria (red)-derived reactive oxygen (ROS) and reactive nitrosative species (RNS).[43-46, 312-313]

2.2.1.1. Glycolysis and Tricarboxylic Acid Cycle

Diabetes-induced hyperglycemia can cause up to a fourfold increase in neuronal glucose levels.[44] The neuronal response to glucose accumulation is to up-regulate the primary and alternate metabolic pathways. In this regard, glycolysis and the TCA Cycle are the first line of defense against glucotoxicity. Several of these metabolic steps use the oxidizing coenzymes NAD^+ (nicotinamide adenine dinucleotide, oxidized) and FAD (flavin adenine dinucleotide, oxidized), which reduce to NADH and $FADH_2$, respectively.[312] Each glucose molecule yields roughly ten NADH and two $FADH_2$, which are then subjected to oxidative phosphorylation to collectively produce 26-28 molecules of ATP.[312] However, the metabolic capacity of hexokinase (rate-limiting step) is overwhelmed in diabetic nerves, intensifying metabolic demands upon the mitochondria and depleting NAD^+ and FAD levels.[44] Consequently, excess glucose must be shunted to alternative metabolic routes.

2.2.1.2. Polyol (Sorbitol) Pathway

The polyol (sorbitol) pathway provides the bulk of reinforcing metabolic support (**Figure 5**). When hexokinase is overwhelmed, glucose levels quickly approach the K_M of

aldose reductase (AR; K_d: AR >> hexokinase).[44] AR reduces glucose to sorbitol using NADPH (nicotinamide adenine dinucleotide phosphate, reduced).[43-44, 46] This coenzyme is also used by glutathione reductase to convert oxidized glutathione (GSSH) back to reduced glutathione (GSH), for use as an antioxidant. Consequently, cellular antioxidant defenses are weakened.[43-45]

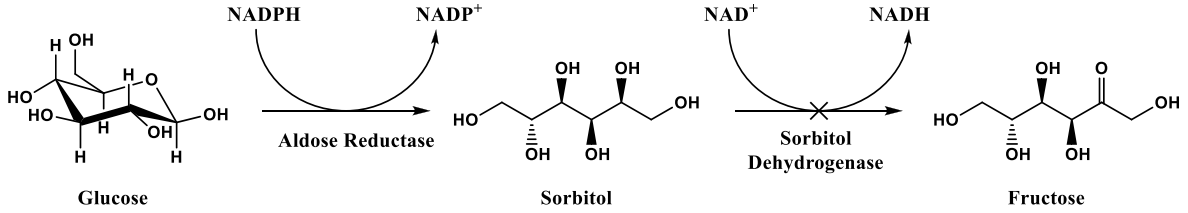

Figure 5. Polyol (sorbitol) pathway. (Adapted from Tomlinson and Gardiner)[44]

Sorbitol is normally oxidized to fructose by sorbitol dehydrogenase and NAD^+.[46] However, NAD^+ depletion in glycolysis and in the TCA Cycle hinder this conversion.[46] This causes the build-up of impermeable, hydrophilic sorbitol, which results in hypertonicity and the efflux of numerous osmolytes, including myo-inositol (MI).[43-45, 314] MI also serves as a metabolic precursor to phosphatidylinositol (PI), whose various phosphorylation states serve as important secondary messengers in multiple signaling cascades.[314] In the sciatic nerves of experimental Type 1 diabetic steptozotocin (STZ)-induced rats, significant reductions in MI concentrations, Na^+/K^+-ATPase activity, and MNCV have been noted after only 2-4 weeks of diabetes.[315-316] MI supplementation can prevent the reductions in Na^+/K^+-ATPase activity and MNCV.[315] Both AR genetic deletions and pretreatments with Fidarestat (aldose reductase inhibitor) prevent GSH depletion and reductions in MNCV and SNCV in STZ-diabetic mice.[317] These conditions also suppress superoxide levels and related DNA damage in these diabetic mice.[317] This is encouraging for the pharmacologic development of ARIs as antipathogenics for DSPN treatment.

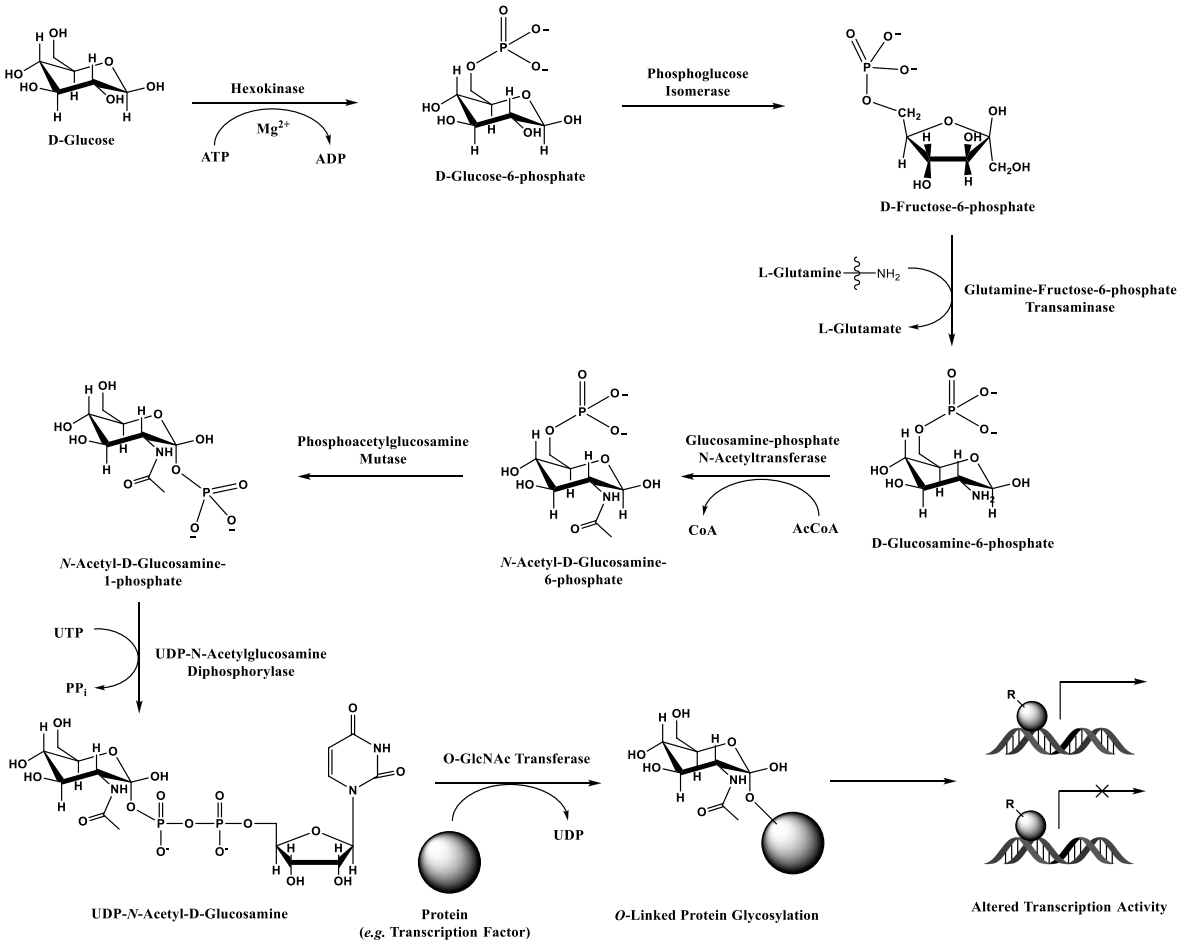

Figure 6. *O*-GlcNAcylation and the hexosamine pathway.[44-45, 318-319]

2.2.1.3. Hexosamine Pathway

Augmented metabolic support is also provided through the hexosamine pathway, which consumes the fructose 6-phosphate intermediate from glycolysis (**Figure 6**).[44-45, 318-319] Shunting of fructose 6-phosphate via the hexosamine pathway leads to an over-production of UDP-*O*-GlcNAc (uridine diphosphate-*N*-acetyl-D-glucosamine).[44-45, 318-319] *O*-GlcNAc transferase (OGT) uses this metabolite to post-translationally modify (*O*-GlcNAcylate) key regulatory sites (serine/threonine residues) of transcription factors and signaling proteins.[44-45, 318-319] These modifications usually serve as an adaptive response to various stressors, such as heat, hypoxia, and heavy metals.[319-322] In this regard, extensive "cross-talk" between

O-GlcNAcylation and phosphorylation tightly regulate gene transcription, translation, and protein trafficking and degradation.[319-322] *O*-GlcNAcylation and phosphorylation can either work together to fine-tune protein activity or antagonize each other.[319-322]

Disrupting the fine balance between *O*-GlcNAcylation and phosphorylation can have devastating effects. In fact, alterations to the hexosamine pathway, protein kinase activity, and regulatory site mutations have been implicated in the pathological progression of numerous diseases, including cancer and diabetes.[323-327]

In cancer, the transcription factor c-Myc is often up-regulated and phosphorylated to enhance pro-survival protein expression.[325-327] *O*-GlcNAcylation of c-Myc's Thr(58) prevents phosphorylation and activation at this same site.[327] In contrast, when the tumor suppressor p53 (mutated in about half of human cancers) is *O*-GlcNAcylated at Ser(149), phosphorylation at Ser(155) is blocked.[325, 328] This prevents p53 proteolytic degradation and promotes pro-apoptotic gene transcription.[328] Thus, *O*-GlcNAcylation and phosphorylation can either promote or inhibit gene transcription.

In diabetes, cardiovascular complications are partially linked to the transcription factor Sp1.[45, 271, 329] *O*-GlcNAcylation activates Sp1, which permits the expression of several glucose-induced housekeeping genes, such as plasminogen activator inhibitor-1 (PAI-1) and transforming growth factor-β1 (TGF-β1).[45, 271, 329] PAI-1 inhibits tissue plasminogen activator (tPA) and urokinase, thereby impeding fibrinolysis and promoting microvascular thrombosis (blood clotting) and nerve ischemia.[45] Increases in PAI-1 activity have been noted in sural nerve biopsies from T2DM patients, where tPA levels in epineurial and endoneurial microvessels were reduced nearly sixfold.[330] *In vitro* studies in rat DRG have shown that TGF-β1 treatment suppresses neurite outgrowth and that TGF-β1 levels are

elevated in the DRG and sciatic nerves of 12-week STZ-diabetic rats.[331] Hence, Sp1 *O*-GlcNAcylation in diabetes likely enhances nerve ischemia and disrupts neuritogenic efforts.

O-GlcNAcylation can also contribute to the development of insulin resistance. High levels of *O*-GlcNAc in adipocyte-like 3T3-L1 cells can increase *O*-GlcNAcylation of IRS-1 and IRS-2.[324] This prevents IRS-1 and IRS-2 phosphorylation and associated PI3K/Akt-dependent GLUT-4 vesicle translocation (discussed in-depth in **Altered Insulin-Associated Neurotrophism in Diabetes Mellitus**).[324] While the functional implications are currently unclear, several insulin signaling components can be *O*-GlcNAcylated, including: β chains of the insulin receptor, Akt-1, Akt-2, GSK-3β (glycogen synthase kinase-3β), PDK1 (phosphoinositide-dependent kinase-1), PI3K, and endothelial GLUT-1.[324] Furthermore, insulin signaling normally causes PIP3 (phosphatidylinositol 3,4,5-triphosphate) to recruit OGT from the nucleus to the plasma membrane.[332] These data suggest that OGT has a critical role in normal insulin signaling and DSPN pathogenesis.

To summarize, *O*-GlcNAcylation can alter gene transcription and protein expression, trafficking, and degradation, which can favor or hinder cell viability. This is especially true for diabetic neurons that endure massive amounts of metabolic flux through the hexosamine pathway. However, non-enzymatic protein glycosylation (glycation) also contributes.

2.2.1.4. Advanced Glycation End-Products

Glycation is a naturally occurring process that simply becomes amplified with diabetes-induced hyperglycemia. Advanced glycation end-products (AGEs) significantly affect the pathological progression of DSPN.[46] These AGEs result from the degradation of early glycation adducts and the formation of adducts with glucose-derived α-oxoaldehydes.[333-334]

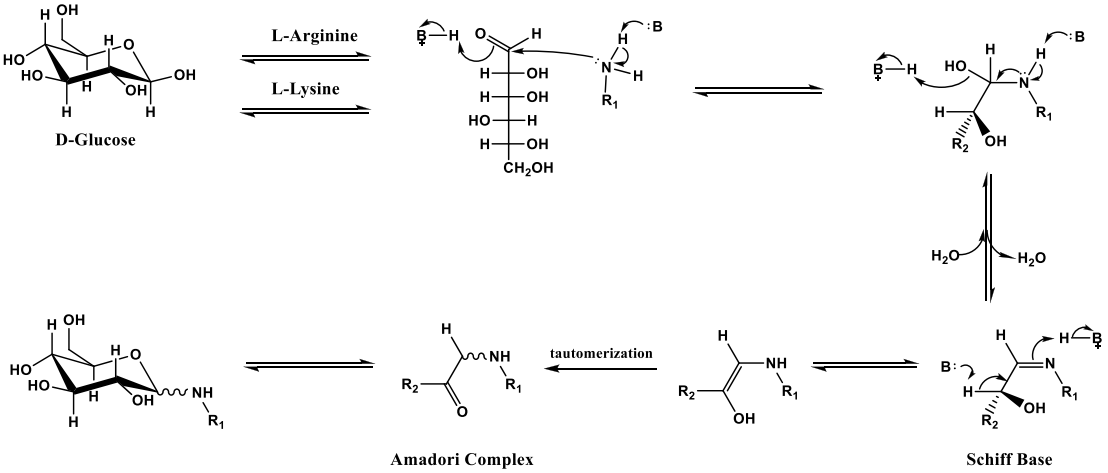

Figure 7. Formation of early glycation adducts. R_1 = remainder of lysine.[335-337]

2.2.1.4.1. Formation of Early Glycation Adducts

Early glycation adducts form via the Amadori rearrangement.[39, 43-46, 335-336] During this process, the anomeric carbon of glucose is attacked by the ε-amino group of lysine or the primary amine of arginine's δ-guanidino group (**Figure 7**). This results in the protonation of glucose's anomeric oxygen and the deprotonation of the attacking amine.[335-336] Nitrogen lone pair electrons then establish a Schiff base with the anomeric carbon, causing further protonation of the anomeric oxygen, the release as H_2O, and deprotonation of the imine.[335-336] Deprotonation at the C-2 position then gives the 1,2-enolamine.[335-336] This tautomerizes to afford the "Amadori complex" (N-ε-fructosyl-lysine or N'-fructosyl-arginine), which can cyclize to form pyranose or furanose ring structures for added stability.[335-337] The most well-known of these complexes is glycated hemoglobin. Since HbA_{1C} remains detectible for up to 120 days (lifespan of most erythrocytes), it makes a great biomarker for physicians to assess long-term changes in plasma glucose levels and to diagnose diabetes.[39, 337-338]

2.2.1.4.2. Formation of AGEs

Amadori complexes are readily oxidized by iron-containing enzymes, phosphates, nitrates, reactive oxygen species (ROS), and reactive nitrosative species (RNS) (discussed

in-depth in **Mitochondrial Dysfunction and Oxidative and Nitrosative Stress**).[333-334, 339] This generates the "glycoxidation products" N-ε-(carboxymethyl)lysine (CML) or 3-(N-ε-lysine)-lactic acid (**Figure 8**).[333-334, 339-341] These AGEs are produced with the pH-dependent oxidation of the 2,3-enediol intermediate of the Amadori complex.[333-334, 339-340]

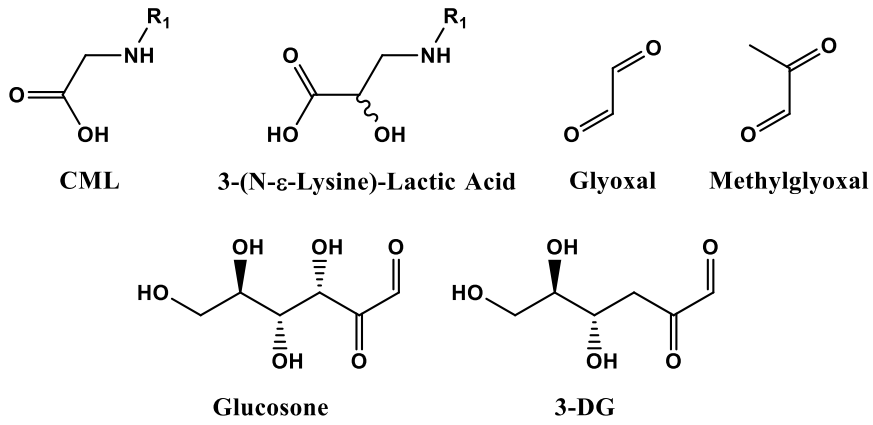

Figure 8. Structures of advanced glycation end-products. R_1 = remainder of lysine.[333-334, 339-341]

Glucose also degrades over time to generate several electrophilic α-oxoaldehydes. For example, C-2 deprotonation and C-3 dehydroxylation of acyclic glucose gives the 2,3-enol, which tautomerizes to yield 3-deoxyglucosone (**3-DG**).[334] Retroaldol reactions between the C-3 and C-4 positions of the 2,3-enol forms 2-hydroxy-propenal (and glyceraldehyde), which tautomerizes to **methylglyoxal**.[334] Deprotonation at C-2 can also give the 1,2-enediol, which undergoes monosaccharide autoxidation to form **glucosone** and H_2O_2.[334] Finally, retroaldol reactions between the C-2 and C-3 positions of acyclic glucose generates **glyoxal** and erythritol or glycolaldehyde and erythrose.[334] In the latter case, glycolaldehyde further oxidizes to produce glyoxal and H_2O_2.[334] All of these α-oxoaldehydes are highly susceptible to nucleophilic attack by proteins, lipids, and DNA and can permanently alter the encountered molecule.[342]

2.2.1.4.3. Impact of AGEs on Peripheral Nerves

Hyperglycemia accelerates AGE production, and disrupts homeostasis.[343] In neurons, AGEs can affect cytoskeletal proteins (*e.g.* tubulin, actin, and neurofilaments) as well as Na^+/K^+-ATPase, thus impairing axonal transport, neurite outgrowth, and NCV and promoting axonal atrophy.[344-345] AGEs involving extracellular matrix proteins (*e.g.* laminin, fibronectin, and collagen) can also impair neurite outgrowth/regeneration.[43, 271, 344-345] AGEs involving the myelin structural proteins P_0 and myelin basic protein (MBP) are also thought to contribute to demyelination.[344-345] Furthermore, AGE formation can alter vasoreactivity by quenching the vasodilator nitric oxide, thus enhancing nerve ischemia.[43, 344-345]

Plasma protein AGEs serve as extracellular ligands for AGE receptors (RAGEs) found on macrophages, smooth muscle cells, vascular endothelial cells, DRG, and SCs.[271, 344-345] In DRG, RAGE signaling induces ROS production, DNA degradation, caspase-3 activation, and apoptosis.[271, 347] RAGE signaling also triggers nuclear factor-κB (NF-κB) translocation to the nucleus.[271, 347] NF-κB enhances proinflammatory cytokine [interleukin-1β (IL-1β) and TNF-α] expression, which are linked to hypoalgesia in DSPN.[344, 346] This is further supported by diabetes studies in RAGE knockout mice, wherein hypoalgesia, NCV deficits, and axonal atrophy are blunted as compared to wild-type diabetic counterparts.[271, 346-347] Finally, NF-κB signaling causes hyperpermeability, atherosclerosis, stenosis, and thrombosis in the blood vessels of the epineurium and the dermal *vasa nervorum*. This compromises essential blood support to the peripheral nerves.[344] Hence, diabetes-induced hyperglycemia can significantly increase AGE concentrations, which can have grave consequences in diabetic nerves.

2.2.1.5. Diacylglycerol-Protein Kinase C Pathway

Dysfunctional insulin signaling causes starvation in adipose tissues, thereby inducing lipolysis and unregulated FFA entry into the blood.[348] The resulting hyperlipidemia compromises neuronal viability in two ways. First, it promotes atherosclerosis through the deposition of small lipoproteins, such as low-density lipoprotein (LDL)-cholesterol, forming hardened plaques in the vasculature that reduce blood flow.[349] Second, it promotes *de novo* 1,2-diacylglycerol (DAG) synthesis in non-adipose tissues, which inhibits IRS-1 and IRS-2 phosphorylation and subsequent insulin signaling.[248, 250-253] This exacerbates neuronal glucotoxicity. DAG also affects blood flow to the nerves via PKC.

DAG activates several PKC isoforms.[348] Once primed by PDK1, PKCs remain auto-inhibited until secondary messengers bind to the C1/C2 domains or the proper stimulus is encountered.[350] Conventional PKCs (α, β, and γ) have DAG-sensitive C1 domains and Ca^{2+}-sensitive C2 domains.[350] It is the PKC-β isoform that is primarily implicated in DSPN.[350] Overactivation of PKC-β reduces microvascular support to diabetic nerves by altering the expression of PAI-1, TGF-β, NF-κB, and vascular endothelial growth factor (VEGF), a pro-angiogenic.[46, 271, 351-352] PKC-β also suppresses flow-mediated nitric oxide release and vasodilation.[353] Hence, PKC-β has emerged as a target for pharmaceutical development (discussed in **PKC-β Inhibitors**)

In contrast, novel PKC isoforms (δ, ε, η, and θ) have inverted C1 and C2 domains that are DAG- and Ca^{2+}-insensitive.[350] Although the endogenous ligands for novel PKCs remain elusive, recent neuronal studies suggest that activating PKC-δ or redox-sensitive PKC-ε could promote neuritogenesis.[350-351, 354-357] Thus, targeting select PKC isoforms could have therapeutic potential.

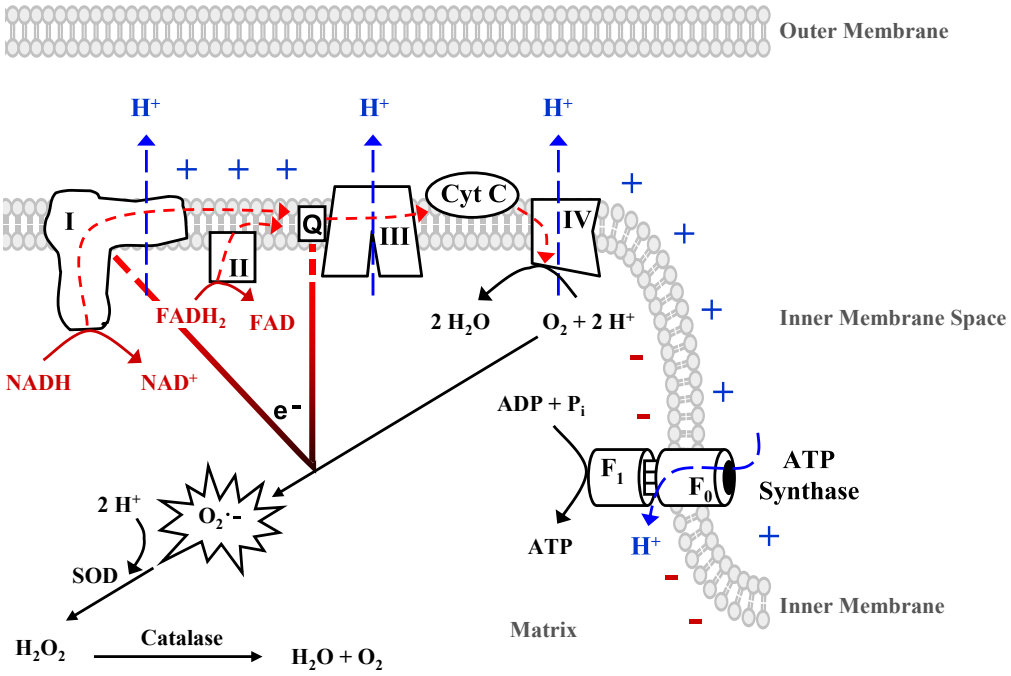

Figure 9. Mitochondrial respiration and generation of superoxide. Electron transfer (red) and proton transport (blue) are denoted by hashed arrows. Single electrons (e^-) lost from complex I and coenzyme Q/complex III converge (red/black hashed lines) and react with O_2 to generate superoxide ($O_2^{\cdot -}$). Blue and red charges along the membrane depict an established electrostatic gradient. (Adapted from Figueroa-Romero *et al.*)[45]

2.2.1.6. Mitochondrial Dysfunction and Oxidative and Nitrosative Stress

Increased metabolic demands impose significant stress upon the mitochondria, which jeopardizes neuronal function and survival. During mitochondrial respiration, a single pair of electrons are transferred from the reducing substrates NADH and $FADH_2$ to respiratory complexes I and II, respectively (**Figure 9**).[45] These electrons are transported through the respiratory complexes, establishing an electrochemical (proton) gradient across the inner mitochondrial membrane.[45] Upon reaching complex IV, the electrons are used to reduce O_2 to H_2O in the matrix.[45] As the protons are released back into the matrix, the proton motive force supplies the energy needed to drive ATP synthesis via ATP synthase.[45]

About 1-4% of O_2 fails to completely reduce to H_2O at complex IV, which generates the free radical ROS superoxide ($O_2^{\cdot -}$) (**Figure 9**).[44-46] Superoxide is thought to arise due to a

reverse single electron transfer (e^-) at complex I or the autoxidation of the ubisemiquinone radical intermediate ($QH^{\cdot}$) at complex III.[45] Superoxide dismutase (SOD) converts superoxide to H_2O_2, where it is reduced to H_2O and O_2 by catalase.[45] The breakdown of H_2O_2 is normally augmented by glutathione peroxidase.[44-46] However, this enzyme requires reduced glutathione (GSH) to convert H_2O_2 to H_2O.[44-45] As NADPH and GSH resources deplete and respiratory demands increase with chronic hyperglycemia, superoxide and hydrogen peroxide levels increase.

Superoxide is highly reactive and can generate a chain reaction that produces additional free radicals if it is not neutralized ("free radical theory" of aging).[44-45] This chain reaction has become known as the Haber-Weiss reaction.[358] It initiates with the reduction of Fe(III) to Fe(II) by superoxide, which restores O_2 (**Equation 1**).[358] H_2O_2 then reacts with Fe(II) to replenish Fe(III) and to give the ROS hydroxyl radical ($\cdot OH$) and hydroxide (OH^-) (**Equation 2**).[358] The net reaction is shown in **Equation 3**. What's more, nitrite (NO_2) can also react with superoxide to produce the highly unstable RNS peroxynitrite ($ONOO^-$). Peroxynitrite also forms when superoxide reacts with endogenous nitric oxide.[44-45]

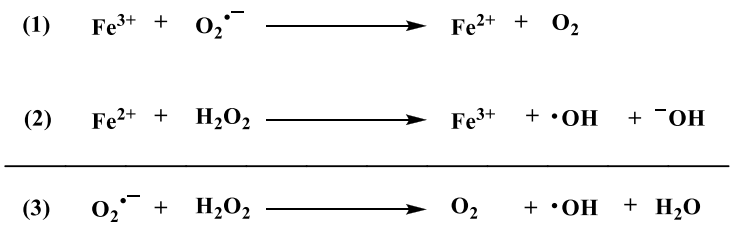

Figure 10. Haber-Weiss Reaction. (Adapted from Haber and Weiss)[358]

ROS and RNS can severely damage any encountered protein, membrane lipid, or DNA molecule in the mitochondria, compromising the functional integrity of the mitochondria and thereby promoting pro-apoptotic signaling (*i.e.* cytochrome C release).[45-46] Recent studies in excised STZ-diabetic and high-glucose-treated DRG and SCs have shown

significant alterations to the mitochondrial proteome, mitochondrial membrane potentials, respiratory chain activities, and bioenergetics.[359-363] Although ROS and RNS can not readily diffuse across mitochondrial membranes, permeability transition pores may likely permit free radicals to exit the outer mitochondrial membrane and enter the cytosol.[45] This can drastically impair other neuronal and SC functions. Common indicators of oxidative and nitrosative stress include: 4-hydroxynonenal, a lipid peroxidation product; nitrotyrosine, a peroxynitrite nitrosylation product; and carbonylation, which results from the oxidation of amino acid side-chain hydroxyl groups.[46, 364]

Interestingly, somatic nerve fibers become increasingly dependent upon mitochondrial sources of ATP as one travels distally down the nerve.[45] Hence, hyperglycemia-induced mitochondrial dysfunction, alongside aforementioned nerve ischemia, may partly explain the dying-back pattern typically observed in DSPN.[45-46]

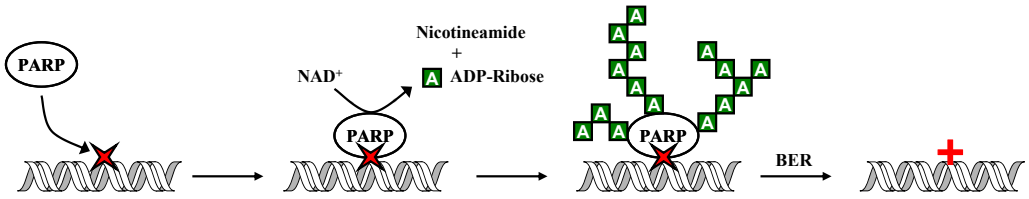

Figure 11. Poly(ADP-ribose) polymerase (PARP) and DNA repair. PARP flags nicked DNA for base excision repair with poly(ADP-ribose), designated as the chains of [A].[46, 313]

2.2.1.7. Poly(ADP-ribose) Polymerase Pathway

ROS and RNS can nick and severely damage DNA. Poly(ADP-ribose) polymerase (PARP) helps repair single-strand DNA breaks (**Figure 11**).[313, 365] PARP cannibalizes NAD^+ to form ADP-ribose and nicotineamide, and then polymerizes these ADP-ribose metabolites to form poly(ADP-ribose), or PAR.[46, 313] PAR is covalently attached to select nuclear proteins (*e.g.* histones) or displayed by PARP at the damage site.[313] PARylation is an SOS beacon that triggers the recruitment of DNA repair enzymes for base excision repair

(BER).[313] This process also depletes NAD^+ stores during a time of metabolic crisis, which ironically intensifies oxidative/nitrosative stress and further DNA damage.[45-46, 271, 313]

PARP hyperactivity has been implicated in NCV deficits, neurovascular dysfunction, thermal and mechanical hyper- and hypoalgesia, tactile allodynia, and demyelination in diabetic nerves.[45-46, 271, 365] PARylated proteins are present after 4 weeks of STZ-diabetes and cultured human SCs.[365] Recent evidence also suggests that PARP overactivation occurs before the development of diabetes-related oxidative/nitrosative stress, suggesting a more pivotal role in DSPN pathogenesis.[46] This is further supported by the fact that mice devoid of PARP-1 do not develop small-fiber neuropathy with STZ-diabetes.[46, 366-367] Hence, PARP may be a viable target for pharmacotherapy.

In summary, diabetes-induced hyperglycemia drives peripheral nerves to the point of metabolic exhaustion while continuing to subject them to worsening ischemic conditions. Chronic exposure to metabolic stress depletes coenzyme stores and antioxidant defenses. This increases the likelihood of mitochondrial dysfunction, ROS/RNS production, DNA damage, pro-apoptotic signaling, aberrant post-translational modifications, and detrimental alterations in molecular trafficking. However, this metabolic distress is accompanied diminished neurotrophic support, which has a much more direct impact upon peripheral nerve function and viability. The effects of this altered neurotrophism are reviewed below.

2.2.2. Altered Insulin-Associated Neurotrophism in Diabetes Mellitus

In addition to regulating postprandial glucose uptake in muscle, adipose, and hepatic tissues, insulin signaling is required during early development to sustain neuronal viability and function throughout the nervous system.[194-195, 269, 277, 368-371] These neurotrophic effects of insulin are normally augmented by insulin-like growth factor-I (IGF-I).[368-371] However,

IGF-I signaling also diminishes in diabetes.[372-378] Dysfunctional insulin and IGF-I signaling are also linked to the pathological progression of central neurodegenerative disorders, such as Alzheimer's, Parkinson's, and Huntington's diseases.[269] While insulin and IGF-I do have critical roles in the CNS, only peripheral neurotrophic effects will be discussed below. To better understand the impact of altered neurotrophism in DSPN, ligand bioavailability, receptor localization, and ligand-induced molecular signaling are reviewed herein.

2.2.2.1. Insulin and Insulin-Like Growth Factor (IGF) Bioavailability

As previously discussed, peripheral insulin supply depends exclusively upon pancreatic β cells, which are compromised in T1DM and T2DM. In adults, IGF-I is expressed in the DRG, the SCs, the sympathetic ganglia, the ventral horn of the spinal cord, and the targeted tissues.[269, 368] Another IGF isoform, IGF-II, is also secreted by SCs and skeletal muscle cells to reinforce neurotrophic support.[269, 368] These IGFs support nerve viability, neuronal migration, and neuritogenesis, which may promote nerve regeneration in DSPN.[269, 368]

Table 1. Insulin, IGF-I, and IGF-II IC_{50} values. IC_{50} values in nM concentrations. (From Urban *et al.*; Adapted from Belfiore *et al.* and Benyoucef *et al.*)[206, 269, 379]

Isoform	***Ligand (IC_{50}, nM)***
IR-A[†]	Insulin (0.2) < IGF-II (2.2) < IGF-I (9.0)
IR-B	Insulin (0.5) < IGF-II (10.0) < IGF-I (90.0)
IGF-IR	IGF-I (0.8) < IGF-II (4.4) < Insulin (>100)

2.2.2.2. Insulin and IGF-I Receptor Structure and Localization

Insulin receptors (IRs) and IGF-I receptors (IGF-IRs) are tetrameric proteins that consist of two extracellular ligand-binding domains (α-subunits) and two receptor tyrosine kinase (RTK) domains (β-subunits).[206, 269] While insulin, IGF-I, and IGF-II can all bind to IGF-IR

[†] Receptor lacks exon 11, which enhances ligand binding affinity

and to both IR isoforms (IR-A and IR-B), differences in receptor compositions substantially alter these ligands' relative binding affinities (**Table 1**).[206, 269, 379-380]

In adipose, muscle, and hepatic tissues, the metabolic effects of insulin are enhanced via selective expression of the IR-B isoform over the IR-A.[206, 269] It is thought that alterations to these relative IR-B:IR-A expression ratios promotes insulin resistance.[206] Conversely, IR-A is believed to be the dominant isoform in neurons, where it exhibits a much stronger binding affinity for all three ligands compared to IR-B.[206, 379-380] In peripheral nerves, IRs primarily localize to the DRG and the sympathetic ganglia.[368, 381] IGF-IRs are mainly expressed in small, nociceptive DRG (Aδ- or C-fiber), motor neurons, sympathetic ganglia, and SCs.[368, 381] Most of these regions are implicated in DSPN and DAN, suggesting an etiologic link between DPN and dysfunctional insulin and IGF-I signaling.[206, 269]

2.2.2.3. Insulin and IGF-I Signaling

Upon ligand binding, receptor autophosphorylation activates intrinsic RTK domains, which phosphorylate and activate regulatory effector proteins, such as IRS-1, IRS-2, Shc [Src (Rous sarcoma) homology 2 domain-containing], and Grb2 (growth factor receptor-bound protein-2) (**Figure 12**).[206, 269] This activation is ligand-, receptor-, and tissue-dependent and essentially directs which signaling effects are induced.[206, 269, 368]

2.2.2.3.1. Metabolic Effects

The metabolic effects of insulin are mediated via induction of the PI3K/Akt pathway in IR-B-heavy tissues (**Figure 12**).[206, 269] IRS-1/IRS-2 phosphorylation triggers the recruitment and activation of PI3K, which converts PIP2 (phosphatidylinositol 4,5-bisphosphate) to PIP_3.[206] This permits PDK-mediated Thr(308)Akt phosphorylation, or pThr(308)Akt.[324] pThr(308)Akt enhances GLUT-4 vesicle transit velocity, docking, and incorporation into the

cell membrane to facilitate glucose uptake.[207-209, 324] As discussed, insulin resistance can develop through the deterioration of PI3K/Akt signaling.[206] Again, this can result from either genetic defects or biochemical inhibitions.[240, 248-254, 257-259, 324]

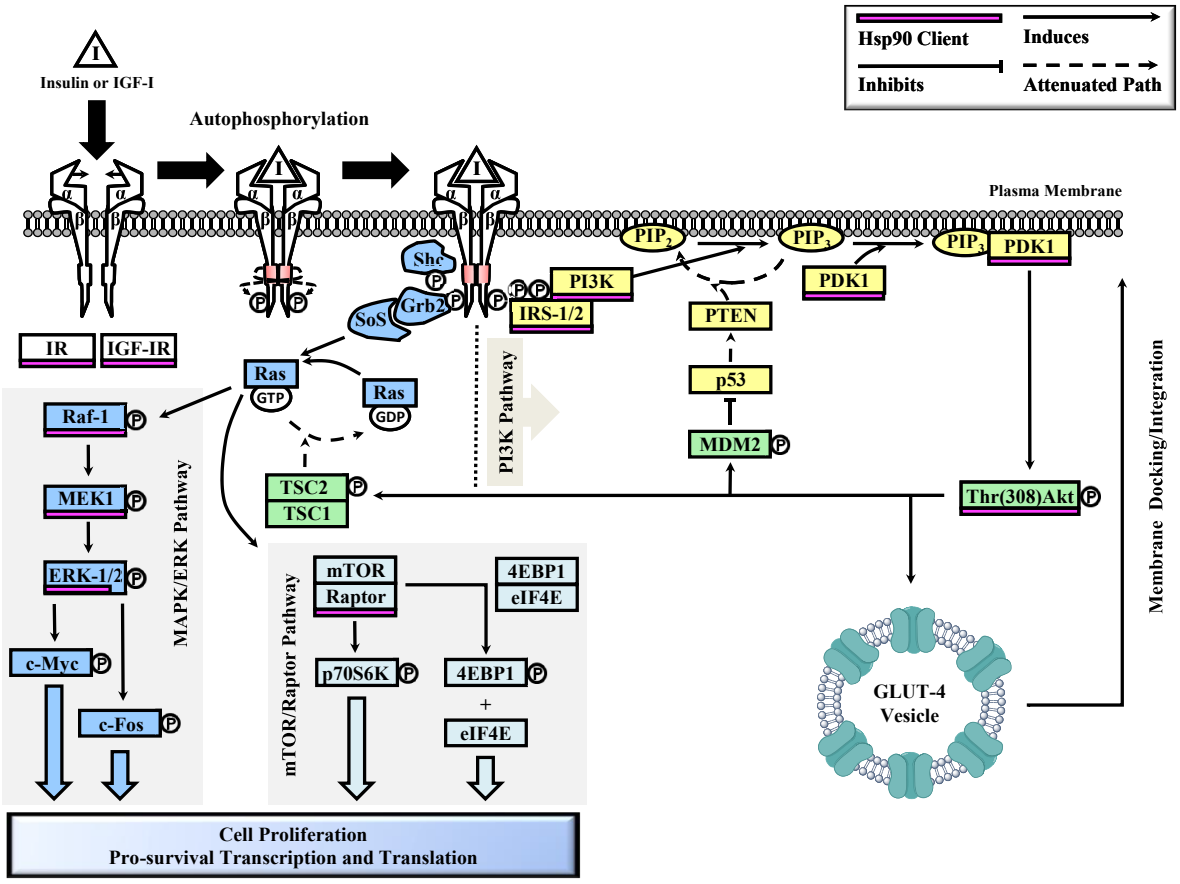

Figure 12. Metabolic effects and cytoprotection via insulin and IGF-I signaling. Ligand binding triggers receptor autophosphorylation and RTK (red) activation, allowing for IRS-1, IRS-2, Shc, or Grb2 phosphorylation. Mitogenic signaling pursues via Grb2-mediated activation of the GEF son of sevenless (SoS), enabling Ras activation. Ras initiates the MAPK/ERK pathway through Raf-1 phosphorylation and enhances mTOR/raptor signaling, collectively inducing cell growth, proliferation, protein expression, and viability. Induction of the PI3K/Akt pathway in muscle, adipose, and hepatic tissues enhances GLUT-4 vesicle integration into the cell membrane, enabling glucose uptake. Hsp90 client proteins (**SECTION 4** and **CHAPTER II**) are indicated with a pink bar and serve critical roles in regulating insulin and IGF-I signaling. (Adapted from Urban *et al.*)[269]

2.2.2.3.2. Cytoprotective Effects

Generalized cytoprotective effects are normally afforded by partial shunting through the MAPK/ERK (mitogen-activated protein kinase/extracellular-signal-regulated kinase) and

mTOR/raptor (mammalian target of rapamycin/regulatory-associated protein of mTOR) pathways (**Figure 12**).[206, 269] Receptor-mediated Ras ("rat sarcoma") activation induces the MAPK/ERK pathway, which enhances transcription factors that promote proliferation, cell growth, and survival (*e.g.* c-Fos and c-Myc).[206] Ras also induces mTOR/raptor signaling, which stimulates p70S6 kinase- and eIF4E (eukaryotic translation initiation factor-4E)-regulated cell growth, autophagy, metabolism, ribosome biogenesis, and translation.[206, 269]

The MAPK/ERK and mTOR/raptor signaling pathways also receive input from Akt.[206, 269] Akt phosphorylates TSC2 (tuberous sclerosis complex 2), which prevents the hydrolysis of Ras-bound GTP and signal termination (**Figure 12**).[206] Further, Akt-mediated MDM2 (murine double minute-2) phosphorylation allows p53 to be sequestered, ubiquitinated, and degraded.[382] This reduces the expression of TSC2, IGFBP-3 (IGF-binding protein-3), and PTEN (phosphatase and tensin homolog).[382] IGFBP-3 disrupts IGF-I:receptor interactions, whereas PTEN dephosphorylates PIP_3.[382] Hence, Akt enhances MAPK/ERK and mTOR/raptor signaling, which collectively promotes pro-survival transcription, translation, and cell proliferation in insulin/IGF-I-responsive cells.[206, 269] However, the bulk of insulin and IGF-I's neurotrophic support in stems from other PI3K signaling effects.

2.2.2.3.3. Neurotrophic Effects

While the specifics of insulin signaling in peripheral nerves are still under investigation, several mechanistic clues suggest that insulin and IGF-I signaling share common neurotrophic signaling pathways.[194, 206] These include: (1) ligand interchangeability between receptors; (2) similar phenotypic improvements upon ligand treatment; and (3) reports of identical activated downstream signaling molecules. These correlations will be emphasized below.

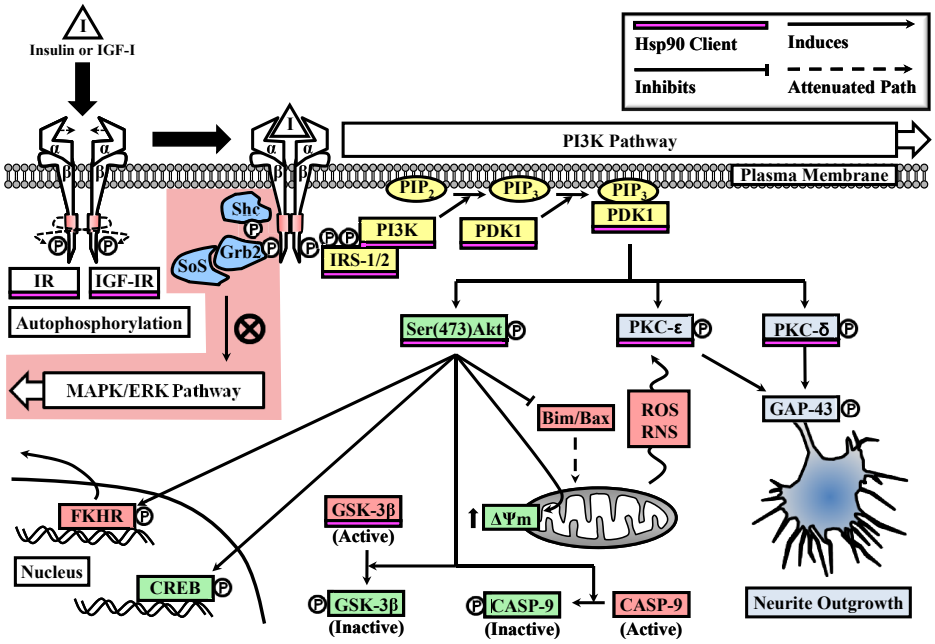

Figure 13. Insulin and IGF-I neurotrophic signaling in dorsal root ganglia. RTK (red)-induced IRS-1/IRS-2 phosphorylation selectively induces PI3K/pSer(473)Akt and PI3K/PKC-ε/PKC-δ signaling, which enhances neuronal viability and function as well as neuritogenesis, respectively. Hsp90 client proteins (**SECTION 4** and **CHAPTER II**) are indicated with a pink bar.[194, 269, 350, 354-356, 361, 383-397]

In DRG, IGF-I selectively activates PI3K signaling over the MAPK/ERK and the mTOR/Raptor pathways (**Figure 13**).[269, 383] Since IRS-2 mRNA levels in adult mouse lumbar DRG are ~ 27 times greater than IRS-1, it is conceivable that selective signaling via IRS-2 affords neurotrophic effects.[195] Further, DRG from Type 1 (STZ-induced) and Type 2 (*ob/ob*) diabetic mice demonstrate significant reductions in IRS-2 protein expression levels in conjunction with elevated IRS-2 inhibitory phosphorylations.[195] These phosphorylations are thought to destabilize IRS-2:receptor associations, resulting in IRS-2 degradation and signal deterioration.[195] However, these effects may likely be region-specific, given that peripheral nerve IRS-1 and IRS-2 mRNA levels in STZ-diabetic foot pads are unaffected.[194]

In diabetic DRG, IR mRNA levels increase, which suggests possible attempts to increase insulin sensitivity.[194] What's more, IGF-IR mRNA and protein expression levels decrease

in diabetic DRG, but recover with insulin treatments.[194, 375, 381, 391] This raises the question: does insulin have direct neurotrophic effects or does it merely act by increasing IGF-IR? In this regard, DRG explants treated with insulin alone (no IGF-I) display vast improvements in mitochondrial function and neurite outgrowth, indicative of direct neurotrophic effects.[361] However, this does not rule out the possibility that insulin could act via IGF-IR nor does it negate possible synergistic or additive neurotrophic effects in the added presence of IGF-I. In any case, these neurotrophic effects appear contingent on PI3K signaling.

2.2.2.3.3.1. Effects on Mitochondria Bioenergetics and Neuronal Viability

In DRG, IGF-I induced PI3K signaling triggers PDK1-mediated Akt phosphorylation at Ser(473) (**Figure 13)**. This enhances Akt's intrinsic kinase abilities, inducing the activation of pro-survival transcription factor CREB (cAMP-response element binding) as well as the nuclear exportation of forkhead and deactivation of GSK-3β (pro-apoptotic effectors).[361, 383-388] Under high glucose conditions, pSer(473)Akt prevents the detrimental trafficking of permeabilizing Bim/Bax to DRG mitochondria and phosphorylates/deactivates caspase-9; both of these conditions prevent caspase-3 activation and apoptosis.[383, 389-391] Similar effects have been seen in SCs, where IGF-I-induced pSer(473)Akt enhances SC motility and promotes myelination in SC-DRG co-cultures.[398-406] IGF-I- and insulin-induced pSer(473)Akt increases mitochondrial inner membrane potentials ($\Delta\Psi m$) in adult rat DRG to nearly twofold that of untreated control DRG.[361] Hence, insulin and IGF-I signaling can improve DRG and SC mitochondrial viability and function via pSer(473)Akt.[361]

2.2.2.3.3.2. Effects on Neuritogenesis

It is thought that somatosensory nerve fibers remain in a state of perpetual growth, and that these nerve fibers can respond to local manipulation.[194] Growth-associated protein-43

(GAP-43) is an IGF-I- and insulin-responsive "plasticity" protein that is locally expressed in neuronal growth cones and non-myelinating SCs during development and nerve fiber regeneration.[194, 392-396] In DRG, GAP-43 promotes F-actin accumulation, morphogenic activity, and prevents growth cone retraction.[397] GAP-43 reductions have been noted in the lumbar DRG and the foot pads of STZ-diabetic rats and in the nerve fibers of early Type 2 diabetic skin biopsies.[194, 407-412] IGF-I can improve distal somatosensory nerve fiber atrophy, iENF density, and attenuate SC vacuolization and peripheral nerve demyelination.[369, 378]

GAP-43 is activated by PKC-δ/PKC-ε-mediated Ser(41) phosphorylation (**Figure 13)**. This process initiates after PKC is phosphorylated and primed by PDK1.[350, 354-356, 397] While neither PKC-δ nor PKC-ε expression levels change in DRG from STZ-diabetics rats, pThr(505)PKC-δ levels reduce by ~ 40%.[413-415] Further, PKC-δ over-expression can restore neurite outgrowth in diabetic DRG.[414] To the best of our knowledge, the effects of PKC-ε phosphorylation [pThr(566) or pSer(729)] in DSPN are unexplored.[355] However, data from PC12 cells suggests that PKC-ε is redox-sensitive and can induce neuritogenesis and CREB phosphorylation when confronted with oxidative stress.[355] Hence, targeting PKC-δ and PKC-ε may be excellent therapeutic strategies for DSPN.

Improvements in mitochondrial function and neuritogenesis likely contribute to insulin- and IGF-I-induced recoveries in MNCV, SNCV, thermal hypoalgesia, and mobility as well as the stabilization of mechanical hyperalgesia in STZ-diabetes.[371, 378, 416] However, these recoveries may also benefit from improvements in synaptic plasticity.

2.2.2.3.3.3. Effects on Synaptic Plasticity

Insulin deprivation can significantly affect nociceptive signaling. In painful neuropathy studies involving STZ-diabetic rats, nociceptive DRG over-express metabotropic glutamate

receptors (mGluR5) at presynaptic terminals.[417] This enhances glutamate (*N*-methyl-D-aspartic acid, or NMDA) release and amplifies nociceptive signaling to postsynaptic neurons in the spinal cord.[417] Postsynaptic NMDA receptor (NMDAR) phosphorylation also increases in the lumbar spinal cords of STZ-diabetic rats, which potentiates nociceptive signaling.[418] Reductions in $GABA_B$ (GABA class B) receptor expression also occur in the lumbar spinal cords of STZ-diabetic rats, suggesting that GABAergic inhibitory signaling needed to suppress nociceptive transmission is compromised.[419] Overall, these data suggest that insulin deprivation alters synaptic plasticity and deregulates nociceptive signaling.

In summary, dysfunctional insulin and IGF-I signaling causes numerous hyperglycemic and neurotrophic insults, which compromise the functional integrity and survival of the peripheral nerves and the relay of nociceptive information. Thus, DSPN is a multifaceted neurodegenerative disorder that demands a multifaceted therapeutic approach.

SECTION 3. MODERN PHARMACOTHERAPEUTIC APPROACHES FOR DSPN

The Diabetes Control and Complications Trial (DCCT, 1983-1993) demonstrated that while controlled insulin therapy does significantly decelerate the rate of progression of diabetes, DSPN and other complications still develop.[23-25] Modern pharmacotherapeutic approaches for DSPN are limited in that they mainly target single pathogenic mechanisms associated with hyperglycemia or provide monosymptomatic relief for positive symptoms.[26] Current drug treatment options for managing diabetes and DSPN are reviewed herein.

3.1. Targeting Hyperglycemia

3.1.1. Insulin

By 1920, the best therapeutic options for diabetes mellitus were purgation and extreme dieting, which were techniques utilized by Aretaeus ~ 3,500 years ago.[264-265] Consequently,

Type 1 diabetics, like "J.L.," suffered from extreme malnutrition and rapidly progressive diabetic complications (**Figure 14A**).[265, 420] Sadly, a T1DM diagnosis at that time was essentially a death sentence, with most patients dying within a year.[265, 420] Luckily, that changed with the discovery and administration of extracted pancreatic insulin by Banting, McCleod, Best, and Collip in 1922.[55] Exogenous insulin administration induced profound physiological improvements in Type 1 diabetics, which appreciably enhanced patient survivability (**Figure 14B)**.[55, 265, 420] This marked the first major pharmacotherapeutic breakthrough for diabetes and its associated complications.[55, 265, 420-421]

A.  **B.** 

Figure 14. "J.L." (A) Before (*December 15, 1922 – Age: 3 years; Weight: 15 lbs*) and (B) after insulin treatment (*February 15, 1923 – Age: 3 years; Weight 29 lbs*).[265]

Insulin therapy has its drawbacks. Acute hyperinsulinism ("insulin shock") causes neuroglycopenia, which deprives the brain of essential glucose.[422] This can cause fatigue, confusion, seizure, temporary loss of consciousness, or even coma or death.[422] Conversely, hypoinsulinism can lead to excessive fatty acid β-oxidation in the liver, which generates large amounts of β-hydroxybutyrate and "ketone bodies" (*i.e.* acetoacetate and acetone).[423] The low pKa's of β-hydroxybutyrate (~ 4.7) and acetoacetate (~ 3.6) result in near complete deprotonation in blood (pH ~ 7.4), thus increasing blood acidity.[423] This overwhelms the bicarbonate buffering system and causes diabetic ketoacidosis (DKA).[423] DKA can also result in severe brain damage, coma, or death.[423] Hence, both extremes of mismanaged

insulin therapy can have dire consequences. These issues are further convoluted by varying pharmacodynamic effects associated with different insulin preparations (rapid-, short-, intermediate-, and extended-acting), insulin mimetics (*e.g.* L-783,281), and adjunctive therapies for postprandial glucose management.[424]

3.1.2. Insulin Secretagogues

Insulin secretagogues are prescribed as an adjunct to insulin therapy.[27] These drugs enhance insulin secretion from β cells, making them most effective during the early stages of T2DM.[425] These mainly consist of first-generation (*e.g.* tolbutamide, chlorpropamide, tolazamide, and acetohexamide) and second-generation (*e.g.* glyburide, glipizide, gliclazide, and glimepiride) sulfonylureas.[27, 424-425] Both of these generations block β cell K_{ATP} channels, causing membrane depolarization, Ca^{2+} ion influx, and insulin secretion.[426] These drugs also inhibit pancreatic α cell K_{ATP} channels alongside secreted Zn^{2+} ions to prevent glucagon release.[150, 424-425] Alternatively, the third-generation sulfonylurea, glimepiride, mainly acts by enhancing GLUT-4 vesicle translocation in muscle, adipose, and liver tissues.[425] Although structurally dissimilar to sulfonylureas, repaglinide (meglitinide) and nateglinide also block pancreatic K_{ATP} channels.[424-425] However, these insulin secretagogues are generally more fast-acting than sulfonylureas.[424-425]

3.1.3. Biguanides

Metformin is the only Food and Drug Administration (FDA)-approved biguanide available for use in the United States due to lactic acidosis dangers associated with other biguinides.[424-425, 427] As opposed to altering pancreatic secretions, metformin enhances AMP-dependent protein kinase (AMPK) activity in the liver, thereby increasing fatty acid β-oxidation and decreasing gluconeogenesis.[424-425, 427] Metformin also reduces intestinal

glucose absorption and improves insulin signaling in muscle and fat.[424-425, 427] With that said, metformin's mechanism of action is still poorly understood.

3.1.4. Thiazolidinediones

Thiazolidinediones (*e.g.* rosiglitazone, pioglitazone, and troglitazone), which are commonly referred to as "insulin sensitizers" or "glitazones," are selective PPAR-γ agonists.[255, 424-425] PPAR-γ enhances the expression of genes linked to adipocyte differentiation and glucose/FFA metabolism, thus increasing viability and preventing the release of pro-inflammatory cytokines and FFAs.[169] PPAR-γ also enhances GLUT-4 expression in adipose and skeletal muscle tissues.[428] Hence, these drugs are mainly intended to improve insulin resistance in Type 2 diabetic patients.

3.1.5. α-Glucosidase Inhibitors

α-Glucosidase inhibitors, such as acarbose and miglitol, reduce intestinal glucose absorption by slowing the hydrolysis of starch, dextrin, and various disaccharides.[424-425] These sugar mimics essentially blunt the postprandial plasma glucose spikes that are characteristically experienced in all diabetics.[424-425]

3.1.6. Other Glucose-Regulating Agents

Postprandial plasma glucose levels can also be managed by enhancing GLP-1-mediated insulin secretion and by suppressing glucagon release. Both of these goals can be accomplished using GLP-1R agonists (*e.g.* exenatide, liraglutide, lixisenatide, albiglutide, langlenatide, and dulaglutide).[429] Similar effects can also be attained by slowing GLP-1 degradation with diaminopeptidase-4 (DPP-4) inhibitors (*e.g.* vildagliptin, sitagliptin, saxagliptin, linagliptin, and alogliptin).[429] Further, glucagon can also be suppressed with pramlintide, a non-aggregating, human recombinant amylin.[430] GLP-1Rs are also found on

DRG and SCs.[431] In STZ-diabetic rodents, exenatide treatment can strangely improve MNCV and iENF density without affecting plasma glucose levels (as intended).[431] What's more, STZ-diabetes intervention with the DPP-4 inhibitor PKF275-055 also improves MNCV, Na^+/K^+-ATPase activity, and nociceptive thresholds.[432] Hence, GLP-1 may have neuroprotective effects in peripheral nerves that are independent from glucose regulation.

To conclude, the inability to prevent DSPN via targeting hyperglycemia alone has led many researchers to pursue alternative pharmacotherapeutic approaches that directly improve nerve viability and function in diabetes. This includes targeting single, putative pathogenic mechanisms associated with hyperglycemia.

3.2. Targeting Hyperglycemia-Associated Pathogenic Mechanisms

3.2.1. Aldose Reductase Inhibitors

As mentioned, pretreatment with the ARI fidarestat prevents MNCV, SNCV, and GSH reductions in STZ-diabetic mice and suppresses superoxide accumulation.[317] As such, diverting metabolic flux away from the polyol pathway via ARIs has become an attractive therapeutic approach. ARIs mainly consist of: acetic acid compounds (*e.g.* epalrestat); spirohydantoins (*e.g.* sorbinil and fidarestat); and succinimides (*e.g.* ranirestat).[433] However, due to undesirable/unsafe side effects from most of the acetic acid compounds, only epalrestat is in use today (only in Japan).[433] Despite fidarestat's initial promising results, further study results halted this drug's marketing in Japan (indefinitely).[433] While ranirestat has recently completed Phase III clinical trials in the United States, the results have not been published.[434] Nonetheless, earlier clinical studies with ranirestat showed vast improvements in MNCV after 52 weeks of treatment in T1DM and T2DM patients. However, SNCV results in this study were questionable due to placebo effects.[434-435]

3.2.2. PKC-β Inhibitors

PKC-β inhibitors can offer neuroprotection by improving peripheral neurovascular support.[351, 414] Selective PKC-β inhibitors, such as the bisindolylmaleimide ruboxistaurin (LY333531) and JTT-010, have been shown to improve MNCV and SNCV deficits in STZ-diabetic rats.[351, 436-438] In DSPN patients (T1DM and T2DM), ruboxistaurin can improve neuropathic pain scores.[439] Even so, the current status for advancing ruboxistaurin and other PKC-β inhibitors is unclear at this point.

3.2.3. PARP Inhibitors

Genetic deletion studies suggest that PARP-1 significantly contributes to DSPN in STZ-diabetic mice.[46, 366-367] In this regard, PARP inhibitors, such as 3-aminobenzamide, 1,5-isoquinolinediol, PJ34, GPI-15427, and nicotinamide, have been shown to improve neurovascular support, NCV deficits, and metabolic activities in STZ-diabetic rats.[366-367] Furthermore, intervention with the PARP inhibitor GPI-15427 can improve thermal hypoalgesia, mechanical hyperalgesia, tactile allodynia, and iENF density in STZ-diabetic rats.[440] Although PARP inhibitors have entered clinical trials as cancer treatments, their use in treating DSPN is still in preclinical stages.[434]

3.2.4. Antioxidants

Since hyperglycemia compromises endogenous antioxidant defense mechanisms, antioxidants could be therapeutically beneficial. In this regard, oral administration of the antioxidant α-lipoic acid can reduce neuropathic pain scores by as much as 50%.[441] Further, α-Lipoic acid is already sold as a dietary supplement in the United States and is approved for DSPN treatment in Germany.[271] The antioxidant QR333 (containing quercetin, ascorbyl palmitate, and vitamin D) has recently completed Phase II clinical trials for DSPN

treatment.[434, 442] Studies have shown that topical application of QR333 to DSPN patients' feet can improve NCV deficits.[442] The antioxidant properties of taurine can also improve mechanical hyperalgesia.[440] Finally, the carotenoid lycopene (commercially available dietary supplement) can improve thermal hyperalgesia presumably through the inhibition of TNF-α and nitric oxide release in STZ-diabetic mice.[443] These data suggest that increasing resilience to hyperglycemia-induced oxidative/nitrosative stress can improve DSPN.

3.2.5. Hexosamine Pathway Inhibitors

While there are no current inhibitors for the hexosamine pathway, fructose-6-phosphate can be shunted away from glycolysis towards the pentose phosphate pathway via thiamine-dependent activation of transketolase.[271] Curiously, both thiamine and transketolase levels are reduced in diabetic patients.[271] In this regard, the combination therapy of thiamine plus pyridoxine can improve neuropathic pain scores in DSPN patients.[444] Benfotiamine, a lipid-soluble thiamine derivative that also improves DSPN-associated neuropathic pain, is currently awaiting Phase III clinical trials to assess its therapeutic influence upon iENF density in DSPN.[434, 445] It is thought that these neuroprotective effects arise by diverting glucose away from the hexosamine pathway and restoring normal *O*-GlcNAcylation.[271]

3.2.6. Antihypertensive Agents

Given the compromised state of neurovascular support in DSPN, various FDA-approved antihypertensive agents are being prescribed. Angiotensin-converting enzyme (ACE) inhibitors (*e.g.* enalapril) can slow the renal conversion of angiotensin I to angiotensin II, which can prevent angiotensin II-induced vasoconstriction.[424-425] Antihypertensive therapies can help ensure adequate blood flow to the peripheral nerves.

3.3. Targeting Growth Factors

Intervention with exogenous growth factors, such as nerve growth factor (NGF), brain-derived neurotrophic factor (BDNF), and neurotrophin-3 (NT-3), have had limited success in clinical trials despite promising preclinical results.[307, 446] NGF can significantly enhance neuritogenesis, collateral branching, and viability in STZ-diabetic rodent DRG.[446] However, despite its improvements to mechanical sensation in humans, NGF's use during Phase III clinical trials was terminated due to injection site hyperalgesia.[446] In contrast, IGF-I has never entered clinical trials for DSPN management, even though it *inhibits hyperalgesia* in rodents. Hence, boosting endogenous IGF-I signaling may be a viable therapeutic approach (discussed in-depth in **SECTION 4**).

3.4. Targeting DSPN Symptoms

Monosymptomatic treatments are a large part of modern DSPN pharmacotherapy. Since there are no FDA-approved drugs to treat DSPN's negative symptoms, this section will focus entirely upon drugs prescribed for pain management.

3.4.1. Non-Steroidal Antiinfammatory Drugs

Non-steroidal antiinfammatory drugs (NSAIDs) inhibit select cyclooxygenases, thereby slowing the production of pro-inflammatory prostaglandins and reducing inflammatory-related pain.[424-425] In this regard, several COX inhibitors are frequently used to manage pain, including: aspirin (COX-1 inhibitor); ibuprofen (non-selective COX-1 and COX-2 inhibitor); and acetaminophen (COX-2 inhibitor).

3.4.2. Opioids

Opioid analgesics alter the perception of pain. Activation of various opioid receptors in the descending inhibitory neurons of the periaqueductal gray (PAG) antagonizes nociceptive

transmissions relayed from the DRG to the dorsal horn lamina of the spinal cord.[300] This blunts the perception of pain. Several opioids (*e.g.* morphine, oxycodone, tapentadol, and tramadol) can effectively mitigate pain in DSPN.[271] However, these drugs are typically plagued by numerous side effects, including gastrointestinal irregularities, nausea, vertigo, and drug tolerance and dependence.[424-425] Hence, this type of therapy is usually a last resort.

3.4.3. Anticonvulsants

Anticonvulsants are sometimes used for pain management since they can reduce neuronal hyperactivity. In hyperalgesic DSPN cases, nociceptive signaling may include excessive glutamatergic signaling from nociceptive DRG. Anticonvulsants essentially blunt this signaling. Commonly prescribed anticonvulsants for pain management include gabapentin (Neurontin) and pregabalin (Lyrica).[447] These anticonvulsants block presynaptic VDCCs, thus preventing Ca^{2+} ion influx required for neurotransmitter secretion.[300, 424-425, 447] Other commonly prescribed anticonvulsants include the voltage-gated sodium channel blockers (*e.g.* oxcarbazepine, lamotrigine, lacosamide, valproate, and topiramate[†]).[300, 424-425, 447] These drugs temporarily prevent neuronal depolarization and the generation of action potentials, thus inhibiting the relay of nociceptive information.[300, 424-425]

3.4.4. Antidepressants

As mentioned, pain is a complex interpretation of sensory outputs combined with *emotional* experiences.[300-301, 303, 308] Nociceptive signaling feeds into the limbic system via the paleospinothalamic tract.[300] These limbic connections are implicated in pain's emotional components of pain.[300] These drugs are thought to provide analgesic effects by improving the patient's mood and by activating the descending inhibitory neurons of the PAG.[300, 424-425]

[†] Also activates postsynaptic ionotropic $GABA_A$ receptors, which enables Cl^- influx into the neurons, resulting in hyperpolarization and inhibition

Selective serotonin reuptake inhibitors (SSRIs) prevent the presynaptic reuptake of serotonin, which increases its synaptic cleft dwell time and promotes postsynaptic signaling.[300, 424-425] Similarly, serotonin-norepinephrine reuptake inhibitors (SNRIs) prevent the reuptake of serotonin and norepinephrine.[300, 424-425] In this manner, SSRIs and SNRIs enhance input to the limbic system, improving the patient's mood and reducing the perception of pain.[300, 424-425, 448] The PAG receives stimulatory serotoninergic and noradrenergic input from the raphe nuclei and the locus coeruleus, respectively. Again, this blunts nociceptive signaling. While SNRIs (*e.g.* duloxetine and venlafaxine) can reduce pain scores by as much as half, SSRIs (*e.g.* fluoxetine, paroxetine, and citalopram) are usually slightly less effective.[448] Of these antidepressents, duloxetine is the only drug that is specifically FDA-approved for treating pain management in DSPN.[271, 448]

3.4.5. Topical Analgesics

The topical analgesics lidocaine and capsaicin are also used for pain management in DSPN. Lidocaine is a voltage-gated sodium channel blocker.[271, 448] Capsaicin (extracted from chili peppers) depletes substance P, another neurotransmitter in nociceptive DRG.[271, 448] Both lidocaine and capsaicin patches are FDA-approved for neuropathic pain.[271, 448]

In conclusion, medicinal treatment options for DSPN are problematic in that they mainly target single, pathogenic mechanisms associated with hyperglycemia or simply help manage pain. There are no FDA-approved drugs available to manage DSPN's negative symptoms.[26, 296] Compounds that improve sensorimotor and NCV deficits in STZ-diabetic animals usually fail to exhibit clinical efficacy.[296, 299] Hence, morphological assessments may be more adept to predicting clinical efficacy since they can alleviate interspecies mechanistic differences.[296] For these reasons, DSPN could benefit from a more multifaceted therapeutic

approach that impacts psychophysical, electrophysiological, and morphological indices. Targeting heat shock proteins improves all three.

SECTION 4. TARGETING HEAT SHOCK PROTEINS (HSPS)

4.1. Prelude

Several heat shock proteins (Hsps) serve as molecular chaperones that assist in the folding of nascent polypeptides, or "client proteins," into their mature conformations.[269, 449-452] These chaperones also assist in the refolding of damaged proteins that arise under various cellular stressors, such as heat shock, nutrient deprivation, oxidative and nitrosative stress, and other various insults to the cell.[449-452] These Hsps also serve as intracellular triage units that tag irreparable proteins for proteolytic degradation, stabilize protein complexes, solubilize protein aggregates, and facilitate intracellular trafficking.[449-453]

The neuroprotective qualities of Hsps have led to new treatment paradigms for several neurodegenerative disorders.[269] Pharmacologic Hsp induction can help mitigate proteotoxic threats associated with: Alzheimer's (AD), Parkinson's (PD), and Huntington's diseases (HD); amyotrophic lateral sclerosis (ALS); multiple sclerosis (MS); and spinal & bulbar muscular atrophy (SBMA).[452] Although it is unlikely that the pathogenesis of DSPN is attributed to the accumulation of any *one* particular misfolded protein, diabetes-induced hyperglycemia does cause significant increases in ROS and RNS in diabetic nerves.[46, 359, 454-455] These reactive species can denature proteins and disrupt protein folding, refolding, and transport initiatives.[44-46, 271, 359-363, 454-458] In support of this, recent studies have shown the myelin structural protein PMP22 (peripheral myelin protein 22) is extensively carbonylated and aggregated in the sciatic nerves of Type 2 diabetic mice, suggesting a direct oxidative link to demyelination and NCV deficits in DSPN.[364] Intriguingly, in SC-DRG co-cultures

developed from PMP22 over-expressing mice, pharmacologic Hsp induction can improve PMP22 solubility and turnover in SCs.[459] Hence, targeting Hsp expression may be a viable option in alleviating potential proteotoxic threats in DSPN.

To better understand the therapeutic potential of augmented Hsp support in DSPN, the physiological roles of Hsps are reviewed herein with a special emphasis on pharmacologic induction of the heat shock response (HSR). This chapter will conclude with a brief review of our preliminary work (2010 Master's Thesis), which supports the proof-of-principle that C-terminal heat shock protein 90 (Hsp90) modulators can be an effective therapeutic approach for DSPN.[28] Objectives and hypotheses for the current work will also be covered.

4.2. Heat Shock Protein 90

Heat shock protein 90 (Hsp90) is a 90-kDa, homodimeric cytosolic protein that interacts with over 200 client proteins and roughly 50 co-chaperones.[269, 449-451, 460-461] While the mechanistic details surrounding client protein folding remain unsolved, the folding machinery involved in this process has been established.

4.2.1. Hsp90 and Protein Folding

Protein folding initiates with the co-chaperones Hsp70 and Hsp40, which recognize and bind select polypeptide substrates.[269, 461] These are recruited into a larger, more stabilized heteroprotein complex with Hsp90 and HOP (Hsp70/Hsp90-organizing protein).[461] This stabilized complex enables client protein transfer to the Hsp90 homodimer, thus permitting Hsp70, Hsp40, and (in some cases) HOP dissociation.[461] Additional co-chaperones and immunophilins aid ATP binding within the N-terminal nucleotide-binding domain of Hsp90, which promotes N-termini dimerization and "clamping" of the client protein.[461] Recruitment of the co-chaperone p23 further stabilizes the clamped protein complex and

modulates nucleotide hydrolysis by altering Hsp90's intrinsic ATPase activity.[461] AHA1 (ATPase homologue 1) then initiates ATP hydrolysis to provide the energy needed for conformational changes (*i.e.* folding) and release.[461]

N-terminal Hsp90 inhibitors block ATP-mediated dimerization and clamping of the client protein, thereby destabilizing the complex and resulting in premature release of the client protein.[269, 462] Failure to produce mature client proteins is progressively cytotoxic as protein turnover surpasses production rates.[461-462]

4.2.2. Hsp90 and the Heat Shock Response

Under normal conditions, Hsp90 binds to heat shock factor 1 (HSF1), and this complex prevents the induction of the pro-survival heat shock response (HSR) (**Figure 15**).[269, 463-464] Upon stress or heat shock, Hsp90 releases HSF1 and induces the HSR following its hyperphosphorylation, trimerization, and translocation into the nucleus.[463-464] The HSR is characterized, in part, by the increased expression of Hsp90, Hsp70, Hsp40, Hsp27, and other genes.[463-464] Small molecule Hsp90 inhibitors mimic cellular stress by disrupting the Hsp90:HSF1 complex.[465]

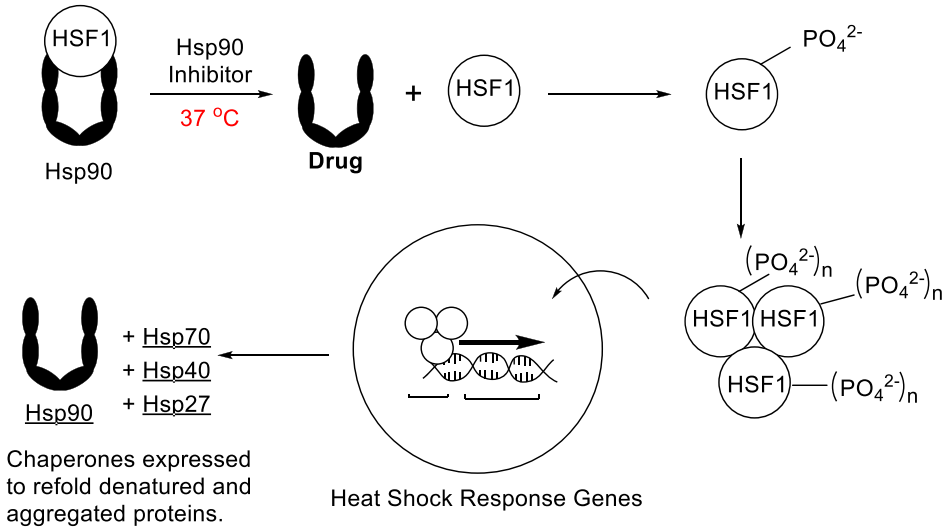

Figure 15. Hsp90 and HSR regulation. (Adapted from Donnelly and Blagg)[466]

Table 2. Hallmarks of cancer. (As defined by Hanahan and Weinberg)[467]

Hallmark	***Hsp90 Client Proteins***
Self-sufficient growth signals	Raf-1, Akt, ErbB2, MEK, Bcr-Abl
Insensitive to anti-growth signals	Plk, Wee1, Myt1, CDK4, CDK6
Evasion of apoptosis	RIP, Akt, mutant p53, c-Met, Apaf-1, Survivin
Limitless replicative potential	Telomerase (h-Tert)
Sustained angiogenesis	FAK, Akt, Hif-1α, VEGF-R, Flt-3
Tissue invasion and metastasis	c-Met, v-src

4.3. Targeting Hsp90

4.3.1. N-Terminal Hsp90 Inhibitors

Therapeutically, the development of N-terminal Hsp90 inhibitors may provide effective chemotherapeutic strategies given that numerous Hsp90 client proteins are also oncoproteins (*e.g.* mutant p53, v-Src, Bcr-Abl, Akt, and ErbB2).[269, 449-450, 468] As such, inhibiting Hsp90 has become an attractive target for cancer therapy since it simultaneously targets multiple molecular components within all six hallmarks of cancer (**Table 2**).[449, 467, 469] However, the chemotherapeutic potential for these inhibitors is often confounded by a narrow therapeutic window (**Figure 16**).[450] N-terminal Hsp90 inhibitors, such as the benzoquinone ansamycin antibiotic geldanamycin (**GDA**) and the structural analog 17-(allylamino)-17-demethoxy geldanamycin (**17-AAG**), fail to effectively dissociate client protein degradation from HSR induction (**Figure 16**).[450] Since HSR induction enhances pro-survival Hsp70 and Hsp90 expression, these Hsps antagonize the desired endpoint of cytotoxicity in cancer cells by increasing oncoprotein folding.[449-452, 469] These compounds have also exhibited hepatotoxic side effects in preclinical (GDA) and clinical (17-AAG) trials.[450, 460] Other N-terminal inhibitors, such as **celastrol**, **gedunin**, and **H_2-gamendazole** (**Figure 16**), also induce client protein degradation by disrupting Hsp90 interactions with the kinase co-chaperone Cdc37

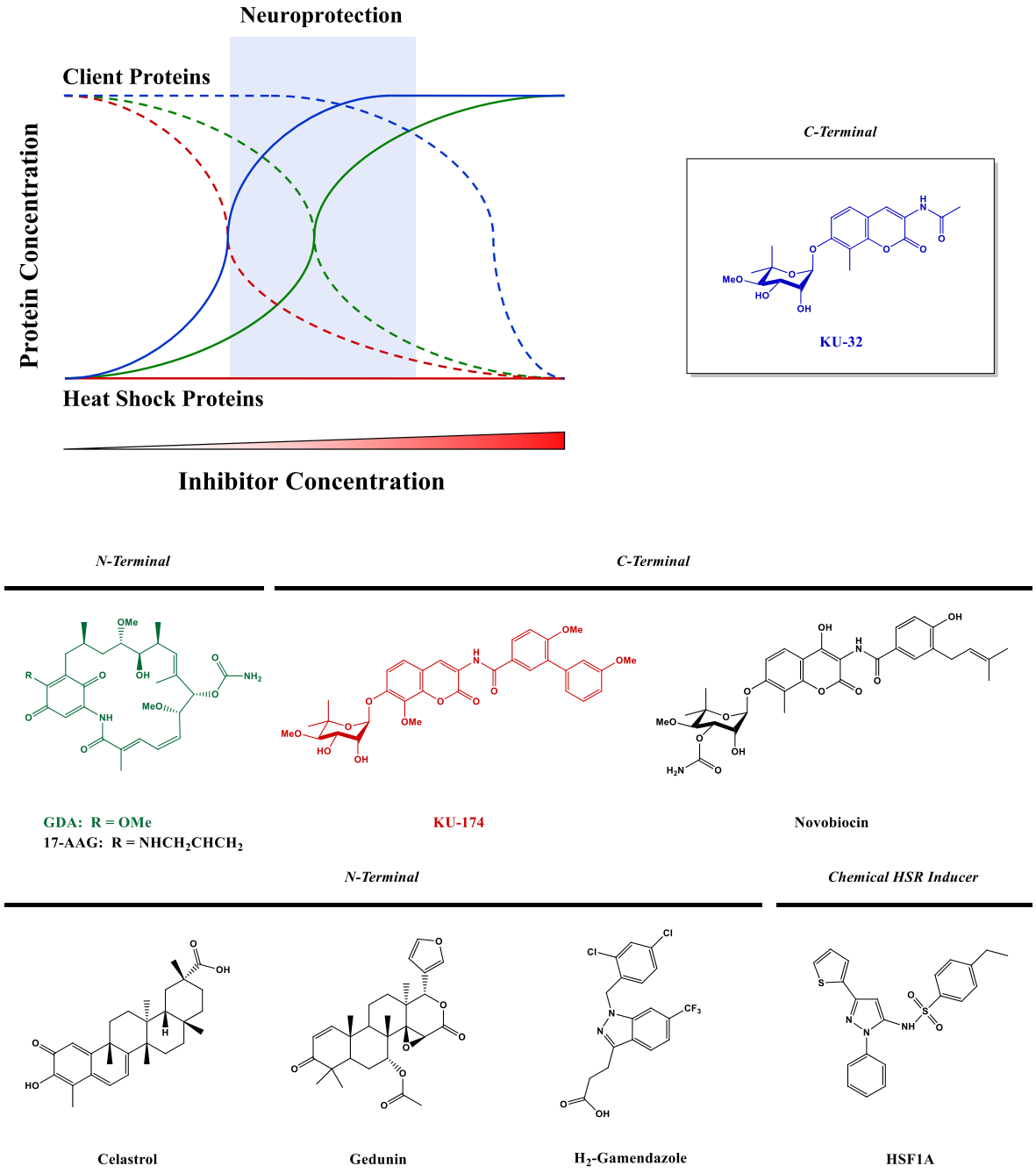

Figure 16. Differential Hsp90 inhibitors and HSR inducers. Structures of N-terminal Hsp90 inhibitors [GDA (green), 17-AAG, Celastrol, Gedunin, and H_2-Gamendazole]; C-terminal Hsp90 inhibitors [**KU-32** (inset; blue), KU-174 (red), and Novobiocin]; and chemical HSR inducer HSF1A. Upper left graph depicts the differential effects of GDA (green), KU-174 (red), and KU-32 (blue) upon client protein expression (hashed) and HSR induction (solid) as a function of inhibitor concentration; blue shading represents the neuroprotective therapeutic window associated with KU-32. KU-174 represents compounds in chemotherapeutic development. (Adapted from Urban *et al.*)[269, 470]

(cell division cycle 37 homolog, *S. cerevisiae*).[471] However, these inhibitors are also plagued by narrow therapeutic windows.[471]

In contrast to selecting for cytotoxicity, it is thought that HSR induction can promote the disaggregation of misfolded proteins linked to several neurodegenerative disorders.[269] In this regard, N-terminal Hsp90 inhibitors can decrease Aβ and tau aggregation in AD, prevent mutant huntingtin (mHtt) aggregation in HD, and improve motor function in SBMA.[472-476] However, as with cancer therapies, selecting for neuroprotection ultimately requires a therapeutic window that minimizes the risk of cytotoxicity. This can be accomplished with C-terminal Hsp90 inhibition.

4.3.2. C-Terminal Hsp90 Inhibitors

The C-terminus of Hsp90 contains an additional nucleotide-binding domain that also binds the natural product **novobiocin** (**Figure 16**), an ATP-binding site inhibitor of DNA gyrase.[269, 477] Although novobiocin is a poor inducer of client protein degradation and the HSR, higher affinity and more potent C-terminal Hsp90 inhibitors have been developed using its coumarin scaffold.[477-478] Through structure-activity relationship studies, HSR induction and associated cytoprotection have been divested from client protein degradation and associated cytotoxicity, expanding the dose range for neuroprotection. A representative example is **KU-32** (**Figure 16**), or *N*-(7-((2R,3R,4S,5R)-3,4-dihydroxy-5-methoxy-6,6-dimethyl-tetrahydro-2H-pyran-2-yloxy)-2-oxo-2-methyl-chromen-3-yl)acetamide, which protects against Aβ-induced death in cortical neurons, glucose-induced cell death in DRG, and agonist-induced demyelination of SC-DRG co-cultures.[470, 479-480] Moreover, we have shown that KU-32 can effectively reverse NCV deficits and sensory hypoalgesia in STZ-diabetes without any overt cytotoxicity (discussed in-depth in **Preliminary Work**).[28, 470]

4.4. Targeting the Heat Shock Response

It should be noted that chemical induction of the HSR can also be achieved without pharmacologic Hsp90 inhibition.[269] For example, **HSF1A** (**Figure 16**) induces the HSR presumably through interactions with the chaperonin TRiC [TCP1 (tailless complex polypeptide 1)-ring complex] independent of Hsp90 binding.[481] In neuroprogenitor cells, riluzole (used to treat ALS) can reduce HSF1 turnover while boosting the expression and activation of HSF1 and glutamate transporters.[482] The latter enhances presynaptic glutamate recovery, reducing the likelihood of excitotoxicity (implicated in painful DSPN, ALS, AD, PD, and HD).[482] However, the mechanisms by which HSF1A and riluzole specifically induce the HSR remain under investigation.[482] Finally, the flavonoid antioxidant quercetin can disrupt the DNA:HSF1 binding interface, thus preventing the transcription of Hsp mRNA (especially Hsp70).[483]

4.5. Heat Shock Factor 1 Roles in the Absence of Heat Shock

HSF1 regulates several genes in the absence of heat shock. For instance, siRNA-mediated HSF1 down-regulation in cervical carcinoma cells modulates the expression of 378 genes linked to cell cycle regulation and proliferation.[269, 484] This suggests that HSF1 maintains the expression of several proteins required for survival under stressful conditions (*i.e.* cancerous) in the privation of heat shock.[464, 484] Under non-cancerous conditions, HSF1 works with NFATC2 (nuclear factor of activated T-cells-2) to regulate αB-crystallin (small Hsp) expression and the scaffolding protein PDZK3 (PSD-95/Dlg-A/ZO-1 (PDZ) domain-containing-3).[485] This enables αB-crystallin to disaggregate mHtt in over-expressing R6/2 HD mice.[485] In the insulin-like signaling pathway of *C. elegans*, the FoxO (forkhead box "other") family transcription factor DAF-16 (abnormal dauer formation-16) works with

HSF1 to regulate genes that promote life expectancy.[463] Hence, HSF1 activation promotes cell survival under both normal and stressful conditions.

4.6. Targeting Hsp70, Hsp40, and Hsp27

Independent of Hsp90, Hsp70 and Hsp40 form heteroprotein complexes that offer additional neuroprotective attributes.[269] J-domain-containing proteins (J proteins), such as Hsp40 and CSPα (cysteine string protein α), can bind and enhance the intrinsic ATPase activities of inducible Hsp70 (Hsp72) and the constitutively expressed Hsp70 isoform Hsc70 (heat shock cognate 70).[486] Although binding affinities differ between these isoforms, a degree of interchangeability exists with various J proteins.[486] These specialized neuronal J protein:Hsp70 interactions can help facilitate synaptic vesicle protein repair, vesicle cycling (via calcium channel regulation and clathrin exchange), GEF activities with G-protein coupled receptors, toxic protein aggregate solubilization, and protein ubiquitination.[486]

Hsp70 and Hsc70 interact with BAG-1 (Bcl-2-associated athanogene) and CHIP (C-terminus of Hsc70/Hsp70-interacting protein) to flag irreparable proteins with ubiquitin for proteolytic degradation.[269, 458] Alternatively, BAG-2 enables Hsp70-mediated (ubiquitin-independent) delivery of irreparable proteins directly to 20S proteasomes for degradation.[487] Upon Hsp70/BAG-2 saturation, clearance duties are reinforced by the Hsp70/BAG-1/CHIP complex.[487] Such triage management has been implicated in tau clearance (AD), where effective Hsp70 chaperoning becomes exhausted.[487] These data suggest that targeting select Hsp70 isoforms via chemical modulators could feasibly enhance desired neuronal J protein interactions and discourage unfavorable associations (*e.g.* tau triage), thus improving neuronal function.[483, 488] Although selective Hsp70 inhibition provides promise as neuroprotective and chemotherapeutics, characterization of isoform-selective scaffolds that

modulate Hsp70 (*e.g.* dihydropyrimidines, polyamines, and ATP mimics) are still underway.[483, 488]

4.7. Preliminary Work

We have demonstrated that Hsp70 induction with the KU-32 can effectively reverse several clinical indices associated with both small and large fiber dysfunction in DSPN.[28, 470] After 12 weeks of STZ-diabetes in C57BL/6 mice, weekly intraperitoneal (IP) injections of 20 mg/kg KU-32 (~ 40 mM Captisol/saline vehicle) for 6 weeks progressively improved mechanical and thermal hypoalgesia and MNCVs and SNCVs back to control levels.[28, 470] These improvements occurred without affecting systemic insulin, FPG, or HbA_{1C} levels, suggesting that KU-32's neuroprotective effects are not attributed to metabolic control.[28, 470]

To explore KU-32's mechanism of action, we investigated whether the removal of HSR-inducible Hsps could negate KU-32's neuroprotective effects or expedite the pathological progression of DSPN.[28, 470] Since Hsp90 genetic deletion is lethal, we focused our attention on alternative knockout (KO) models.[28, 470] We had shown (by immunoblotting) that KU-32 dose-dependently increases Hsp70 expression in MCF7 (human breast adenocarcinoma) cells and sciatic nerves of KU-32-treated C57BL/6 mice.[28, 470] This data, combined with knowledge of Hsp70's physiological roles with and without Hsp90, led us to perform a nearly identical 12-week intervention study in Hsp70 double KO mice, in which both inducible Hsp70 genes in mice (Hsp70.1 and Hsp70.3) were removed.[28, 470] While the pathological timeline of STZ-diabetes in Hsp70 KO mice was nearly identical to wild-type C57BL/6 mice, KU-32 was ineffective.[28, 470] Hence, while inducible Hsp70 is required for KU-32's neuroprotective effects, its privation has no affect upon DSPN development.[28, 470] However, this does not rule out compensatory support from other Hsp70 isoforms.

Overall, our preliminary studies provided proof-of-principal that C-terminal Hsp90 modulators could improve psychophysical and electrophysiological aspects of DSPN in experimental T1DM animal models without affecting systemic metabolic control. We concluded that hyperglycemia may adversely impact the folding and refolding capabilities of newly synthesized or mildly damaged proteins in diabetic peripheral nerves.

4.8. Objectives and Hypotheses

4.8.1 Part 1 (Chapter II)

Although the efficacy of KU-32 requires the expression of inducible Hsp70, little insight was gained in these early studies to determine how KU-32 specifically improves psychophysical and electrophysiological aspects of DSPN. With that said, it should be reemphasized that compounds that improve sensory and NCV deficits in rodents historically fail to exhibit clinical efficacy.[296, 299] Thus, morphological assessments, such as iENF density analyses, may likely alleviate interspecies mechanistic differences to expedite drug development.[296] To better observe morphological alterations, an animal model capable of surviving more chronic stages of DSPN was needed. Hence, we elected to use a more hardy strain of mice, the genetically out-bred Swiss-Webster (SW) mice, which enables better morphological comparisons that may be more comparable to human DSPN. Also, given hyperglycemia's adverse affects upon mitochondrial function and viability as well as its implications in DSPN development, we assessed mitochondrial bioenergetic profiles to determine KU-32 affects upon metabolic resiliency.[359-360]

4.8.1.1. Objective 1

The main objective of this research is to determine whether KU-32 can improve clinical indices of chronic DSPN and its effects on iENF density and mitochondrial bioenergetics.

4.8.1.2. Hypothesis 1

We hypothesize that KU-32 intervention will improve morphological, psychophysical, electrophysiological, and bioenergetic indices of DSPN at more chronic stages.

4.8.2. Part 2 (Chapter III)

In our preliminary work, pharmacokinetic (PK) analyses demonstrated that a single intraperitoneal injection of KU-32 at a dose of 2 mg/kg (5% Captisol/saline vehicle) resulted in rapid drug absorption and distribution to the brain within 5 minutes.[470] KU-32 was eliminated from the blood and the brain within ~ 8 hours.[470] While these PK studies yielded promising results, they did not assess KU-32's levels in DSPN-relevant tissues, such as the DRG, foot pads, and sciatic, tibial, and sural nerves. Moreover, oral PK profiles have not been assessed. Demonstrating oral drug efficacy would be advantageous to a patient's quality of life and expedite drug progression. It would also help establish comparable dose ranges needed to initiate oral gavage (OG) intervention studies. Therefore, PK profiles for IP and OG KU-32 treatments were assessed.

4.8.2.1. Objective 2

The second objective of this research is to characterize the KU-32's pharmacokinetic profiles in DSPN-relevant tissues after IP or OG administration.

4.8.2.2. Hypothesis 2

We hypothesize that both intraperitoneal and oral KU-32 administration will result in successful drug delivery to DSPN-relevant tissues in a route-dependent manner.

SECTION 5. REFERENCES

1. International Diabetes Federation. IDF Diabetes Atlas: 5th Ed., 2012 Update 2012, p. 2. www.idf.org/diabetesatlas.
2. Guariguata, L. *Diabetes Res Clin Pract* **2012,** *98* (3), 524-5.
3. Whiting, D. R.; Guariguata, L.; Weil, C.; Shaw, J. *Diabetes Res Clin Pract* **2011,** *94* (3), 311-21.

4. American Diabetes, A. *Diabetes Care* **2013,** *36 Suppl 1*, S67-74.
5. Mathers, C. D.and Loncar, D. *PLoS Med* **2006,** *3* (11), e442.
6. United Nations General Assembly. A/RES/61/225: World Diabetes Day. United Nations: New York, 2007; p 2.
7. Lam, D. W.and LeRoith, D. *Curr Opin Endocrinol Diabetes Obes* **2012,** *19* (2), 93-6.
8. Danaei, G.; Finucane, M. M.; Lu, Y.; Singh, G. M.; Cowan, M. J.; Paciorek, C. J.; Lin, J. K.; Farzadfar, F.; Khang, Y. H.; Stevens, G. A.*, et al. Lancet* **2011,** *378* (9785), 31-40.
9. World Health Organization. *Global status report on noncommunicable diseases 2010*; WHO: Geneva, 2011; p 176.
10. Abegunde, D. O.; Mathers, C. D.; Adam, T.; Ortegon, M.; Strong, K. *Lancet* **2007,** *370* (9603), 1929-38.
11. Rabi, D. M.; Edwards, A. L.; Southern, D. A.; Svenson, L. W.; Sargious, P. M.; Norton, P.; Larsen, E. T.; Ghali, W. A. *BMC Health Serv Res* **2006,** *6*, 124.
12. American Diabetes, A. *Diabetes Care* **2013,** *36* (4), 1033-46.
13. Leone, T.; Coast, E.; Narayanan, S.; de Graft Aikins, A. *Global Health* **2012,** *8*, 39.
14. van Dieren, S.; Beulens, J. W.; van der Schouw, Y. T.; Grobbee, D. E.; Neal, B. *Eur J Cardiovasc Prev Rehabil* **2010,** *17 Suppl 1*, S3-8.
15. Maruthur, N. M. *Curr Diab Rep* **2013**.
16. Harris, M. I.; Klein, R.; Welborn, T. A.; Knuiman, M. W. *Diabetes Care* **1992,** *15* (7), 815-9.
17. Cowie, C. C.; Rust, K. F.; Byrd-Holt, D. D.; Eberhardt, M. S.; Flegal, K. M.; Engelgau, M. M.; Saydah, S. H.; Williams, D. E.; Geiss, L. S.; Gregg, E. W. *Diabetes Care* **2006,** *29* (6), 1263-8.
18. Ryden, L.; Standl, E.; Bartnik, M.; Van den Berghe, G.; Betteridge, J.; de Boer, M. J.; Cosentino, F.; Jonsson, B.; Laakso, M.; Malmberg, K.*, et al. Eur Heart J* **2007,** *28* (1), 88-136.
19. Anselmino, M.and Sillano, D. *Curr Vasc Pharmacol* **2012,** *10* (6), 680-3.
20. Centers for Disease Control and Prevention. National diabetes fact sheet: national estimates and general information on diabetes and prediabetes in the United States, 2011. http://apps.nccd.cdc.gov/DDTSTRS/FactSheet.aspx.
21. Boyle, J. P.; Thompson, T. J.; Gregg, E. W.; Barker, L. E.; Williamson, D. F. *Popul Health Metr* **2010,** *8*, 29.
22. American Diabetes Association. Living With Diabetes > Complications > Mental Health 2013. http://www.diabetes.org/living-with-diabetes/complications/mental-health/.
23. The Diabetes Control and Complications Trial Research Group. *N Engl J Med* **1993,** *329* (14), 977-86.
24. Martin, C. L.; Albers, J.; Herman, W. H.; Cleary, P.; Waberski, B.; Greene, D. A.; Stevens, M. J.; Feldman, E. L. *Diabetes Care* **2006,** *29* (2), 340-4.
25. Maser, R. E.; Steenkiste, A. R.; Dorman, J. S.; Nielsen, V. K.; Bass, E. B.; Manjoo, Q.; Drash, A. L.; Becker, D. J.; Kuller, L. H.; Greene, D. A. *Diabetes* **1989,** *38* (11), 1456-61.
26. Vincent, A. M.; Callaghan, B. C.; Smith, A. L.; Feldman, E. L. *Nat Rev Neurol* **2011,** *7* (10), 573-83.
27. Triplitt, C. *Diabetes Spectrum* **2006,** *19* (4), 202-211.
28. Urban, M. J. A small molecule modulator of Hsp90 improves experimental diabetic neuropathy. M.S., University of Kansas, Ann Arbor, 2010.
29. Expert Committee on the Diagnosis and Classification of Diabetes Mellitus. *Diabetes Care* **1997,** *20* (7), 1183-97.
30. National Diabetes Data Group. *Diabetes* **1979,** *28* (12), 1039-57.
31. WHO Expert Committee on Diabetes Mellitus. *World Health Organ Tech Rep Ser* **1980,** *646*, 1-80.
32. World Health Organization. *World Health Organ Tech Rep Ser* **1985,** *727*, 1-113.
33. Expert Committee on the Diagnosis and Classification of Diabetes Mellitus. *Diabetes Care* **2003,** *26* (11), 3160-7.
34. Alberti, K. G.and Zimmet, P. Z. *Diabet Med* **1998,** *15* (7), 539-53.

35. World Health Organization-International Diabetes Federation. *Definition and diagnosis of diabetes mellitus and intermediate hyperglycaemia*; WHO-IDF: Geneva, 2006; p 50.
36. Perry, R. C.and Baron, A. D. *Diabetes Care* **1999,** *22* (6), 883-5.
37. World Health Organization. *Br Med J* **1980,** *281* (6254), 1512-3.
38. American Diabetes Association. *Diabetes Care* **2010,** *33 Suppl 1*, S4-10.
39. Glenn, J. V.and Stitt, A. W. *Biochim Biophys Acta* **2009,** *1790* (10), 1109-16.
40. World Health Organization. *Use of Glycated Haemoglobin (HbA1c) in the Diagnosis of Diabetes Mellitus*; WHO: Geneva, 2011; p 25.
41. Gillett, M. J. *Clin Biochem Rev* **2009,** *30* (4), 197-200.
42. Nathan, D. M.; Turgeon, H.; Regan, S. *Diabetologia* **2007,** *50* (11), 2239-44.
43. Zochodne, D. W. *Muscle Nerve* **2007,** *36* (2), 144-66.
44. Tomlinson, D. R.and Gardiner, N. J. *Nat Rev Neurosci* **2008,** *9* (1), 36-45.
45. Figueroa-Romero, C.; Sadidi, M.; Feldman, E. L. *Rev Endocr Metab Disord* **2008,** *9* (4), 301-14.
46. Obrosova, I. G. *Biochim Biophys Acta* **2009,** *1792* (10), 931-40.
47. Amadori, M. *Atti Accad Naz Lincei* **1925,** *6* (2), 337-342.
48. Kürti, L. s.and Czakó, B. *Strategic applications of named reactions in organic synthesis : background and detailed mechanisms*. Elsevier Academic Press: Amsterdam ; Boston, 2005; p lii, 758 p.
49. World Health Organization. Diagnostic criteria and classification of hyperglycaemia first detected in pregnancy. WHO, Ed. WHO Press: Geneva, 2013; p. 63. http://apps.who.int/iris/bitstream/10665/85975/1/WHO_NMH_MND_13.2_eng.pdf.
50. Stanescu, D. E.; Lord, K.; Lipman, T. H. *Endocrinol Metab Clin North Am* **2012,** *41* (4), 679-94.
51. Menke, A.; Orchard, T. J.; Imperatore, G.; Bullard, K. M.; Mayer-Davis, E.; Cowie, C. C. *Epidemiology* **2013,** *24* (5), 773-4.
52. Howden, L. M. M., J. A. Age and Sex Composition: 2010. U.S. Department of Commerce: U.S. Census Bureau, Ed. Washington, D.C., 2011.
53. Atkinson, M. A. *Cold Spring Harb Perspect Med* **2012,** *2* (11).
54. Mahaffy, J. M.and Edelstein-Keshet, L. *SIAM Journal on Applied Mathematics* **2007,** *67* (4), 915-37.
55. Banting, F. G.; Best, C. H.; Collip, J. B.; Campbell, W. R.; Fletcher, A. A. *Can Med Assoc J* **1922,** *12* (3), 141-6.
56. von Herrath, M.; Sanda, S.; Herold, K. *Nat Rev Immunol* **2007,** *7* (12), 988-94.
57. Eisenbarth, G. S. *N Engl J Med* **1986,** *314* (21), 1360-8.
58. Herold, K. C.; Vignali, D. A.; Cooke, A.; Bluestone, J. A. *Nat Rev Immunol* **2013,** *13* (4), 243-56.
59. Eisenbarth, G. S.; Srikanta, S.; Jackson, R.; Rabinowe, S.; Dolinar, R.; Aoki, T.; Morris, M. A. *Diabetes Res* **1985,** *2* (6), 271-6.
60. Stiller, C. R.; Dupre, J.; Gent, M.; Jenner, M. R.; Keown, P. A.; Laupacis, A.; Martell, R.; Rodger, N. W.; von Graffenried, B.; Wolfe, B. M. *Science* **1984,** *223* (4643), 1362-7.
61. Nokoff, N.and Rewers, M. *Ann N Y Acad Sci* **2013,** *1281*, 1-15.
62. Lempainen, J.and Ilonen, J. *Curr Diab Rep* **2012,** *12* (5), 447-55.
63. Atkinson, M. A.; Bluestone, J. A.; Eisenbarth, G. S.; Hebrok, M.; Herold, K. C.; Accili, D.; Pietropaolo, M.; Arvan, P. R.; Von Herrath, M.; Markel, D. S.*, et al. Diabetes* **2011,** *60* (5), 1370-9.
64. La Torre, D.and Lernmark, A. *Adv Exp Med Biol* **2010,** *654*, 537-83.
65. Bluestone, J. A.; Herold, K.; Eisenbarth, G. *Nature* **2010,** *464* (7293), 1293-300.
66. Knip, M. *Horm Res* **2002,** *57 Suppl 1*, 6-11.
67. Lernmark, A.and Larsson, H. E. *Nat Rev Endocrinol* **2013,** *9* (2), 92-103.

68. Meier, J. J.; Bhushan, A.; Butler, A. E.; Rizza, R. A.; Butler, P. C. *Diabetologia* **2005,** *48* (11), 2221-8.
69. Matveyenko, A. V.and Butler, P. C. *Diabetes Obes Metab* **2008,** *10 Suppl 4*, 23-31.
70. Akirav, E.; Kushner, J. A.; Herold, K. C. *Diabetes* **2008,** *57* (11), 2883-8.
71. Lund, F. E.and Randall, T. D. *Nat Rev Immunol* **2010,** *10* (4), 236-47.
72. Aly, H.and Gottlieb, P. *Curr Opin Endocrinol Diabetes Obes* **2009,** *16* (4), 286-92.
73. Chase, H. P.; MacKenzie, T. A.; Burdick, J.; Fiallo-Scharer, R.; Walravens, P.; Klingensmith, G.; Rewers, M. *Pediatr Diabetes* **2004,** *5* (1), 16-9.
74. Muhammad, B. J.; Swift, P. G.; Raymond, N. T.; Botha, J. L. *Arch Dis Child* **1999,** *80* (4), 367-9.
75. Bober, E.; Dundar, B.; Buyukgebiz, A. *J Pediatr Endocrinol Metab* **2001,** *14* (4), 435-41.
76. Acharjee, S.; Ghosh, B.; Al-Dhubiab, B. E.; Nair, A. B. *Can J Diabetes* **2013,** *37* (4), 269-76.
77. Redondo, M. J.; Fain, P. R.; Eisenbarth, G. S. *Recent Prog Horm Res* **2001,** *56*, 69-89.
78. Condon, J.; Shaw, J. E.; Luciano, M.; Kyvik, K. O.; Martin, N. G.; Duffy, D. L. *Twin Res Hum Genet* **2008,** *11* (1), 28-40.
79. Hyttinen, V.; Kaprio, J.; Kinnunen, L.; Koskenvuo, M.; Tuomilehto, J. *Diabetes* **2003,** *52* (4), 1052-5.
80. Redondo, M. J.; Yu, L.; Hawa, M.; Mackenzie, T.; Pyke, D. A.; Eisenbarth, G. S.; Leslie, R. D. *Diabetologia* **2001,** *44* (3), 354-62.
81. Kyvik, K. O.; Green, A.; Beck-Nielsen, H. *BMJ* **1995,** *311* (7010), 913-7.
82. Redondo, M. J.; Jeffrey, J.; Fain, P. R.; Eisenbarth, G. S.; Orban, T. *N Engl J Med* **2008,** *359* (26), 2849-50.
83. Pociot, F.; Akolkar, B.; Concannon, P.; Erlich, H. A.; Julier, C.; Morahan, G.; Nierras, C. R.; Todd, J. A.; Rich, S. S.; Nerup, J. *Diabetes* **2010,** *59* (7), 1561-71.
84. Concannon, P.; Rich, S. S.; Nepom, G. T. *N Engl J Med* **2009,** *360* (16), 1646-54.
85. Steck, A. K.and Rewers, M. J. *Clin Chem* **2011,** *57* (2), 176-85.
86. Burren, O. S.; Adlem, E. C.; Achuthan, P.; Christensen, M.; Coulson, R. M.; Todd, J. A. *Nucleic Acids Res* **2011,** *39* (Database issue), D997-1001.
87. Gough, S. C.and Simmonds, M. J. *Curr Genomics* **2007,** *8* (7), 453-65.
88. Klein, J.and Sato, A. *N Engl J Med* **2000,** *343* (10), 702-9.
89. Liao, Y.; Xiang, Y.; Zhou, Z. *Front Med* **2012,** *6* (3), 243-7.
90. Noble, J. A.; Valdes, A. M.; Cook, M.; Klitz, W.; Thomson, G.; Erlich, H. A. *Am J Hum Genet* **1996,** *59* (5), 1134-48.
91. Pugliese, A.; Gianani, R.; Moromisato, R.; Awdeh, Z. L.; Alper, C. A.; Erlich, H. A.; Jackson, R. A.; Eisenbarth, G. S. *Diabetes* **1995,** *44* (6), 608-13.
92. Erlich, H.; Valdes, A. M.; Noble, J.; Carlson, J. A.; Varney, M.; Concannon, P.; Mychaleckyj, J. C.; Todd, J. A.; Bonella, P.; Fear, A. L.*, et al. Diabetes* **2008,** *57* (4), 1084-92.
93. Baker, P. R., 2ndand Steck, A. K. *Curr Diab Rep* **2011,** *11* (5), 445-53.
94. Tait, B. D.; Colman, P. G.; Morahan, G.; Marchinovska, L.; Dore, E.; Gellert, S.; Honeyman, M. C.; Stephen, K.; Loth, A. *Tissue Antigens* **2003,** *61* (2), 146-53.
95. Zikherman, J.and Weiss, A. *Arthritis Res Ther* **2009,** *11* (1), 202.
96. Lempainen, J.; Hermann, R.; Veijola, R.; Simell, O.; Knip, M.; Ilonen, J. *Diabetes* **2012,** *61* (4), 963-6.
97. Vang, T.; Congia, M.; Macis, M. D.; Musumeci, L.; Orru, V.; Zavattari, P.; Nika, K.; Tautz, L.; Tasken, K.; Cucca, F.*, et al. Nat Genet* **2005,** *37* (12), 1317-9.
98. Nielsen, L. B.; Porksen, S.; Andersen, M. L.; Fredheim, S.; Svensson, J.; Hougaard, P.; Vanelli, M.; Aman, J.; Mortensen, H. B.; Hansen, L.*, et al. BMC Med Genet* **2011,** *12*, 41.
99. Petrone, A.; Galgani, A.; Spoletini, M.; Alemanno, I.; Di Cola, S.; Bassotti, G.; Picardi, A.; Manfrini, S.; Osborn, J.; Pozzilli, P.*, et al. Diabetes Metab Res Rev* **2005,** *21* (3), 271-5.
100. Harbo, H. F.; Celius, E. G.; Vartdal, F.; Spurkland, A. *Tissue Antigens* **1999,** *53* (1), 106-10.

101. Seidl, C.; Donner, H.; Fischer, B.; Usadel, K. H.; Seifried, E.; Kaltwasser, J. P.; Badenhoop, K. *Tissue Antigens* **1998,** *51* (1), 62-6.
102. Vaidya, B.; Pearce, S. H.; Charlton, S.; Marshall, N.; Rowan, A. D.; Griffiths, I. D.; Kendall-Taylor, P.; Cawston, T. E.; Young-Min, S. *Rheumatology (Oxford)* **2002,** *41* (2), 180-3.
103. Djilali-Saiah, I.; Schmitz, J.; Harfouch-Hammoud, E.; Mougenot, J. F.; Bach, J. F.; Caillat-Zucman, S. *Gut* **1998,** *43* (2), 187-9.
104. Agarwal, K.; Jones, D. E.; Daly, A. K.; James, O. F.; Vaidya, B.; Pearce, S.; Bassendine, M. F. *J Hepatol* **2000,** *32* (4), 538-41.
105. Donner, H.; Rau, H.; Walfish, P. G.; Braun, J.; Siegmund, T.; Finke, R.; Herwig, J.; Usadel, K. H.; Badenhoop, K. *J Clin Endocrinol Metab* **1997,** *82* (1), 143-6.
106. Rudd, C. E. *Nat Rev Immunol* **2008,** *8* (2), 153-60.
107. Kavvoura, F. K.and Ioannidis, J. P. *Am J Epidemiol* **2005,** *162* (1), 3-16.
108. Ghaderi, A. *Iran J Immunol* **2011,** *8* (3), 127-49.
109. Jeker, L. T.; Bour-Jordan, H.; Bluestone, J. A. *Cold Spring Harb Perspect Med* **2012,** *2* (3), a007807.
110. Steck, A. K.; Zhang, W.; Bugawan, T. L.; Barriga, K. J.; Blair, A.; Erlich, H. A.; Eisenbarth, G. S.; Norris, J. M.; Rewers, M. J. *Diabetes* **2009,** *58* (4), 1028-33.
111. Kukko, M.; Kimpimaki, T.; Korhonen, S.; Kupila, A.; Simell, S.; Veijola, R.; Simell, T.; Ilonen, J.; Simell, O.; Knip, M. *J Clin Endocrinol Metab* **2005,** *90* (5), 2712-7.
112. Vafiadis, P.; Bennett, S. T.; Todd, J. A.; Nadeau, J.; Grabs, R.; Goodyer, C. G.; Wickramasinghe, S.; Colle, E.; Polychronakos, C. *Nat Genet* **1997,** *15* (3), 289-92.
113. Moriyama, H.; Abiru, N.; Paronen, J.; Sikora, K.; Liu, E.; Miao, D.; Devendra, D.; Beilke, J.; Gianani, R.; Gill, R. G.*, et al. Proc Natl Acad Sci U S A* **2003,** *100* (18), 10376-81.
114. Peng, H.and Hagopian, W. *Rev Endocr Metab Disord* **2006,** *7* (3), 149-62.
115. Berg, A. K.; Korsgren, O.; Frisk, G. *Diabetologia* **2006,** *49* (11), 2697-703.
116. Christen, U.; McGavern, D. B.; Luster, A. D.; von Herrath, M. G.; Oldstone, M. B. *J Immunol* **2003,** *171* (12), 6838-45.
117. Schulte, B. M.; Lanke, K. H.; Piganelli, J. D.; Kers-Rebel, E. D.; Bottino, R.; Trucco, M.; Huijbens, R. J.; Radstake, T. R.; Engelse, M. A.; de Koning, E. J.*, et al. Diabetes* **2012,** *61* (8), 2030-6.
118. von Herrath, M. G.; Fujinami, R. S.; Whitton, J. L. *Nat Rev Microbiol* **2003,** *1* (2), 151-7.
119. Bach, J. F.and Chatenoud, L. *Cold Spring Harb Perspect Med* **2012,** *2* (2), a007799.
120. Gale, E. A. *Diabetologia* **2002,** *45* (4), 588-94.
121. Beyan, H.; Valorani, M. G.; Pozzilli, P. *Diabetologia* **2003,** *46* (2), 301-2; author reply 302.
122. Mathis, D.and Benoist, C. *Immunol Rev* **2012,** *245* (1), 239-49.
123. Moran, G. W.; Dubeau, M. F.; Kaplan, G. G.; Panaccione, R.; Ghosh, S. *Inflamm Bowel Dis* **2013**.
124. Giongo, A.; Gano, K. A.; Crabb, D. B.; Mukherjee, N.; Novelo, L. L.; Casella, G.; Drew, J. C.; Ilonen, J.; Knip, M.; Hyoty, H.*, et al. ISME J* **2011,** *5* (1), 82-91.
125. Koletzko, B. *Early nutrition and its later consequences : new opportunities : perinatal programming of adult health - EC supported research*. Springer: Dordrecht ; New York, 2005; p xvii, 237 p.
126. Hanninen, A.; Salmi, M.; Simell, O.; Jalkanen, S. *Diabetes* **1993,** *42* (11), 1656-62.
127. Wilkin, T. J. *Diabetologia* **2001,** *44* (7), 914-22.
128. Norris, J. M.; Barriga, K.; Klingensmith, G.; Hoffman, M.; Eisenbarth, G. S.; Erlich, H. A.; Rewers, M. *JAMA* **2003,** *290* (13), 1713-20.
129. Ziegler, A. G.; Schmid, S.; Huber, D.; Hummel, M.; Bonifacio, E. *JAMA* **2003,** *290* (13), 1721-8.
130. Gerstein, H. C. *Diabetes Care* **1994,** *17* (1), 13-9.

131. Vaarala, O.; Ilonen, J.; Ruohtula, T.; Pesola, J.; Virtanen, S. M.; Harkonen, T.; Koski, M.; Kallioinen, H.; Tossavainen, O.; Poussa, T.*, et al. Arch Pediatr Adolesc Med* **2012,** *166* (7), 608-14.
132. Diaz, J. L.and Wilkin, T. *Diabetes* **1987,** *36* (1), 66-72.
133. Lempainen, J.; Vaarala, O.; Makela, M.; Veijola, R.; Simell, O.; Knip, M.; Hermann, R.; Ilonen, J. *J Autoimmun* **2009,** *33* (2), 155-64.
134. TRIGR Study Group. *Pediatr Diabetes* **2007,** *8* (3), 117-37.
135. Bingley, P. J. *J Clin Endocrinol Metab* **2010,** *95* (1), 25-33.
136. Skyler, J. S. *Clin Pharmacol Ther* **2007,** *81* (5), 768-71.
137. Winter, W. E.and Schatz, D. A. *Clin Chem* **2011,** *57* (2), 168-75.
138. Wenzlau, J. M.; Moua, O.; Sarkar, S. A.; Yu, L.; Rewers, M.; Eisenbarth, G. S.; Davidson, H. W.; Hutton, J. C. *Ann N Y Acad Sci* **2008,** *1150*, 256-9.
139. Verge, C. F.; Gianani, R.; Kawasaki, E.; Yu, L.; Pietropaolo, M.; Jackson, R. A.; Chase, H. P.; Eisenbarth, G. S. *Diabetes* **1996,** *45* (7), 926-33.
140. Baekkeskov, S.; Aanstoot, H. J.; Christgau, S.; Reetz, A.; Solimena, M.; Cascalho, M.; Folli, F.; Richter-Olesen, H.; De Camilli, P. *Nature* **1990,** *347* (6289), 151-6.
141. Palmer, J. P.; Asplin, C. M.; Clemons, P.; Lyen, K.; Tatpati, O.; Raghu, P. K.; Paquette, T. L. *Science* **1983,** *222* (4630), 1337-9.
142. Bottazzo, G. F.; Florin-Christensen, A.; Doniach, D. *Lancet* **1974,** *2* (7892), 1279-83.
143. Wenzlau, J. M.; Juhl, K.; Yu, L.; Moua, O.; Sarkar, S. A.; Gottlieb, P.; Rewers, M.; Eisenbarth, G. S.; Jensen, J.; Davidson, H. W.*, et al. Proc Natl Acad Sci U S A* **2007,** *104* (43), 17040-5.
144. Bingley, P. J.; Gale, E. A.; European Nicotinamide Diabetes Intervention Trial, G. *Diabetologia* **2006,** *49* (5), 881-90.
145. Steck, A. K.; Johnson, K.; Barriga, K. J.; Miao, D.; Yu, L.; Hutton, J. C.; Eisenbarth, G. S.; Rewers, M. J. *Diabetes Care* **2011,** *34* (6), 1397-9.
146. Kanatsuna, N.; Papadopoulos, G. K.; Moustakas, A. K.; Lenmark, A. *Anat Res Int* **2012,** *2012*, 457546.
147. Chimienti, F.; Devergnas, S.; Favier, A.; Seve, M. *Diabetes* **2004,** *53* (9), 2330-7.
148. Kawasaki, E. *Endocr J* **2012,** *59* (7), 531-7.
149. Fu, Z.; Gilbert, E. R.; Liu, D. *Curr Diabetes Rev* **2013,** *9* (1), 25-53.
150. Slucca, M.; Harmon, J. S.; Oseid, E. A.; Bryan, J.; Robertson, R. P. *Diabetes* **2010,** *59* (1), 128-34.
151. Richardson, C. C.; Dromey, J. A.; McLaughlin, K. A.; Morgan, D.; Bodansky, H. J.; Feltbower, R. G.; Barnett, A. H.; Gill, G. V.; Bain, S. C.; Christie, M. R. *Diabetologia* **2013**.
152. Vaziri-Sani, F.; Oak, S.; Radtke, J.; Lernmark, K.; Lynch, K.; Agardh, C. D.; Cilio, C. M.; Lethagen, A. L.; Ortqvist, E.; Landin-Olsson, M.*, et al. Autoimmunity* **2010,** *43* (8), 598-606.
153. Howson, J. M.; Krause, S.; Stevens, H.; Smyth, D. J.; Wenzlau, J. M.; Bonifacio, E.; Hutton, J.; Ziegler, A. G.; Todd, J. A.; Achenbach, P. *Diabetologia* **2012,** *55* (7), 1978-84.
154. Sladek, R.; Rocheleau, G.; Rung, J.; Dina, C.; Shen, L.; Serre, D.; Boutin, P.; Vincent, D.; Belisle, A.; Hadjadj, S.*, et al. Nature* **2007,** *445* (7130), 881-5.
155. Winkler, C.; Raab, J.; Grallert, H.; Ziegler, A. G. *PLoS One* **2012,** *7* (4), e35410.
156. Graham, J.; Hagopian, W. A.; Kockum, I.; Li, L. S.; Sanjeevi, C. B.; Lowe, R. M.; Schaefer, J. B.; Zarghami, M.; Day, H. L.; Landin-Olsson, M.*, et al. Diabetes* **2002,** *51* (5), 1346-55.
157. Ge, X.; James, E. A.; Reijonen, H.; Kwok, W. W. *J Autoimmun* **2011,** *36* (2), 155-60.
158. Eerligh, P.; van Lummel, M.; Zaldumbide, A.; Moustakas, A. K.; Duinkerken, G.; Bondinas, G.; Koeleman, B. P.; Papadopoulos, G. K.; Roep, B. O. *Genes Immun* **2011,** *12* (6), 415-27.
159. Taneera, J.; Jin, Z.; Jin, Y.; Muhammed, S. J.; Zhang, E.; Lang, S.; Salehi, A.; Korsgren, O.; Renstrom, E.; Groop, L.*, et al. Diabetologia* **2012,** *55* (7), 1985-94.
160. Soltani, N.; Qiu, H.; Aleksic, M.; Glinka, Y.; Zhao, F.; Liu, R.; Li, Y.; Zhang, N.; Chakrabarti, R.; Ng, T.*, et al. Proc Natl Acad Sci U S A* **2011,** *108* (28), 11692-7.

161. Mendu, S. K.; Akesson, L.; Jin, Z.; Edlund, A.; Cilio, C.; Lernmark, A.; Birnir, B. *Mol Immunol* **2011,** *48* (4), 399-407.
162. Braun, M.; Ramracheya, R.; Bengtsson, M.; Clark, A.; Walker, J. N.; Johnson, P. R.; Rorsman, P. *Diabetes* **2010,** *59* (7), 1694-701.
163. Wendt, A.; Birnir, B.; Buschard, K.; Gromada, J.; Salehi, A.; Sewing, S.; Rorsman, P.; Braun, M. *Diabetes* **2004,** *53* (4), 1038-45.
164. Pietropaolo, M.; Towns, R.; Eisenbarth, G. S. *Cold Spring Harb Perspect Med* **2012,** *2* (10).
165. Libman, I. M.; Pietropaolo, M.; Trucco, M.; Dorman, J. S.; LaPorte, R. E.; Becker, D. *Diabetes Care* **1998,** *21* (11), 1824-7.
166. Torii, S. *Endocr J* **2009,** *56* (5), 639-48.
167. Pinero-Pilona, A.and Raskin, P. *J Diabetes Complications* **2001,** *15* (6), 328-35.
168. World Health Organization. Diabetes Fact sheet N°312. http://www.who.int/mediacentre/factsheets/fs312/en/index.html.
169. Nolan, C. J.; Damm, P.; Prentki, M. *Lancet* **2011,** *378* (9786), 169-81.
170. Kahn, S. E. *Diabetologia* **2003,** *46* (1), 3-19.
171. Springer, S. C.; Silverstein, J.; Copeland, K.; Moore, K. R.; Prazar, G. E.; Raymer, T.; Shiffman, R. N.; Thaker, V. V.; Anderson, M.; Spann, S. J.*, et al. Pediatrics* **2013,** *131* (2), e648-64.
172. D'Adamo, E.and Caprio, S. *Diabetes Care* **2011,** *34 Suppl 2*, S161-5.
173. Phillips, J.and Phillips, P. J. *Aust Fam Physician* **2009,** *38* (9), 699-703.
174. Mayer-Davis, E. J.; Beyer, J.; Bell, R. A.; Dabelea, D.; D'Agostino, R., Jr.; Imperatore, G.; Lawrence, J. M.; Liese, A. D.; Liu, L.; Marcovina, S.*, et al. Diabetes Care* **2009,** *32 Suppl 2*, S112-22.
175. Liu, L. L.; Yi, J. P.; Beyer, J.; Mayer-Davis, E. J.; Dolan, L. M.; Dabelea, D. M.; Lawrence, J. M.; Rodriguez, B. L.; Marcovina, S. M.; Waitzfelder, B. E.*, et al. Diabetes Care* **2009,** *32 Suppl 2*, S133-40.
176. Writing Group for the, S. f. D. i. Y. S. G.; Dabelea, D.; Bell, R. A.; D'Agostino, R. B., Jr.; Imperatore, G.; Johansen, J. M.; Linder, B.; Liu, L. L.; Loots, B.; Marcovina, S.*, et al. JAMA* **2007,** *297* (24), 2716-24.
177. Giannini, C.and Caprio, S. *Curr Diab Rep* **2013,** *13* (1), 89-95.
178. American Diabetes, A. *Diabetes Care* **2013,** *36 Suppl 1*, S11-66.
179. Ahima, R. S. *J Clin Invest* **2011,** *121* (6), 2076-9.
180. Weyer, C.; Bogardus, C.; Mott, D. M.; Pratley, R. E. *J Clin Invest* **1999,** *104* (6), 787-94.
181. Knowler, W. C.; Pettitt, D. J.; Saad, M. F.; Bennett, P. H. *Diabetes Metab Rev* **1990,** *6* (1), 1-27.
182. Pavkov, M. E.; Hanson, R. L.; Knowler, W. C.; Bennett, P. H.; Krakoff, J.; Nelson, R. G. *Diabetes Care* **2007,** *30* (7), 1758-63.
183. National Institutes of Health - National Heart, L., and Blood Institute. *Obes Res* **1998,** *6 Suppl 2*, 51S-209S.
184. Ma, R. C.and Chan, J. C. *Ann N Y Acad Sci* **2013,** *1281*, 64-91.
185. Yoon, K. H.; Lee, J. H.; Kim, J. W.; Cho, J. H.; Choi, Y. H.; Ko, S. H.; Zimmet, P.; Son, H. Y. *Lancet* **2006,** *368* (9548), 1681-8.
186. Lee, J. W.; Brancati, F. L.; Yeh, H. C. *Diabetes Care* **2011,** *34* (2), 353-7.
187. Zhang, Q.; Wang, Y.; Huang, E. S. *Ethn Health* **2009,** *14* (5), 439-57.
188. Borrell, L. N.; Crawford, N. D.; Dallo, F. J.; Baquero, M. C. *Public Health Rep* **2009,** *124* (5), 702-10.
189. Retnakaran, R.and Zinman, B. *Diabetes Obes Metab* **2012,** *14 Suppl 3*, 161-6.
190. Laffel, L.and Svoren, B. Epidemiology, presentation, and diagnosis of type 2 diabetes mellitus in children and adolescents 2013. UpToDate. www.uptodate.com.
191. Kahn, S. E.; Suvag, S.; Wright, L. A.; Utzschneider, K. M. *Diabetes Obes Metab* **2012,** *14 Suppl 3*, 46-56.

192. Turner, R. C.; Cull, C. A.; Frighi, V.; Holman, R. R. *JAMA* **1999,** *281* (21), 2005-12.
193. Holman, R. R. *Diabetes Res Clin Pract* **1998,** *40 Suppl*, S21-5.
194. Guo, G.; Kan, M.; Martinez, J. A.; Zochodne, D. W. *Neurobiol Dis* **2011,** *43* (2), 414-21.
195. Grote, C. W.; Morris, J. K.; Ryals, J. M.; Geiger, P. C.; Wright, D. E. *Exp Diabetes Res* **2011,** *2011*, 212571.
196. Mithieux, G. *Curr Opin Clin Nutr Metab Care* **2005,** *8* (4), 445-9.
197. Bell, G. I.; Kayano, T.; Buse, J. B.; Burant, C. F.; Takeda, J.; Lin, D.; Fukumoto, H.; Seino, S. *Diabetes Care* **1990,** *13* (3), 198-208.
198. Thorens, B. *J Intern Med* **2013,** *274* (3), 203-14.
199. Efrat, S. *Nat Genet* **1997,** *17* (3), 249-50.
200. Minkowski, O. *Diabetes* **1989,** *38* (1), 1-6.
201. Mering, J. V.and Minkowski, O. *Zentralbl Klin Med* **1889,** *10*, 393.
202. De Vos, A.; Heimberg, H.; Quartier, E.; Huypens, P.; Bouwens, L.; Pipeleers, D.; Schuit, F. *J Clin Invest* **1995,** *96* (5), 2489-95.
203. Renner, R. *FEBS Lett* **1973,** *32* (1), 87-90.
204. Freychet, P.; Roth, J.; Neville, D. M., Jr. *Proc Natl Acad Sci U S A* **1971,** *68* (8), 1833-7.
205. Crofford, O. B.; Minemura, T.; Kono, T. *Adv Enzyme Regul* **1970,** *8*, 219-38.
206. Belfiore, A.; Frasca, F.; Pandini, G.; Sciacca, L.; Vigneri, R. *Endocr Rev* **2009,** *30* (6), 586-623.
207. Kanzaki, M. *Endocr J* **2006,** *53* (3), 267-93.
208. Evans, G. J.; Barclay, J. W.; Prescott, G. R.; Jo, S. R.; Burgoyne, R. D.; Birnbaum, M. J.; Morgan, A. *J Biol Chem* **2006,** *281* (3), 1564-72.
209. Kern, M.; Wells, J. A.; Stephens, J. M.; Elton, C. W.; Friedman, J. E.; Tapscott, E. B.; Pekala, P. H.; Dohm, G. L. *Biochem J* **1990,** *270* (2), 397-400.
210. Magnani, P.; Cherian, P. V.; Gould, G. W.; Greene, D. A.; Sima, A. A.; Brosius, F. C., 3rd. *Metabolism* **1996,** *45* (12), 1466-73.
211. Muona, P.; Sollberg, S.; Peltonen, J.; Uitto, J. *Diabetes* **1992,** *41* (12), 1587-96.
212. Gerhart, D. Z.; Broderius, M. A.; Borson, N. D.; Drewes, L. R. *Proc Natl Acad Sci U S A* **1992,** *89* (2), 733-7.
213. Brooks-Worrell, B.; Narla, R.; Palmer, J. P. *Diabetes Obes Metab* **2013,** *15 Suppl 3*, 137-40.
214. Brooks-Worrell, B. M.; Reichow, J. L.; Goel, A.; Ismail, H.; Palmer, J. P. *Diabetes Care* **2011,** *34* (1), 168-73.
215. Goel, A.; Chiu, H.; Felton, J.; Palmer, J. P.; Brooks-Worrell, B. *Diabetes* **2007,** *56* (8), 2110-5.
216. Brooks-Worrell, B. M.; Juneja, R.; Minokadeh, A.; Greenbaum, C. J.; Palmer, J. P. *Diabetes* **1999,** *48* (5), 983-8.
217. Brooks-Worrell, B.and Palmer, J. P. *Clin Exp Immunol* **2012,** *167* (1), 40-6.
218. Gottsater, A.; Landin-Olsson, M.; Fernlund, P.; Lernmark, A.; Sundkvist, G. *Diabetes Care* **1993,** *16* (6), 902-10.
219. Donath, M. Y.; Boni-Schnetzler, M.; Ellingsgaard, H.; Ehses, J. A. *Physiology (Bethesda)* **2009,** *24*, 325-31.
220. Donath, M. Y.; Schumann, D. M.; Faulenbach, M.; Ellingsgaard, H.; Perren, A.; Ehses, J. A. *Diabetes Care* **2008,** *31 Suppl 2*, S161-4.
221. Boni-Schnetzler, M.; Ehses, J. A.; Faulenbach, M.; Donath, M. Y. *Diabetes Obes Metab* **2008,** *10 Suppl 4*, 201-4.
222. Butler, A. E.; Janson, J.; Bonner-Weir, S.; Ritzel, R.; Rizza, R. A.; Butler, P. C. *Diabetes* **2003,** *52* (1), 102-10.
223. Verchere, C. B.; D'Alessio, D. A.; Palmiter, R. D.; Weir, G. C.; Bonner-Weir, S.; Baskin, D. G.; Kahn, S. E. *Proc Natl Acad Sci U S A* **1996,** *93* (8), 3492-6.
224. Jurgens, C. A.; Toukatly, M. N.; Fligner, C. L.; Udayasankar, J.; Subramanian, S. L.; Zraika, S.; Aston-Mourney, K.; Carr, D. B.; Westermark, P.; Westermark, G. T.*, et al. Am J Pathol* **2011,** *178* (6), 2632-40.

225. Johnson, K. H.; O'Brien, T. D.; Betsholtz, C.; Westermark, P. *N Engl J Med* **1989,** *321* (8), 513-8.
226. Montane, J.; Klimek-Abercrombie, A.; Potter, K. J.; Westwell-Roper, C.; Bruce Verchere, C. *Diabetes Obes Metab* **2012,** *14 Suppl 3*, 68-77.
227. Westwell-Roper, C. Y.; Ehses, J. A.; Verchere, C. B. *Diabetes* **2013**.
228. Tfayli, H.; Bacha, F.; Gungor, N.; Arslanian, S. *Diabetes Care* **2010,** *33* (3), 632-8.
229. Brooks-Worrell, B. M.; Greenbaum, C. J.; Palmer, J. P.; Pihoker, C. *J Clin Endocrinol Metab* **2004,** *89* (5), 2222-7.
230. Palmer, J. P.; Hampe, C. S.; Chiu, H.; Goel, A.; Brooks-Worrell, B. M. *Diabetes* **2005,** *54 Suppl 2*, S62-7.
231. Tobin, A. M.; Ahern, T.; Rogers, S.; Collins, P.; O'Shea, D.; Kirby, B. *Int J Dermatol* **2013,** *52* (8), 927-32.
232. Yang, L.; Zhou, Z. G.; Tan, S. Z.; Huang, G.; Jin, P.; Yan, X.; Li, X.; Peng, H.; Hagopian, W. *Ann N Y Acad Sci* **2008,** *1150*, 263-6.
233. Hass, D. J.; Brensinger, C. M.; Lewis, J. D.; Lichtenstein, G. R. *Clin Gastroenterol Hepatol* **2006,** *4* (4), 482-8.
234. Sandovici, I.; Hammerle, C. M.; Ozanne, S. E.; Constancia, M. *Cell Mol Life Sci* **2013,** *70* (9), 1575-95.
235. Poulsen, P.; Kyvik, K. O.; Vaag, A.; Beck-Nielsen, H. *Diabetologia* **1999,** *42* (2), 139-45.
236. Medici, F.; Hawa, M.; Ianari, A.; Pyke, D. A.; Leslie, R. D. *Diabetologia* **1999,** *42* (2), 146-50.
237. Strawbridge, R. J.; Dupuis, J.; Prokopenko, I.; Barker, A.; Ahlqvist, E.; Rybin, D.; Petrie, J. R.; Travers, M. E.; Bouatia-Naji, N.; Dimas, A. S.*, et al. Diabetes* **2011,** *60* (10), 2624-34.
238. Schafer, S. A.; Tschritter, O.; Machicao, F.; Thamer, C.; Stefan, N.; Gallwitz, B.; Holst, J. J.; Dekker, J. M.; t Hart, L. M.; Nijpels, G.*, et al. Diabetologia* **2007,** *50* (12), 2443-50.
239. Villareal, D. T.; Robertson, H.; Bell, G. I.; Patterson, B. W.; Tran, H.; Wice, B.; Polonsky, K. S. *Diabetes* **2010,** *59* (2), 479-85.
240. Dupuis, J.; Langenberg, C.; Prokopenko, I.; Saxena, R.; Soranzo, N.; Jackson, A. U.; Wheeler, E.; Glazer, N. L.; Bouatia-Naji, N.; Gloyn, A. L.*, et al. Nat Genet* **2010,** *42* (2), 105-16.
241. Ling, C.and Groop, L. *Diabetes* **2009,** *58* (12), 2718-25.
242. Dang, M. N.; Buzzetti, R.; Pozzilli, P. *Diabetes Metab Res Rev* **2013,** *29* (1), 8-18.
243. Jirtle, R. L.and Skinner, M. K. *Nat Rev Genet* **2007,** *8* (4), 253-62.
244. Laird, P. W. *Nat Rev Cancer* **2003,** *3* (4), 253-66.
245. Pinney, S. E.and Simmons, R. A. *Curr Diab Rep* **2012,** *12* (1), 67-74.
246. Vohr, B. R.and Boney, C. M. *J Matern Fetal Neonatal Med* **2008,** *21* (3), 149-57.
247. Volkmar, M.; Dedeurwaerder, S.; Cunha, D. A.; Ndlovu, M. N.; Defrance, M.; Deplus, R.; Calonne, E.; Volkmar, U.; Igoillo-Esteve, M.; Naamane, N.*, et al. EMBO J* **2012,** *31* (6), 1405-26.
248. Ye, J. *Front Med* **2013,** *7* (1), 14-24.
249. Roberts, C. K.; Hevener, A. L.; Barnard, R. J. *Compr Physiol* **2013,** *3* (1), 1-58.
250. Soumaya, K. *Adv Exp Med Biol* **2012,** *771*, 240-51.
251. Schmitz-Peiffer, C. *Ann N Y Acad Sci* **2002,** *967*, 146-57.
252. Turban, S.and Hajduch, E. *FEBS Lett* **2011,** *585* (2), 269-74.
253. Boden, G. *Exp Clin Endocrinol Diabetes* **2003,** *111* (3), 121-4.
254. Tanti, J. F.and Jager, J. *Curr Opin Pharmacol* **2009,** *9* (6), 753-62.
255. Elbein, S. C. *J Diabetes Sci Technol* **2009,** *3* (4), 685-9.
256. Deeb, S. S.; Fajas, L.; Nemoto, M.; Pihlajamaki, J.; Mykkanen, L.; Kuusisto, J.; Laakso, M.; Fujimoto, W.; Auwerx, J. *Nat Genet* **1998,** *20* (3), 284-7.
257. Rung, J.; Cauchi, S.; Albrechtsen, A.; Shen, L.; Rocheleau, G.; Cavalcanti-Proenca, C.; Bacot, F.; Balkau, B.; Belisle, A.; Borch-Johnsen, K.*, et al. Nat Genet* **2009,** *41* (10), 1110-5.
258. Voight, B. F.; Scott, L. J.; Steinthorsdottir, V.; Morris, A. P.; Dina, C.; Welch, R. P.; Zeggini, E.; Huth, C.; Aulchenko, Y. S.; Thorleifsson, G.*, et al. Nat Genet* **2010,** *42* (7), 579-89.

259. Barbieri, M.; Rizzo, M. R.; Papa, M.; Boccardi, V.; Esposito, A.; White, M. F.; Paolisso, G. *J Gerontol A Biol Sci Med Sci* **2010,** *65* (3), 282-6.
260. Fischer, J.; Koch, L.; Emmerling, C.; Vierkotten, J.; Peters, T.; Bruning, J. C.; Ruther, U. *Nature* **2009,** *458* (7240), 894-8.
261. International Association of, D.; Pregnancy Study Groups Consensus, P.; Metzger, B. E.; Gabbe, S. G.; Persson, B.; Buchanan, T. A.; Catalano, P. A.; Damm, P.; Dyer, A. R.; Leiva, A.*, et al. Diabetes Care* **2010,** *33* (3), 676-82.
262. Fong, A.; Serra, A.; Herrero, T.; Pan, D.; Ogunyemi, D. *J Diabetes Complications* **2013**.
263. American Diabetes, A. *Diabetes Care* **2003,** *26 Suppl 1*, S103-5.
264. Aretaeus; Adams, F.; Banov, L. *Aretaiou Kappadokou ta sozomena = The extant works of Aretaeus, the Cappadocian*. Milford House: Boston, 1972; p xx, 510 p.
265. Bliss, M. *The discovery of insulin*. University of Chicago Press: Chicago, 1982; p 304 p., [16] p. of plates.
266. Engelhardt, D. v. *Diabetes, its medical and cultural history : outlines, texts, bibliography*. Springer-Verlag: Berlin ; New York, 1989; p x, 491 p.
267. Loriaux, D. L. *The Endocrinologist* **2006,** *16* (2), 55-56.
268. American Diabetes Association. Diabetes Basics > Symptoms 2013. http://www.diabetes.org/diabetes-basics/symptoms/.
269. Urban, M. J.; Dobrowsky, R. T.; Blagg, B. S. *Trends Pharmacol Sci* **2012,** *33* (3), 129-37.
270. Boulton, A. J.; Malik, R. A.; Arezzo, J. C.; Sosenko, J. M. *Diabetes Care* **2004,** *27* (6), 1458-86.
271. Farmer, K. L.; Li, C.; Dobrowsky, R. T. *Pharmacol Rev* **2012,** *64* (4), 880-900.
272. Tesfaye, S.and Selvarajah, D. *Diabetes Metab Res Rev* **2012,** *28 Suppl 1*, 8-14.
273. Callaghan, B. C.; Cheng, H. T.; Stables, C. L.; Smith, A. L.; Feldman, E. L. *Lancet Neurol* **2012,** *11* (6), 521-34.
274. Dyck, P. J.; Albers, J. W.; Andersen, H.; Arezzo, J. C.; Biessels, G. J.; Bril, V.; Feldman, E. L.; Litchy, W. J.; O'Brien, P. C.; Russell, J. W.*, et al. Diabetes Metab Res Rev* **2011**.
275. Tesfaye, S.; Boulton, A. J.; Dyck, P. J.; Freeman, R.; Horowitz, M.; Kempler, P.; Lauria, G.; Malik, R. A.; Spallone, V.; Vinik, A.*, et al. Diabetes Care* **2010,** *33* (10), 2285-93.
276. Boulton, A. J. *Curr Opin Endocrinol Diabetes Obes* **2007,** *14* (2), 141-5.
277. Christianson, J. A.; Ryals, J. M.; Johnson, M. S.; Dobrowsky, R. T.; Wright, D. E. *Neuroscience* **2007,** *145* (1), 303-13.
278. Cheer, K.; Shearman, C.; Jude, E. B. *BMJ* **2009,** *339*, b4905.
279. Thomas, P. K. *Diabetes* **1997,** *46 Suppl 2*, S54-7.
280. Vinik, A.; Mehrabyan, A.; Colen, L.; Boulton, A. *Diabetes Care* **2004,** *27* (7), 1783-8.
281. Perkins, B. A.; Olaleye, D.; Bril, V. *Diabetes Care* **2002,** *25* (3), 565-9.
282. Fleischer, J. *J Diabetes Sci Technol* **2012,** *6* (5), 1207-15.
283. Vinik, A. I.; Maser, R. E.; Mitchell, B. D.; Freeman, R. *Diabetes Care* **2003,** *26* (5), 1553-79.
284. Berthoud, H. R.and Neuhuber, W. L. *Auton Neurosci* **2000,** *85* (1-3), 1-17.
285. Low, P. A.; Benrud-Larson, L. M.; Sletten, D. M.; Opfer-Gehrking, T. L.; Weigand, S. D.; O'Brien, P. C.; Suarez, G. A.; Dyck, P. J. *Diabetes Care* **2004,** *27* (12), 2942-7.
286. Gordon Smith, A.and Robinson Singleton, J. *J Neurol Sci* **2006,** *242* (1-2), 9-14.
287. Smith, A. G.; Russell, J.; Feldman, E. L.; Goldstein, J.; Peltier, A.; Smith, S.; Hamwi, J.; Pollari, D.; Bixby, B.; Howard, J.*, et al. Diabetes Care* **2006,** *29* (6), 1294-9.
288. Sumner, C. J.; Sheth, S.; Griffin, J. W.; Cornblath, D. R.; Polydefkis, M. *Neurology* **2003,** *60* (1), 108-11.
289. Singleton, J. R.; Smith, A. G.; Bromberg, M. B. *Diabetes Care* **2001,** *24* (8), 1448-53.
290. Knowler, W. C.; Barrett-Connor, E.; Fowler, S. E.; Hamman, R. F.; Lachin, J. M.; Walker, E. A.; Nathan, D. M.; Diabetes Prevention Program Research, G. *N Engl J Med* **2002,** *346* (6), 393-403.

291. The Diabetes Control and Complications Trial Research Group. *Ann Intern Med* **1995,** *122* (8), 561-8.
292. Partanen, J.; Niskanen, L.; Lehtinen, J.; Mervaala, E.; Siitonen, O.; Uusitupa, M. *N Engl J Med* **1995,** *333* (2), 89-94.
293. Chong, P. S.and Cros, D. P. *Muscle Nerve* **2004,** *29* (5), 734-47.
294. Chong, P. S.and Cros, D. P. Reproducibility Studies on QST 2004. http://www.aanem.org/Practice/Technology-Reviews.aspx.
295. Dyck, P. J.; Kratz, K. M.; Karnes, J. L.; Litchy, W. J.; Klein, R.; Pach, J. M.; Wilson, D. M.; O'Brien, P. C.; Melton, L. J., 3rd; Service, F. J. *Neurology* **1993,** *43* (4), 817-24.
296. Calcutt, N. A.; Cooper, M. E.; Kern, T. S.; Schmidt, A. M. *Nat Rev Drug Discov* **2009,** *8* (5), 417-29.
297. Loseth, S.; Stalberg, E.; Jorde, R.; Mellgren, S. I. *J Neurol* **2008,** *255* (8), 1197-202.
298. Quattrini, C.; Tavakoli, M.; Jeziorska, M.; Kallinikos, P.; Tesfaye, S.; Finnigan, J.; Marshall, A.; Boulton, A. J.; Efron, N.; Malik, R. A. *Diabetes* **2007,** *56* (8), 2148-54.
299. Beiswenger, K. K.; Calcutt, N. A.; Mizisin, A. P. *Neurosci Lett* **2008,** *442* (3), 267-72.
300. Kandel, E. R.; Schwartz, J. H.; Jessell, T. M. *Principles of neural science*. 4th ed.; McGraw-Hill, Health Professions Division: New York, 2000; p xli, 1414 p.
301. Todd, A. J. *Nat Rev Neurosci* **2010,** *11* (12), 823-36.
302. Gasser, H. S. *The Ohio Journal of Science* **1941,** *41* (3), 145-159.
303. Julius, D.and Basbaum, A. I. *Nature* **2001,** *413* (6852), 203-10.
304. Lehmann, H. C.and Hoke, A. *CNS Neurol Disord Drug Targets* **2010,** *9* (6), 801-6.
305. Nave, K. A.and Schwab, M. H. *Nat Neurosci* **2005,** *8* (11), 1420-2.
306. McGuire, J. F.; Rouen, S.; Siegfreid, E.; Wright, D. E.; Dobrowsky, R. T. *Diabetes* **2009,** *58* (11), 2677-86.
307. Dobrowsky, R. T.; Rouen, S.; Yu, C. *J Pharmacol Exp Ther* **2005,** *313* (2), 485-91.
308. Sandkuhler, J. *Physiol Rev* **2009,** *89* (2), 707-58.
309. Hargreaves, K.; Dubner, R.; Brown, F.; Flores, C.; Joris, J. *Pain* **1988,** *32* (1), 77-88.
310. Beissner, F.; Brandau, A.; Henke, C.; Felden, L.; Baumgartner, U.; Treede, R. D.; Oertel, B. G.; Lotsch, J. *PLoS One* **2010,** *5* (9), e12944.
311. Haines, D. E. *Neuroanatomy : an atlas of structures, sections, and systems*. 7th ed.; Wolters Kluwer Health/Lippincott Williams & Wilkins: Philadelphia, 2008; p x, 341 p.
312. Nelson, D. L.; Cox, M. M.; Lehninger, A. L. *Lehninger principles of biochemistry*. 4th ed.; W.H. Freeman: New York, 2005; p 1 v. (various pagings).
313. Banasik, M.; Stedeford, T.; Strosznajder, R. P. *Mol Neurobiol* **2012,** *46* (1), 55-63.
314. Arner, R. J.; Prabhu, K. S.; Krishnan, V.; Johnson, M. C.; Reddy, C. C. *Biochem Biophys Res Commun* **2006,** *339* (3), 816-20.
315. Greene, D. A.and Lattimer, S. A. *J Clin Invest* **1983,** *72* (3), 1058-63.
316. Clements, R. S., Jr.and Stockard, C. R. *Diabetes* **1980,** *29* (3), 227-35.
317. Ho, E. C.; Lam, K. S.; Chen, Y. S.; Yip, J. C.; Arvindakshan, M.; Yamagishi, S.; Yagihashi, S.; Oates, P. J.; Ellery, C. A.; Chung, S. S.*, et al. Diabetes* **2006,** *55* (7), 1946-53.
318. ExplorEnz: The Enzyme Database. UDP-N-acetylglucosamine Biosynthesis. http://www.enzyme-database.org/reaction/polysacc/UDPGlcN.html.
319. Zachara, N. E.; O'Donnell, N.; Cheung, W. D.; Mercer, J. J.; Marth, J. D.; Hart, G. W. *J Biol Chem* **2004,** *279* (29), 30133-42.
320. Hart, G. W.; Slawson, C.; Ramirez-Correa, G.; Lagerlof, O. *Annu Rev Biochem* **2011,** *80*, 825-58.
321. Butkinaree, C.; Park, K.; Hart, G. W. *Biochim Biophys Acta* **2010,** *1800* (2), 96-106.
322. Hu, P.; Shimoji, S.; Hart, G. W. *FEBS Lett* **2010,** *584* (12), 2526-2538.
323. Lefebvre, T.; Dehennaut, V.; Guinez, C.; Olivier, S.; Drougat, L.; Mir, A. M.; Mortuaire, M.; Vercoutter-Edouart, A. S.; Michalski, J. C. *Biochim Biophys Acta* **2010,** *1800* (2), 67-79.

324. Whelan, S. A.; Dias, W. B.; Thiruneelakantapillai, L.; Lane, M. D.; Hart, G. W. *J Biol Chem* **2010,** *285* (8), 5204-11.
325. Weinberg, R. A. *The biology of cancer*. Garland Science: New York, NY, 2007; p 1 v. (various pagings).
326. Fiordaliso, F.; Leri, A.; Cesselli, D.; Limana, F.; Safai, B.; Nadal-Ginard, B.; Anversa, P.; Kajstura, J. *Diabetes* **2001,** *50* (10), 2363-75.
327. Chou, T. Y.; Hart, G. W.; Dang, C. V. *J Biol Chem* **1995,** *270* (32), 18961-5.
328. Yang, W. H.; Kim, J. E.; Nam, H. W.; Ju, J. W.; Kim, H. S.; Kim, Y. S.; Cho, J. W. *Nat Cell Biol* **2006,** *8* (10), 1074-83.
329. Du, X. L.; Edelstein, D.; Rossetti, L.; Fantus, I. G.; Goldberg, H.; Ziyadeh, F.; Wu, J.; Brownlee, M. *Proc Natl Acad Sci U S A* **2000,** *97* (22), 12222-6.
330. Hafer-Macko, C. E.; Ivey, F. M.; Sorkin, J. D.; Macko, R. F. *Neurology* **2007,** *69* (3), 268-74.
331. Anjaneyulu, M.; Berent-Spillson, A.; Inoue, T.; Choi, J.; Cherian, K.; Russell, J. W. *Exp Neurol* **2008,** *211* (2), 469-79.
332. Yang, X.; Ongusaha, P. P.; Miles, P. D.; Havstad, J. C.; Zhang, F.; So, W. V.; Kudlow, J. E.; Michell, R. H.; Olefsky, J. M.; Field, S. J.*, et al. Nature* **2008,** *451* (7181), 964-9.
333. Ahmed, N.; Argirov, O. K.; Minhas, H. S.; Cordeiro, C. A.; Thornalley, P. J. *Biochem J* **2002,** *364* (Pt 1), 1-14.
334. Thornalley, P. J.; Langborg, A.; Minhas, H. S. *Biochem J* **1999,** *344 Pt 1*, 109-16.
335. Amadori, M. *Atti. accad. Lincci* **1925,** *6* (2), 337-342.
336. Kürti, L.and Czakó, B. *Strategic applications of named reactions in organic synthesis : background and detailed mechanisms*. Elsevier Academic Press: Amsterdam ; Boston, 2005; p lii, 758 p.
337. Ansari, N. A.and Dash, D. *Aging Dis* **2013,** *4* (1), 50-6.
338. Shemin, D.and Rittenberg, D. *J Biol Chem* **1946,** *166* (2), 627-36.
339. O'Brien, J. Non-Enzymatic Degradation Pathways of Lactose and Their Significance in Dairy Products. In *Advanced Dairy Chemistry*, McSweeney, P.; Fox, P. F., Eds. Springer New York: 2009; pp 231-294.
340. Henning, C.; Smuda, M.; Girndt, M.; Ulrich, C.; Glomb, M. A. *J Biol Chem* **2011,** *286* (52), 44350-6.
341. Oliveira, M. I. A.; Souza, E. M. d.; Pedrosa, F. d. O.; Réa, R. R.; Alves, A. d. S. C.; Picheth, G.; Rego, F. G. d. M. *Jornal Brasileiro de Patologia e Medicina Laboratorial* **2013,** *49*, 97-108.
342. Synold, T.; Xi, B.; Wuenschell, G. E.; Tamae, D.; Figarola, J. L.; Rahbar, S.; Termini, J. *Chem Res Toxicol* **2008,** *21* (11), 2148-55.
343. Hosseini, A.and Abdollahi, M. *Oxid Med Cell Longev* **2013,** *2013*, 168039.
344. Sugimoto, K.; Yasujima, M.; Yagihashi, S. *Curr Pharm Des* **2008,** *14* (10), 953-61.
345. Wada, R.and Yagihashi, S. *Ann N Y Acad Sci* **2005,** *1043*, 598-604.
346. Bierhaus, A.; Haslbeck, K. M.; Humpert, P. M.; Liliensiek, B.; Dehmer, T.; Morcos, M.; Sayed, A. A.; Andrassy, M.; Schiekofer, S.; Schneider, J. G.*, et al. J Clin Invest* **2004,** *114* (12), 1741-51.
347. Toth, C.; Rong, L. L.; Yang, C.; Martinez, J.; Song, F.; Ramji, N.; Brussee, V.; Liu, W.; Durand, J.; Nguyen, M. D.*, et al. Diabetes* **2008,** *57* (4), 1002-17.
348. Wiggin, T. D.; Sullivan, K. A.; Pop-Busui, R.; Amato, A.; Sima, A. A.; Feldman, E. L. *Diabetes* **2009,** *58* (7), 1634-40.
349. Dokken, B. B. *Diabetes Spectrum* **2008,** *21* (3), 160-165.
350. Barnett, M. E.; Madgwick, D. K.; Takemoto, D. J. *Cell Signal* **2007,** *19* (9), 1820-9.
351. Geraldes, P.and King, G. L. *Circ Res* **2010,** *106* (8), 1319-31.
352. Madonna, R.and De Caterina, R. *Vascul Pharmacol* **2011,** *54* (3-6), 68-74.
353. Bohlen, H. G. *Am J Physiol Heart Circ Physiol* **2004,** *286* (2), H492-7.
354. Oehrlein, S. A.; Parker, P. J.; Herget, T. *Biochem J* **1996,** *317 (Pt 1)*, 219-24.

355. Gopalakrishna, R.; Gundimeda, U.; Schiffman, J. E.; McNeill, T. H. *J Biol Chem* **2008,** *283* (21), 14430-44.
356. Sakaue, Y.; Sanada, M.; Sasaki, T.; Kashiwagi, A.; Yasuda, H. *Neuroreport* **2003,** *14* (3), 431-6.
357. Zhang, Y.; Wang, Y. H.; Zhang, X. H.; Ge, H. Y.; Arendt-Nielsen, L.; Shao, J. M.; Yue, S. W. *Exp Brain Res* **2008,** *189* (2), 199-209.
358. Haber, F.and Weiss, J. *Proc. R. Soc. Lond. A* **1934,** *147* (861), 332-351.
359. Chowdhury, S. K.; Dobrowsky, R. T.; Fernyhough, P. *Mitochondrion* **2011,** *11* (6), 845-54.
360. Akude, E.; Zherebitskaya, E.; Chowdhury, S. K.; Smith, D. R.; Dobrowsky, R. T.; Fernyhough, P. *Diabetes* **2011,** *60* (1), 288-97.
361. Huang, T. J.; Verkhratsky, A.; Fernyhough, P. *Mol Cell Neurosci* **2005,** *28* (1), 42-54.
362. Zhang, L.; Zhao, H.; Blagg, B. S.; Dobrowsky, R. T. *J Proteome Res* **2012,** *11* (4), 2581-93.
363. Zhang, L.; Yu, C.; Vasquez, F. E.; Galeva, N.; Onyango, I.; Swerdlow, R. H.; Dobrowsky, R. T. *J Proteome Res* **2010,** *9* (1), 458-71.
364. Hamilton, R. T.; Bhattacharya, A.; Walsh, M. E.; Shi, Y.; Wei, R.; Zhang, Y.; Rodriguez, K. A.; Buffenstein, R.; Chaudhuri, A. R.; Van Remmen, H. *PLoS One* **2013,** *8* (6), e65725.
365. Obrosova, I. G.and Julius, U. A. *Curr Vasc Pharmacol* **2005,** *3* (3), 267-83.
366. Stevens, M. J.; Li, F.; Drel, V. R.; Abatan, O. I.; Kim, H.; Burnett, D.; Larkin, D.; Obrosova, I. G. *J Pharmacol Exp Ther* **2007,** *320* (1), 458-64.
367. Obrosova, I. G.; Li, F.; Abatan, O. I.; Forsell, M. A.; Komjati, K.; Pacher, P.; Szabo, C.; Stevens, M. J. *Diabetes* **2004,** *53* (3), 711-20.
368. Sullivan, K. A.; Kim, B.; Feldman, E. L. *Endocrinology* **2008,** *149* (12), 5963-71.
369. Toth, C.; Brussee, V.; Zochodne, D. W. *Diabetologia* **2006,** *49* (5), 1081-8.
370. Zochodne, D. W.and Cheng, C. *J Anat* **2000,** *196 (Pt 2)*, 279-83.
371. Brussee, V.; Cunningham, F. A.; Zochodne, D. W. *Diabetes* **2004,** *53* (7), 1824-30.
372. Ekstrom, A. R.; Kanje, M.; Skottner, A. *Brain Res* **1989,** *496* (1-2), 141-7.
373. Kamiya, H.; Murakawa, Y.; Zhang, W.; Sima, A. A. *Diabetes Metab Res Rev* **2005,** *21* (5), 448-58.
374. Wuarin, L.; Guertin, D. M.; Ishii, D. N. *Exp Neurol* **1994,** *130* (1), 106-14.
375. Migdalis, I. N.; Kalogeropoulou, K.; Kalantzis, L.; Nounopoulos, C.; Bouloukos, A.; Samartzis, M. *Diabet Med* **1995,** *12* (9), 823-7.
376. Bitar, M. S.; Pilcher, C. W.; Khan, I.; Waldbillig, R. J. *Diabetes Res Clin Pract* **1997,** *38* (2), 73-80.
377. Guo, H.; Yang, Y.; Geng, Z.; Zhu, L.; Yuan, S.; Zhao, Y.; Gao, Y.; Fu, H. *Chin Med J (Engl)* **1999,** *112* (1), 76-9.
378. Chu, Q.; Moreland, R.; Yew, N. S.; Foley, J.; Ziegler, R.; Scheule, R. K. *Mol Ther* **2008,** *16* (8), 1400-8.
379. Benyoucef, S.; Surinya, K. H.; Hadaschik, D.; Siddle, K. *Biochem J* **2007,** *403* (3), 603-13.
380. Denley, A.; Bonython, E. R.; Booker, G. W.; Cosgrove, L. J.; Forbes, B. E.; Ward, C. W.; Wallace, J. C. *Mol Endocrinol* **2004,** *18* (10), 2502-12.
381. Craner, M. J.; Klein, J. P.; Black, J. A.; Waxman, S. G. *Neuroreport* **2002,** *13* (13), 1649-52.
382. Feng, Z.and Levine, A. J. *Trends Cell Biol* **2010,** *20* (7), 427-34.
383. Leinninger, G. M.; Backus, C.; Uhler, M. D.; Lentz, S. I.; Feldman, E. L. *FASEB J* **2004,** *18* (13), 1544-6.
384. Dill, J.; Wang, H.; Zhou, F.; Li, S. *J Neurosci* **2008,** *28* (36), 8914-28.
385. Lonze, B. E.; Riccio, A.; Cohen, S.; Ginty, D. D. *Neuron* **2002,** *34* (3), 371-85.
386. Tang, E. D.; Nunez, G.; Barr, F. G.; Guan, K. L. *J Biol Chem* **1999,** *274* (24), 16741-6.
387. Edstrom, A.and Ekstrom, P. A. *J Neurosci Res* **2003,** *74* (5), 726-35.
388. Christie, K. J.; Webber, C. A.; Martinez, J. A.; Singh, B.; Zochodne, D. W. *J Neurosci* **2010,** *30* (27), 9306-15.

389. Leinninger, G. M.; Backus, C.; Sastry, A. M.; Yi, Y. B.; Wang, C. W.; Feldman, E. L. *Neurobiol Dis* **2006,** *23* (1), 11-22.
390. Cardone, M. H.; Roy, N.; Stennicke, H. R.; Salvesen, G. S.; Franke, T. F.; Stanbridge, E.; Frisch, S.; Reed, J. C. *Science* **1998,** *282* (5392), 1318-21.
391. Kamiya, H.; Zhang, W.; Sima, A. A. *Diabetologia* **2006,** *49* (11), 2763-74.
392. Goslin, K.; Schreyer, D. J.; Skene, J. H.; Banker, G. *Nature* **1988,** *336* (6200), 672-4.
393. Goslin, K.and Banker, G. *J Cell Biol* **1990,** *110* (4), 1319-31.
394. Goslin, K.; Schreyer, D. J.; Skene, J. H.; Banker, G. *J Neurosci* **1990,** *10* (2), 588-602.
395. Bergman, E.; Carlsson, K.; Liljeborg, A.; Manders, E.; Hokfelt, T.; Ulfhake, B. *Brain Res* **1999,** *832* (1-2), 63-83.
396. Curtis, R.; Stewart, H. J.; Hall, S. M.; Wilkin, G. P.; Mirsky, R.; Jessen, K. R. *J Cell Biol* **1992,** *116* (6), 1455-64.
397. Aigner, L.and Caroni, P. *J Cell Biol* **1995,** *128* (4), 647-60.
398. Stewart, H. J.; Bradke, F.; Tabernero, A.; Morrell, D.; Jessen, K. R.; Mirsky, R. *Eur J Neurosci* **1996,** *8* (3), 553-64.
399. Cheng, H. L.; Steinway, M. L.; Xin, X.; Feldman, E. L. *J Neurochem* **2001,** *76* (3), 935-43.
400. Delaney, C. L.; Cheng, H. L.; Feldman, E. L. *J Neurobiol* **1999,** *41* (4), 540-8.
401. Delaney, C. L.; Russell, J. W.; Cheng, H. L.; Feldman, E. L. *J Neuropathol Exp Neurol* **2001,** *60* (2), 147-60.
402. Liang, G.; Cline, G. W.; Macica, C. M. *Glia* **2007,** *55* (6), 632-41.
403. Russell, J. W.; Cheng, H. L.; Golovoy, D. *Journal of Neuropathology and Experimental Neurology* **2000,** *59* (7), 575-584.
404. Cheng, H. L.; Russell, J. W.; Feldman, E. L. *Ann N Y Acad Sci* **1999,** *883*, 124-30.
405. Ogata, T.; Iijima, S.; Hoshikawa, S.; Miura, T.; Yamamoto, S.; Oda, H.; Nakamura, K.; Tanaka, S. *J Neurosci* **2004,** *24* (30), 6724-32.
406. Cheng, H. L.; Steinway, M.; Delaney, C. L.; Franke, T. F.; Feldman, E. L. *Mol Cell Endocrinol* **2000,** *170* (1-2), 211-5.
407. Maeda, K.; Fernyhough, P.; Tomlinson, D. R. *Brain Res Mol Brain Res* **1996,** *37* (1-2), 166-74.
408. Pekiner, C.; Dent, E. W.; Roberts, R. E.; Meiri, K. F.; McLean, W. G. *Diabetes* **1996,** *45* (2), 199-204.
409. Mohiuddin, L.; Fernyhough, P.; Tomlinson, D. R. *Diabetes* **1995,** *44* (1), 25-30.
410. Mohiuddin, L.and Tomlinson, D. R. *Diabetes* **1997,** *46* (12), 2057-62.
411. Bursova, S.; Dubovy, P.; Vlckova-Moravcova, E.; Nemec, M.; Klusakova, I.; Belobradkova, J.; Bednarik, J. *J Neurol Sci* **2011**.
412. Scott, J. N.; Clark, A. W.; Zochodne, D. W. *Brain* **1999,** *122 (Pt 11)*, 2109-18.
413. Borghini, I.; Ania-Lahuerta, A.; Regazzi, R.; Ferrari, G.; Gjinovci, A.; Wollheim, C. B.; Pralong, W. F. *J Neurochem* **1994,** *62* (2), 686-96.
414. Shangguan, Y.; Hall, K. E.; Neubig, R. R.; Wiley, J. W. *J Neurochem* **2003,** *86* (4), 1006-14.
415. Cenni, V.; Doppler, H.; Sonnenburg, E. D.; Maraldi, N.; Newton, A. C.; Toker, A. *Biochem J* **2002,** *363* (Pt 3), 537-45.
416. Zhuang, H. X.; Snyder, C. K.; Pu, S. F.; Ishii, D. N. *Exp Neurol* **1996,** *140* (2), 198-205.
417. Li, J. Q.; Chen, S. R.; Chen, H.; Cai, Y. Q.; Pan, H. L. *J Neurochem* **2010,** *112* (1), 162-72.
418. Daulhac, L.; Maffre, V.; Mallet, C.; Etienne, M.; Privat, A. M.; Kowalski-Chauvel, A.; Seva, C.; Fialip, J.; Eschalier, A. *Eur J Pain* **2011,** *15* (2), 169 e1-169 e12.
419. Wang, X. L.; Zhang, Q.; Zhang, Y. Z.; Liu, Y. T.; Dong, R.; Wang, Q. J.; Guo, Y. X. *Neurosci Lett* **2011,** *490* (2), 112-5.
420. Bliss, M. *Horm Res* **2005,** *64 Suppl 2*, 98-102.
421. Banting, F. G. Nobel Lecture: Diabetes and Insulin. The Nobel Foundation: Stockholm, Sweden, 1923.

422. Dalan, R.; Leow, M. K.; George, J.; Chian, K. Y.; Tan, A.; Han, H. W.; Cheow, S. P. *Diabet Med* **2009,** *26* (1), 105-9.
423. Cartwright, M. M.; Hajja, W.; Al-Khatib, S.; Hazeghazam, M.; Sreedhar, D.; Li, R. N.; Wong-McKinstry, E.; Carlson, R. W. *Crit Care Clin* **2012,** *28* (4), 601-31.
424. Goodman, L. S.; Hardman, J. G.; Limbird, L. E.; Gilman, A. G. *Goodman & Gilman's the pharmacological basis of therapeutics*. 10th ed.; McGraw-Hill, Medical Pub. Division: New York, 2001; p xxvii, 2148 p.
425. Williams, D. A.and Lemke, T. L. *Foye's principles of medicinal chemistry*. 5th ed.; Lippincott Williams & Wilkins: Philadelphia, 2002; p xii, 1114 p.
426. Malaisse, W. J.and Lebrun, P. *Diabetes Care* **1990,** *13 Suppl 3*, 9-17.
427. Russo, G. L.; Russo, M.; Ungaro, P. *Biochem Pharmacol* **2013,** *86* (3), 339-50.
428. Tan, M. H. *Int J Clin Pract Suppl* **2000,** (113), 54-62.
429. Nadkarni, P.; Chepurny, O. G.; Holz, G. G. *Prog Mol Biol Transl Sci* **2014,** *121*, 23-65.
430. Cao, P.; Abedini, A.; Wang, H.; Tu, L. H.; Zhang, X.; Schmidt, A. M.; Raleigh, D. P. *Proc Natl Acad Sci U S A* **2013,** *110* (48), 19279-84.
431. Jolivalt, C. G.; Fineman, M.; Deacon, C. F.; Carr, R. D.; Calcutt, N. A. *Diabetes Obes Metab* **2011,** *13* (11), 990-1000.
432. Bianchi, R.; Cervellini, I.; Porretta-Serapiglia, C.; Oggioni, N.; Burkey, B.; Ghezzi, P.; Cavaletti, G.; Lauria, G. *J Pharmacol Exp Ther* **2012,** *340* (1), 64-72.
433. Schemmel, K. E.; Padiyara, R. S.; D'Souza, J. J. *J Diabetes Complications* **2010,** *24* (5), 354-60.
434. National Institutes of Health. ClinicalTrials.gov 2014. http://clinicaltrials.gov/ct2/home.
435. Bril, V.; Hirose, T.; Tomioka, S.; Buchanan, R.; Ranirestat Study, G. *Diabetes Care* **2009,** *32* (7), 1256-60.
436. Nakamura, J.; Kato, K.; Hamada, Y.; Nakayama, M.; Chaya, S.; Nakashima, E.; Naruse, K.; Kasuya, Y.; Mizubayashi, R.; Miwa, K.*, et al. Diabetes* **1999,** *48* (10), 2090-5.
437. Sasase, T.; Yamada, H.; Sakoda, K.; Imagawa, N.; Abe, T.; Ito, M.; Sagawa, S.; Tanaka, M.; Matsushita, M. *Diabetes Obes Metab* **2005,** *7* (5), 586-94.
438. Cameron, N. E.and Cotter, M. A. *Diabetes Metab Res Rev* **2002,** *18* (4), 315-23.
439. Casellini, C. M.; Barlow, P. M.; Rice, A. L.; Casey, M.; Simmons, K.; Pittenger, G.; Bastyr, E. J., 3rd; Wolka, A. M.; Vinik, A. I. *Diabetes Care* **2007,** *30* (4), 896-902.
440. Obrosova, I. G.; Xu, W.; Lyzogubov, V. V.; Ilnytska, O.; Mashtalir, N.; Vareniuk, I.; Pavlov, I. A.; Zhang, J.; Slusher, B.; Drel, V. R. *Free Radic Biol Med* **2008,** *44* (6), 972-81.
441. Ziegler, D.; Ametov, A.; Barinov, A.; Dyck, P. J.; Gurieva, I.; Low, P. A.; Munzel, U.; Yakhno, N.; Raz, I.; Novosadova, M.*, et al. Diabetes Care* **2006,** *29* (11), 2365-70.
442. Valensi, P.; Le Devehat, C.; Richard, J. L.; Farez, C.; Khodabandehlou, T.; Rosenbloom, R. A.; LeFante, C. *J Diabetes Complications* **2005,** *19* (5), 247-53.
443. Kuhad, A.; Sharma, S.; Chopra, K. *Eur J Pain* **2008,** *12* (5), 624-32.
444. Abbas, Z. G.and Swai, A. B. *East Afr Med J* **1997,** *74* (12), 803-8.
445. Stracke, H.; Gaus, W.; Achenbach, U.; Federlin, K.; Bretzel, R. G. *Exp Clin Endocrinol Diabetes* **2008,** *116* (10), 600-5.
446. Pittenger, G.and Vinik, A. *Exp Diabesity Res* **2003,** *4* (4), 271-85.
447. Finnerup, N. B.; Sindrup, S. H.; Jensen, T. S. *Pain* **2010,** *150* (3), 573-81.
448. Singh, R.; Kishore, L.; Kaur, N. *Pharmacol Res* **2013**.
449. Chaudhury, S.; Welch, T. R.; Blagg, B. S. *ChemMedChem* **2006,** *1* (12), 1331-40.
450. Chiosis, G.; Rodina, A.; Moulick, K. *Anticancer Agents Med Chem* **2006,** *6* (1), 1-8.
451. Luo, W.; Sun, W.; Taldone, T.; Rodina, A.; Chiosis, G. *Mol Neurodegener* **2010,** *5*, 24.
452. Peterson, L. B.and Blagg, B. S. *Future Med Chem* **2009,** *1* (2), 267-83.
453. Fujimoto, M.and Nakai, A. *FEBS J* **2010,** *277* (20), 4112-25.
454. Akude, E.; Zherebitskaya, E.; Roy Chowdhury, S. K.; Girling, K.; Fernyhough, P. *Neurotox Res* **2010,** *17* (1), 28-38.

455. Giacco, F.and Brownlee, M. *Circ Res* **2010,** *107* (9), 1058-70.
456. Muchowski, P. J.and Wacker, J. L. *Nat Rev Neurosci* **2005,** *6* (1), 11-22.
457. Baseler, W. A.; Dabkowski, E. R.; Williamson, C. L.; Croston, T. L.; Thapa, D.; Powell, M. J.; Razunguzwa, T. T.; Hollander, J. M. *Am J Physiol Regul Integr Comp Physiol* **2011,** *300* (2), R186-200.
458. Pratt, W. B.; Morishima, Y.; Peng, H. M.; Osawa, Y. *Experimental Biology and Medicine* **2010,** *235* (3), 278-289.
459. Rangaraju, S.; Madorsky, I.; Pileggi, J. G.; Kamal, A.; Notterpek, L. *Neurobiol Dis* **2008,** *32* (1), 105-15.
460. Peterson, L. B.and Blagg, B. S. *Future Med Chem* **2009,** *1* (2), 267-283.
461. Whitesell, L.and Lindquist, S. L. *Nat Rev Cancer* **2005,** *5* (10), 761-72.
462. Hadden, M. K.; Lubbers, D. J.; Blagg, B. S. *Curr Top Med Chem* **2006,** *6* (11), 1173-82.
463. Anckar, J.and Sistonen, L. *Annu Rev Biochem* **2011,** *80*, 1089-115.
464. Whitesell, L.and Lindquist, S. *Expert Opin Ther Targets* **2009,** *13* (4), 469-78.
465. Blagg, B. S.and Kerr, T. D. *Med Res Rev* **2006,** *26* (3), 310-38.
466. Donnelly, A.and Blagg, B. S. *Curr Med Chem* **2008,** *15* (26), 2702-17.
467. Hanahan, D.and Weinberg, R. A. *Cell* **2011,** *144* (5), 646-74.
468. Hayden, M. R.; Tyagi, S. C.; Kerklo, M. M.; Nicolls, M. R. *JOP* **2005,** *6* (4), 287-302.
469. Amolins, M. W.and Blagg, B. S. *Mini Rev Med Chem* **2009,** *9* (2), 140-52.
470. Urban, M. J.; Li, C.; Yu, C.; Lu, Y.; Krise, J. M.; McIntosh, M. P.; Rajewski, R. A.; Blagg, B. S.; Dobrowsky, R. T. *ASN Neuro* **2010,** *2* (4), 189-199.
471. Matts, R. L.; Brandt, G. E.; Lu, Y.; Dixit, A.; Mollapour, M.; Wang, S.; Donnelly, A. C.; Neckers, L.; Verkhivker, G.; Blagg, B. S. *Bioorg Med Chem* **2011,** *19* (1), 684-92.
472. Evans, C. G.; Wisen, S.; Gestwicki, J. E. *J Biol Chem* **2006,** *281* (44), 33182-91.
473. Sittler, A.; Lurz, R.; Lueder, G.; Priller, J.; Lehrach, H.; Hayer-Hartl, M. K.; Hartl, F. U.; Wanker, E. E. *Hum Mol Genet* **2001,** *10* (12), 1307-15.
474. Luo, W.; Dou, F.; Rodina, A.; Chip, S.; Kim, J.; Zhao, Q.; Moulick, K.; Aguirre, J.; Wu, N.; Greengard, P.*, et al. Proc Natl Acad Sci U S A* **2007,** *104* (22), 9511-6.
475. Dickey, C. A.; Kamal, A.; Lundgren, K.; Klosak, N.; Bailey, R. M.; Dunmore, J.; Ash, P.; Shoraka, S.; Zlatkovic, J.; Eckman, C. B.*, et al. J Clin Invest* **2007,** *117* (3), 648-58.
476. Waza, M.; Adachi, H.; Katsuno, M.; Minamiyama, M.; Sang, C.; Tanaka, F.; Inukai, A.; Doyu, M.; Sobue, G. *Nat Med* **2005,** *11* (10), 1088-95.
477. Marcu, M. G.; Chadli, A.; Bouhouche, I.; Catelli, M.; Neckers, L. M. *J Biol Chem* **2000,** *275* (47), 37181-6.
478. Marcu, M. G.; Schulte, T. W.; Neckers, L. *J Natl Cancer Inst* **2000,** *92* (3), 242-8.
479. Ansar, S.; Burlison, J. A.; Hadden, M. K.; Yu, X. M.; Desino, K. E.; Bean, J.; Neckers, L.; Audus, K. L.; Michaelis, M. L.; Blagg, B. S. *Bioorg Med Chem Lett* **2007,** *17* (7), 1984-90.
480. Lu, Y.; Ansar, S.; Michaelis, M. L.; Blagg, B. S. *Bioorg Med Chem* **2009,** *17* (4), 1709-15.
481. Neef, D. W.; Turski, M. L.; Thiele, D. J. *PLoS Biol* **2010,** *8* (1), e1000291.
482. Liu, A. Y.; Mathur, R.; Mei, N.; Langhammer, C. G.; Babiarz, B.; Firestein, B. L. *J Biol Chem* **2011,** *286* (4), 2785-94.
483. Brodsky, J. L.and Chiosis, G. *Curr Top Med Chem* **2006,** *6* (11), 1215-25.
484. Page, T. J.; Sikder, D.; Yang, L.; Pluta, L.; Wolfinger, R. D.; Kodadek, T.; Thomas, R. S. *Mol Biosyst* **2006,** *2* (12), 627-39.
485. Hayashida, N.; Fujimoto, M.; Tan, K.; Prakasam, R.; Shinkawa, T.; Li, L.; Ichikawa, H.; Takii, R.; Nakai, A. *EMBO J* **2010,** *29* (20), 3459-69.
486. Zhao, X.; Braun, A. P.; Braun, J. E. *Cell Mol Life Sci* **2008,** *65* (15), 2385-96.
487. Carrettiero, D. C.; Hernandez, I.; Neveu, P.; Papagiannakopoulos, T.; Kosik, K. S. *J Neurosci* **2009,** *29* (7), 2151-61.
488. Evans, C. G.; Chang, L.; Gestwicki, J. E. *J Med Chem* **2010,** *53* (12), 4585-602.

SECTION 1. MATERIALS AND METHODS

1.1. Animals

Male, six-week old, outbred Swiss-Webster (SW) mice were purchased from Harlan Laboratories (Indianapolis, IN) and acclimated for two weeks prior to starting the study. All animals were maintained on a 12 hour light/dark cycle at 70°F and 70% humidity with *ad libitum* access to water and Purina diet 5001 chow. All animal procedures (*e.g.* tagging, handling, fasting, blood draw, drug administration, euthanasia, and colony management) were performed according to Institutional Animal Care and Use Committee (IACUC) regulations and protocols as well as the standards and regulations for care and use of laboratory rodents established by the National Institutes of Health (NIH).

1.2. Induction of Diabetes

Streptozoticin [**STZ**, or 2-deoxy-2-(3-(methyl-3-nitrosoureido)-D-glucopyranose; Sigma Aldrich, St. Louis, MO] was used to chemically induce experimental T1DM in select SW mice (**Figure 17**). STZ is a nitrosourea alkyating agent whose glucose-moiety permits GLUT-2-mediated transport into rodent pancreatic β cells.[1-2] Upon entry, STZ methylates pancreatic β cell DNA, thereby inhibiting transcription and promoting cytotoxicity.[1-2] This destroys the majority of insulin-producing β cells to achieve a Type 1 diabetogenic state.[1-3]

Prior to inducing diabetes, all mice were designated into weight-matched, diabetic and non-diabetic treatment groups. After a six hour fast, mice identified for diabetes were administered a single intraperitoneal injection of 100 mg/kg STZ in 200 µl sterile saline buffered solution (10 mM sodium citrate; 154 mM NaCl; pH 4.5). Given STZ's instability in solution, pre-weighed STZ was mixed with the saline vehicle immediately prior to each

injection.[3] Fasted, non-diabetic mice received only the 200 µl saline vehicle. All injection sites were cleaned with 70% ethanol prior to injection. Food was reintroduced just after injection. This entire process was repeated the next day. Altogether, diabetes-designated mice received a total of 200 mg/kg STZ and *all* mice received a total of 400 µl saline vehicle. Fasting blood glucose (FBG) levels were measured (as described below) one week after the final STZ injection. Mice with FBG levels above 290 mg/dl were deemed diabetic and were admitted into the study. FBG measurements were conducted at study completion to assess the animal's acute metabolic state. HbA_{1C} levels (as described below) were also determined at study completion to gauge more long-term metabolic alterations.

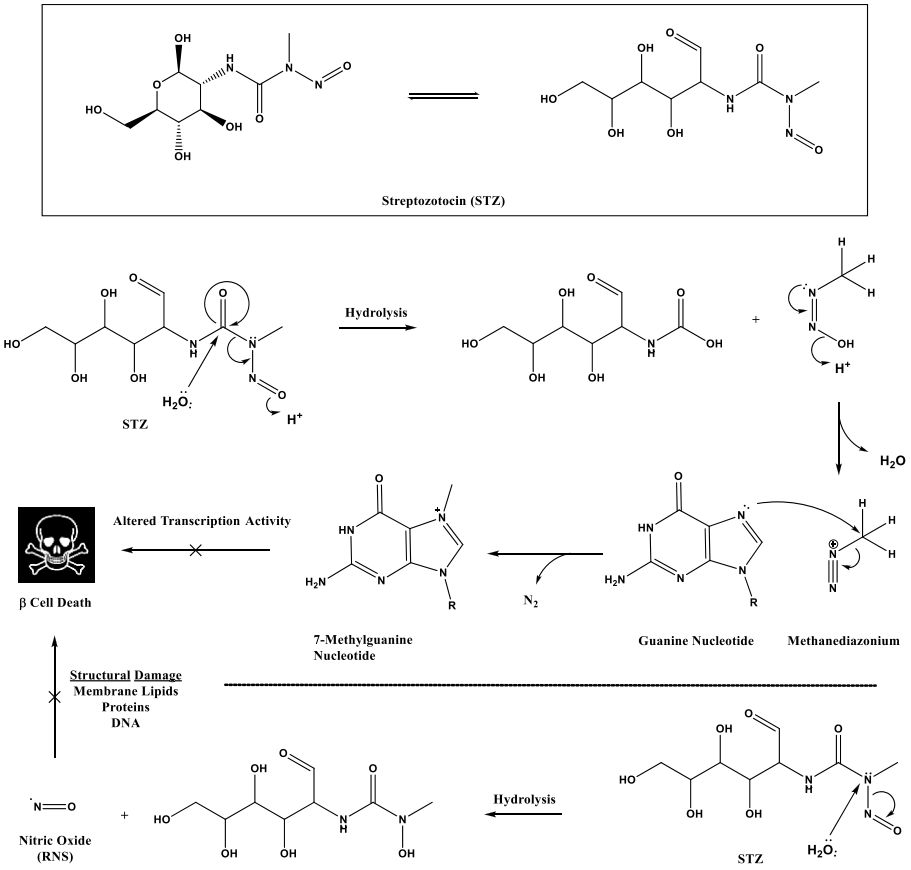

Figure 17. Proposed mechanism of action for streptozotocin in pancreatic β cells. STZ hydrolysis generates the DNA alkylating agent methanediazonium and the RNS nitric oxide. These species cause irreparable structural damage to DNA, proteins, and membrane lipids, thus resulting in pancreatic β cell death and a Type 1 diabetogenic state.[1-3]

In compliance with veterinary oversight and IACUC approval, a body condition score (BCS) was used to assess overall health deterioration in diabetic mice.[4] BCS1 denotes advanced muscular atrophy and extreme loss of subcutaneous fat deposits, which causes prominent indentions between the vertebrae and sharp protuberances of spinal processes (ileum and sacrum).[4] Throughout this study, a conscious effort was made to avoid BCS1. A $BCS1^+$ status was characterized by less severe fat loss and milder bony protuberances.[4] $BCS1^+$ diabetic mice that exhibited a hunched posture, sunken or closed eyes, lethargy, and seemed unlikely to improve, were generally euthanized after veterinary consult.

1.3. Fasting Blood Glucose and Glycated Hemoglobin Measurements

Venous blood was drawn from the tip of the tail for all FBG and HbA_{1C} measurements. FBG levels were determined using a commercial One-Touch Ultra glucometer (Lifescan, Milpitas, CA) following a 16-hour, overnight fast. Percent HbA_{1C} levels were measured using the A1C Now^+ multi test A1C kit (Bayer Healthcare, Sunnyvale, CA). HbA_{1C} levels at or above 6.5% were considered diabetic (comparable to humans).[5-7]

1.4. Drug Formulation and Treatments

STZ-diabetic mice were designated into untreated (**STZ + Veh**) and KU-32-treated (**STZ + KU-32**) groups after 16 weeks of STZ-diabetes. Non-diabetic mice were likewise divided into untreated (**Veh + Veh**) and KU-32-treated (**Veh + KU-32**) groups. In both cases, mice were weight-matched and BCS-matched so as to alleviate treatment bias.

KU-32 [*N*-(7-((2R,3R,4S,5R)-3,4-dihydroxy-5-methoxy-6,6-dimethyl-tetrahydro-2H-pyran-2-yloxy)-2-oxo-2-methyl-chromen-3-yl)acetamide] was synthesized and its structural purity was verified (> 95%) according to published procedures.[8-10] To overcome solubility constraints, KU-32 was dissolved in 0.1 M Captisol (CyDex Pharmaceuticals, Lenexa, KS)

in sterile 1X phosphate buffered saline (PBS) (137 mM NaCl; 2.7 mM KCl; 100 mM Na_2HPO_4; 2 mM KH_2PO_4; pH 7.4). 0.1 M Captisol and 5 mg/ml KU-32 (0.1 M Captisol) stock solutions were prepared fresh and sterile-filtered the morning prior to injections.

After 16 weeks, all mice received weekly intraperitoneal injections of 20 mg/kg KU-32 or a corresponding vehicle equivalent for 10 weeks. Treatments were based on the mass of the specimen (kg) the day prior to injection. Aliquots of 5 mg/ml KU-32 (0.1 M Captisol) stock needed for each 20 mg/kg dose were dispensed into sterile 1.7-ml microcentrifuge tubes. 200 µl of sterile 1X PBS was then added to help facilitate injections, giving a final working concentration of 20 mg/kg KU-32 in ~ 350 µl of ~ 43 mM Captisol. Each injection was performed using a sterile 1-ml syringe fitted with a 27-gauge, 3/4-inch long hypodermic needle (BD, Franklin Lakes, NJ) at injection sites precleaned with 70% ethanol. Control diabetic and non-diabetic mice were administered mass-dependent equivalents of 0.1 M Captisol with 200 µl of sterile 1X PBS, or ~ 350 µl of ~ 43 mM Captisol.

1.5. Assessment of Thermal Hypoalgesia

A Hargreaves Analgesiometer (Ugo Basile, Comerio, Italy) was used to assess responses to noxious thermal stimuli.[11-13] Mice were placed under a 1 L glass beaker on a glass platform and allowed to acclimate for 30-40 minutes. A focused beam of intensifying, radiating heat (0.3°C/s) was applied to the plantar surface of alternating hindpaws to determine paw withdrawal latencies (seconds). Individual paw readings were collected every five minutes to avoid hyperalgesia. Paw withdrawal latencies were measured 3-4 times per animal and then averaged. Hargreaves testing was conducted once during weeks 5, 9, and 13, and then weekly from weeks 15 to 26. The analgesiometer was calibrated prior at the start of each session using a heat flux radiometer (Ugo Basile). As discussed, the

Hargreaves test measures behavioral responses to slow, dull burning sensations as detected by polymodal nociceptors located on unmyelinated C-fibers.[13-15]

1.6. Assessment of Mechanical Hypoalgesia

A Dynamic Plantar Aesthesiometer (Ugo Basile) was used to monitor responses to noxious mechanical stimuli.[11-12, 16-17] Mice were acclimated for 30-40 minutes within a covered plastic cubicle, which rested upon a wire mesh platform. The upward application of a stiff von Frey monofilament (0.5 mm diameter steel fiber fitted to a force actuator) to the plantar surface of alternating hindpaws was used to assess pricking pain thresholds. As mentioned, pricking sensations are transduced by mechanical nociceptors found on thinly myelinated Aδ-fibers.[14, 18] Preliminary experiments found that applying the monofilament with an upward force of 10 g and a ramp speed of 2 seconds was necessary to provide a sufficient dynamic range to detect mechanical hypoalgesia in diabetic SW mice. Using these settings, a series of 5 recordings were collected roughly every 5 minutes per foot, measuring the force (grams) needed to trigger paw withdrawal and the latency associated with each response; these recordings were averaged for each animal. Von Frey testing was conducted once during weeks 4, 8, and 12, and then weekly from weeks 15 to 26. The anesthesiometer was calibrated using a 50 g steel weight prior to each testing session.

1.7. Nerve Conduction Velocity Measurements

NCV measurements were performed according to published procedures.[11-12] These measurements were conducted at weeks 16 (benchmark) and 26 (study completion). All mice were anesthetized via intraperitoneal injection of 100 mg/kg ketamine with 10 mg/kg xylazine. Mice were only operated upon after general anesthesia was confirmed using toe pinch and eye blink reflex methods. Electromyography for motor and sensory NCV

assessments were performed using a using a TECA™ Synergy N2-EMG Monitoring System (Carefusion, San Diego, CA) with 12 mm subdermal disposable platinum/iridium bipolar needle electrodes (Cardinal Health Neurocare, Madison, WI). Throughout this procedure, body temperature was monitored using a rectal probe and Physitemp TCAT-2DF Controller (Physitemp Instruments, Clifton, NJ) and was maintained at 37°C using a heat lamp.

1.7.1. Motor Nerve Conduction Velocity

To determine MNCV, electromyograms (EMGs) for proximal and distal compound muscle action potentials (CMAPs) were collected.[11-12] A stimulatory electrode was inserted through either the sciatic notch (proximal) or just above the calcaneous between the Achilles tendon and the tibia/fibula (distal). A recording electrode was embedded in the first plantar interosseous muscle. Three additional electrodes were implanted in nearby skin and muscle tissues to improve the signal:noise ratio. Electrical stimuli consisted of a 9.9 mA 0.05 ms duration square wave pulse. Resulting waveforms were filtered with low (3 kHz) and high (10 kHz) settings. Latencies were defined as the time between stimulus artifact and the onset of negative M-wave deflection. Each distal EMG was followed by a proximal EMG. MNCV (m/s) was calculated by dividing the physical straight line distance between proximal and distal stimulatory electrodes by the time difference between proximal and distal latencies. Three MNCV measurements were collected for each mouse and averaged.

1.7.2. Sensory Nerve Conduction Velocity

To determine SNCV, a series of 10 EMGs for sensory nerve action potentials (SNAPs) were collected and averaged to generate a single waveform.[11-12] A stimulatory electrode was inserted into the tip of the second hind toe. The recording electrode was emplaced just above the calcaneous between the Achilles tendon and the tibia/fibula. Electrical stimuli

consisted of ten 2.4-3.0 mA 0.05 ms duration square wave pulses. The resulting average waveform was filtered with low (3 kHz) and high (10 kHz) settings. Latency was defined as the time difference between stimulus artifact to the onset of peak negative deflection. SNCV (m/s) was determined by dividing the physical straight line distance between stimulating and recording electrodes by the latency. Since this was derived from an average of 10 SNAP EMGs, SNCV was calculated only once per animal.

1.8. Euthanasia and Tissue Harvesting

All mice were euthanized according to NIH guidelines and IACUC regulations and approved protocols. Upon completing NCV measurements, animals were euthanized by cardiac excision and then decapitation. Mice identified for euthanasia based upon BCS and veterinary consult were terminated using CO_2 asphyxiation and then decapitation. In all cases, select tissues and organs were harvested immediately thereafter.

Sciatic, tibial, and sural nerves were dissected and pooled from both hind limbs and cut into smaller segments in 200 µl mRIPA (modified radioimmunoprecipitation assay) buffer (50 mM Tris-HCl, pH 7.5; 1 mM EDTA; 1% Nonidet P-40; 0.5% deoxycholate; 0.1% SDS; 150 mM Na_3VO_4; 0.5 mM Na_2MoO_4; 40 mM NaF; and 10 mM β-glycerophosphate) containing 1X complete protease inhibitor cocktail (Roche Diagnostics, Indianapolis, IN) on ice. Tissues were homogenized using a Polytron fitted with a micro tissue tearor and centrifuged at 10,000 x g at 4°C for 10 minutes. The supernatant was collected, flash frozen on dry ice, and stored at – 20°C. With the exception of 3 representative mice from each treatment group at week 26, L4-L6 DRG were dissected from the lumbar intervertebral foramena for each mouse using a dissecting microscope (roots removed during extraction). DRG were processed in the same manner described for the nerves. The remaining 12 mice

at week 26 were used to establish adult DRG cultures to assess mitochondrial bioenergetics (described in **Establishment of Adult Sensory Neuron Cultures**).

Blood serum was collected for future processing after cardiac excision. Whole blood was vortexed with 50 µl of 0.3 M EDTA (ethylenediaminetetraacetic acid) containing 1X complete protease inhibitor cocktail. EDTA's calcium chelation properties serve as an artificial anticoagulant. Whole blood was centrifuged at 1,500 x g at 4°C for 15 minutes and the sera (supernatant) was collected, flash frozen on dry ice, and stored at – 80°C. Brain, liver, muscle, adipose, and kidney samples were also collected, flash frozen on dry ice, and stored at – 80°C for future processing.

The plantar integument ("foot pads") of both hindpaws were dissected and fixed with Zamboni's fixative (3% paraformaldehyde and 15% picric acid; Newcomer Supply, Middleton, WI) overnight at 4°C. All foot pads were washed 3 times with cold (4°C) PBS buffer with 3 mM NaN_3 (pH 7.4) and dehydrated in 30% sucrose (cryoprotectant) overnight at 4°C. These tissues were then embedded in Tissue-Tek optimal cutting temperature compound (OCT) (Sakura USA, Torrence, CA) on dry ice and stored at – 80°C for cryosectioning. Frozen foot pads were cut into 30 µm sections using a Leica CM3050 S Cryostat (Leica Biosystems, Buffalo Grove, IL). Samples were collected on Fisherbrand Superfrost Plus microscope slides (ThermoFisher Scientific, Waltham, MA) that were coded to obscure treatment and then stored at – 80°C until iENF density analysis.

1.9. Intraepidermal Nerve Fiber Density Analysis

For iENF density analysis, immunohistochemistry (IHC) was performed using rabbit anti-PGP 9.5 (ubiquitin C-terminal hydrolase) antibody (AbD Serotec, Oxford, UK) and a Vectastain Elite ABC-Peroxidase kit for rabbit IgG (Vector Laboratories, Burlingame, CA).

Slides were blocked in normal goat serum (NGS)-containing blocking buffer for 30 minutes and then incubated in a 1:1,000 dilution of anti-PGP 9.5 antibody in NGS-blocking buffer for 3 hours at room temperature. Slides were rinsed with PBS, incubated with secondary antibody for 1 hour at room temperature, and then rinsed again with cold PBS. The slides were then incubated in an avidin-biotin complex solution (ABC solution) for 1 hour at room temperature, rinsed with PBS, and then incubated with NovaRED peroxidase substrate solution (Vector Laboratories, Burlingame, CA) for 2-3 minutes. Slides were counterstained with hematoxylin (Vector Laboratories, Burlingame, CA) and coverslipped with Permount (ThermoFisher Scientific, Waltham, MA). Twelve digital images per animal were captured using a Zeiss Axioplan-2 light microscope (Carl Zeiss Microimaging, Thornwood, NY) with a color CCD digital camera (Diagnostic Instruments Inc., Sterling Heights, MI). Single immunopositive nerve fibers crossing the dermal/epidermal junction were quantified by blinded observers (branching within the epidermis was disregarded).[19] iENF density was calculated by dividing the number of fibers by the length of the dermal/epidermal junction (fibers/mm). Treatment effects upon dermal nerve fiber density were also assessed by tracing individual PGP 9.5-immunopositive nerve fibers and summing fiber area using ImageJ software (http://imagej.nih.gov/ij/). This was divided by the total dermal area to generate a percentage of fiber-occupied space in the dermis.

1.10. Measuring Mitochondrial Bioenergetics in Adult Sensory Neurons

1.10.1. Establishment of Adult Sensory Neuron Cultures

Three representative mice from each treatment group were used to establish adult sensory neuron cultures at 26 weeks. This was conducted according to published protocols with minor modifications.[20] Lumbar spinal columns were removed and transported in 1X

PBS to a sterile hood[†], where the spinal cord was dislodged using a gentle stream of sterile 1X PBS delivered through a 10 ml syringe. L4-L6 DRG were excised using a dissecting microscope and pooled by treatment group (n = 3 mice/group) in 1 ml of Ham's F10 medium (Corning cellgro/Mediatech, Manassas, VA) containing 10% fetal calf serum (Atlas Biologicals, Fort Collins, CO) on ice. After trimming the nerve roots and connective tissue, pooled DRG were transferred to 1 ml of serum-free F10 medium. DRG were then dissociated by adding 1 ml of 1.25% collagenase (Gibco/Invitrogen, Carlsbad, CA) for 45 minutes (37°C) and then adding 1 ml of 2% trypsin (Gibco/Invitrogen) for 30 minutes (37°C). Cells were isolated from the media by centrifugation at 1,000 x g at 4°C for 5 minutes, and the cell pellet was resuspended in serum-free F10 medium and triturated using a fire-polished glass pipette. The cell suspension was carefully layered on top of a 10 ml gradient of iso-osmotic Percoll [0.9 ml of 10X PBS; 6.485 ml ddH_2O; 2.615 ml Percoll (Sigma-Aldrich, St. Louis, MO)] and centrifuged at 800 x g at 4°C for 20 minutes to remove cell debris and myelin fragments. The pellet was resuspended in 5 ml of serum-free F10 medium and filtered through a 40 μm nylon sieve (Mt. Baker Bio, Everett, WA); the sieve was rinsed with 5 ml of fresh medium. Sensory neurons were recovered by centrifugation and were resuspended in F10 (6.1 mM glucose) maintenance medium containing 50 ng/ml NGF (Harlan Biosciences, Indianapolis, IN), 1 ng/ml NT-3 (Harlan), and N2 supplement (Invitrogen) without insulin. These neurons were seeded on a specialized 96-well plate [XF96 Cell Culture Microplate (Seahorse Biosciences, North Billerica, MA)] that was pre-coated with poly-DL-ornithine (0.5 mg/ml overnight) and then laminin (2 mg/ml for 3 hours). For each treatment group, pooled neurons were plated on 4-5 wells at 5 x 10^3 cells/well containing maintenance medium and maintained for 48 hours *ex vivo* (**Figure 18**).

[†] Subsequent procedures conducted under sterile conditions

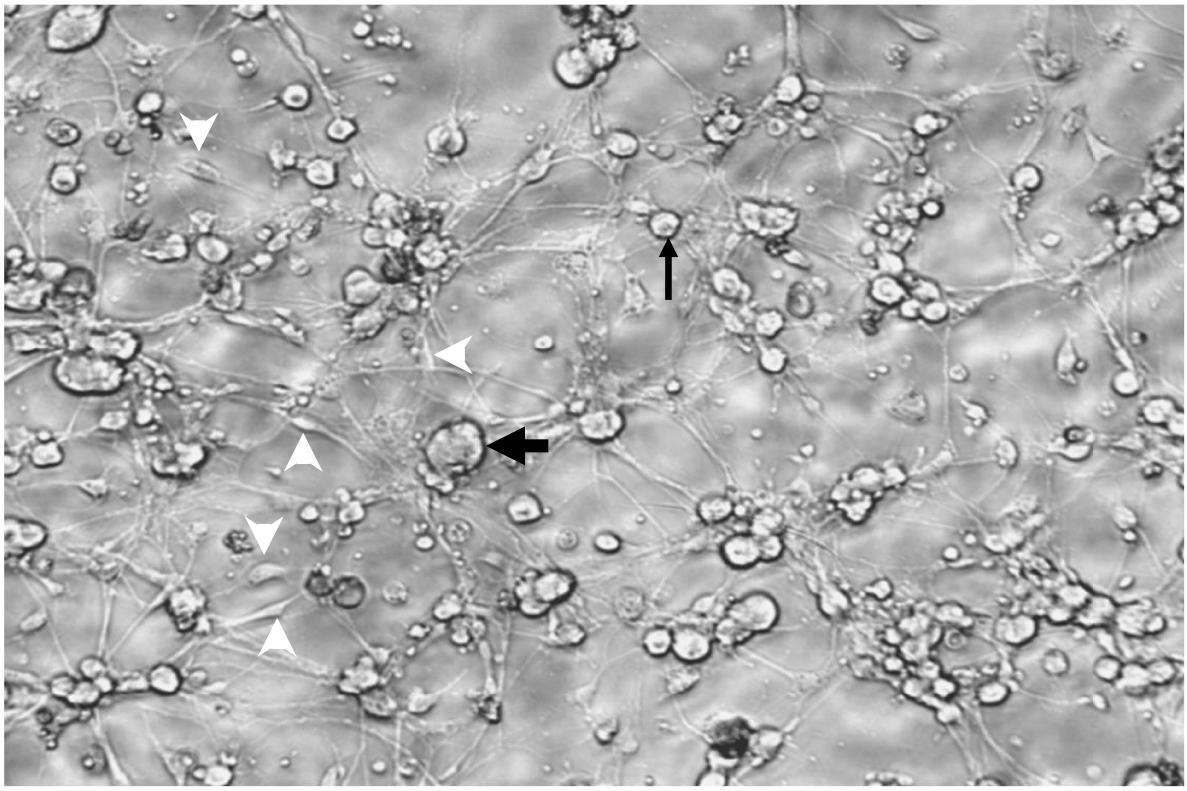

Figure 18. Neurite outgrowth in intact adult sensory neuron cultures. Phase contrast image shows axons extending from large (*e.g.* thick arrow) and small (*e.g.* thin arrow) DRG after 48 hours in culture. Examples of non-neurons are indicated by white arrowheads.

1.10.2. Assessment of Mitochondrial Bioenergetics

The 96-well Extracellular Flux (XF96) Analyzer (Seahorse Biosciences) uses two calibrated optic sensors to non-invasively assess oxygen consumption rates (OCRs) in viable cells that remain attached to the bottom of the microplate wells.[21] After 48 hours in culture, adult sensory neurons were incubated in bicarbonate-free DMEM (5.5 mM D-glucose) for 1 hour at 37°C. Basal OCR readings (**teal; Figure 19**) were collected in the XF96 Analyzer using 4 measurement loops that each consisted of a 2 minute mix and 5 minute measurement cycle. These measurement loops were repeated after injecting each respiratory chain inhibitor. ATP-coupled oxygen consumption (**blue**) was calculated as a percent basal OCR sensitive to 1 μg/ml oligomycin (Sigma), an ATP synthase inhibitor. Maximal functional

assessments of the respiratory chain [maximal respiratory capacity, or MRC (**red**)] were also conducted by depolarizing the mitochondrial inner membrane potential with 1 µM FCCP [carbonylcyanide-4-(trifluoromethoxy)-phenylhydrazone] (Sigma); protonophore effects were expressed as percent basal OCR. Working oligomycin and FCCP concentrations (indicated above) were optimized in earlier experiments. Spare respiratory capacity, or SRC (**magenta**), is the arithmetic difference between the MRC and the basal OCR and depicts how close the mitochondria are to operating at their bioenergetic limit. Non-mitochondrial (**green**) OCRs values were obtained from other wells. After respiratory measures, cells were harvested and rate values for each well were normalized to relative protein content. To determine protein content, each well was washed three times with cold (4°C) 1X PBS and cells were lysed in cold (4°C) mRIPA buffer with 1X complete protease inhibitor cocktail on ice. Protein levels were determined (in triplicate) using lysate aliquots and the DC Protein Assay (Bio-Rad, Berkeley, CA).

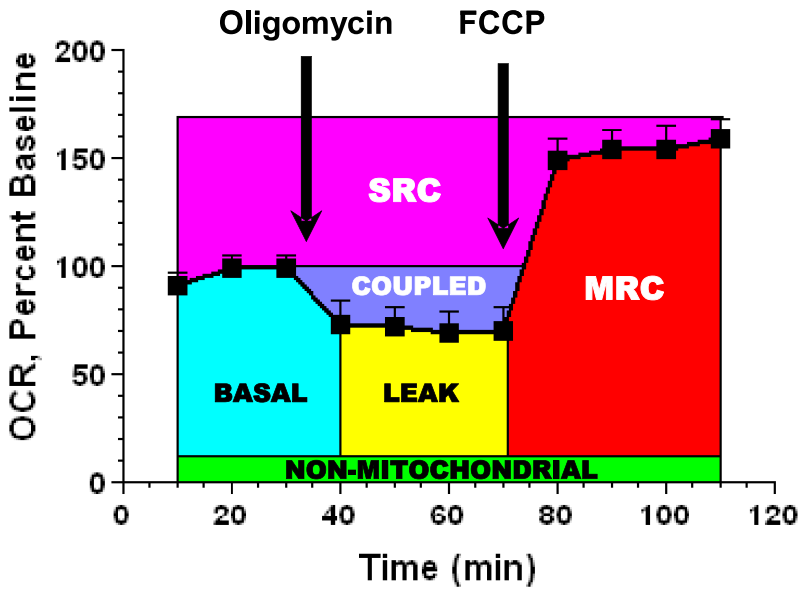

Figure 19. Schematic Seahorse XF96 Analyzer graph interpretation. Abbreviations: OCR (oxygen consumption rate); SRC (spare respiratory capacity); MRC (maximal respiratory capacity); and FCCP [carbonylcyanide-4-(trifluoromethoxy)-phenylhydrazone]. See text for in-depth description. (Adapted from Brand and Nicholls).[21]

1.11. Immunoblot Analyses

Immunoblotting (IB) was performed on tissue homogenates. Protein samples were thawed on ice and quantified via DC Protein Assay to determine the sample volume needed for 10 μg of protein. This sample volume was used to generate a 40 μl sample solution containing 10 μl of 4X Sample Buffer [20% glycerol; 6% β-mercaptoethanol; 4% SDS (sodium dodecyl sulfate); 0.5% bromphenol blue; and 6.25% 4X Upper Tris buffer (0.5 M Tris HCl; 4% SDS; pH 6.8)]. Samples were boiled at 100°C for 5 minutes, separated by SDS-PAGE (polyacrylamide gel electrophoresis), transferred to a nicrocellulose membrane overnight, and stored in PBS-T (PBS buffer with Tween-20) at 4°C. Membranes were blocked with three 20-minute washes of 5% milk in PBS-T via gentle rocking; 5% bovine serum albumin alternatively used to detect phosphorylated proteins. Membranes were then incubated with primary antibodies (diluted in blocking buffer) overnight (16-17 hours) at 4°C, with the exception of β–actin (two hours at room temperature). These membranes were washed in 5% blocking buffer three times for ten minutes each. Upon completion, membranes were incubated with appropriate secondary antibodies for 1 hour at room temperature (β–actin) or 3 hours at 4°C (all others). All membranes were washed three times for 5 minutes with PBS-T and incubated with an HRP-conjugated chemiluminescence detection kit (ECL Plus Western Blotting Detection Reagents, Amersham Biosciences, Buckinghamshire, UK). Autoradiography film was exposed to this chemiluminescent signal, developed, and the bands were quantified via densitometry using ImageJ software. **Table 3** summarizes the key antibodies used for presented data.

Table 3. List of antibodies used.

Antibody	*Use*	*Manufacturer*	*Catalog*
PGP 9.5	IHC	AbD Serotec	7863-0504
Hsp72	IB	Stressgen	ADI-SPA-812
GAP-43	IB	Neuromics	RA22115
pSer(41)GAP-43	IB	Santa Cruz Biotechnology	SC-17109-R
pSer(473)Akt	IB	Cell Signaling Technology	4060S
β-actin	IB	Santa Cruz Biotechnology	SC-47778
Goat anti-Rabbit HRP	IB	Santa Cruz Biotechnology	SC-2004
Goat anti-Mouse HRP	IB	Santa Cruz Biotechnology	SC-2005

1.12. Statistical Analyses

All data are presented as mean ± SEM. After verifying equality of variances, differences between treatment groups were determined using one-way/two-way ANOVA. Significant differences between group means were established using the Tukey HSD posthoc test. Statistical analyses were performed using Systat 12 (Systat Software, Chicago, IL) and portrayed using Graphpad Prism (Graphpad Software, Inc., La Jolla, CA).

SECTION 2. EXPERIMENTAL DESIGN

To test the hypothesis that *KU-32 intervention will improve morphological, psychophysical, electrophysiological, and bioenergetic indices of DSPN at more chronic stages*, a 16-week intervention study was designed using SW mice (**Figure 20**). Although these mice were expected to be more resilient to the effects of chronic experimental T1DM as compared to C57BL/6 mice, some disease-associated mortality was still anticipated and considered in the study design. Hence, STZ-diabetes was induced in 42 of 73 mice (~ 58%) at week 0, while 31 mice (~ 42%) were kept non-diabetic. To alleviate sex and body weight bias upon drug efficacy, only male mice were used and all mice were weight-matched. After 4 weeks, periodic Hargreaves and Von Frey testing were conducted to monitor

progressive hypoalgesia. At 16 weeks, representative STZ-diabetic (n = 4) and non-diabetic (n = 4) mice were euthanized to confirm NCV deterioration and for benchmark tissue collection. FBG and HbA_{1C} readings were taken to verify altered metabolic states. Select control (n = 13) and STZ-diabetic (n = 14) mice were administered (IP) 20 mg/kg KU-32 or corresponding vehicle equivalents (all other mice) on a weekly basis for ten weeks. Weekly Hargreaves and von Frey testing commenced one week prior to injections (week 15) and lasted until study completion at 26 weeks. Injections were conducted each week after behavioral testing so as to minimize possible influences of injection site soreness on behavioral responses. At 26 weeks, NCV, FBG, and HbA_{1C} measurements were collected for all mice and tissues were harvested and stored as described. Mitochondrial bioenergetic, iENF density, and molecular assessments were conducted shortly after study completion.

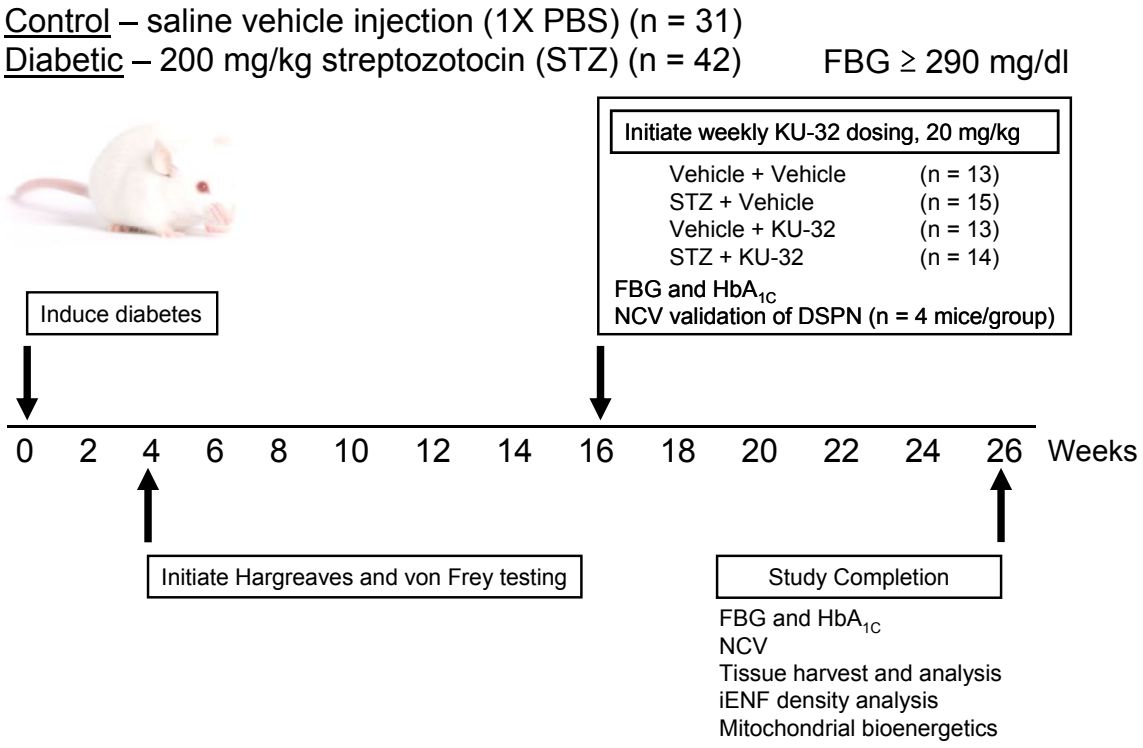

Figure 20. Experimental design for 16-week intervention study in SW mice.

SECTION 3. RESULTS

3.1. KU-32 Does Not Alter Overall Glycemic Control

After 26 weeks of untreated STZ-diabetes, body weight was significantly decreased and both FBG and HbA_{1C} were significantly elevated relative to untreated non-diabetic mice (**Table 4**). As expected, KU-32 intervention at 16 weeks had no impact upon body weight, FBG, and HbA_{1C} levels as compared to untreated diabetic and non-diabetic controls. These results are similar to those in our previous 12-week intervention studies in C57BL/6 mice and indicate that variations in mouse strain and drug schedule are insufficient to improve overall glycemic control.[12] It is interesting to note that during the drug intervention period, almost half (7 of 15) of untreated diabetic mice abruptly died (4) or required early euthanizing (3) due to a poor BCS. In contrast, none of the KU-32-treated animals abruptly died and only 3 of 14 mice were euthanized early due to a poor BCS.

Table 4. Effects of STZ-diabetes and KU-32 on metabolic parameters.

Treatment	*Body Weight (g)*	*n*	*FBG (mg/dl)*	*HbA_{1C} (%)*	*n*
Veh + Veh	46.9 ± 5.0	11	101 ± 19	4.6 ± 0.6	6
Veh + KU-32	44.3 ± 3.2	9	109 ± 29	4.6 ± 0.4	6
STZ + Veh	36.0 ± 6.6*	8	533 ± 114*	11.8 ± 1.1*	6
STZ + KU-32	37.7 ± 4.0*	11	571 ± 55*	11.9 ± 0.3*	6

*, $p < 0.001$ versus Veh + Veh

3.2. KU-32 Rescues Electrophysiological Deficits

After 16 weeks of diabetes, MNCV decreased 17% from 58.6 ± 1.0 to 48.9 ± 2.0 m/s ($p < 0.001$; $n = 4$), whereas SNCV reductions were more modest from 40 ± 0.1 to 36.2 ± 1.1 m/s ($p < 0.05$; $n = 4$). After 26 weeks of untreated diabetes, MNCV and SNCV remained significantly lower than untreated non-diabetic controls (**Figure 21**). In untreated diabetics, MNCV decreased to 41.3 ± 4.1 m/s by 26 weeks (30% total reduction). KU-32 intervention

at 16 weeks not only prevented further MNCV decline but also reversed the pre-existing deficit to within normal control levels. Similarly, KU-32 rescued diabetic SNCV deficits at 16 weeks (37.4 ± 0.8 m/s) to within normal control levels by 26 weeks. These NCV results reflect those observed in previous 12-week intervention studies in C57BL/6 mice, with the exception that SNCV reductions in diabetic SW mice were only half that of diabetic C57BL/6 mice.[12] This is most likely attributed to differences between mouse strains.

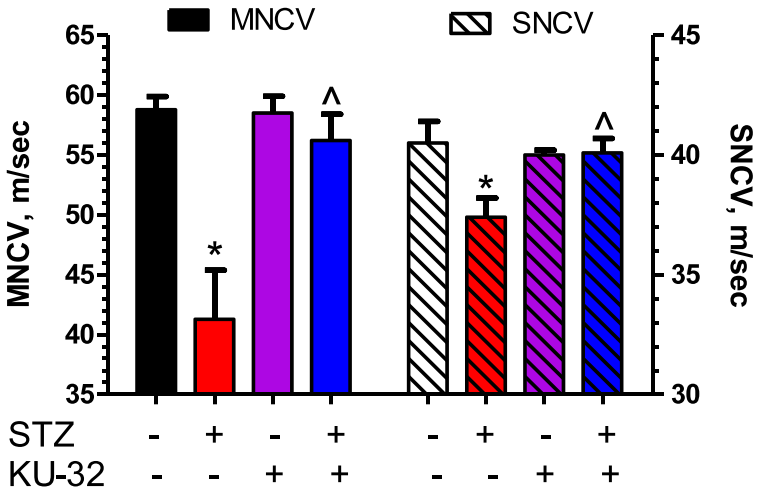

Figure 21. KU-32 rescues NCV deficits. Ten weeks of KU-32 treatment significantly improved diabetes-induced MNCV (solid bars; left axis) and SNCV (striped bars; right axis). *, $p < 0.05$ versus Veh + Veh; ^, $p < 0.05$ versus STZ + Veh.

3.3. KU-32 Improves Sensory Hypoalgesia

After 4 weeks of STZ-diabetes, mechanical and thermal pain thresholds were assessed on alternate weeks. These measurements were collected once every 4 weeks until week 15, where both tests were performed each week until study completion at 26 weeks.

3.3.1. Improvements to Mechanical Hypoalgesia

While the mechanical (pricking) pain thresholds (force in grams) necessary to trigger paw withdrawal in untreated non-diabetic mice remained steady at ~ 5.5 g, untreated diabetic mice demonstrated a significant increase in stimuli intensity requirements by 4

weeks (**Figure 22**). These thresholds progressively worsened until 18 weeks, where force requirements plateaued at ~ 9.5 g for the remainder of the study. Relative to untreated diabetic mice, KU-32 induced a time-dependent recovery in diabetic mechanical sensitivity after only one week of treatment. After six weeks, mechanical thresholds for KU-32-treated diabetic mice were indistinguishable from untreated non-diabetic mice. KU-32 had no adverse effects in non-diabetic mice.

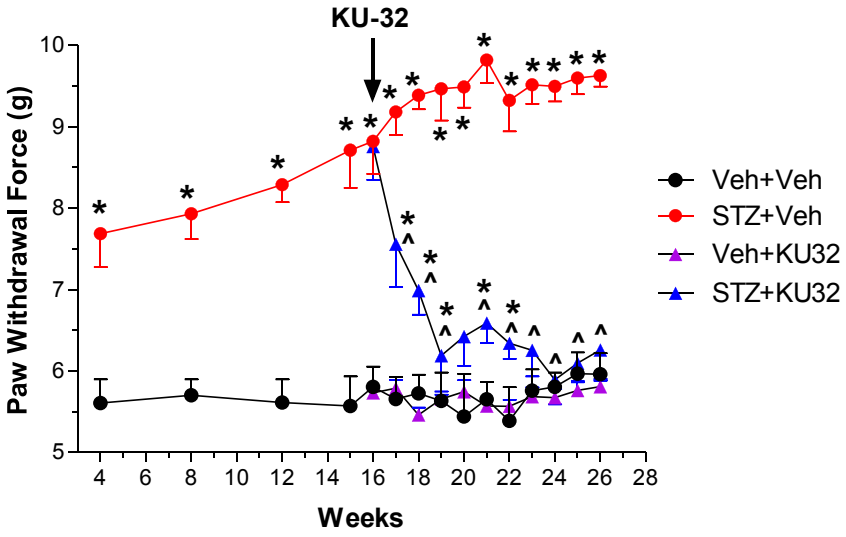

Figure 22. KU-32 restores normal mechanical thresholds. Responses to pricking stimuli (von Frey monofilament) applied at an increasing intensity (force in grams) were assessed. These mechanical pain thresholds gradually increased and maxed at ~ 18 weeks in untreated diabetic mice. KU-32 intervention at 16 weeks restored these mechanical thresholds back to non-diabetic levels. *, $p < 0.05$ versus time-matched Veh + Veh; ^, $p < 0.05$ versus time-matched STZ + Veh.

3.3.2. Improvements to Thermal Hypoalgesia

STZ-diabetes caused a significant increase in paw withdrawal latency to intensifying thermal stimuli (thermal pain thresholds) by 5 weeks (**Figure 23**). While paw withdrawal latencies averaged 5.5 s for non-diabetic mice throughout this study, untreated diabetic mice plateaued at ~ 10 s between 14 and 24 weeks. While KU-32 had no adverse effects in untreated non-diabetic mice, the drug induced a significant, time-dependent improvement in

diabetic paw withdrawal latencies throughout the study. Thermal thresholds for KU-32-treated diabetic mice became indistinguishable from non-diabetics only at 10 weeks of drug treatment. Though KU-32 improved both thermal and mechanical thresholds, the rate of recovery differed substantially. This suggests that KU-32 may affect myelinated and unmyelinated nociceptive nerve fibers differently.

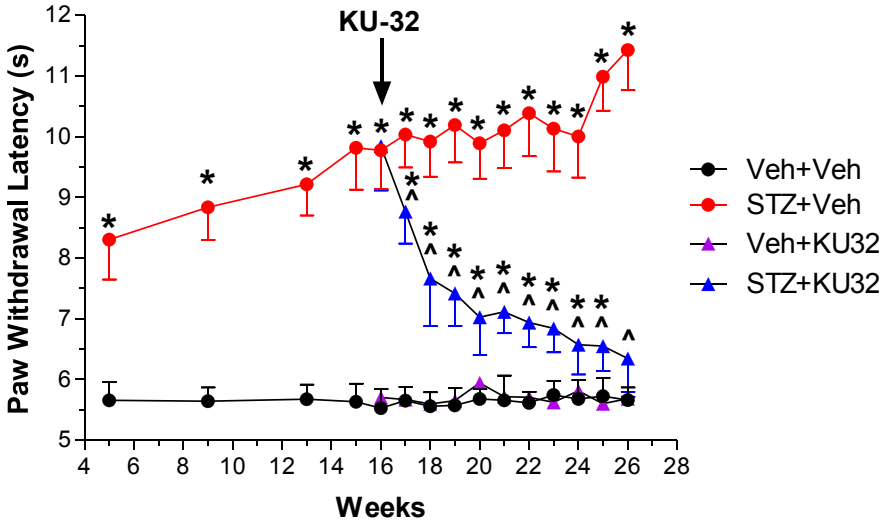

Figure 23. KU-32 reestablishes normal thermal thresholds. Paw withdrawal latencies (seconds) to intensifying thermal stimuli were assessed. These latencies gradually increased and plateaued between 14 and 24 weeks in untreated diabetic mice. Over 10 weeks, KU-32 restored thermal thresholds back to non-diabetic levels. *, $p < 0.05$ versus time-matched Veh + Veh; ^, $p < 0.05$ versus time-matched STZ + Veh.

3.4. KU-32 Partly Improves Cutaneous Innervation

3.4.1. Improvements to iENF Density

Recovery of normal thermal thresholds can occur without any improvements to iENF density.[22-24] To explore KU-32's neuroprotective effects, iENF density was assessed at 16 and 26 weeks (**Figure 24**). Prior to drug intervention at 16 weeks, diabetic mice exhibited a 31% reduction in iENF density. This deficit allowed us to determine whether KU-32 could improve this morphological index of DSPN and to assess its correlation with

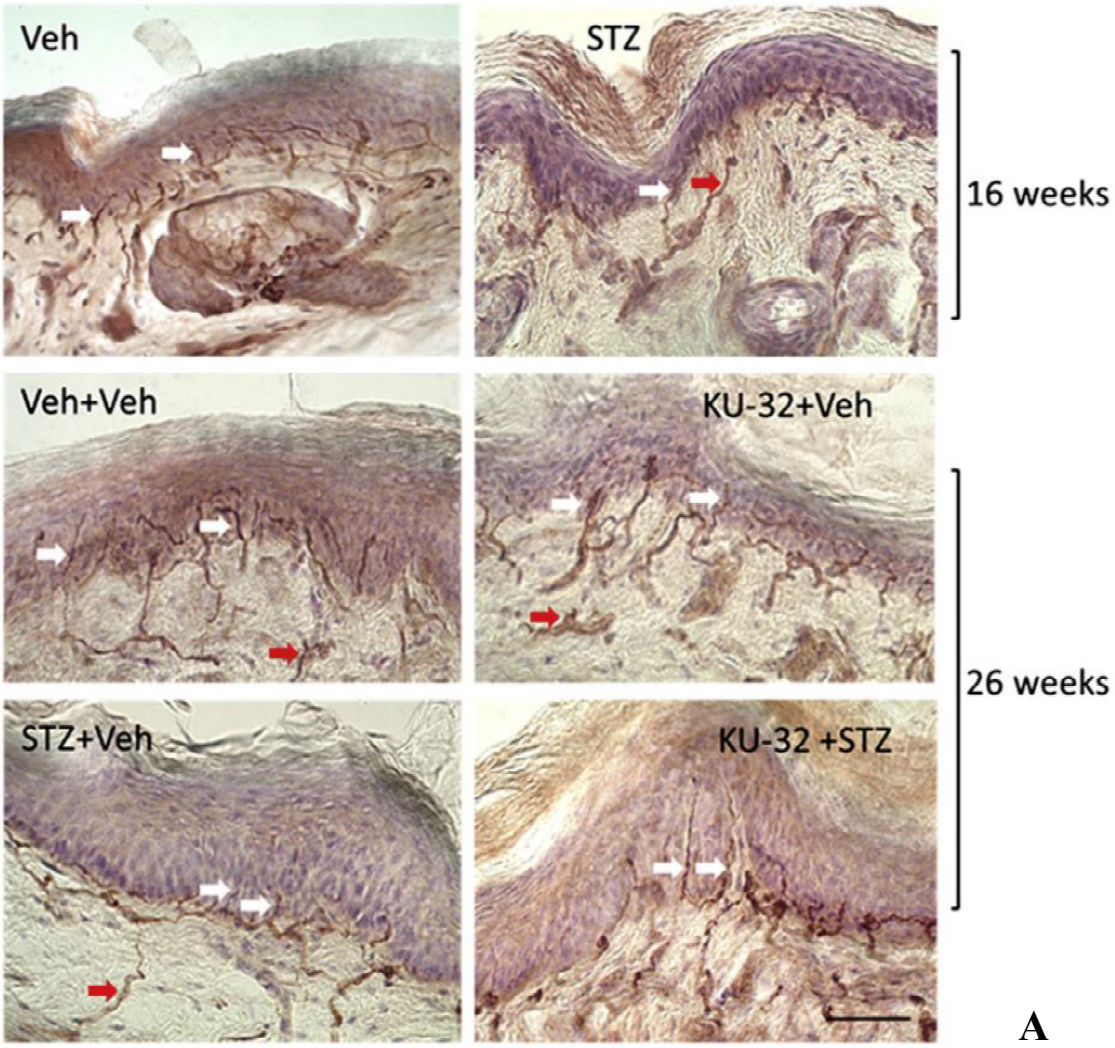

Figure 24. KU-32 improves cutaneous innervation. (A) Representative IHC images for 16- and 26-week treatment groups; scale bar = 40 µm. Arrows show examples of iENFs (white) and dermal nerve fibers (red) that were counted. (B) Analysis of iENF densities. **, $p < 0.01$ versus Veh + Veh; ^, $p < 0.05$ versus STZ + Veh.

improvements in thermal pain thresholds. After 26 weeks of untreated diabetes, iENF density was 29% less than untreated controls (unchanged compared to 16-week diabetics). KU-32 intervention in diabetic mice significantly improved iENF density to within 11% of untreated controls. These effects were not observed in previous intervention studies due to a lack of measureable iENF loss and excessive mortality in STZ-diabetic C57BL/6 mice.[11-12] KU-32 had no effect on iENF density in non-diabetic mice.

3.4.2. Correlations Between iENF Density and Thermal Hypoalgesia

After plotting each animal's thermal paw withdrawal latency versus its iENF density, a significant inverse correlation was established between untreated diabetic and non-diabetic mice (**Figure 25**). K-means cluster analysis revealed that while most KU-32-treated diabetic mice (7) statistically clustered with non-diabetic mice, a subpopulation of KU-32-treated diabetic mice (4) remained more closely associated with untreated diabetic mice. These KU-32-treated diabetic mice had significantly fewer fibers than the other drug-treated mice ($p < 0.006$, Mann-Whitney test), but still showed significant improvements in thermal pain thresholds. Why this recovery occurred without iENF density improvements remains unclear. One possibility may lie with the genetic heterogeneity of the outbred strain, but a larger sample size is needed to determine this. Other explanations may involve alterations to thermal nociceptor expression or nociceptive information relay. Although we can not distinguish whether KU-32 invigorates new fiber growth or suppresses degeneration, morphological improvements are still evident and provide great promise towards treating more humanistic hallmarks of DSPN. However, given the lack of additional nerve fiber loss between 16 and 26 weeks of diabetes, it seems reasonable that KU-32 may enhance neurite outgrowth. KU-32-treated non-diabetic mice remained clustered with untreated controls.

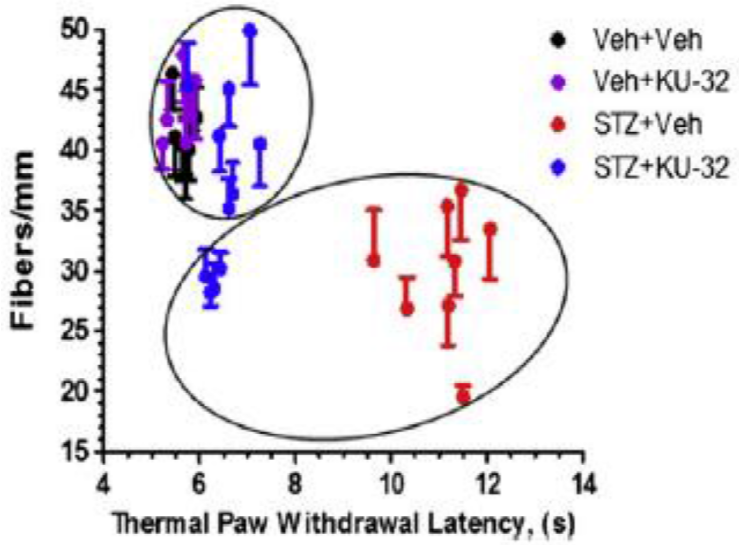

Figure 25. Thermal thresholds correlate to reductions in iENF density. Thermal paw withdrawal latency (s) was plotted against iENF density for each animal and subjected to k-means cluster analysis. Encircled regions indicate cluster membership and show that only a small subset of KU-32-treated diabetic mice (n = 4) demonstrated significant recoveries in thermal thresholds without improving iENF density.

3.4.3. Drug Intervention Does Not Alter Dermal Nerve Fiber Density

The percent area occupied by PGP 9.5-immunopositive dermal nerve fibers were normalized to the total dermal area. Although diabetes trended toward decreasing dermal fiber area, no significant differences were observed between treatment groups (Veh + Veh, 5.9 ± 1.0%; Veh + KU-32, 5.7 ± 1.9%; STZ + Veh, 4.8 ± 1.7%; STZ + KU-32, 5.2 ± 1.1%).

3.5. KU-32 Improves Mitochondrial Function in Diabetic Sensory Neurons

Adult sensory neurons were isolated from L4-L6 DRG at week 26 since they generate the myelinated and unmyelinated nerve fibers mainly affected by DSPN and KU-32. A key advantage to working with adult sensory neurons is that they have been exposed to the physiological milieu of experimental T1DM and exhibit molecular deficits associated with a diabetogenic phenotype.[25-27] Using intact sensory neurons also avoids artifacts commonly associated with mitochondrial isolation from DRG. However, one drawback is that the

primary cultures are not pulsed with anti-mitotics, which helps alleviate Schwann cell and fibroblast contamination, which are normally eradicated during the establishment of embryonic primary cultures.[28] Even so, this enriched neuronal preparation promotes neurite outgrowth and temporarily retains an adult neuronal phenotype.[29]

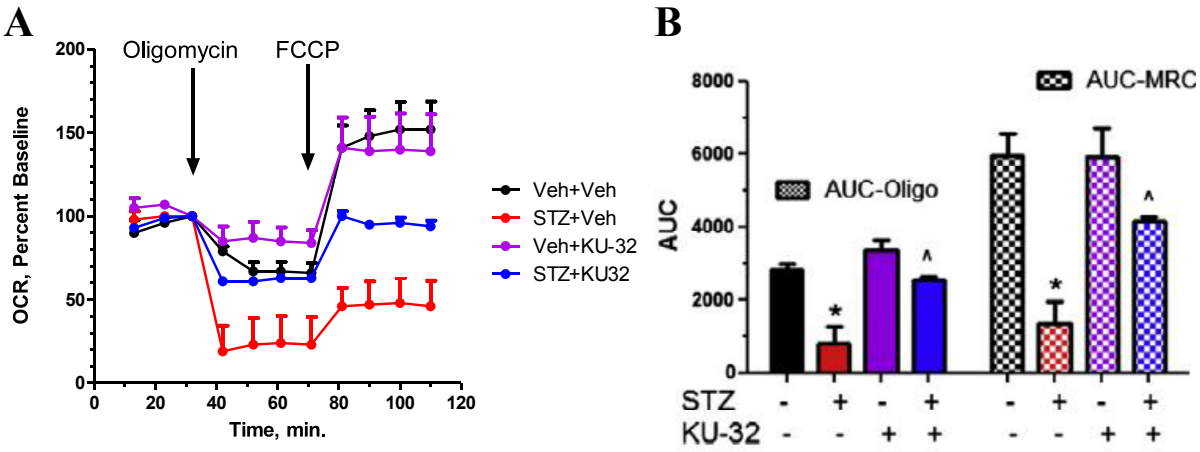

Figure 26. KU-32 improves mitochondrial function in diabetic sensory neurons. (A) Graph of XF96 Seahorse data showing oligomycin and FCCP effects on OCR in adult sensory neurons isolated from each treatment group (n = 4-5 wells derived from 3 mice per group) at 26 weeks. (B) Area under the curve (AUC) analysis indicates significantly altered ATP-coupled respiration (solid bars) as determined by oligomycin-sensitivity and decreased MRC (hatched bars) as determined by FCCP-sensitivity. Both parameters were significantly enhanced in KU-32-treated diabetic mice compared to untreated diabetics. *, $p < 0.05$ versus time-matched Veh + Veh; ^, $p < 0.05$ versus time-matched STZ + Veh.

Sensory neurons isolated from 26-week untreated diabetic mice exhibited an ~ 80% decrease in oligomycin-sensitive OCR (**rate 7; Figure 26A**). This was over twice that of sensory neurons from untreated controls (~ 35%). Since oligomycin inhibits ATP synthase, these data suggest that diabetic sensory neurons devote most of their basal O_2 consumption to ATP synthesis, which may be a compensatory measure for compromised electron transport through the respiratory complexes. Sensory neurons from KU-32-treated diabetic mice demonstrated a significant improvement in oligomycin-sensitive OCR to ~ 40%, which about half that of untreated diabetics. This suggests that KU-32 can either enhance ATP

synthesis efficiency or reduce overall ATP requirements in chronically stressed diabetic sensory neurons. After FCCP (protonophore) injection, sensory neurons from KU-32-treated diabetic mice exhibited a much higher and significant rebound in MRC compared to untreated diabetic sensory neurons (**rate 11; Figure 26A**). However, neither diabetic group successfully generated an SRC to reinforce metabolic support, suggesting that diabetic sensory neurons already operate at maximal capacity. Even so, the improved MRC indicates that KU-32 promotes resiliency in sensory neurons subjected to prolonged metabolic stress. In all cases, statistical significance between treatment groups was determined by integrating the area under the curve (AUC) for rates 4-7 (oligomycin-sensitive) and rates 8-11 (FCCP-sensitive) (**Figure 26B**).

Since completing this study, we have adopted a new method to assess non-mitochondrial oxygen consumption through a final coinjection of rotenone[†] and antimycin A[†], which inhibits respiratory complexes I and III and halts mitochondrial respiration.[30] Regardless of whether non-mitochondrial OCRs are altered in DSPN, it does not detract from the fact that oligomycin- and FCCP-sensitive differences in OCRs occurred between treatment groups. In addition, 1 mM pyruvate is not incorporated into the bicarbonate-free DMEM medium prior to XF96 analysis to establish a more pronounced MRC and SRC across all treatment groups.[30] Even so, all sensory neurons in this study had free access to 5.5 mM glucose-rich medium and endogenous pyruvate stores, which permits an appropriate measure of basal and drug-sensitive OCR changes. The fact that OCRs remained largely consistent throughout each measurement loop suggests that these resources were never fully depleted during these measurements, which further validates the results of this study.

[†] 1 mM working concentration

SECTION 4. DISCUSSION AND CONCLUDING REMARKS

These results support our previous proposal that pharmacologic Hsp90 modulators can provide sensory neurons and peripheral nerves with the edge needed to endure the austere physiological milieu associated with DSPN. In our previous work, we demonstrated that our novel C-terminal Hsp90 modulator, KU-32, improves several clinical indices of negative symptoms associated with small and large fiber dysfunction without affecting metabolic control of the disease.[12] We also established that these effects were dependent upon the functional expression of inducible Hsp70 (Hsp70.1 and Hsp70.3 in mice).[12] In this study, we have shown that KU-32 significantly improves *electrophysiological*, *psychophysical*, *morphological*, and *bioenergetic* indices of DSPN at more chronic stages of development, thus supporting our hypothesis. Most importantly, this pharmacotherapeutic strategy may represent the first effective treatment option for the negative symptoms of DSPN. However, the resounding question still reverberates: "How does KU-32 afford these neuroprotective effects in DSPN?"

4.1. KU-32's Impact on Hsp90

It is unclear as to whether KU-32 elicits an HSR in diabetic sensory neurons and peripheral nerves or simply alters normal Hsp90 interactions via allosteric modulation. While KU-32 does induce a robust HSR (especially Hsp70) in cultured embryonic sensory neurons, evidence of HSR induction in adult diabetic tissues has been inconsistent.[12, 31] Then again, the fact that most DRG differentiate and adopt distinct phenotypes as they mature [*e.g.* fiber type, fiber length, sensory modality(ies), and neuropeptide expression] may partly explain these differences.[32-34] Variations in KU-32-induced recovery rates for mechanical and thermal hypoalgesia in diabetic mice support the notion of differential drug

effects by fiber type. It must also be considered that most tissues from intervention studies are collected at study completion, which is 6-10 weeks after the first KU-32 injection and nearly one week after the final injection.[12] In contrast to *in vitro* drug treatments, *in vivo* pharmacokinetics can also significantly alter the amount and extent of drug exposure in diabetes-relevant tissues.[35] Hence, if KU-32 only induces a transient HSR immediately after an injection or only during the initial weeks of treatment, then evidence of a robust HSR could be missed.

Alternatively, it should be considered that an HSR may not be required. Novobiocin (**Figure 27**) is thought to bind to Hsp90's C-terminal nucleotide-binding domain and disrupt normal co-chaperone interactions, though this has not been proven.[36-38] The benzamide sidechain of novobiocin presumably extends into Hsp90's dimerization domain, infringing upon dimerization and promoting proteotoxicity.[36-37] Structure-activity relationship (SAR) studies have shown that replacing the benzamide sidechain with an acetamide reduces toxicity.[36, 39] KU-32 is a descendent of A4-inspired novobiocin analogs, which possess this acetamide substitution.[8-10] It is thought that these analogs bind to Hsp90 in a similar manner as novobiocin, but induce only allosteric modulation versus dimer disruption.[36, 38-39] While this could dislodge HSF1 to elicit an HSR, it could also alter normal protein interactions with Hsp90. Either way, the Hsp90-dependent and independent roles of Hsp70 could be enhanced, suggesting that a robust HSR may not be crucial for drug efficacy.[40]

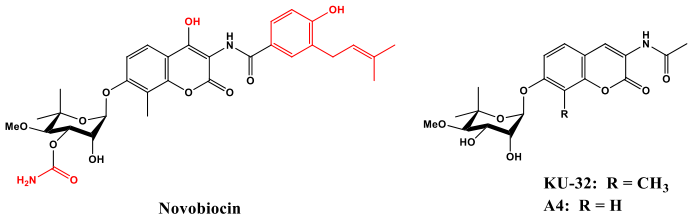

Figure 27. Structures of novobiocin, A4, and KU-32. Modified regions of novobiocin for A4-inspired analogs (*e.g.* KU-32) are indicated in red.[8-10, 36-39]

4.2. Hypothetical Mechanisms of Action

To an extent, oncogenesis can be viewed as a "survival guide" to decipher new ways to withstand prolonged periods of metabolic distress and growth inhibition. This could aid the development of new and effective neuroprotective agents that target similar obstacles encountered in DSPN and other neurodegenerative disorders.[40] KU-32 represents a novel pharmacotherapeutic approach that capitalizes upon lessons learned from Hsp involvement in oncogenesis to empower sensory neurons and peripheral nerves with increased resiliency and neurite outgrowth. Potential mechanisms surrounding KU-32's neuroprotective effects will be discussed drawing upon lessons learned from Hsp actions in oncogenesis.

4.2.1. Mechanisms for Improving iENF Density and Thermal Hypoalgesia

KU-32's improvements to iENF density in diabetic SW mice strongly correspond to its reestablishment of normal thermal pain thresholds. As mentioned, somatosensory nerve fibers are thought to linger in a state of perpetual growth and could be responsive to local manipulation.[41] The lack of further iENF loss between 16 and 26 weeks in untreated diabetic mice would argue that KU-32 likely enhances nerve fiber growth rather than just slowing the rate of progressive fiber degeneration. Since KU-32 has no affect on systemic metabolic parameters, it seems reasonable to suspect that these neuroprotective effects are attributed to enhanced neurotrophic support.[12]

Oncogenesis requires the acquisition of self-sufficient growth signaling, which supports cancer cell survival, proliferation, and migration (metastasis).[42] In several types of cancer (*e.g.* gastrointestinal, lung, breast, prostate, gynecological, pancreatic, and osteosarcomas), this requirement is fulfilled by enhancing IGF-I signaling.[43-47] This occurs by either increasing IGF-I secretion, improving ligand binding interactions, or promoting the

expression of IGF-I signaling components.[47-48] Several IGF-I signaling components rely upon Hsps for post-translational modifications, transport, and functional integrity. Hsp90 client proteins include the IGF-IR, IRS-1, IRS-2, PI3K, PDK1, Akt, PKC-δ, PKC-ε, Raf-1, ERK-1, MEK-1 (MAPK/ERK kinase 1), and GSK-3β (**Figures 12 and 13; CHAPTER I**).[44-46, 49-61] Hsp90 also binds raptor to enhance mTOR signaling.[62] Even so, most of this client protein data comes from cancer studies and must be verified in normal tissues.[44-46, 49-61]

The chemotherapeutic potential for targeting IGF-I signaling has not gone unrealized, and has resulted in the development of several IGF-IR inhibitors.[63] Alas, many cancer strains have developed resistance to this treatment by augmenting IR-A expression.[48, 64] This has led to the development of RTK inhibitors that dually target the IGF-IR and the IR.[48, 64] Of note, IR maturation also depends heavily upon Hsp90-mediated trafficking of the pro-receptor through the ER.[65] During this process, Hsp90 exports dysfunctional IRs to the cytoplasm for degradation.[66] Hence, targeting Hsp90 in these drug-resistant strains may simultaneously affect both IR and IGF-IR signaling.

In contrast, enhancing Hsp support could boost insulin and IGF-I neurotrophic signaling in diabetic sensory neurons and peripheral nerves. IGF-IR levels spike in the distal axons of degenerating sural nerves in T1DM and T2DM patients, suggesting that a natural response to late stages of DSPN is to invigorate IGF-I signaling.[67] It is interesting to note that Hsp90 and Hsp70 localize to regenerating growth cones of sciatic nerves following nerve crush.[68] What's more, Hsp70 expression levels increase in the more distal regions (isolated from the soma), suggesting Hsp70 can be locally translated in response to neurotrauma.[68] Further, Hsp70 expression levels inexplicably deplete alongside IGF-IR in the small nociceptive DRG and Schwann cells of STZ-diabetic rats.[69] While inducible Hsp70 depletion has no

impact upon DSPN progression, it is required for KU-32's neuroprotective effects.[12] Hence, it seems reasonable that restoring local Hsp70 support to more distal regions of nociceptive nerve fibers could amplify endogenous neurotrophic signaling. This is supported by findings in IGF-I intervention studies in STZ-diabetic rodents, which elicits very similar neuroprotective effects as KU-32 (**Table 5**).[70-73]

Table 5. Neuroprotective effects of KU-32 and IGF-I in STZ-diabetes.[12, 70-73]

Neuroprotective Effect	***KU-32***	***IGF-I***
Improves iENF Density	+	+
Stimulates Neuritogenesis		+
Reduces Distal Axon Atrophy		+
Improves Thermal Hypoalgesia	+	+
Improves Mechanical Hypoalgesia	+	*
Improves MNCV	+	+
Improves SNCV	+	+
Improves Mitochondrial Bioenergetics	+	
Improves Mitochondrial Inner Membrane Potential		+

(+) effective; (*) stabilizes hyperalgesia; and (blank) unknown effects

Unfortunately, molecular evidence of increased IGF-I signaling has been inconclusive in 26-week pooled nerve samples, as represented by pSer(473)Akt in **Figure 28**. As such, we speculated that KU-32 could have more distinct effects at the more distal regions of diabetic peripheral nerves (*i.e.* foot pads). Since all foot pad samples from this study were fixed for iENF density analysis, additional foot pad samples were acquired from a follow-up 16-week intervention SW study conducted by Jiacheng Ma and homogenized. Although immunoblots from these tissues were not entirely conclusive due the fluctuating β-actin (loading control) levels, some general trends were noticed. Inducible Hsp70 levels generally decreased in diabetic foot pads (as expected), but there was no evidence of a robust HSR. pSer(473)Akt levels were also unaffected by KU-32 as well as diabetes. However, a notable

trending increase in pSer(41)GAP-43 appeared in KU-32-treated diabetic and non-diabetic mice, but not GAP-43. As previously discussed, GAP-43 is a "plasticity" protein that is locally expressed in neuronal growth cones and non-myelinating SCs during regeneration.[41, 74-78] GAP-43 phosphorylation by PKC promotes morphogenic activity and prevents growth cone retraction in DRG.[79] While it is unknown whether Hsps directly interact with GAP-43, insulin- and IGF-I-responsive PKCs, such as PKC-δ and PKC-ε, are Hsp90 client proteins.[59-60] While these IB results suggest that KU-32 may enhance pSer(41)GAP-43, but not Hsp70 or pSer(473)Akt in diabetic foot pads, more evidence is needed. Importantly, there were no adverse signs of excessive collateral branching or hyperalgesia in either KU-32 treatment group. Hence, while pSer(41)GAP-43 may favor neurite outgrowth, there are most likely other regulatory factors at play. More work is needed to confirm these results and to further explore potential KU-32 affects upon the IGF-I/PKC/GAP-43 signaling axis.

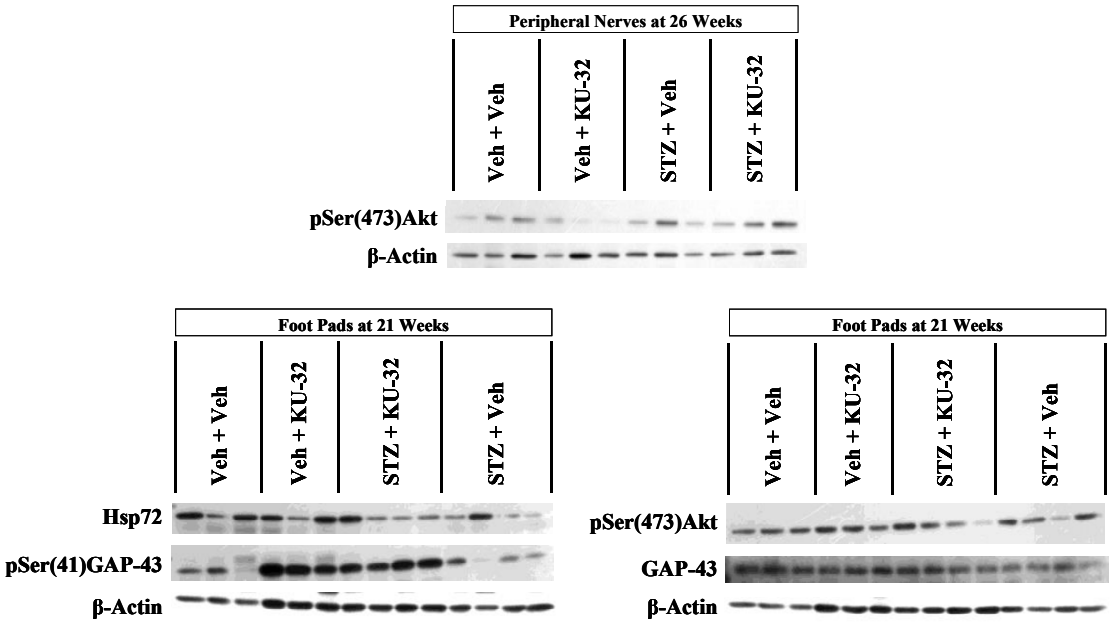

Figure 28. Representative IB of peripheral nerve and foot pad homogenates. (Top) Pooled sciatic, tibial, and sural nerve homogenates from 16-week intervention SW mice at study completion (26 weeks) were analyzed for pSer(473)Akt and β-actin. (Bottom) Foot pad homogenates from a separate, 16-week intervention SW mice were analyzed for inducible Hsp70 (Hsp72), pSer(41)GAP-43, pSer(473)Akt, GAP-43, and β-actin.

4.2.2. Mechanisms for Improving Mitochondrial Function and Other Indices

High-energy axonal functions, such as growth cone motility, molecular transport, and excitation, require a dedicated and sufficient supply of ATP.[29] Substantial changes to the mitochondrial proteome have been reported in STZ-diabetic and high glucose-stressed sensory neurons and SCs, which alter mitochondrial membrane potentials, respiratory chain activities, and bioenergetics.[25, 29, 80-83] Thus, improving mitochondrial support and function in diabetic sensory neurons could significantly improve multiple aspects of DSPN.

In cancer, tumor biomass expansion and signaling are partially driven by advantageous metabolic alterations.[84] To meet biosynthetic demands, cancer cell mitochondria must function efficiently under extreme conditions, including nutrient deprivation and oxidative stress.[84] This requires adequate biomaterial flux, protein folding and stabilization, and the neutralization of impending proteotoxic threats.[84] Increases in mitochondria-localized Hsp90 and its homolog TRAP-1 (TNF receptor-associate protein-1) in tumor cells serve to stabilize and repair damaged mitochondrial proteins (*e.g.* respiratory complex II), thus sustaining mitochondrial operations.[84] Mitochondria-localized Hsp90 can also bind cyclophilin D to prevent mitochondrial membrane permeabilization and apoptosis.[85] Along these lines, Hsp70 induction inhibits the activation and translocation of pro-apoptotic Bax to the mitochondria and stabilizes anti-apoptotic Bcl-2.[86-87] Furthermore, Hsp90 and Hsp70 largely facilitate mitochondrial protein trafficking.[60, 88-89] These Hsps deliver preproteins to the mitochondrial membrane transporter TOM70 (translocase of outer mitochondrial membrane 70-kDa).[90-91] TOM70 imports these preproteins into the mitochondria for mtHsp70 (mitochondrial Hsp70)-mediated transport to Hsp60.[90-91] Hsp60 then folds these preproteins into their mature conformations.[90-91] In this manner, nearly 99% of the

mitochondrial proteome is dependent upon Hsp90 and Hsp70.[92] Hence, Hsp90 and Hsp70 promote structural and functional integrity in cancer cell mitochondria, making them more adept to handling chronic metabolic stress.

We have shown that KU-32 significantly improves mitochondrial bioenergetics at more chronic stages of DSPN, which likely contributes to electrophysiological, psychophysical, and morphological effects as well. In proteomic studies in high glucose-stressed embryonic rat DRG, KU-32 greatly increased the translation of several mitochondrial respiratory components and bolstered endogenous antioxidant defenses (*e.g.* manganese SOD, an Hsp90 client protein).[81] With that said, a definitive mechanistic cause for improved mitochondrial bioenergetics in diabetic sensory neurons is still under investigation. If the enhanced neurotrophic signaling hypothesis holds true, then Hsp90 modulation should likely affect pSer(473)Akt. After all, Hsp90 over-expression alone can increase pSer(473)Akt levels in HEK293 cells.[57] In DRG, IGF-I-induced pSer(473)Akt improves mitochondrial inner membrane potential ($\Delta\Psi m$), inhibits Bim/Bax translocation, triggers CREB-mediated pro-survival transcription, and deactivates caspase-9, FKHR (forkhead in rhabdomyosarcoma), and GSK-3β.[25, 69, 93-100] Alas, the IB results seemingly refute this possibility, unless KU-32's effects are indeed more transient. To thoroughly assess this possibility, more tissues have to be collected immediately after each weekly KU-32 injection. This requires a substantially larger population size (n) and a better understanding of KU-32's IP pharmacokinetic profiles (addressed in **CHAPTER III**).

4.2.3. Other Mechanistic Considerations

While the enhancement of IGF-I neurotrophic signaling seems a likely candidate for KU-32's neuroprotective effects, it is possible that other neurotrophic signaling pathways

(*e.g.* NGF or NT-3) are being affected. Of note, most of these pathways result in the downstream activation of identical signaling molecules, which synergistically afford neuroprotective effects.[101-102] Hence, if Hsp90 modulation enhances the activation of downstream neurotrophic signaling molecules, then the neurotrophic factors themselves may be less important. Hence more, this pharmacotherapeutic approach may likely bypass the painful side effects linked to exogenous NGF treatments.[101]

Given the vastness of the Hsp90 and the Hsp70 interactomes, it should be considered that each of the neuroprotective effects of KU-32 could be attributed to multiple molecular signaling alterations. While this is not ideal from a drug development perspective, it is possible. To effectively rule this out requires a broad assessment of the proteome/RNAome at several regions of diabetic peripheral nerves, given that Hsp70 can be locally expressed.[68] This type of analysis is problematic for distal somatosensory nerve fibers in foot pads since they can not be readily isolated from the surrounding tissues. Hence, costly analytical techniques, such as high content screening or RNA microarrays, would be plagued by tissue contamination issues; this is a concern for IB as well. To exclusively analyze protein expression in the nerve fibers of the dermis/epidermis requires IHC.

Proteomics can be used to assess disease and drug-induced alterations in protein levels in adult sensory neurons and remaining portions of sciatic, tibial, and sural nerves. However, previous pulse SILAC (stable isotope labeling of amino acids in culture) methods used to assess KU-32's effects in embryonic sensory neurons require 7 days in culture.[81] This poses survivability issues in adult primary cultures. More importantly, failure to fully reproduce the physiological milieu of experimental T1DM would likely alter protein expression. Thus, an alternative proteomic approach is needed. iTRAQ (isobaric tags for relative and absolute

quantification) enables protein/peptide labeling in tissue homogenates, which enables snapshot comparisons between various treatment groups.[103] While this technique does not eliminate contamination issues, changes in whole nerve and DRG protein levels could be characterized. This would help govern subsequent molecular analyses and determine regions differences overall protein expression. This is important given the dying back pattern of nerve attrition in DSPN. However, this generates two concerns: (1) which time points should be assessed and (2) if KU-32 has distinct effects in different nerve fibers, will background noise suppress real changes in affected nerve fibers. The bottom line is that employing a pharmacotherapeutic approach that targets molecular chaperones runs the "risk" of affecting multiple molecular signaling pathways. To fully understand KU-32's effects will require either proteomics or genetic knockdown studies (if possible) upon discovery of a putative neuroprotective mechanism.

There are additional risks associated with targeting heat shock proteins in DSPN.[40] The first is the risk for drug-drug interactions with insulin and/or adjunctive therapies for glycemic control. If KU-32 does boost neurotrophic signaling, it could also generate risks similar to mismanaged insulin therapy if metabolic insulin signaling is also affected. In this regard, it must first be noted that complete annihilation of insulin production is lethal and our previous 12-week intervention studies in C57Bl/6 mice demonstrated that STZ-diabetic mice still retained ~ 40% of normal circulating insulin levels.[12] While KU-32 has not been administered alongside insulin or other diabetes adjunctive therapies, we have shown that FBG and HbA_{1C} levels are unaffected by KU-32 treatments in diabetic and non-diabetic animals. This effectively negates possible enhancement of metabolic insulin signaling. The second risk is the promotion of cancer. While this is a practical concern, all intervention

studies to date involving KU-32-treated diabetic and non-diabetic mice have been devoid of signs of overt toxicity or tumorigenesis.[12] With that said, clinical effects can often differ from preclinical studies with regard to drug pharmacodynamics and pharmacokinetics. If KU-32 exhibits any undesirable side effects, these could be overcome by readjusting primary treatment regimens, insulin and adjunctive therapies, or by developing an Hsp90 modulator with less robust effects.[12]

4.3. Concluding Remarks

In summary, pharmacologic Hsp90 modulation significantly improves psychophysical, electrophysiological, morphological, and bioenergetic indices at more chronic stages of DSPN development. The finding that KU-32 promotes iENF recovery argues against a purely neurochemical correction for NCV improvements, which may transcend interspecies mechanistic differences to help expedite drug development.[104-105] However, the molecular mechanisms underlying these neuroprotective effects require further attention. KU-32 represents a novel pharmacotherapeutic approach that draws upon oncogenic methods to improve resiliency to hyperglycemic and neurotrophic insults that contribute to DSPN.

SECTION 5. REFERENCES

1. Szkudelski, T. *Physiol Res* **2001,** *50* (6), 537-46.
2. Bennett, R. A.and Pegg, A. E. *Cancer Res* **1981,** *41* (7), 2786-90.
3. Junod, A.; Lambert, A. E.; Stauffacher, W.; Renold, A. E. *J Clin Invest* **1969,** *48* (11), 2129-39.
4. Ullman-Cullere, M. H.and Foltz, C. J. *Lab Anim Sci* **1999,** *49* (3), 319-23.
5. Gillett, M. J. *Clin Biochem Rev* **2009,** *30* (4), 197-200.
6. World Health Organization. *Use of Glycated Haemoglobin (HbA1c) in the Diagnosis of Diabetes Mellitus*; WHO: Geneva, 2011; p 25.
7. American Diabetes, A. *Diabetes Care* **2013,** *36 Suppl 1*, S67-74.
8. Burlison, J. A.; Neckers, L.; Smith, A. B.; Maxwell, A.; Blagg, B. S. *J Am Chem Soc* **2006,** *128* (48), 15529-36.
9. Donnelly, A. C.; Mays, J. R.; Burlison, J. A.; Nelson, J. T.; Vielhauer, G.; Holzbeierlein, J.; Blagg, B. S. *J Org Chem* **2008,** *73* (22), 8901-20.
10. Huang, Y. T.and Blagg, B. S. *J Org Chem* **2007,** *72* (10), 3609-13.
11. McGuire, J. F.; Rouen, S.; Siegfreid, E.; Wright, D. E.; Dobrowsky, R. T. *Diabetes* **2009,** *58* (11), 2677-86.

12. Urban, M. J.; Li, C.; Yu, C.; Lu, Y.; Krise, J. M.; McIntosh, M. P.; Rajewski, R. A.; Blagg, B. S.; Dobrowsky, R. T. *ASN Neuro* **2010,** *2* (4), 189-199.
13. Hargreaves, K.; Dubner, R.; Brown, F.; Flores, C.; Joris, J. *Pain* **1988,** *32* (1), 77-88.
14. Gasser, H. S. *The Ohio Journal of Science* **1941,** *41* (3), 145-159.
15. Kandel, E. R.; Schwartz, J. H.; Jessell, T. M. *Principles of neural science*. 4th ed.; McGraw-Hill, Health Professions Division: New York, 2000; p xli, 1414 p.
16. Julius, D.and Basbaum, A. I. *Nature* **2001,** *413* (6852), 203-10.
17. Sandkuhler, J. *Physiol Rev* **2009,** *89* (2), 707-58.
18. Beissner, F.; Brandau, A.; Henke, C.; Felden, L.; Baumgartner, U.; Treede, R. D.; Oertel, B. G.; Lotsch, J. *PLoS One* **2010,** *5* (9), e12944.
19. Lauria, G.; Cornblath, D. R.; Johansson, O.; McArthur, J. C.; Mellgren, S. I.; Nolano, M.; Rosenberg, N.; Sommer, C.; European Federation of Neurological, S. *Eur J Neurol* **2005,** *12* (10), 747-58.
20. Delree, P.; Leprince, P.; Schoenen, J.; Moonen, G. *J Neurosci Res* **1989,** *23* (2), 198-206.
21. Brand, M. D.and Nicholls, D. G. *Biochem J* **2011,** *435* (2), 297-312.
22. Beiswenger, K. K.; Calcutt, N. A.; Mizisin, A. P. *Neurosci Lett* **2008,** *442* (3), 267-72.
23. Chen, Y. S.; Chung, S. S.; Chung, S. K. *Diabetes* **2005,** *54* (11), 3112-8.
24. Stavniichuk, R.; Drel, V. R.; Shevalye, H.; Maksimchyk, Y.; Kuchmerovska, T. M.; Nadler, J. L.; Obrosova, I. G. *Exp Neurol* **2011,** *230* (1), 106-13.
25. Huang, T. J.; Verkhratsky, A.; Fernyhough, P. *Mol Cell Neurosci* **2005,** *28* (1), 42-54.
26. Vincent, A. M.; Edwards, J. L.; McLean, L. L.; Hong, Y.; Cerri, F.; Lopez, I.; Quattrini, A.; Feldman, E. L. *Acta Neuropathol* **2010,** *120* (4), 477-89.
27. Zherebitskaya, E.; Akude, E.; Smith, D. R.; Fernyhough, P. *Diabetes* **2009,** *58* (6), 1356-64.
28. Yu, C.; Rouen, S.; Dobrowsky, R. T. *Glia* **2008,** *56* (8), 877-87.
29. Chowdhury, S. K.; Dobrowsky, R. T.; Fernyhough, P. *Mitochondrion* **2011,** *11* (6), 845-54.
30. Ma, J.; Farmer, K. L.; Pan, P.; Urban, M. J.; Zhao, H.; Blagg, B. S.; Dobrowsky, R. T. *J Pharmacol Exp Ther* **2014,** *348* (2), 281-92.
31. Li, C.; Ma, J.; Zhao, H.; Blagg, B. S.; Dobrowsky, R. T. *ASN Neuro* **2012,** *4* (7), e00102.
32. Liu, Y.and Ma, Q. *Curr Opin Neurobiol* **2011,** *21* (1), 52-60.
33. Schneider, S. P.and Perl, E. R. *J Neurosci* **1988,** *8* (6), 2062-73.
34. De Biasi, S.and Rustioni, A. *Proc Natl Acad Sci U S A* **1988,** *85* (20), 7820-4.
35. Goodman, L. S.; Hardman, J. G.; Limbird, L. E.; Gilman, A. G. *Goodman & Gilman's the pharmacological basis of therapeutics*. 10th ed.; McGraw-Hill, Medical Pub. Division: New York, 2001; p xxvii, 2148 p.
36. Burlison, J. A.; Avila, C.; Vielhauer, G.; Lubbers, D. J.; Holzbeierlein, J.; Blagg, B. S. *J Org Chem* **2008,** *73* (6), 2130-7.
37. Marcu, M. G.; Chadli, A.; Bouhouche, I.; Catelli, M.; Neckers, L. M. *J Biol Chem* **2000,** *275* (47), 37181-6.
38. Matts, R. L.; Brandt, G. E.; Lu, Y.; Dixit, A.; Mollapour, M.; Wang, S.; Donnelly, A. C.; Neckers, L.; Verkhivker, G.; Blagg, B. S. *Bioorg Med Chem* **2011,** *19* (1), 684-92.
39. Donnelly, A.and Blagg, B. S. *Curr Med Chem* **2008,** *15* (26), 2702-17.
40. Urban, M. J.; Dobrowsky, R. T.; Blagg, B. S. *Trends Pharmacol Sci* **2012,** *33* (3), 129-37.
41. Guo, G.; Kan, M.; Martinez, J. A.; Zochodne, D. W. *Neurobiol Dis* **2011,** *43* (2), 414-21.
42. Hanahan, D.and Weinberg, R. A. *Cell* **2011,** *144* (5), 646-74.
43. Jerome, V.; Leger, J.; Devin, J.; Baulieu, E. E.; Catelli, M. G. *Growth Factors* **1991,** *4* (4), 317-27.
44. Martins, A. S.; Ordonez, J. L.; Garcia-Sanchez, A.; Herrero, D.; Sevillano, V.; Osuna, D.; Mackintosh, C.; Caballero, G.; Otero, A. P.; Poremba, C.*, et al. Cancer Res* **2008,** *68* (15), 6260-70.
45. Breinig, M.; Mayer, P.; Harjung, A.; Goeppert, B.; Malz, M.; Penzel, R.; Neumann, O.; Hartmann, A.; Dienemann, H.; Giaccone, G.*, et al. Clin Cancer Res* **2011,** *17* (8), 2237-49.

46. Lang, S. A.; Moser, C.; Gaumann, A.; Klein, D.; Glockzin, G.; Popp, F. C.; Dahlke, M. H.; Piso, P.; Schlitt, H. J.; Geissler, E. K.*, et al. Clin Cancer Res* **2007,** *13* (21), 6459-68.
47. Boone, D. N.and Lee, A. V. *Crit Rev Oncog* **2012,** *17* (2), 161-73.
48. Belfiore, A.; Frasca, F.; Pandini, G.; Sciacca, L.; Vigneri, R. *Endocr Rev* **2009,** *30* (6), 586-623.
49. Basso, A. D.; Solit, D. B.; Chiosis, G.; Giri, B.; Tsichlis, P.; Rosen, N. *J Biol Chem* **2002,** *277* (42), 39858-66.
50. Fujita, N.; Sato, S.; Ishida, A.; Tsuruo, T. *J Biol Chem* **2002,** *277* (12), 10346-53.
51. Lochhead, P. A.; Kinstrie, R.; Sibbet, G.; Rawjee, T.; Morrice, N.; Cleghon, V. *Mol Cell* **2006,** *24* (4), 627-33.
52. Schulte, T. W.; Blagosklonny, M. V.; Romanova, L.; Mushinski, J. F.; Monia, B. P.; Johnston, J. F.; Nguyen, P.; Trepel, J.; Neckers, L. M. *Mol Cell Biol* **1996,** *16* (10), 5839-45.
53. Fukushima, T.; Okajima, H.; Yamanaka, D.; Ariga, M.; Nagata, S.; Ito, A.; Yoshida, M.; Asano, T.; Chida, K.; Hakuno, F.*, et al. Mol Cell Endocrinol* **2011,** *344* (1-2), 81-9.
54. Stancato, L. F.; Silverstein, A. M.; Owens-Grillo, J. K.; Chow, Y. H.; Jove, R.; Pratt, W. B. *J Biol Chem* **1997,** *272* (7), 4013-20.
55. Taherian, A.; Krone, P. H.; Ovsenek, N. *Biochem Cell Biol* **2008,** *86* (1), 37-45.
56. O'Rahilly, S. *Nature* **2009,** *462* (7271), 307-14.
57. Cortes-Gonzalez, C.; Barrera-Chimal, J.; Ibarra-Sanchez, M.; Gilbert, M.; Gamba, G.; Zentella, A.; Flores, M. E.; Bobadilla, N. A. *Cell Physiol Biochem* **2010,** *26* (4-5), 657-68.
58. Yoshikawa, N.; Nemoto, T.; Satoh, S.; Maruta, T.; Yanagita, T.; Chosa, E.; Wada, A. *Neurochem Int* **2010,** *56* (1), 42-50.
59. Gould, C. M.; Kannan, N.; Taylor, S. S.; Newton, A. C. *J Biol Chem* **2009,** *284* (8), 4921-35.
60. Budas, G. R.; Churchill, E. N.; Disatnik, M. H.; Sun, L.; Mochly-Rosen, D. *Cardiovasc Res* **2010,** *88* (1), 83-92.
61. Zitzmann, K.; Ailer, G.; Vlotides, G.; Spoettl, G.; Maurer, J.; Goke, B.; Beuschlein, F.; Auernhammer, C. J. *Int J Oncol* **2013,** *43* (6), 1824-32.
62. Ohji, G.; Hidayat, S.; Nakashima, A.; Tokunaga, C.; Oshiro, N.; Yoshino, K.; Yokono, K.; Kikkawa, U.; Yonezawa, K. *J Biochem* **2006,** *139* (1), 129-35.
63. Buck, E.and Mulvihill, M. *Expert Opin Investig Drugs* **2011,** *20* (5), 605-21.
64. Malaguarnera, R.and Belfiore, A. *Front Endocrinol (Lausanne)* **2011,** *2*, 93.
65. Ramos, R. R.; Swanson, A. J.; Bass, J. *Proc Natl Acad Sci U S A* **2007,** *104* (25), 10470-5.
66. Imamura, T.; Haruta, T.; Takata, Y.; Usui, I.; Iwata, M.; Ishihara, H.; Ishiki, M.; Ishibashi, O.; Ueno, E.; Sasaoka, T.*, et al. J Biol Chem* **1998,** *273* (18), 11183-8.
67. Grandis, M.; Nobbio, L.; Abbruzzese, M.; Banchi, L.; Minuto, F.; Barreca, A.; Garrone, S.; Mancardi, G. L.; Schenone, A. *Muscle Nerve* **2001,** *24* (5), 622-9.
68. Willis, D.; Li, K. W.; Zheng, J. Q.; Chang, J. H.; Smit, A.; Kelly, T.; Merianda, T. T.; Sylvester, J.; van Minnen, J.; Twiss, J. L. *J Neurosci* **2005,** *25* (4), 778-91.
69. Kamiya, H.; Zhang, W.; Sima, A. A. *Diabetologia* **2006,** *49* (11), 2763-74.
70. Brussee, V.; Cunningham, F. A.; Zochodne, D. W. *Diabetes* **2004,** *53* (7), 1824-30.
71. Zhuang, H. X.; Snyder, C. K.; Pu, S. F.; Ishii, D. N. *Exp Neurol* **1996,** *140* (2), 198-205.
72. Chu, Q.; Moreland, R.; Yew, N. S.; Foley, J.; Ziegler, R.; Scheule, R. K. *Mol Ther* **2008,** *16* (8), 1400-8.
73. Toth, C.; Brussee, V.; Zochodne, D. W. *Diabetologia* **2006,** *49* (5), 1081-8.
74. Goslin, K.; Schreyer, D. J.; Skene, J. H.; Banker, G. *Nature* **1988,** *336* (6200), 672-4.
75. Goslin, K.and Banker, G. *J Cell Biol* **1990,** *110* (4), 1319-31.
76. Goslin, K.; Schreyer, D. J.; Skene, J. H.; Banker, G. *J Neurosci* **1990,** *10* (2), 588-602.
77. Bergman, E.; Carlsson, K.; Liljeborg, A.; Manders, E.; Hokfelt, T.; Ulfhake, B. *Brain Res* **1999,** *832* (1-2), 63-83.
78. Curtis, R.; Stewart, H. J.; Hall, S. M.; Wilkin, G. P.; Mirsky, R.; Jessen, K. R. *J Cell Biol* **1992,** *116* (6), 1455-64.

79. Aigner, L.and Caroni, P. *J Cell Biol* **1995,** *128* (4), 647-60.
80. Akude, E.; Zherebitskaya, E.; Chowdhury, S. K.; Smith, D. R.; Dobrowsky, R. T.; Fernyhough, P. *Diabetes* **2011,** *60* (1), 288-97.
81. Zhang, L.; Zhao, H.; Blagg, B. S.; Dobrowsky, R. T. *J Proteome Res* **2012,** *11* (4), 2581-93.
82. Zhang, L.; Yu, C.; Vasquez, F. E.; Galeva, N.; Onyango, I.; Swerdlow, R. H.; Dobrowsky, R. T. *J Proteome Res* **2010,** *9* (1), 458-71.
83. Courchesne, S. L.; Karch, C.; Pazyra-Murphy, M. F.; Segal, R. A. *J Neurosci* **2011,** *31* (5), 1624-34.
84. Chae, Y. C.; Angelin, A.; Lisanti, S.; Kossenkov, A. V.; Speicher, K. D.; Wang, H.; Powers, J. F.; Tischler, A. S.; Pacak, K.; Fliedner, S.*, et al. Nat Commun* **2013,** *4*, 2139.
85. Kang, B. H.; Plescia, J.; Dohi, T.; Rosa, J.; Doxsey, S. J.; Altieri, D. C. *Cell* **2007,** *131* (2), 257-70.
86. Yang, X.; Wang, J.; Zhou, Y.; Wang, Y.; Wang, S.; Zhang, W. *Cancer Lett* **2012**.
87. Li, H.; Liu, L.; Xing, D.; Chen, W. R. *FEBS Lett* **2010,** *584* (22), 4672-8.
88. Barksdale, K. A.and Bijur, G. N. *J Neurochem* **2009,** *108* (5), 1289-99.
89. Fan, A. C.; Bhangoo, M. K.; Young, J. C. *J Biol Chem* **2006,** *281* (44), 33313-24.
90. Hood, D. A.; Adhihetty, P. J.; Colavecchia, M.; Gordon, J. W.; Irrcher, I.; Joseph, A. M.; Lowe, S. T.; Rungi, A. A. *Med Sci Sports Exerc* **2003,** *35* (1), 86-94.
91. Young, J. C.; Hoogenraad, N. J.; Hartl, F. U. *Cell* **2003,** *112* (1), 41-50.
92. Schmidt, O.; Pfanner, N.; Meisinger, C. *Nat Rev Mol Cell Biol* **2010,** *11* (9), 655-67.
93. Leinninger, G. M.; Backus, C.; Uhler, M. D.; Lentz, S. I.; Feldman, E. L. *FASEB J* **2004,** *18* (13), 1544-6.
94. Dill, J.; Wang, H.; Zhou, F.; Li, S. *J Neurosci* **2008,** *28* (36), 8914-28.
95. Lonze, B. E.; Riccio, A.; Cohen, S.; Ginty, D. D. *Neuron* **2002,** *34* (3), 371-85.
96. Tang, E. D.; Nunez, G.; Barr, F. G.; Guan, K. L. *J Biol Chem* **1999,** *274* (24), 16741-6.
97. Edstrom, A.and Ekstrom, P. A. *J Neurosci Res* **2003,** *74* (5), 726-35.
98. Christie, K. J.; Webber, C. A.; Martinez, J. A.; Singh, B.; Zochodne, D. W. *J Neurosci* **2010,** *30* (27), 9306-15.
99. Leinninger, G. M.; Backus, C.; Sastry, A. M.; Yi, Y. B.; Wang, C. W.; Feldman, E. L. *Neurobiol Dis* **2006,** *23* (1), 11-22.
100. Cardone, M. H.; Roy, N.; Stennicke, H. R.; Salvesen, G. S.; Franke, T. F.; Stanbridge, E.; Frisch, S.; Reed, J. C. *Science* **1998,** *282* (5392), 1318-21.
101. Pittenger, G.and Vinik, A. *Exp Diabesity Res* **2003,** *4* (4), 271-85.
102. Dobrowsky, R. T.; Rouen, S.; Yu, C. *J Pharmacol Exp Ther* **2005,** *313* (2), 485-91.
103. He, Q.; Man, L.; Ji, Y.; Zhang, S.; Jiang, M.; Ding, F.; Gu, X. *J Proteome Res* **2012,** *11* (6), 3077-89.
104. Calcutt, N. A. *ASN Neuro* **2010,** *2* (4), e00042.
105. Calcutt, N. A.; Cooper, M. E.; Kern, T. S.; Schmidt, A. M. *Nat Rev Drug Discov* **2009,** *8* (5), 417-29.

CHAPTER III: KU-32 PHARMACOKINETIC ANALYSES

SECTION 1. EXPERIMENTAL DESIGN

Despite marked improvements in several standard indices of DSPN, there was a need to characterize KU-32's intraperitoneal pharmacokinetic (**IP-PK**) profile in DSPN-relevant tissues to verify successful drug distribution and elimination from these tissues. We further sought to characterize KU-32's PK profiles after oral gavage (**OG-PK**) to develop comparable dose ranges for future oral intervention studies.

To test the hypothesis that both intraperitoneal and oral KU-32 administration will result in successful drug delivery to DSPN-relevant tissues in a route-dependent manner, we conducted four experiments. In Experiment 1, drug tissue levels in 20 mg/kg KU-32 IP-treated wild-type C57BL/6 (WT B6) and Hsp70.1/70.3 double knockout (Hsp70 KO) mice were compared to determine if previous reported differences in KU-32-responsiveness[†] between these strains were the result of unequal drug distribution.[1-2] In Experiment 2, pharmacokinetic profiles for DSPN-relevant tissues were assessed following 20 mg/kg KU-32 IP treatments in WT B6 and Hsp70 KO mice. In Experiment 3, drug tissue levels were measured after an 8-week intervention study in Swiss-Webster (SW) mice[††] to confirm total drug elimination in STZ-diabetic and non-diabetic tissues at the point the next weekly treatment would typically occur.[1] Finally, in Experiment 4, pharmacokinetic profiles for DSPN-relevant tissues and blood plasma were examined after 10 or 20 mg/kg KU-32 OG treatments in SW mice. KU-32 analyte levels in tissue/plasma were measured using liquid chromatography-tandem (triple quadrupole) mass spectrometry (LC/MS/MS).

[†] Both WT B6 and Hsp70 KO studies consisted of 12 weeks of STZ-diabetes followed by 6 weekly 20 mg/kg KU-32 IP treatments. In contrast to KU-32-responsive diabetic WT B6 mice, KU-32 intervention in diabetic HSP70 KO mice had no effect on standard indices of DSPN.

[††] Treatments entailed 6 weekly 2, 10, or 20 mg/kg KU-32 IP treatments after 8 weeks of STZ-diabetes.

SECTION 2. MATERIALS AND METHODS

2.1. Animals

Three strains of mice were used for these experiments. Male, six-week old, outbred SW mice were purchased from Harlan Laboratories (Indianapolis, IN) and acclimated for two weeks prior to use. Male and female WT B6 and Hsp70 KO (C57BL/6 background) mice were obtained from in-house breeding colonies. WT B6 mice were initially purchased from Harlan Laboratories, and Hsp70 KO mice were originally acquired from the Mutant Mouse Resource Center (San Diego, CA). Animals were maintained on a 12 hour light/dark cycle at 70°F and 70% humidity and given *ad libitum* access to Purina diet 5001 chow and water. All procedures were conducted according to IACUC regulations and protocols as well as the standards and regulations for care and use of laboratory rodents established by the NIH.

2.2. Drug Formulations and Treatments

All KU-32 treatments were based on the weight (kg) of the mouse on the day prior to injection. KU-32 was synthesized and prepared as a 5 mg/ml stock (0.1 M Captisol) as previously described (**CHAPTER II**). In addition, a 2.5 mg/ml KU-32 stock (0.1 M Captisol) was also prepared for 10 mg/kg KU-32 OG treatments to allow consistent vehicle loading for both OG treatments. For each KU-32-treated animal, an aliquot of fresh 5 mg/ml KU-32 (0.1 M Captisol) or 2.5 mg/ml KU-32 (0.1 M Captisol) stock needed for each dose was dispensed into a sterile 1.7-ml microcentrifuge tube. To help facilitate IP injections, sterile 1X PBS (200 µl) was added to each tube, bringing the final working concentrations to: 2 mg/kg KU-32 (in ~ 215 µl of ~ 7 mM Captisol); 10 mg/kg KU-32 (~ 275 µl of ~ 27 mM Captisol); and 20 mg/kg KU-32 (~ 350 µl of ~ 43 mM Captisol). Vehicle-treated controls for IP experiments were given mass-dependent volume equivalents of 0.1 M Captisol plus

200 µl of sterile 1X PBS, or ~ 350 µl of ~ 43 mM Captisol (vehicle equivalent for 20 mg/kg KU-32 treatments). To minimize dilution effects on drug absorption, no additional saline was added to OG treatments. Hence, final working concentrations for OG treatments were: 10 mg/kg KU-32 (in ~ 125 µl of 0.1 M Captisol) and 20 mg/kg KU-32 (in ~ 125 µl of 0.1 M Captisol). Vehicle-treated controls for OG experiments were given mass-dependent volume equivalents of 0.1 M Captisol, or ~ 125 µl of 0.1 M Captisol (vehicle equivalent for both 10 mg/kg KU-32 and 20 mg/kg KU-32 OG treatments).

IP treatments were conducted using a sterile 1-ml syringe fitted with a sterile 27-gauge, 3/4-inch long hypodermic needle (BD, Franklin Lakes, NJ). Injection sites were pre-cleaned with 70% ethanol. For OG treatments, mice were anesthetized by open-drop exposure to isoflurane. During this procedure, animals were placed on a perforated plastic platform inside a slightly vented desiccation chamber, which contained a 2 x 2-inch gauze doused with 30% v/v isoflurane/propylene glycol underneath. Each bolus was then loaded into a primed[†] 1-ml syringe fitted with a reusable curved feeding needle (20-gauge; 1.5-inch long; and 2.25-mm ball diameter) (Cadence Science, Staunton, VA), inserted gently down the anesthetized animal's esophagus, and injected directly into the stomach. Upon full recovery from anesthesia (~ 15 seconds), mice were returned to their home cages. To minimize food influences on drug absorption, animals were fasted four hours before and one hour after OG treatment; animals always had *ad libitum* access to water. For better comparisons between drug delivery routes, IP-treated animals in Experiments 1 and 2 were likewise fasted. Only SW mice from the 8-week intervention study were treated without fasting.

[†] Needles were primed with appropriate solutions of 5 mg/ml KU-32, 2.5 mg/ml KU-32, or 0.1 M Captisol stock to avoid gastric distension and physical discomfort and to ensure complete dose delivery. Each dose was slowly drawn into the needle/syringe and any air trapped in the tip of the needle was expelled prior to injection. Pressure during gavage ceased upon initial contact of the plunger tip with the end of the syringe barrel.

2.3. Experiments

2.3.1. Experiment 1: KU-32 Tissue Levels in WT B6 and Hsp70 KO Mice

The first experiment was conducted using WT B6 and Hsp70 KO mice (**Table 6**). Each animal was administered a single IP injection of either 20 mg/kg KU-32 or a Captisol/saline vehicle equivalent. Vehicle-treated controls were included for quality assurance purposes. All animals were euthanized 2 or 4 hours after treatment for tissue collection (described in **Euthanasia and Tissue/Plasma Collection**). KU-32 levels were measured in the dorsal root ganglia (DRG), foot pads, and pooled sciatic, tibial, and sural nerves ("pooled nerves") of both strains at each time point.

Table 6. Treatment groups for Experiment 1.

WT B6 Treatments	*Time Point*	*n*		*Hsp70 KO Treatments*	*Time Point*	*n*
Veh	2 h	1		Veh	2 h	1
Veh	4 h	1		Veh	4 h	1
20 mg/kg KU-32	2 h	3		20 mg/kg KU-32	2 h	3
20 mg/kg KU-32	4 h	3		20 mg/kg KU-32	4 h	3

2.3.2. Experiment 2: Intraperitoneal Pharmacokinetic Time Profiles for KU-32

In the second experiment, 2- and 4-hour data from Experiment 1 were augmented by two earlier time points using Hsp70 KO mice (**Table 7**). These mice were intraperitoneally injected with 20 mg/kg KU-32 or a Captisol/saline vehicle and euthanized 30 or 60 minutes later for tissue collection. Since 2- and 4-hour KU-32 tissue levels (Experiment 1) were indistinguishable between WT B6 and Hsp70 KO mice, strain data were pooled at each time point. Hence, IP-PK time profiles were established using 0.5-hour (n = 3 mice), 1-hour (n = 3 mice), 2-hour (n = 6 mice), and 4-hour (n = 6 mice) time points in DRG, foot pads, and pooled nerves. Vehicle-treated controls were also included for quality assurance. Since

our pilot study revealed no detectable traces of KU-32 at 8 hours (data not presented), IP-PK time profiles were not extended beyond 4 hours.

Table 7. Augmented treatment groups for Experiment 2.

Hsp70 KO Treatments	*Time Point*	*n*
Veh	0.5 h	1
Veh	1 h	1
20 mg/kg KU-32	0.5 h	3
20 mg/kg KU-32	1 h	3

2.3.3. Experiment 3: KU-32 Tissue Levels After an 8-Week Intervention Study

In this 8-week intervention study, STZ-diabetes was induced in SW mice and monitored using the same methods and BCS considerations described in **CHAPTER II**. After 8 weeks, STZ-diabetic and non-diabetic animals identified for tissue analysis received six weekly IP treatments of 2, 10, or 20 mg/kg KU-32 (**Table 8**). All animals were euthanized 7-9 days after the sixth (final) treatment and the DRG, foot pads, and pooled nerves were collected.

Table 8. Treatment groups for Experiment 3.

SW Treatments	*n*
Veh + 20 mg/kg KU-32	7
STZ + 2 mg/kg KU-32	6
STZ + 10 mg/kg KU-32	7
STZ + 20 mg/kg KU-32	5

2.3.4. Experiment 4: Oral Gavage Pharmacokinetic Time Profiles for KU-32

In the final experiment, SW mice were orally administered 10 mg/kg KU-32, 20 mg/kg KU-32, or Captisol/saline vehicle-equivalent doses (**Table 9**). Vehicle-treated controls were included for quality assurance purposes. All animals were euthanized 1, 2, 4, 8, or 24 hours after gavage. In addition to DRG, foot pads, and pooled nerves, OG-PK time profiles for blood plasma were also established.

Table 9. Treatment groups for Experiment 4.

SW Treatments	*Time Point*	*n*	*SW Treatments*	*Time Point*	*n*
10 mg/kg KU-32	1 h	4	20 mg/kg KU-32	1 h	4
10 mg/kg KU-32	2 h	4	20 mg/kg KU-32	2 h	4
10 mg/kg KU-32	4 h	4	20 mg/kg KU-32	4 h	4
10 mg/kg KU-32	8 h	4	20 mg/kg KU-32	8 h	4
10 mg/kg KU-32	24 h	4	20 mg/kg KU-32	24 h	4
Veh	1 h	2			

2.4. Euthanasia and Tissue/Plasma Collection

All animals were euthanized in accordance with NIH guidelines, IACUC regulations, and approved animal use protocols. For Experiments 1, 2, and 4, mice were euthanized by CO_2 asphyxiation, followed by cardiac excision and then decapitation. After standard NCV measurements in the 8-week intervention study (as described in **CHAPTER II**), mice from Experiment 3 mice were euthanized via cardiac excision and then decapitation.

All tissues were collected immediately after euthanasia. Sciatic, tibial, and sural nerves were dissected and pooled from both hind limbs, flash frozen on dry ice, and then stored at - 80°C. The plantar integument (foot pad) for each hindpaw was also dissected, pooled, flash frozen on dry ice, and stored at – 80°C. L4-L6 DRG were excised from the lumbar intervertebral foramena using a dissecting microscope (roots trimmed during extraction), pooled for each mouse, flash frozen on dry ice, and stored at – 80°C. In Experiment 4, blood samples were collected after cardiac excision and promptly vortexed with 50 µl of 0.3 M ethylenediaminetetraacetic acid (EDTA) containing 1X complete protease inhibitor cocktail (Roche Diagnostics, Indianapolis, IN). Samples were centrifuged at 1,500 x g for 15 minutes at 4°C and plasma was collected, flash frozen on dry ice, and stored at – 80°C. Pooled nerves, foot pads, DRG, and plasma were also collected from wholly untreated mice (no vehicle) to serve as negative controls (tissue and plasma blanks) and for standard curve

generation in LC/MS/MS analyses (n = 30 mice). All tissues were later weighed in fresh, dry 2-ml microcentrifuge tubes at room-temperature in preparation for LC/MS/MS. These tissues were immediately refrozen on dry ice and re-stored at – 80°C alongside frozen plasma samples.

2.5. KU-32 Measurements and Pharmacokinetic Analyses

2.5.1. KU-32 Extraction

While the extraction procedure for KU-32 was largely conserved across all sample types and experiments, different extraction solvent volumes were used based on the amount of sample available and each distinct matrix.[1] These methods are described below. Drug extractions and LC/MS/MS analyses were performed with technical consult and equipment provided by Joanna Krise and Dr. Roger Rajewski at The University of Kansas's Biotechnology Innovation and Optimization Center.

2.5.1.1. KU-32 Extraction from Pooled Sciatic, Tibial, and Sural Nerves

All 2-ml microcentrifuge tubes containing frozen pooled nerve samples and standards were slowly warmed to room temperature (RT). Millipure H_2O was carefully added to each tube using a mass scale to achieve a 25 mg tissue/g H_2O suspension. All tissues were then pulverized by intense sonication for 30 seconds at RT. Each homogenate was vortexed for 10 seconds and a 200-µl aliquot was transferred to a safe-lock 2-ml microcentrifuge tube. For each standard, 5 µl of appropriate 1X KU-32 (50% dimethyl sulfoxide; DMSO) stock solution was added, vortexed for 10 seconds, and incubated for 5 minutes at RT to generate 1, 10, 50, 100, 250, 500, and 1,000 ng KU-32/g tissue standards. Each 1X KU-32 stock was vortexed for 10 seconds prior to use and 5 µl of 50% DMSO was added to each sample for consistency and vortexed for 10 seconds. All standards and samples were then spiked with

5 µl of 50 ng/ml trideutero KU-32 (d3KU-32) (50% DMSO) internal standard and vortexed for 10 seconds to give a 50 ng d3KU-32/g tissue mixture; d3KU-32 stock was also vortexed for 5 seconds before use. Approximately 1 ml of methyl *tert*-butyl ether (MTBE) was added to each tube, vortexed for 5 minutes, and centrifuged at 12,000 rpm for 5 minutes at RT. Roughly 950 µl of the organic layer was transferred to a new 1.7-ml microcentrifuge tube and evaporated to dryness using a speed vacuum (high temperature) for ~ 20 minutes. Each sample and standard was then reconstituted in 50 µl of 20% v/v (CH_3CN/H_2O), vortexed for 10 seconds, and centrifuged at 12,000 rpm for 5 minutes at RT. Upon completion, 45-µl of supernatant was transferred to autosampler vials with glass inserts for LC/MS/MS analysis.

2.5.1.2. KU-32 Extraction from Foot Pads

All 2-ml microcentrifuge tubes containing pooled frozen foot pad samples and standards were slowly warmed to RT. Millipure H_2O was carefully added to each tube using a mass scale to achieve a 100 mg tissue/g H_2O suspension. Tissues were then pulverized by intense sonication for 90 seconds at RT. Each homogenate was vortexed for 10 seconds and a 125-µl aliquot was transferred to a safe-lock 2-ml microcentrifuge tube. For each standard, 12.5 µl of appropriate 1X KU-32 (50% DMSO) stock solution was added, vortexed for 10 seconds, and incubated for 5 minutes at RT to generate 1, 10, 50, 100, 250, 500, and 1,000 ng KU-32/g tissue standards. Each 1X KU-32 stock solution was vortexed for 10 seconds before use and 12.5 µl of 50% DMSO was added to each sample for consistency and vortexed for 10 seconds. All tubes were spiked with 12.5 µl of 50 ng/ml d3KU-32 (50% DMSO) internal standard and vortexed for 10 seconds to give a 50 ng d3KU-32/g tissue mixture; d3KU-32 stock solution was vortexed for 5 seconds before use. Roughly 625 µl of MTBE was added to each tube, vortexed for 5 minutes, and centrifuged at

12,000 rpm for 5 minutes at RT. About 600 µl of the organic layer was transferred to a fresh 1.7-ml microcentrifuge tube and evaporated to dryness using a speed vacuum (high temperature) for ~ 20 minutes. Each sample/standard was reconstituted in 50 µl of 20% v/v (CH_3CN/H_2O), vortexed for 10 seconds, and centrifuged at 12,000 rpm for 5 minutes at RT. Upon completion, 45-µl of supernatant was transferred to autosampler vials with glass inserts for LC/MS/MS analysis.

2.5.1.3. KU-32 Extraction from Dorsal Root Ganglia

2.5.1.3.1. KU-32 Extraction from DRG (IP Experiments)

All 2-ml microcentrifuge tubes containing frozen DRG samples and standards were slowly warmed to RT. Millipure H_2O was carefully added to each tube using a mass scale to achieve a 25 mg tissue/g H_2O suspension. Tissues were then pulverized by intense sonication for 30 seconds at RT. Each homogenate was vortexed for 10 seconds and a 40-µl aliquot was transferred to a safe-lock 2-ml microcentrifuge tube. For each standard, 1 µl of appropriate 1X KU-32 (50% DMSO) stock solution was added, vortexed for 10 seconds, and incubated for 5 minutes at RT to generate 1, 10, 50, 100, 250, 500, and 1,000 ng KU-32/g tissue standards. Each 1X KU-32 stock solution was vortexed for 10 seconds before use and 1 µl of 50% DMSO was added to each sample for consistency and vortexed for 10 seconds. All tubes were spiked with 1 µl of 50 ng/ml d3KU-32 (50% DMSO) internal standard and vortexed for 10 seconds to give a 50 ng d3KU-32/g tissue mixture; d3KU-32 stock solution was vortexed for 5 seconds before use. Roughly 200 µl of MTBE was added to each tube, vortexed for 5 minutes, and centrifuged at 12,000 rpm for 5 minutes at RT. About 180 µl of the organic layer was transferred to a fresh 1.7-ml microcentrifuge tube and evaporated to dryness using a speed vacuum (high temperature) for ~ 20 minutes.

Each sample/standard was reconstituted in 40 µl of 20% v/v (CH_3CN/H_2O), vortexed for 10 seconds, and centrifuged at 12,000 rpm for 5 minutes at RT. Upon completion, 35-µl of supernatant was transferred to autosampler vials with glass inserts for LC/MS/MS analysis.

2.5.1.3.2. KU-32 Extraction from DRG (OG Experiment)

Due to DRG sample mass limitations, the extraction procedure for the OG experiment was modified relative to IP experiments. All 2-ml microcentrifuge tubes containing frozen DRG samples and standards were slowly warmed to RT. Millipure H_2O was added to each tube using a mass scale to achieve a 10 mg tissue/g H_2O suspension. Tissues were then pulverized by intense sonication for 30 seconds at RT. Each homogenate was vortexed for 10 seconds and a 40-µl aliquot was transferred to a safe-lock 2-ml microcentrifuge tube. For each standard, 4 µl of appropriate 0.1X KU-32 (50% DMSO) stock solution was added, vortexed for 10 seconds, and incubated for 5 minutes at RT to generate 1, 10, 50, 100, 250, 500, and 1,000 ng KU-32/g tissue standards. Each KU-32 stock solution was vortexed for 10 seconds before use and 4 µl of 50% DMSO was added to each sample for consistency and vortexed for 10 seconds. All tubes were then spiked with 4 µl of 5 ng/ml d3KU-32 (50% DMSO) internal standard and vortexed for 10 seconds to give a 50 ng d3KU-32/g tissue mixture; d3KU-32 stock solution was vortexed for 5 seconds before use. Roughly 200 µl of MTBE was then added to each tube, vortexed for 5 minutes, and centrifuged at 12,000 rpm for 5 minutes at RT. About 180 µl of the organic layer was transferred to a fresh 1.7-ml microcentrifuge tube and evaporated to dryness using a speed vacuum (high temperature) for ~ 20 minutes. Each sample/standard was reconstituted in 40 µl of 20% v/v (CH_3CN/H_2O), vortexed for 10 seconds, and centrifuged at 12,000 rpm for 5 minutes at RT.

Upon completion, 35-µl of supernatant was transferred to autosampler vials with glass inserts for LC/MS/MS analysis.

2.5.1.4. KU-32 Extraction from Blood Plasma

All 2-ml microcentrifuge tubes containing frozen plasma samples and standards were slowly warmed to RT. Each tube was vortexed for 10 seconds and a 50-µl aliquot was transferred to a safe-lock 2-ml microcentrifuge tube. For each standard, 5 µl of appropriate 10X KU-32 (50% DMSO) stock solution was added, vortexed for 10 seconds, and incubated for 5 minutes at RT to give 1, 10, 50, 100, 250, 500, and 1,000 ng KU-32/ml plasma standards. Each KU-32 stock solution was vortexed for 10 seconds before use and 5 µl of 50% DMSO was added to each sample for consistency and vortexed for 10 seconds. All tubes were spiked with 5 µl of 500 ng/ml d3KU-32 (50% DMSO) internal standard and vortexed for 10 seconds to give a 50 ng d3KU-32/ml plasma mixture; d3KU-32 stock solution was vortexed for 5 seconds before use. Roughly 250 µl of MTBE was added to each tube, vortexed for 5 minutes, and centrifuged at 12,000 rpm for 5 minutes at RT. About 225 µl of the organic layer was transferred to a 1.7-ml microcentrifuge tube and evaporated to dryness using a speed vacuum (high temperature) for ~ 20 minutes. Each sample/standard was then reconstituted in 50 µl of 20% v/v (CH_3CN/H_2O), vortexed for 10 seconds, and centrifuged at 12,000 rpm for 5 minutes at RT. Upon completion, 45-µl of supernatant was transferred to autosampler vials with glass inserts for LC/MS/MS analysis.

2.5.1.5. Tissue and Plasma Blanks

Tissue and plasma blanks were prepared from wholly untreated mice. These blanks were used for purging and as negative controls between standard and sample processing

during LC/MS/MS analysis. Blanks were processed similar to the standards with the exception that KU-32 and d3KU-32 spikes were substituted with 50% DMSO only.

2.5.2. Liquid Chromatography-Tandem Mass Spectrometry (LC/MS/MS)

KU-32 analyte concentrations were measured using an API 3200™ LC/MS/MS System (AB SCIEX, Framingham, MA). Chromatographic separation was performed using a 5-µm Agilent Zorbax SB-C18 column (2.1 x 50 mm) (Agilent Technologies, Santa Clara, CA) and a linear gradient of CH_3CN:H_2O:HCO_2H [(5:95:0.1) to (95:5:0.1) over 8 minutes] with a 300 µl/min flow rate. Average analyte retention time was 3.43 minutes. The effluent was then introduced to a Sciex API3200 Linear Ion Trap (LIT) detector (Framingham, MA) using turbo ion spray in the positive ion mode. During this process, effluent ions were focused by the Q0 quadrupole prior to entering the Q1 quadrupole. The Q1 quadrupole served as an ion filter optimized for 408.223 m/z (KU-32) and 411.140 m/z (d3KU-32) collection. Upon arriving at the Q2 collision chamber [LINAC® (linear accelerator) collision cell], ions were fragmented by nitrogen gas collision. KU-32 (192.100 m/z) and d3KU-32 (193.200 m/z) analytes were then filtered by the Q3 quadrupole before entering the LIT detector to generate quantifiable signals. Standard curves were constructed for each run using 0-1,000 ng KU-32/g tissue or 0-1,000 ng KU-32/ml plasma standards. Analyte recovery ranged between 65-75%, which was determined by comparing d3KU-32 analyte spectra from the zero standard in relation to like spectra from a d3KU-32 (50% DMSO)-spiked 20% v/v (CH_3CN/H_2O) control[†]. KU-32:d3KU-32 analyte ratios and standard curves were used to determine original KU-32 concentrations for each sample. Limit of detection (LOD) calculations for Experiment 3 were based on the linear calibration curves for each

[†] Established as 100% recovery since created post-extraction

LC/MS/MS run: $LOD = 3S_a/b$, where S_a is the residual standard deviation[†] and b is the slope of the calibration curve.[3-4]

2.6. Statistical Analyses and Pharmacokinetic Calculations

Statistical analyses were performed using JMP Pro 11.0.0 (SAS Institute Inc, Cary, NC) and portrayed using Graphpad Prism 6 (Graphpad Software, Inc., La Jolla, CA). Initial assessments of KU-32 analyte concentration data revealed strong evidence of non-normality (Shapiro-Wilks test) and high variance (via O'Brien's, Brown-Forsythe, Levene's, and Bartlett's tests) across treatment groups, thus violating two major assumptions for proper two-way ANOVA use.[5-6] This was not surprising given the small sample sizes for each treatment group (n = 3-6 samples/group). Alternatively, the Kruskal-Wallis test was used to determine differences between group medians, followed by the Wilcoxon Each Pair test for nonparametric multiple comparisons to identify significant differences between specific group pairs.[6-7] The Bonferonni correction (post hoc test) was used to correctly adjust the α-levels to account for inflated error associated with the multiple comparisons.[7] This was achieved by dividing the desired α-level of 0.05 by the number of pairwise comparisons made with 20 mg/kg KU-32 OG at each time point, giving either a new α-level of 0.025 for two comparisons (20 mg/kg KU-32 IP and 10 mg/kg KU-32 OG)[††] or retaining 0.05 for a single pair comparison (10 mg/kg KU-32 OG).[7] The p-values expressed in all figures reflect these corrected α-levels, and all data are presented as mean ± SEM.

IP-PK and OG-PK time profiles (Experiments 2 and 4) for each sample type were established by plotting mean KU-32 analyte concentrations over time. For further analysis, mean analyte concentrations were converted to a natural log scale.[8-13] Linear regression

[†] Defined as "$s_{y.x}$" in JMP Pro 11.0.0
[††] No comparisons were made for 20 mg/kg KU-32 IP:10 mg/kg KU-32 OG

analysis was then performed for each treatment group and the linear regression segments were plotted.[8-13] The r^2-values for each linear regression segment were used to determine whether the drug elimination data supported first-order kinetics.[8-13] Drug elimination rate constants (k_e) were established as the opposite slope of these linear regression segments.[8-13] Drug elimination half-lives for each treatment group and sample type were calculated as: $t_{1/2} = \ln(2)/k_e$.[8-13] Based on the linear equations of each linear regression segment, one-phase exponential decay equations were derived and plotted on the unaltered PK time profiles.

SECTION 3. RESULTS

3.1. Inducible Hsp70 Deletion Does Not Affect Drug Distribution

While KU-32 was detected in the pooled nerves, foot pads, and DRG of 20 mg/kg KU-32 IP-treated WT B6 and Hsp70 KO mice, no significant differences were found between strains at the 2- and 4-hour time points (**Figure 29**); lowest p-value (0.0809) was established for the 2-hour foot pad comparison. Despite clear differences between tissue types, drug elimination between strains appeared equal over this 2-hour duration.

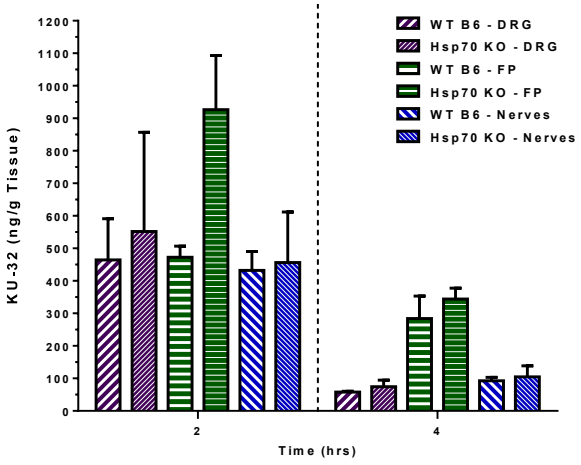

Figure 29. Comparison of KU-32 tissue levels in WT B6 and Hsp70 KO mice. KU-32 levels for the DRG, foot pads, and pooled nerves of WT B6 and Hsp70 KO mice were measured two and four hours after a single 20 mg/kg KU-32 IP injection. No significant differences ($p < 0.05$) between strains were found; error bars denote SEM.

3.2. Intraperitoneal Pharmacokinetic Time Profiles for KU-32

Temporal IP-PK analyses revealed major drug distribution and elimination differences between pooled nerves, foot pads, and DRG. Surprisingly, the highest levels of KU-32 were found at the initial time point at 30 minutes ($C_{i\text{-}30}$) for all tissues (**Table 10**; **Figure 30A-C**), indicating that maximum drug concentrations for these tissues had already been reached and that drug absorption into the blood and tissue distribution occur remarkably fast. Additional analyses were performed using natural log plots of mean KU-32 analyte levels over time (**Figure 30E-G**). The r^2-values for linear regression segments [0.952 (pooled nerves); 0.934 (foot pads), and 0.995 (DRG)] supported first-order elimination kinetics for all tissues.[8-9] While the elimination rate constant (k_e) for pooled nerves was nearly identical to the DRG, the k_e for foot pads was 41% less than that of pooled nerves, resulting in a 67% longer half-life ($t_{1/2}$) in foot pads. Given these half-life and $C_{i\text{-}30}$ data, it was determined that 99.9% of total drug distributed to these tissues was eliminated 6.4 hours (pooled nerves), 10.4 hours (foot pads), and 6.6 hours (DRG) after treatment. These data suggest that foot pads are exposed to KU-32 roughly 60% longer than pooled nerves and DRG. Unfortunately, while AUC calculations are best-suited for comparing the overall extent of drug exposure between tissues (and delivery routes), these calculations required additional (earlier) time points to accurately capture the maximum drug concentrations (C_{max}) and initial distribution from C_o (concentration at time point zero) to the true C_{max}.

Table 10. IP-PK parameters.

Tissue	*(IP Treatment)*	*$C_{i\text{-}30}$ (ng/g)*	*k_e (h^{-1})*	*$t_{1/2}$ (h)*
Pooled Nerves	(20 mg/kg KU-32)	5,720	1.18	0.590
Foot Pads	(20 mg/kg KU-32)	3,680	0.696	0.996
DRG	(20 mg/kg KU-32)	3,250	1.13	0.613

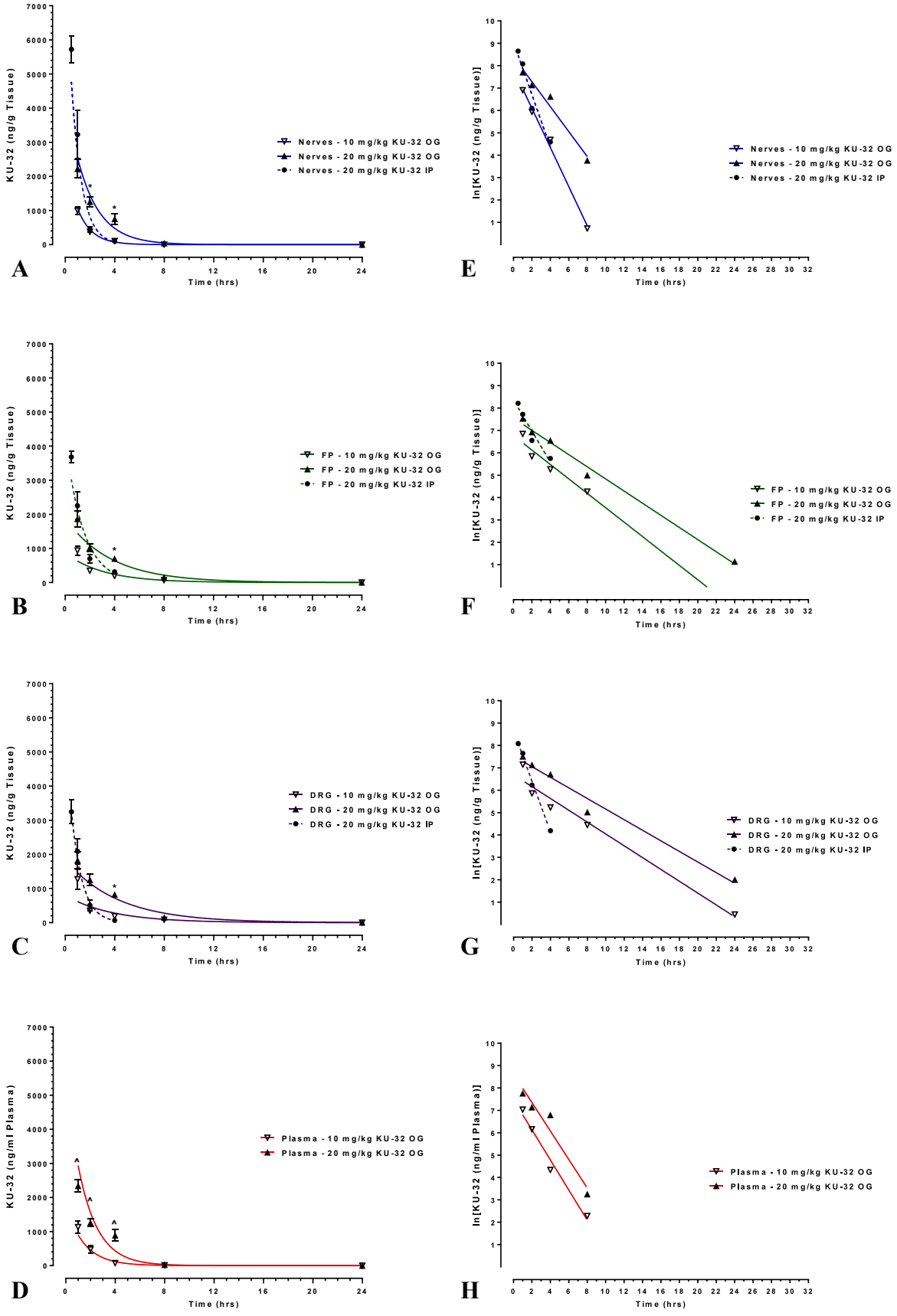
A
KU-32 (ng/g Tissue)
Time (hrs)
Nerves - 10 mg/kg KU-32 OG
Nerves - 20 mg/kg KU-32 OG
Nerves - 20 mg/kg KU-32 IP
E
ln[KU-32 (ng/g Tissue)]
Time (hrs)
Nerves - 10 mg/kg KU-32 OG
Nerves - 20 mg/kg KU-32 OG
Nerves - 20 mg/kg KU-32 IP
B
KU-32 (ng/g Tissue)
Time (hrs)
FP - 10 mg/kg KU-32 OG
FP - 20 mg/kg KU-32 OG
FP - 20 mg/kg KU-32 IP
F
ln[KU-32 (ng/g Tissue)]
Time (hrs)
FP - 10 mg/kg KU-32 OG
FP - 20 mg/kg KU-32 OG
FP - 20 mg/kg KU-32 IP
C
KU-32 (ng/g Tissue)
Time (hrs)
DRG - 10 mg/kg KU-32 OG
DRG - 20 mg/kg KU-32 OG
DRG - 20 mg/kg KU-32 IP
G
ln[KU-32 (ng/g Tissue)]
Time (hrs)
DRG - 10 mg/kg KU-32 OG
DRG - 20 mg/kg KU-32 OG
DRG - 20 mg/kg KU-32 IP
D
KU-32 (ng/ml Plasma)
Time (hrs)
Plasma - 10 mg/kg KU-32 OG
Plasma - 20 mg/kg KU-32 OG
H
ln[KU-32 (ng/ml Plasma)]
Time (hrs)
Plasma - 10 mg/kg KU-32 OG
Plasma - 20 mg/kg KU-32 OG

Figure 30. IP-PK and OG-PK time profiles for KU-32. Mean KU-32 analyte levels and one-phase exponential decay equations for (A) pooled nerves, (B) foot pads, (C) DRG, and (D) plasma were plotted over time following 10 mg/kg KU-32 (OG) or 20 mg/kg KU-32 (OG and IP) treatments; error bars denote ± SEM. Natural log conversions of mean KU-32 analyte levels and linear regression segments for (E) pooled nerves, (F) foot pads, (G) DRG, and (H) plasma were plotted over time. Dashed lines represent IP treatments and solid lines portray OG treatments. *, $p < 0.025$ between 20 mg/kg KU-32 OG and 20 mg/kg KU-32 IP; ^, $p < 0.05$ between 20 mg/kg KU-32 OG and 10 mg/kg KU-32 OG**.**

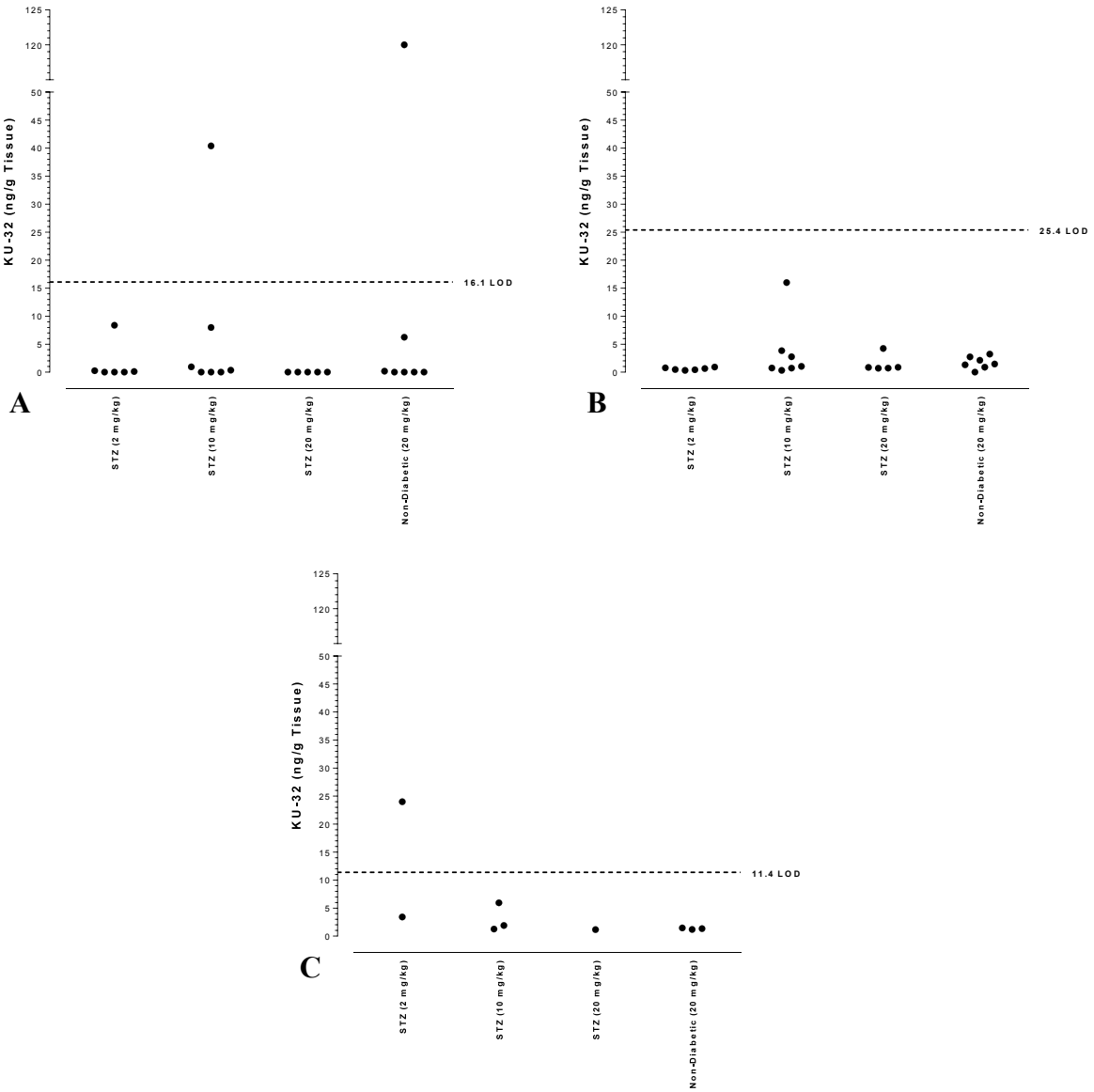

Figure 31. KU-32 levels after an 8-week intervention study. KU-32 analyte levels in the (A) pooled nerves, (B) foot pads, and (C) DRG after an 8-week intervention study in SW mice. All tissues were collected 7-9 days after the sixth (final) weekly IP treatment at the indicated doses. LOD denotes the limit of detection as defined in the methods.

3.3. KU-32 Levels After an 8-Week Intervention Study

Eight-week STZ-diabetic and non-diabetic SW mice were given 2, 10, or 20 mg/kg KU-32 IP treatments once per week for six weeks. One week after the final treatment, LC/MS/MS analysis showed virtually no detectable KU-32 present in pooled nerves, foot pads, and DRG (**Figure 31**). These data suggest that KU-32 was either never distributed to these tissues or that KU-32 was entirely eliminated before sampling. Drug elimination data from Experiment 2 support the latter, predicting that 99.9% of all drug distributed to these tissues is eliminated within 11 hours of treatment. Conversely, the data here reinforce the findings of Experiment 2, suggesting that weekly IP treatments at this dose are insufficient to cause drug accumulation in these tissues, thus ruling out drug accumulation as a possible explanation for the progressive neuroprotective effects elicited by KU-32.[1]

In most cases, KU-32 analyte levels were well below the limit of detection (LOD) for LC/MS/MS (defined in the **LC/MS/MS** section). However, there were three cases in which KU-32 was detected: two in pooled nerves [1x STZ-diabetic (10 mg/kg KU-32) and 1x Non-Diabetic (20 mg/kg KU-32)] and one in DRG [1x STZ-diabetic (2 mg/kg KU-32)]. The reasons for these outliers are unknown but may be linked to individual variations in drug absorption, distribution, and elimination. This is partly supported by the non-normality and high variance observed across treatment groups. While it is tempting to speculate that disease-induced reductions in vascular support could affect drug elimination, it seems unlikely for two reasons. First, while the extremities are the most common site for vascular deterioration in diabetes mellitus[14], KU-32 was not found in time-matched foot pads. Second, trace levels of KU-32 were found in the pooled nerves of non-diabetic mice, which should have normal vasculature to facilitate elimination. Regardless, these levels comprise

less than 2% of initial drug concentrations measured at 30 minutes in Experiment 2, which is far less than the standard deviation for these points. Fortunately, the detection of KU-32 in STZ-diabetic tissues does confirm that at least some drug is distributed to diabetic tissues. Even so, further temporal IP-PK studies in STZ-diabetic mice are needed to assess particular disease influences on KU-32 absorption, distribution, and elimination.

3.4. Oral Gavage Pharmacokinetic Time Profiles for KU-32

Temporal OG-PK analyses revealed several dose-dependent distribution and elimination differences between pooled nerves, foot pads, and DRG and dose-dependent differences in drug absorption and elimination in the plasma. The highest KU-32 levels were found at the initial 60-minute time point ($C_{i\text{-}60}$) for all tissues and plasma, again suggestive of rapid drug absorption into the blood and distribution to the tissues (**Table 11**; **Figure 30A-D**). This rapid drug absorption was corroborated by Dr. Maged Zeineldin (Molecular Biosciences), who performed identical PK analyses on intestinal samples also collected from these mice. He found that KU-32 levels were highest in the superior duodenum, but quickly diminished upon passing posteriorly through the jejunum and ileum (unpublished results). However, with the analyses performed, it was not possible to determine if KU-32 was fully depleted before reaching these regions or if physiological differences affected absorption.

Table 11. OG-PK parameters.

Tissue	*(OG Treatment)*	*$C_{i\text{-}60}$ (ng/g)*	*k_e (h^{-1})*	*$t_{1/2}$ (h)*
Pooled Nerves	(10 mg/kg KU-32)	999	0.874	0.793
Pooled Nerves	(20 mg/kg KU-32)	2,220	0.557	1.25
Foot Pads	(10 mg/kg KU-32)	940	0.322	2.15
Foot Pads	(20 mg/kg KU-32)	1,870	0.271	2.56
DRG	(10 mg/kg KU-32)	1,270	0.264	2.62
DRG	(20 mg/kg KU-32)	1,830	0.237	2.93
Plasma	(10 mg/kg KU-32)	1,130	0.673	1.03
Plasma	(20 mg/kg KU-32)	2,340	0.637	1.09

Further analyses were performed using natural log plots of mean KU-32 analyte levels over time (**Figure 30E-H**). The linear regression segments established for these plots had r^2-values of: 0.993 (10 mg/kg KU-32) and 0.970 (20 mg/kg KU-32) for pooled nerves; 0.969 (10 mg/kg KU-32) and 0.977 (20 mg/kg KU-32) for DRG; 0.992 (10 mg/kg KU-32) and 0.991 (20 mg/kg KU-32) for foot pads; and 0.978 (10 mg/kg KU-32) and 0.944 (20 mg/kg KU-32) for plasma, suggesting that elimination followed first-order kinetics.[8-9] As expected, there were dose-dependent differences in drug absorption, distribution, and elimination. Initial tissue levels ($C_{i\text{-}60}$) for the pooled nerves, foot pads, and plasma of 20 mg/kg KU-32 OG-treated mice were nearly twice that of 10 mg/kg OG-treated mice. Intriguingly, the $C_{i\text{-}60}$ for DRG of 20 mg/kg KU-32 OG-treated mice was 44% higher than those of 10 mg/kg OG-treated mice. Drug elimination rate constants were consistently higher for tissues of 10 mg/kg OG-treated mice [57% (pooled nerves), 18% (foot pads); and 11% (DRG) higher] than those of 20 mg/kg KU-32 OG-treated mice.

In considering half-life and $C_{i\text{-}60}$ data, it was determined that 99.9% of all drug distributed to the tissues of 10 mg/kg KU-32 OG-treated mice is eliminated 8.9 hours (pooled nerves), 22.4 hours (foot pads), and 27.1 hours (DRG) after treatment. Likewise, 99.9% of all drug distributed to the tissues of 20 mg/kg KU-32 OG-treated mice is eliminated 13.5 hours (pooled nerves), 26.5 hours (foot pads), and 30.2 hours (DRG) after oral gavage. Similarly, calculations with plasma half-life and $C_{i\text{-}60}$ data showed that 99.9% of all drug absorbed into the blood is eliminated 11.3 hours (10 mg/kg KU-32) and 11.9 hours (20 mg/kg KU-32) after gavage. Hence, the duration of drug exposure for foot pads and DRG seems to be over twice that of pooled nerves and plasma.

SECTION 4. DISCUSSION AND CONCLUDING REMARKS

4.1. KU-32 Pharmacokinetic Time Profile Comparisons

The results obtained show that KU-32 is rapidly absorbed and distributed to DSPN-relevant tissues within 30 minutes of IP treatment or one hour of gavage. Temporal IP-PK and OG-PK analyses suggest that 99.9% of all drug distributed to the pooled nerves, foot pads, and DRG is eliminated within ~ 30 hours of treatment. These inferences are consistent with findings from the 8-week intervention study, which showed virtually no detectable levels of KU-32 present in the tissues of non-diabetic and diabetic mice one week after final treatment. With that said, there were still distinct differences in drug distribution and elimination between delivery routes, tissues, and doses. Possible explanations for these observations are discussed herein.

Since peripheral nerve fibers stem from the neuronal cell body (soma) located within the DRG, one might expect KU-32 to readily diffuse throughout the neuron, regardless of its site of entry and relative hydrophobicity, thereby resulting in similar drug concentrations and elimination kinetics for DRG that perhaps lag behind those of pooled nerves.[15] This seems to be true for the DRG and pooled nerves of 20 mg/kg KU-32 IP-treated mice, which do demonstrate comparable $C_{i\text{-}30}$, k_e, and $t_{1/2}$ values after temporal PK analyses (**Table 10**). This was not the case for OG-treated mice (**Table 11**). Drug elimination half-lives for the DRG of OG-treated mice (10 and 20 mg/kg KU-32) were 2-3 times greater than those of pooled nerves. In comparing drug elimination half-lives for DRG and pooled nerves between delivery routes (20 mg/kg KU-32 OG versus 20 mg/kg KU-32 IP), it was found that tissues of OG-treated mice had half-lives that were 2.3 hours (DRG) and 0.7 hours (pooled nerves) longer than those of IP-treated mice. Hence, it takes an additional 7.1 hours

(pooled nerves) and 23.6 hours (DRG) to eliminate 99.9% of the total drug distributed to these same tissues in OG-treated mice.

While it was reasonable to expect variations in initial drug distribution based on drug dose and delivery routes, the reasons for differences in elimination kinetics are unknown.[8-10, 12-13] For DRG, we first suspected that differences in extraction solvent:sample mass ratios used during the pulverization step of KU-32 extraction could cause variations in KU-32 analyte recovery. Drug extraction from the DRG of OG-treated mice was performed using 10 mg tissue/g H_2O, whereas extraction from the DRG of IP-treated mice was conducted using 25 mg tissue/g H_2O. Given KU-32's solubility constraints, it seemed reasonable that extra solvent could enhance the amount of total free drug recovered in solution. Moreover, lesser amounts of tissue pulp in near equivalent volumes of water between protocols should lessen the likelihood of KU-32 repartitioning back into the pulverized tissues. While this might be possible, it seems unlikely given that each homogenate was intensely vortexed immediately prior to aliquot collection and that tissue mass-dependent equivalents of d3KU-32 internal standard were recovered at similar rates between delivery routes. Thus, the question remained, why does KU-32 elimination kinetics for DRG (and foot pads and pooled nerves) differ so much between delivery routes?

To answer this, plasma IP-PK and OG-PK time profiles were compared. While plasma samples were not collected during these IP experiments, we have previously reported plasma KU-32 levels after 2 mg/ml KU-32 (5% Captisol) IP injections in Balb/c mice (**Figure 32**).[1] This study also showed rapid drug absorption into the blood with maximum absorption levels occurring within 15 minutes of treatment.[1] In 10 mg/kg KU-32 and 20 mg/kg KU-32 OG-treated mice, drug elimination half-lives for plasma were consistent at about 1.1 hours,

and plasma drug concentrations appeared to be dose-dependent. In the Balb/c study, the drug elimination half-life for plasma was ~ 1.8 hours. However, dosing must be considered.

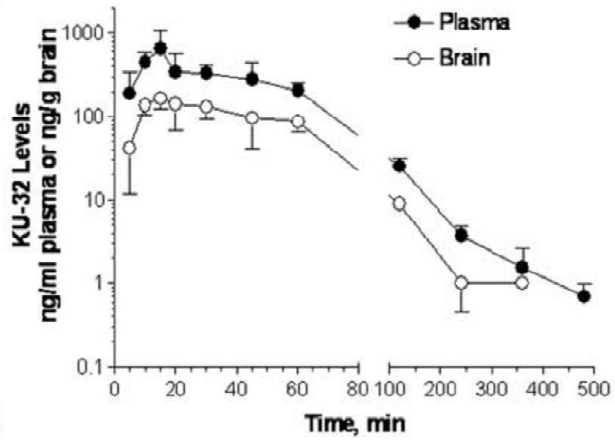

Figure 32. KU-32 IP-PK time profiles for plasma and whole brain. 1 ml of 2 mg/ml KU-32 (5% Captisol) was injected intraperitoneally in Balb/c mice. Plasma and whole brain samples were harvested at the indicated times and analyzed using LC/MS/MS.[1]

Approximately 150 µl of 5 mg/ml KU-32 stock solution was needed for each 20 mg/kg KU-32 OG treatment, meaning that ~ 0.75 mg of KU-32 was administered into each animal. In contrast, 1 ml of 2 mg/ml KU-32 stock solution gives a total of 2 mg KU-32 injected into each Balb/c mouse.[1] Setting aside vehicle differences, the net amount of KU-32 delivered in OG treatments was 37.5% of that used for the IP treatments. Incredibly, the amount of KU-32 circulating in the blood after one hour of OG treatment is over twice that ever achieved in IP-treated Balb/c mice.[1] Given that the $C_{i\text{-}30}$ levels reported herein for pooled nerves, foot pads, and DRG were all above 3,000 ng/g for 20 mg/kg KU-32 IP-treated mice, it seems likely that the majority of IP-administered drug diffuses directly into the tissues rather than first partitioning into the blood for distribution. Conversely, OG requires drug absorption across the gut for systemic blood circulation and then tissue distribution. It seems possible that IP drug delivery could result in more superficial drug penetration into DSPN-relevant tissues. Further, diffusion back out of superficial tissue layers may occur

more rapidly once initial drug distribution is complete. In contrast, more systemic blood circulation (via OG) may afford more thorough penetration into deeper tissue layers. It is important to note that L4-L6 DRG are largely encased in the lumbar intervertebral foramena of the spinal column, which only allows the nerve roots to protrude out into the periphery.[15-16] This makes the DRG less susceptible to IP drug treatments.[17] However, DRG also lack a protective capsular membrane as seen in the blood-brain barrier.[17] Given that the DRG are still highly perfused by capillaries, they are more susceptible to orally bioavailable drugs.[17] In regard to peripheral nerves, the *vasa nervorum* may provide better access to inner nerve fibers by bypassing the protective nerve sheathes (**Figure 33**).[18] For foot pads, higher drug plasma levels would likely increase more remote cutaneous drug distribution via capillaries. Overall, these reasons may partly explain why drug elimination half-lives for DRG, pooled nerves, and foot pads of OG-treated mice are all longer than those of IP-treated mice.

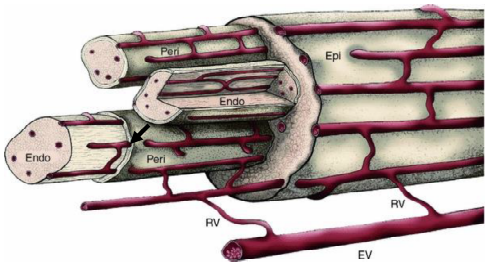

Figure 33. ***Vasa nervorum*.** Radicular vessels (RV) stemming from regional extrinsic vessels (EV) comprise the *vasa nervorum*, or the microvasculature supplying the peripheral nerves. Also shown are the epineurium (Epi), perineurium (Peri), and endoneurium (Endo) nerve sheathes, which are interconnected by microvessels.[18]

4.2. Inducible Hsp70 and KU-32 Pharmacokinetics

In support of the ongoing hypothesis that inducible Hsp70 is essential for KU-32's neuroprotective effects in DSPN, we have shown that KU-32 distribution to the pooled nerves, foot pads, and DRG are indistinguishable between WT B6 and Hsp70 KO mice.[1-2, 19-20] While 2-hour foot pad data did seem to deviate between strains, the difference was insignificant ($p = 0.0809$). Should this deviation become significant with increased sample sizes[†], KU-32 levels would likely become higher for the foot pads of Hsp70 KO mice. Such a distinction would be irrelevant, however, given that *more* KU-32 would be available to tissues of Hsp70 KO mice. Hence, our previous report of KU-32 inefficacy in STZ-diabetic Hsp70 KO mice was not the result of less drug distribution and availability in these tissues, but rather a mechanistic consequence of inducible Hsp70 deletion.[1-2]

4.3. Concluding Remarks and Future Directions

In summary, we have shown that KU-32 is rapidly distributed to DSPN-relevant tissues and readily available for local Hsp90 modulation almost immediately after IP and gavage treatments. The finding that KU-32 is readily eliminated from these tissues within the normal dosing timeframe argues against the notion that mounting drug concentrations are related to KU-32's progressive neuroprotective effects. Interestingly, OG drug delivery seemed to increase the drug elimination half-lives in all examined tissues relative to IP treatments. However, the resounding question still remains, are these concentrations achieved by OG sufficient to elicit the same neuroprotective effects observed with IP treatments? In this regard, dose-dependent improvements in electrophysiological and psychophysical indices of DSPN in 8-week intervention studies have been demonstrated

[†] As described in the **Statistical Analyses and Pharmacokinetic Calculations** section, small sample sizes as well as data non-normality and high variance were all major limitations.

using an IP dose range of 2-20 mg/kg KU-32.[1, 21] Hence, it seems likely that repeated exposure to even low amounts of KU-32 could be beneficial. However, this is contingent upon how the disease impacts drug distribution to these DSPN-relevant tissues.

In **CHAPTER II**, we demonstrated that pharmacologic Hsp90 modulation improves psychophysical, electrophysiological, morphological, and bioenergetic indices at more chronic stages of DSPN development. Previous studies have also shown that KU-32's neuroprotective effects in DSPN are contingent upon the expression of inducible Hsp70.[1-2] Herein, we have established that KU-32 distribution and elimination in DSPN-relevant tissues are unaffected by inducible Hsp70 deletion. While this local drug availability in DSPN-relevant tissues of Hsp70 KO mice does support the mechanistic importance of inducible Hsp70 for KU-32 effectiveness, the molecular mechanisms underlying these neuroprotective effects still remain elusive. However, the confirmation that KU-32 is locally available within the DRG, pooled nerves, and foot pads, combined with the prospect for remote Hsp90 modulation and Hsp70 translation in neurons, opens the door to multiple mechanistic possibilities.[22]

In the future, it will be important to explore whether KU-32 can effectively enhance IGF-I-induced neurite outgrowth and mitochondrial bioenergetic improvements in sensory neurons (DRG) isolated from intervention study mice. Given the extent of Hsp90 client protein involvement in the IGF-I signaling, the body's natural tendency to increase IGF-I signaling during late stages of DSPN, and the highly similar neuroprotective effects elicited by both KU-32 and IGF-I intervention in STZ-diabetic rodents (**CHAPTER II**), boosting endogenous IGF-I signaling may be a valid mechanism of action for KU-32.[22-44] The realization that KU-32 is orally bioavailable and displays different temporal PK patterns

compared to IP treatments in DSPN-relevant tissues clearly warrants further investigation in OG KU-32 intervention studies. Further, additional PK studies are needed to determine whether KU-32 disposition is affected by diabetes and its other associated complications.

In conclusion, KU-32 represents a novel pharmacotherapeutic approach that can effectively treat more humanistic hallmarks of DSPN at acute and chronic stages of development. These neuroprotective qualities, in conjunction with desirable PK attributes, provide great promise as the first effective treatment option for DSPN.

SECTION 5. REFERENCES

1. Urban, M. J.; Li, C.; Yu, C.; Lu, Y.; Krise, J. M.; McIntosh, M. P.; Rajewski, R. A.; Blagg, B. S.; Dobrowsky, R. T. *ASN Neuro* **2010,** *2* (4), 189-199.
2. Urban, M. J. A small molecule modulator of Hsp90 improves experimental diabetic neuropathy. M.S., University of Kansas, Ann Arbor, 2010.
3. Shrivastava, A. and Gupta, V. B. *Chronicles of Young Scientists* **2011,** *2* (1), 21-25.
4. Motulsky, H. GraphPad Prism Version 5.0 Regression Guide. GraphPad Software, Inc.: San Diego, CA, 2007; p. 294. www.graphpad.com.
5. Fujikoshi, Y. *Discrete Mathematics* **1993,** *116* (1–3), 315-334.
6. Forthofer, R. N.; Lee, E. S.; Hernandez, M. *Biostatistics : a guide to design, analysis, and discovery*. 2nd ed.; Elsevier Academic Press: Burlington, MA, 2007; p xvii, 502 p.
7. Weisstein, E. W. Bonferroni Correction. http://mathworld.wolfram.com/BonferroniCorrection.html.
8. Dhillon, S. and Gill, K. Basic Pharmacokinetics. In *Clinical Pharmacokinetics*, Dhillon, S.; Kostrzewski, A., Eds. RPS Publishing: Pharmaceutical Press, 2006; pp 1-43.
9. Williams, D. A. and Lemke, T. L. *Foye's principles of medicinal chemistry*. 5th ed.; Lippincott Williams & Wilkins: Philadelphia, 2002; p xii, 1114 p.
10. Goodman, L. S.; Hardman, J. G.; Limbird, L. E.; Gilman, A. G. *Goodman & Gilman's the pharmacological basis of therapeutics*. 10th ed.; McGraw-Hill, Medical Pub. Division: New York, 2001; p xxvii, 2148 p.
11. Gudzinowicz, B. J.; Younkin, B. T.; Gudzinowicz, M. J. *Drug dynamics for analytical, clinical, and biological chemists*. Dekker: New York, 1984; p vii, 176 p.
12. Rowland, M. and Tozer, T. N. *Clinical pharmacokinetics : concepts and applications*. 3rd ed.; Williams & Wilkins: Baltimore, 1995; p xiv, 601 p.
13. Schoenwald, R. D. *Pharmacokinetics in drug discovery and development*. CRC Press: Boca Raton, 2002; p 426 p.
14. Cheer, K.; Shearman, C.; Jude, E. B. *BMJ* **2009,** *339*, b4905.
15. Kandel, E. R.; Schwartz, J. H.; Jessell, T. M. *Principles of neural science*. 4th ed.; McGraw-Hill, Health Professions Division: New York, 2000; p xli, 1414 p.
16. Todd, A. J. *Nat Rev Neurosci* **2010,** *11* (12), 823-36.
17. Sapunar, D.; Kostic, S.; Banozic, A.; Puljak, L. *J Pain Res* **2012,** *5*, 31-8.
18. Mizisin, A. P. and Weerasuriya, A. *Acta Neuropathol* **2011,** *121* (3), 291-312.
19. Urban, M. J.; Dobrowsky, R. T.; Blagg, B. S. *Trends Pharmacol Sci* **2012,** *33* (3), 129-37.
20. Farmer, K. L.; Li, C.; Dobrowsky, R. T. *Pharmacol Rev* **2012,** *64* (4), 880-900.

21. Ma, J.; Farmer, K. L.; Pan, P.; Urban, M. J.; Zhao, H.; Blagg, B. S.; Dobrowsky, R. T. *J Pharmacol Exp Ther* **2014,** *348* (2), 281-92.
22. Willis, D.; Li, K. W.; Zheng, J. Q.; Chang, J. H.; Smit, A.; Kelly, T.; Merianda, T. T.; Sylvester, J.; van Minnen, J.; Twiss, J. L. *J Neurosci* **2005,** *25* (4), 778-91.
23. Basso, A. D.; Solit, D. B.; Chiosis, G.; Giri, B.; Tsichlis, P.; Rosen, N. *J Biol Chem* **2002,** *277* (42), 39858-66.
24. Fujita, N.; Sato, S.; Ishida, A.; Tsuruo, T. *J Biol Chem* **2002,** *277* (12), 10346-53.
25. Lochhead, P. A.; Kinstrie, R.; Sibbet, G.; Rawjee, T.; Morrice, N.; Cleghon, V. *Mol Cell* **2006,** *24* (4), 627-33.
26. Schulte, T. W.; Blagosklonny, M. V.; Romanova, L.; Mushinski, J. F.; Monia, B. P.; Johnston, J. F.; Nguyen, P.; Trepel, J.; Neckers, L. M. *Mol Cell Biol* **1996,** *16* (10), 5839-45.
27. Fukushima, T.; Okajima, H.; Yamanaka, D.; Ariga, M.; Nagata, S.; Ito, A.; Yoshida, M.; Asano, T.; Chida, K.; Hakuno, F.*, et al. Mol Cell Endocrinol* **2011,** *344* (1-2), 81-9.
28. Martins, A. S.; Ordonez, J. L.; Garcia-Sanchez, A.; Herrero, D.; Sevillano, V.; Osuna, D.; Mackintosh, C.; Caballero, G.; Otero, A. P.; Poremba, C.*, et al. Cancer Res* **2008,** *68* (15), 6260-70.
29. Stancato, L. F.; Silverstein, A. M.; Owens-Grillo, J. K.; Chow, Y. H.; Jove, R.; Pratt, W. B. *J Biol Chem* **1997,** *272* (7), 4013-20.
30. Taherian, A.; Krone, P. H.; Ovsenek, N. *Biochem Cell Biol* **2008,** *86* (1), 37-45.
31. O'Rahilly, S. *Nature* **2009,** *462* (7271), 307-14.
32. Cortes-Gonzalez, C.; Barrera-Chimal, J.; Ibarra-Sanchez, M.; Gilbert, M.; Gamba, G.; Zentella, A.; Flores, M. E.; Bobadilla, N. A. *Cell Physiol Biochem* **2010,** *26* (4-5), 657-68.
33. Breinig, M.; Mayer, P.; Harjung, A.; Goeppert, B.; Malz, M.; Penzel, R.; Neumann, O.; Hartmann, A.; Dienemann, H.; Giaccone, G.*, et al. Clin Cancer Res* **2011,** *17* (8), 2237-49.
34. Yoshikawa, N.; Nemoto, T.; Satoh, S.; Maruta, T.; Yanagita, T.; Chosa, E.; Wada, A. *Neurochem Int* **2010,** *56* (1), 42-50.
35. Lang, S. A.; Moser, C.; Gaumann, A.; Klein, D.; Glockzin, G.; Popp, F. C.; Dahlke, M. H.; Piso, P.; Schlitt, H. J.; Geissler, E. K.*, et al. Clin Cancer Res* **2007,** *13* (21), 6459-68.
36. Gould, C. M.; Kannan, N.; Taylor, S. S.; Newton, A. C. *J Biol Chem* **2009,** *284* (8), 4921-35.
37. Budas, G. R.; Churchill, E. N.; Disatnik, M. H.; Sun, L.; Mochly-Rosen, D. *Cardiovasc Res* **2010,** *88* (1), 83-92.
38. Zitzmann, K.; Ailer, G.; Vlotides, G.; Spoettl, G.; Maurer, J.; Goke, B.; Beuschlein, F.; Auernhammer, C. J. *Int J Oncol* **2013,** *43* (6), 1824-32.
39. Grandis, M.; Nobbio, L.; Abbruzzese, M.; Banchi, L.; Minuto, F.; Barreca, A.; Garrone, S.; Mancardi, G. L.; Schenone, A. *Muscle Nerve* **2001,** *24* (5), 622-9.
40. Brussee, V.; Cunningham, F. A.; Zochodne, D. W. *Diabetes* **2004,** *53* (7), 1824-30.
41. Zhuang, H. X.; Snyder, C. K.; Pu, S. F.; Ishii, D. N. *Exp Neurol* **1996,** *140* (2), 198-205.
42. Chu, Q.; Moreland, R.; Yew, N. S.; Foley, J.; Ziegler, R.; Scheule, R. K. *Mol Ther* **2008,** *16* (8), 1400-8.
43. Toth, C.; Brussee, V.; Zochodne, D. W. *Diabetologia* **2006,** *49* (5), 1081-8.
44. Ohji, G.; Hidayat, S.; Nakashima, A.; Tokunaga, C.; Oshiro, N.; Yoshino, K.; Yokono, K.; Kikkawa, U.; Yonezawa, K. *J Biochem* **2006,** *139* (1), 129-35.